Design, characterization and applications of polyester nanoparticles obtained by enzymatic polymerization in nano-emulsions prepared by low-energy methods

Camille Paulme

Universitat de Barcelona
Facultat de Química
Departamento de enginyeria Quimica
Doctoral program “Ciència i Tecnologia de Materials”

Consejo superior de Investigaciones científicas
Instituto de química avanzada de Catalunya
Departamento de Nanotecnología Química y Biomolecular

DESIGN, CHARACTERIZATION AND APPLICATIONS OF POLYESTER NANOPARTICLES OBTAINED BY ENZYMATIC POLYMERIZATION IN NANO-EMULSIONS PREPARED BY LOW-ENERGY METHODS

A dissertation submitted by **CAMILLE PAULME** in partial fulfillment of the requirements for the degree of Doctor in chemistry of the Universitat de Barcelona.

PhD thesis directed by:

Prof. Conxita Solans Marsà
Instituto de Química Avanzada de Catalunya (IQAC-CSIC)

Dr. Jordi Esquena Moret
Instituto de Química Avanzada de Catalunya (IQAC-CSIC)

Tutora: Dr. Carme González
Department de Chemical engineering
(University de Barcelona)

Barcelona, Febrero 2013

TABLE OF CONTENT

INTRODUCTION

1. INTRODUCTION

1.1. NANO-EMULSIONS

1.1.1. General properties

Nano-emulsions are emulsions, (dispersion of an immiscible liquid in another liquid) **with very small droplet size, generally between 20 and 200 nm** (Figure 1.1). In most of the emulsions (and nano-emulsions), the immiscible liquids are generally a polar solvent, generally water (W) and a non polar liquid, oil (O). Emulsions can be classified by the nature of the dispersed phase in two main types: oil-in-water emulsions (oil droplets dispersed in water, O/W) or water-in-oil emulsions (water droplets dispersed in oil, W/O).

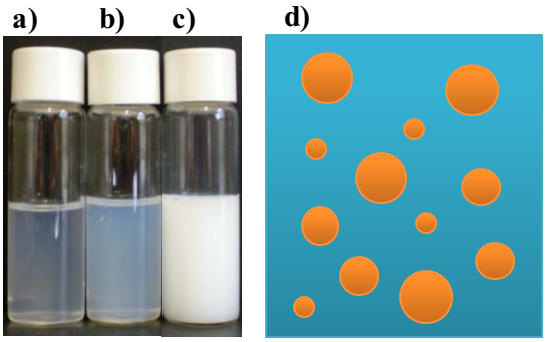

Figure 1.1 : Visual aspect of a) transparent, b) slightly turbid nano-emulsions, c) a conventional emulsion and d) schematic representation of a liquid-liquid dispersion.

Compared to conventional emulsions which size is generally higher than 1 µm and therefore are milky, nano-emulsions are transparent or slightly turbid. Nano-emulsions are also designated as sub-micrometric emulsions (Benita, 1993), namely in the pharmaceutical field, miniemulsions in the literature related to polymerization (Ugelstadt, 1973; Lovell, 1997), ultrafine emulsions (Nakajima, 1997) or instable microemulsions. The terminology nano-emulsion was adopted in this thesis as it gives the size range and avoids misunderstandings with the term microemulsion (Solans, 2005; Mason, 2006; Anton, 2011; McClemens, 2012).

Nano-emulsions, being emulsions, **are thermodynamically unstable systems** due to the relatively large positive free energy associated to the contact of the oil and the water phase and the creation of the interface. The free energy of formation, ΔG, of an emulsion can be expressed by the Gibb's equation:

$$\Delta G = \gamma \Delta A - T \Delta S \quad (1.1)$$

Where γ is the interfacial tension between the two liquids, ΔA is the increment in interfacial area, T the temperature and ΔS the difference of entropy (Tadros, 1983). The entropy of dispersion ΔS is positive but small and therefore, $T\Delta S$ cannot compensate $\gamma \Delta A$ which is large due to the high value of ΔA produced by the formation of a large number of droplets. As a consequence, the Gibbs free energy (ΔG) which is the amount of energy needed to create an emulsion is high and positive and can be brought to the system by either external or internal energy sources (Walstra, 1993). The amount of energy required to form an emulsion can be lowered by decreasing the interfacial tension between the two immiscible liquids by adding surfactant molecules. Although nano-emulsions are thermodynamically unstable, they can present a high kinetic stability when the system properties are optimized.

1.1.2. Stability

Due to their thermodynamic instability, emulsions (as well as nano-emulsions) tend to separate in two or more phases. This process is called phase separation and can occur through various destabilization mechanisms (Figure 1.2) including sedimentation, creaming, flocculation, coalescence and Ostwald ripening. These different mechanisms can take place simultaneously or consecutively. The predominance of one mechanism on the other depends on the emulsion type, the droplet size, the component of the emulsion and/or the emulsion preparation. In this section, each destabilization mechanism will be briefly described.

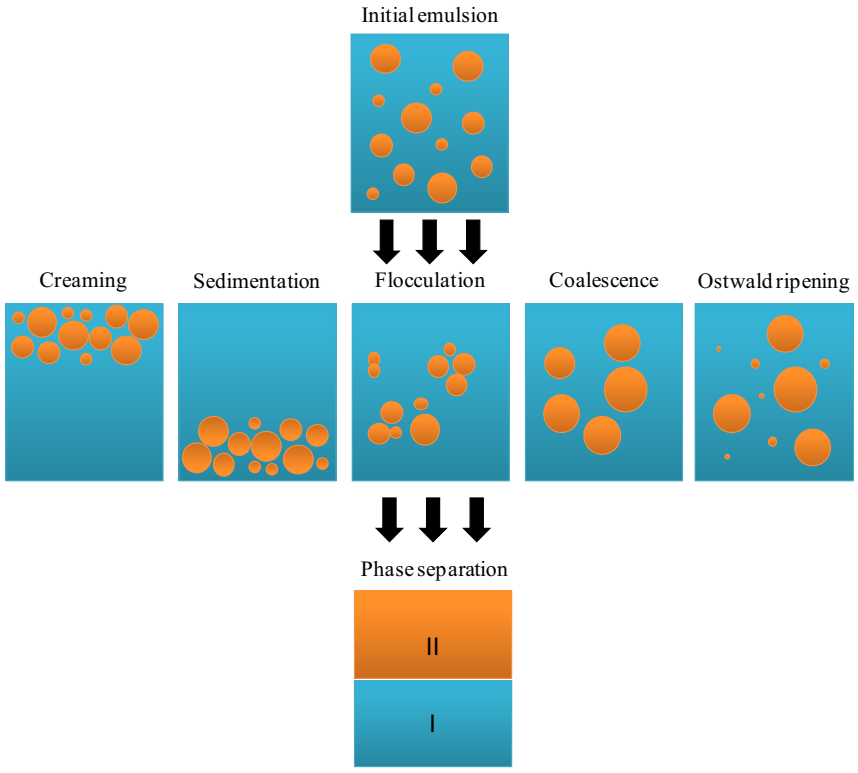

Figure 1.2 : Emulsion instability mechanisms

Creaming or sedimentation describes the upward (or downward) movement of the droplets due to gravity effects and as a result of the density difference between the two liquids (Tadros, 1983). Creaming and sedimentation processes can be generally reversed with a minimal energy input. This migration velocity (m/s) ω_{CR}, can be calculated by the Stockes law described as follow:

$$\omega_{CR} = \frac{2(\rho_d - \rho_c)gr^2}{9\eta} \qquad 1.2$$

Where ρ_d and ρ_c are respectively the density of the dispersed and the continuous phase, g is the acceleration due to the gravity, r is the radius of the droplets and η the viscosity of the continuous phase. The migration velocity can be reduced by decreasing the density difference between the two phases, by increasing the viscosity of the continuous phase and/or by decreasing the droplet radius. In the case of nano-emulsions, the droplet radius is extremely small, thus the migration velocity is low. The Brownian motion, which is relatively high for small droplets, overcomes any migration processes. Therefore, due to their small droplet size, **nano-emulsions are stable systems against sedimentation or creaming** (Tadros, 2004; Mason, 2006; McClemens, 2011).

Flocculation is defined as the reversible aggregation of the droplets into clusters. The flocculation of the emulsion droplets can be described by the DLVO theory (Derjaguin and

Landau (Derjaguin, 1941) and Verwey and Overbeek (Verwey, 1948)) which states that the stability of an emulsion is determined by the sum of the attractive (E_A) and repulsive (E_R) forces that exist between two droplets as they approach each other due to the Brownian motion they are undergoing.

$$E_T = E_A + E_R \quad 1.3$$

E_A, the potential due to attractive forces (Van Der Waals forces), is expressed as:

$$E_A = -A/(12\,\pi\,x^2) \quad 1.4$$

Where A is the Hamaker constant and x is the distance between two droplets. E_R, the potential due to the repulsive forces of electrostatic origin (electrical double layer), is a far more complex function and can be described as:

$$E_R = 2\,\pi\,\varepsilon\,r\,\xi^2\,\exp(-\kappa x) \quad 1.5$$

Where r is the droplet radius, ε is the solvent permeability, κ is a function of the ionic composition and ξ is the zeta potential.

According to this theory, an energy barrier resulting from the repulsive force may prevent two particles to approach and to adhere to one another (Figure 1.3). When two droplets collide with sufficient energy to overcome this barrier (V_{max}), the attractive forces pull them into contact and the drops adhere strongly and irreversibly together ("primary minimum"). To avoid this effect (flocculation), a sufficiently high repulsion between the droplets is required. In certain conditions (such as high salt concentrations), a possible "secondary minimum" can be observed corresponding to a weak flocculation of the droplets. These weak flocs are sufficiently stable not to be broken up by Brownian motion, but may dissociate under an externally applied force such as vigorous agitation.

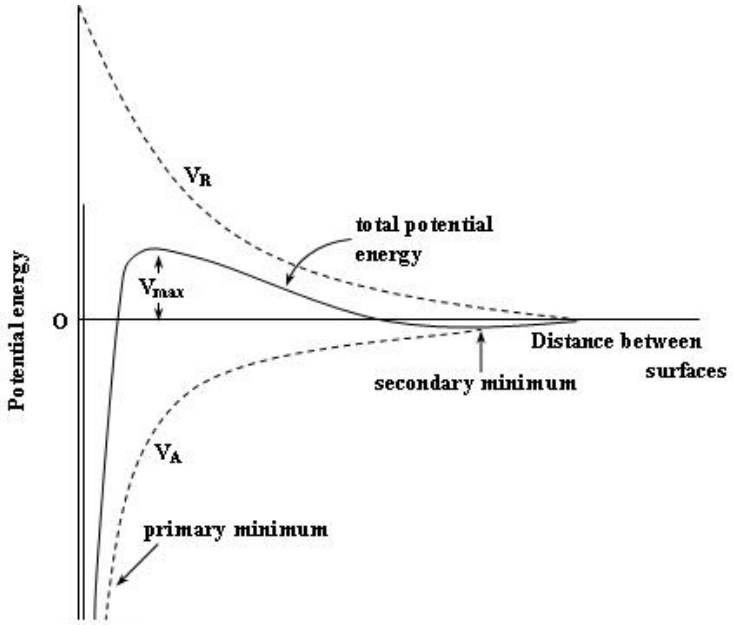

Figure 1.3 : Schematic diagram of the variation of free energy with droplet separation according to DLVO theory.

Due to the small droplet size of nano-emulsions, the curvature of the interface is high and the region of contact between the drops is low thus, reducing the probability of two drops to aggregate. Therefore, some authors considered **nano-emulsions stable against flocculation** (Tadros, 2004).

Another approach consists in saying that flocculation rate depends on how often the droplets encounter each other and how long they stay in contact. In nano-emulsions, the droplets are extremely small, the Brownian movement is high and thus the probability of collision between the droplets increases. Therefore, some authors considered that **nano-emulsions can destabilize by flocculation** (Wang, 2008 and 2009). Flocculation can be prevented either by addition of nonionic surfactants with large hydrophilic groups that act as a steric barrier or by addition of co-adsorbed ionic surfactants that increase the emulsion droplet surface charge and act as an electrostatic barrier.

Coalescence is the process whereby two or more droplets collide and merge into a bigger droplet, which has less specific interfacial area. Coalescence is an irreversible phenomenon, which clearly differentiates it from the aforementioned mechanisms, as the thin film between the droplets breaks (Walstra, 1993). Deminière *et al.* proposed a mechanism describing the spontaneous break of the interface of concentrated emulsions (Deminière, 1998) and considering that the limiting step for the rupture is only controlled by the thinning of the film up to molecular contact.

Following the Deminière theory, the coalescence rate ω_{CO} , for emulsions can be calculated by the following equation:

$$\omega_{CO} = \left(\frac{1}{{r_0}^2} - \frac{1}{r^2}\right)\frac{3}{8\pi t} \quad 1.6$$

Where r is the droplet radius after a time t, r_0 is the radius at t=0. The velocity of coalescence ω_{CO} can be calculated by the slope of the curve $1/r^2$ as a function of time. **Coalescence is generally considered as a possible destabilization mechanism of nano-emulsions.**

Ostwald Ripening is the process whereby the mean size of the droplets increases over time due to the diffusion of the molecules of the dispersed phase from the small to the large droplet. In 1961, Lifshitz and Slezov (and independently Wagner) proposed an equation to describe the Ostwald ripening velocity (Lifshitz, 1961; Wagner, 1961). The LSW theory assumes that the droplets are spherical, the distance between the droplets is higher than the droplet size and the mass transfer is only due to diffusion. In these conditions, the velocity of Ostwald ripening, ω_{OR}, is determined by the following equation:

$$\omega_{OR} = \frac{dr^3}{dt} = \frac{8C_\infty \gamma V_m D}{9RT\rho} \quad 1.7$$

Where C_∞ is the solubility of the dispersed phase in the continuous phase, γ is the interfacial tension between the two liquids, V_m is the molar volume of the dispersed phase, D is the diffusion coefficient of the dispersed phase into the continuous phase, r is the droplet radius, ρ the density of the dispersed phase, R the gas constant and T the temperature. The Ostwald ripening rate can be determined from the slope of the curve r^3 as a function of time.

In nano-emulsion, the Brownian motion is high due to the small droplet size inducing an increase of the diffusion velocity. Therefore, **Ostwald ripening is considered as the main destabilization mechanism of nano-emulsions**. Moreover, it was described that the polydispersity and the solubility of the dispersed phase in the continuous phase are the main factors affecting the Ostwald ripening (Taisne, 1996; Kabalnov, 1987, Taylor, 1998). It is then necessary to reduce these parameters to decrease the Ostwald ripening rate (Tadros, 2004). The first approach consists in the addition of a second disperse phase component, which is less soluble in the continuous phase such as squalene, hexadecane or squalane to limit the diffusion of the dispersed phase through the continuous phase (Higushi, 1962; Davis, 1981). The second

approach consists in forming low polydispersed emulsions by playing on the surfactant concentration and/or the preparation method.

To conclude on the destabilization mechanisms, **due to their small droplet size, nano-emulsions tend to have a better stability to creaming, sedimentation but worse stability against Ostwald ripening (Taylor, 1994; Tadros, 2004; Izquierdo, 2002) than conventional emulsions.**

1.1.3. Stabilization by surfactants

To form an emulsion of small droplet size, it is necessary to reduce the interfacial tension (Equation 1.1) which can be achieved by the addition of a third component to the system, called emulsifier or stabilizer. Generally, surfactants, solid particles or macromolecules (Holmberg, 2002; Pickering, 1907) among other materials are used to enhance emulsion stability. To form and stabilize nano-emulsions, the most common emulsifiers are the surfactants.

1.1.3.1. General properties of surfactants

Surfactants are amphiphilic molecules containing one hydrophilic head and one hydrophobic tail. The hydrophobic tail generally consists of an alkyl chain that can be linear or branched while the hydrophilic head can be of four types depending on the charge of the head group (anionic, zwitterionic, amphoteric or nonionic). In this thesis, **nonionic surfactants** have been used as they are considered as less toxic than charged surfactant, they are not affected by electrolytes compared to the other types of surfactant but those of ethoxylated type are very temperature dependent.

The main property of surfactants is their spontaneous adsorption at interfaces. In fact, when present at low concentrations in a two-liquid system such as emulsions, they orient themselves in order to avoid unfavorable interactions by having their hydrophilic head in the hydrophilic medium and their hydrophobic tail in a lipophilic medium in a way that reduces the surface tension between the two liquids (Rosen, 1976).

When the surfactant concentration increases, the interfacial tension decreases until a plateau is reached at the Critical Micellar Concentration (CMC). Up to that point, the excess of surfactant spontaneously aggregates into micelles in order to reduce the contact of the alkyl chains with the polar solvent. At higher surfactant concentration, the solubility limit of micelles is reduced and

phase transition (first order of transition) to liquid crystalline phase takes place (Israelachvili, 1976 and 1994).

1.1.3.2. Stabilization of emulsions by surfactants

Due to their amphiphilic structure, surfactants strongly adsorb at the liquid-liquid interface, performing two functions. First, they lower the interfacial tension, γ, and consequently reduce the free energy ΔG needed to create the emulsion (Equation 1.1). Then, they create a monolayer at the droplet interface which acts as a mechanical, steric, and/or electrical barrier. Therefore, they prevent the direct contact between neighboring droplets, and hence avoid flocculation, coalescence or Ostwald ripening. The addition of surfactants into the system is then a key factor for both the formation and stabilization of emulsions.

1.1.3.3. Prediction of the emulsion type

The type of emulsion depends on various factors such as the nature of the surfactant, the process used and/or the volume fraction of dispersed phase. Over the years, many authors have attempted to predict the type of emulsion considering these factors. Bancroft in 1912 first suggested a qualitative rule which states: “the phase in which the surfactant is more soluble constitutes the continuous phase of the emulsion” (Bancroft, 1912). However this rule is not always true.

Therefore, in order to extend this rule to a more quantitative aspect, the concept of hydrophilic-lipophilic balance number, N_{HLB} was introduced and relates quantitatively the polar and apolar groups of the surfactant (Griffin, 1949). For nonionic surfactants with polyoxyethylene groups the N_{HLB} is given by the equation:

$$N_{HLB} = \frac{H}{H + L} \times 20 \qquad 1.8$$

Where H and L are the weight percent of the hydrophilic and lipophilic group of the surfactant, respectively. The number 20 represents an arbitrary scale. It was then showed that surfactants with N_{HLB} higher than 10 have a hydrophilic behavior while those with N_{HLB} lower than 10 have a hydrophobic behavior. The N_{HLB} is a widely used parameter to predict the interfacial activity as well as a useful tool for formulation purposes. Table 1.1 relates the ranges of N_{HLB} numbers and the surfactant properties.

Table 1.1 : Properties of surfactants as a function of the HLB number.

N_{HLB}	Application
4 - 8	Anti-foaming
7 - 11	W/O emulsifier
11 - 14	Wetting agent
12 - 16	O/W emulsifier (detergent)
16 – 20	Solubilizer

Unfortunately, the HLB number does not consider parameters such as the temperature, the pressure, the salinity, the use of cosurfactant or the volume fraction of each phase, although the interfacial activity of surfactants depends on all these factors. For example, in a water/nonionic surfactant/oil system, when the temperature increases, the dehydration of the ethoxylated chains of the nonionic surfactant occurs and hence the surfactant becomes more hydrophobic. This change in the surfactant solubility induces a phase transition from an O/W to a W/O emulsion. Therefore, Shinoda proposed a new concept for poly(oxyethylene) type nonionic surfactants named the phase inversion temperature (PIT or HLB temperature) (Shinoda, 1968) that takes into account all the system parameters. This temperature, where the phase transition occurs is a characteristic and useful parameter of a system to predict the emulsion type at a given temperature.

1.1.4. Preparation methods

The formation of small droplet, such as nano-emulsions droplets implies a high increase of the interfacial area ΔA (Equation 1.1) which can be achieved by inducing a high energy input from either external (high-energy methods) or internal sources (low-energy methods).

1.1.4.1. High-energy methods

During emulsification by high-energy methods, small droplet sizes are obtained by breaking the bigger drops using mechanical devices able to produce intense breaking forces. High-pressure homogenizers, colloidal mills, ultrasounds or high-shear stirrers are generally used to produce the appropriate energy in a relatively short time (Walstra, 1993; Delmas, 2011). High-energy methods are straightforward processes as the higher the energy input the smaller the droplet size is. However, the level of energy required to obtain small droplets is very high and therefore cost-

inefficient, especially knowing that only a small amount (around 0.1%) of the energy produced is used for emulsification.

1.1.4.2. Low-energy methods

Low-energy methods make use of the internal chemical energy of the system components to produce small droplet sizes. Compared to high energy methods, those methods are more energy efficient, as only simple stirring is required, and generally enable the formation of smaller droplets with lower polydispersity. Low-energy methods can be classified in two types, spontaneous emulsification and phase inversion methods depending on whether phase inversion of the spontaneous curvature of the surfactant occurs during emulsification (McClemens, 2011; Solans, 2005 and 2012).

- **Spontaneous emulsification**

Spontaneous emulsification or self-emulsification methods make use of the internal chemical energy released by the system during a dilution process with the continuous phase, generally at constant temperature, without any phase transition taking place. For instance, the formation of nano-emulsions has been reported to take place by dilution of O/W microemulsions with water(Taylor, 1994). During the process, the microemulsion became no longer thermodynamically stable as the surfactant concentration is not high enough to maintain the very low interfacial tension required, thus forming a nano-emulsion. In a recent study, Solè *et al*. reported that nano-emulsions can be obtained starting emulsification from both W/O and O/W microemulsions by selecting an appropriate dilution procedure and composition (Solé, 2012). Nano-emulsions have also been formed by dilution of a direct cubic liquid crystalline phase in mixed non-ionic/ionic surfactant systems (Solé, 2006 and 2008). It should be noted that no change in the surfactant spontaneous curvature is involved during these processes. Therefore, the mechanism by which nano-emulsions are formed is self-emulsification. This process is also called self-nano-emulsifying drug delivery systems (SNEDDS) in the pharmaceutical industry. Its main disadvantage is that nano-emulsions are generally obtained with a low volume fraction of dispersed phase and high concentration of surfactant. However this process has also been carried out without surfactant, so called the Pastis or Ouzo effect, when a large amount of water is added to a mixture made of alcohol and anise-flavored oil to produce nano-emulsions by displacement of some alcohol molecules from the dispersed to the aqueous phase.

- **Inversion Emulsification**

The Phase Inversion Temperature (PIT) method relies on changes in the physicochemical properties (optimum curvature or solubility of ethoxylated non-ionic surfactant) with changing temperature (Figure 1.4) (Shinoda, 1969). This method can only be applied to temperature-sensitive surfactants such as polyethoxylated surfactant. For instance, in a water/ethoxylated nonionic surfactant/oil system, at low temperature (T< PIT), the surfactant, due to the presence of ethylene oxide group, is dissolved in water, resulting in the formation of O/W structures. An increase of the temperature produces the dehydration of the ethoxylated chains of the nonionic surfactant that become more hydrophobic. At high temperature (T>PIT), the surfactant is dissolved in the oil phase, resulting in the formation of W/O structures. At intermediate temperatures, close to the phase inversion (T ≈ PIT), the surfactant is no longer soluble in water or oil and the formation of zero-curvature colloidal structure takes place (lamellar liquid crystal or bicontinuous structure) (Figure 1.4). The interfacial tension between oil and water is then extremely low and the formation of small droplet is favored (equation 1.1). Nevertheless, at low interfacial tension, emulsions destabilize quickly by coalescence. Therefore, practically, this method consists in preparing the sample at the temperature of phase inversion and decreasing (increasing) quickly the temperature to produce O/W (W/O) emulsions avoiding coalescence (Shinoda, 1969).

Various studies showed that phase transitions through lamellar liquid crystalline phase or microemulsions take place during emulsification by the PIT method of water/nonionic surfactant/aliphatic oil systems. Morales *et al.* reported the formation of O/W nano-emulsions with minimum droplet sizes (around 40 nm) in the Water/$C_{16}E_6$/oil system by the PIT method when the surfactant and all the oil components are previously dissolved in the same phase (bicontinuous microemulsion), independent of whether the initial phase equilibrium is single or multiphase. Similar results were observed by Izquierdo *et al.* (Izquierdo, 2005; Morales, 2003 and 2006). Recently, Roger *et al.* introduced the concept of sub-PIT emulsification (Roger, 2010 and 2011). By keeping the W/O ratio constant in the water/$C_{16}E_8$/hexadecane system, O/W nano-emulsions have been obtained by cooling quickly the system from a temperature a few degrees below the PIT (sub-PIT), and their size was similar to that of nano-emulsions obtained cooling from or above the PIT. An advantage of the sub-PIT method over the PIT is the lower temperature at which the emulsification process is initiated by a given concentration of surfactant. Nevertheless, it can be discussed whether this method is a phase inversion emulsification method as no changes in the spontaneous curvature of the surfactant take place.

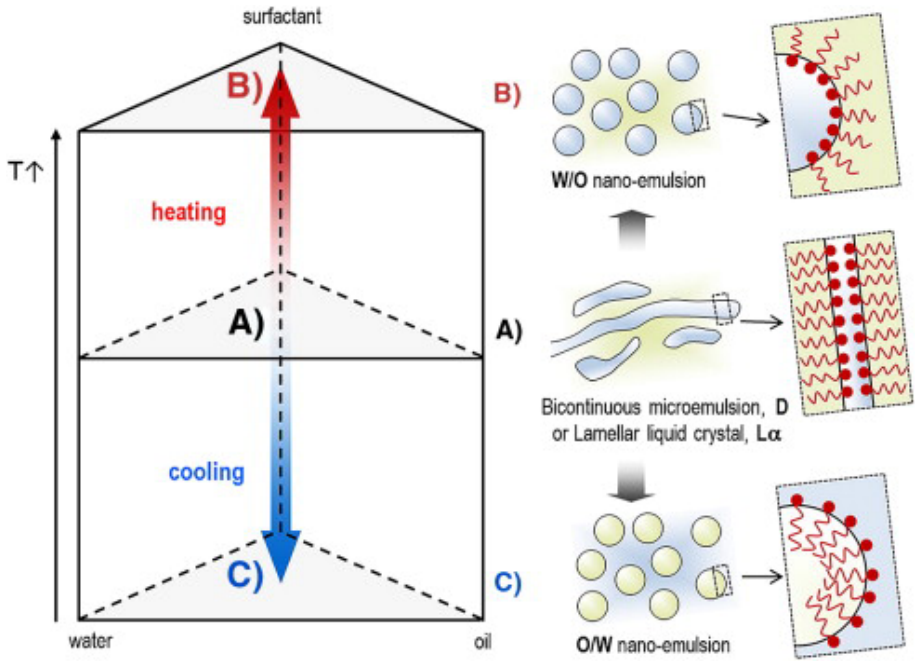

Figure 1.4 : Schematic representation of nano-emulsion formation by the phase inversion temperature method. (Adapted from Solans, 2012)

The Phase Inversion Composition (PIC) method is based on the changes in the surfactant spontaneous curvature during emulsification by changing the composition at constant temperature. This method consists on progressively adding one of the components (water or oil) over a mixture of the other two components (oil-surfactant or water-surfactant, respectively). As the volume fraction of water increases in a water/ nonionic ethoxylated surfactant/oil system, the hydration grade of the ethoxylated chains of the surfactant progressively increases, and the surfactant spontaneous curvature changes from negative to zero. Around the transition composition, the hydrophilic-lipophilic properties of the surfactant are balanced and bicontinuous or lamellar structures are formed. When more water is added to the system, the structures with zero curvature separate into unstable small droplet size nano-emulsion (O/W), which implies a very high positive curvature of the surfactant layer (Figure 1.5). The PIC method has a greater potential for a large-scale production compared to the PIT method as it is experimentally easier to add one component to a large volume of emulsion than to produce a sudden change in temperature. Moreover, it should be noted that this method can be applied to non-temperature sensitive surfactants other than ehtoxylated-type.

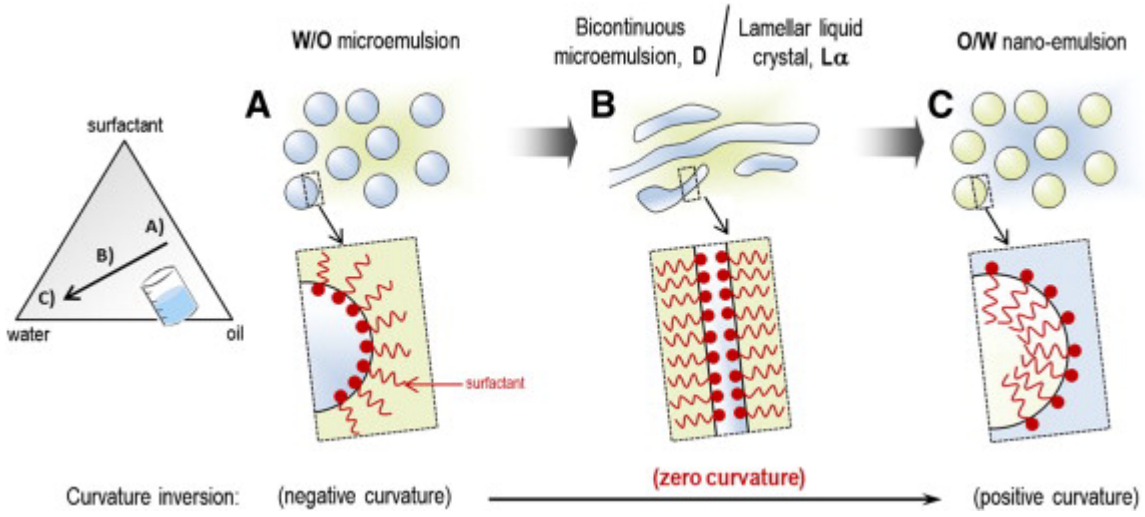

Figure 1.5 : Schematic representation of nano-emulsion formation by the phase inversion composition method. (Adapted from Solans, 2012).

Concerning studies on O/W nano-emulsions by the PIC method, Sagitani *et al.* demonstrated that the formation of a liquid crystal phase during the emulsification process was necessary to obtain droplets of small size and low polydispersity (Sagitani, 1981). Later, Forgiarini *et al.* confirmed the presence of a lamellar liquid crystalline phase during the formation of nano-emulsion in the water/Brij 30/decane system (Forgiarini, 2001). Sonneville-Aubrun *et al.* reported also the presence of zero-curvature lamellar liquid crystalline phases at very short times after water addition to the water/polyethylene glycol 400 monoisostearate/hydrogenated polyisobutene system leading to nano-emulsions with homogenenous size distribution and a mean diameter of 100 nm (Sonneville-Aubrun, 2009). Recently, Roger *et al.* compared the formation of nano-emulsions in the water/$C_{16}E_8$/hexadecane system by the PIC method (Roger, 2011) and the PIT method (Roger, 2010). Emulsification by the PIC method proceeds through the swelling of a reverse micellar phase, followed by the formation of a bicontinuous sponge phase and leading to nano-emulsions with bimodal size distributions were obtained while the same system emulsified by the sub-PIT method presents monomodal distributions. It was concluded that the PIT method was more efficient than the PIC method to obtain small droplets and narrow size distributions. An important factor that should be taken into account in the emulsification by low-energy methods is the kinetics of the process as highly viscous phases might form during the emulsification. Sole *et al.* reported the presence of cubic liquid crystalline phase in the emulsification process, leading to monomodal or bimodal distribution depending on the stirring speed and surfactant concentration (Sole, 2012). In many investigations and practical applications, nano-emulsion formation is achieved by a combination of low-energy methods (phase-inversion and self-emulsification) (Sadurni, 2005; Wang, 2007) or low- and high-energy methods.

1.1.5. Applications

Due to their small droplet size and higher kinetic stability, nano-emulsions have been considered as an improvement of conventional emulsions already on the market. Due to their bluish transparent aspect, they have been used for the incorporation of functional component in transparent products for food, perfumery industry (McClements, 2011; Ziani, 2012) or cosmetics (Sonneville-Aubrun, 2004).

Nano-emulsions have been widely investigated for the encapsulation and release of functional components such as flavors, antimicrobials, vitamins, nutraceuticals or drugs to increase the bioavailability of active components. In the pharmaceutical field, nano-emulsions have brought many benefits for a variety of purposes, namely, nutrition (such as administration of fats, carbohydrates, vitamins, etc.), controlled drug release and targeting of drugs to specific sites in the body, delivery of vaccines or as gene carriers (Benita, 1993; Tamilvanan, 2005). For example, nano-emulsions are advantageous carriers for the parenteral administration. In fact, the small droplet size of nano-emulsions makes them recommendable to avoid the obstruction of the blood vessels. The oral administration of drugs encapsulated in nano-emulsions has also shown some benefits as the absorption of drugs in the gastrointestinal tract increases when incorporated in nano-emulsion and the latter is directly related to the size of the drops (Nicolaos, 2003).

Apart from their applications as drug delivery systems, another application of nano-emulsions is their use as template for the preparation of polymeric nanoparticles (Antonietti, 2002; Asua, 2000). This application will be described in details in section 1.2.1.

1.2. POLYESTER NANOPARTICLES

Polyesters are an important class of polymers. Natural polyesters are generally biodegradable while most of the synthetic polyesters are not. Therefore, the synthesis of biodegradable polymer has attracted much attention over the past decades. On the other hand, nanoparticles have drawn much interest for their use in pharmaceutical or cosmetic applications.

1.2.1. Synthesis of polyesters

The syntheses of polyesters is generally carried out by polycondensation or ring-opening polymerization (ROP) using radical (Siebert, 2012), anionic (Jedliski, 1996; Ruppert, 2010), cationic or metalorganic catalyzed polymerization (Albertsson, 2003; Zhiyuan, 2000). Those methods require the use of organic solvents, catalysts and often, high temperatures and long reaction times that make the process very expensive and unsafe. The need for developing ecofriendly processes and products have conducted to use enzymes as catalysts. Enzymes are known to act efficiently as catalysts outside living systems and can be used even at extreme pH values, high temperature or reduced pressure. Among the large variety of enzymes, **lipases** are able to catalyze the formation of polyesters as they catalyze the hydrolysis of fatty acid esters normally in an aqueous environment in living systems. Using lipase catalysts, polyesters have been synthesized by two polymerization modes: the **ring-opening polymerization (ROP)** of cyclic monomers and the polycondensation between a carboxylic group and an alcohol (Uyama, 2006; Kadokawa, 2010). It has been shown that the Ring-Opening Polymerization method present an important advantage over polycondensation as it enables the control of the molecular weight of the polymer by controlling the monomer/initiator ratio (Kobayashi, 2009 and 2010; Matsumura, 2006; Gross, 2001). The **enzymatic Ring-Opening Polymerization (eROP)** deals with the opening of a cyclic monomer, generally of lactone type (Figure 1.6).

a)

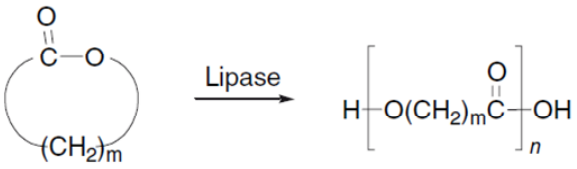

b)

m	Name	
2	β-propiolactone	β-BL
4	δ-valerolactone	δ-VL
5	ε-caprolactone	ε-CL
7	8-octanolide	8-OL
10	11-Undecanolide	UDL
11	12-Dodecanolide	DDL
14	15-Pentadecanolide	PDL
15	16-Hexadecanolide	HDL

Figure 1.6 : a) Reaction of enzymatic ring-opening polymerization (eROP) of lactones of various ring size and b) Example of lactones polymerized by eROP (adapted from Namekawa, 1999).

The first report of an enzymatic ring opening polymerization of lactones was published in 1993 and deals with the polymerization of ε-caprolactone using a lipase PPL (Knani, 1993). Since then, the polymerization of lactones with small (Matsumura, 1998), medium (Kobayashi, 1998a-b; Mei, 2003) and large ring size (Uyama, 1995a-b and 1996; Namekawa, 1998a) has been successfully achieved by lipase ROP in bulk but their polymerizability is dependent on the lactone ring size (Figure 1.6) and enzyme origin (Table 1.2).

Table 1.2 : Effect of the ring size and lipase origin on the conversion of lipase catalyzed-ROP of lactone and the molecular weight of the obtained polymer (Namekawa, 1999).

Lipase-catalyzed ring-opening polymerization of lactones[a]

Lactone	Enzyme	Temperature (°C)	Time (h)	Conversion[b](%)	M_n[b]	M_w/M_n[b]
ε-CL	Lipase CC	60	240	92	1900	2.0
ε-CL	Lipase PC	60	240	84	6100	2.7
ε-CL	Lipase PF	60	240	71	7000	2.2
ε-CL	Lipase PF	75	480	99	12 000	2.3
ε-CL	Lipase RJ	60	240	83	840	1.7
ε-CL	PPL	60	240	95	1300	1.7
UDL	Lipase CC	75	240	95	25 200	2.2
UDL	Lipase PF	75	48	98	19 500	2.5
DDL	Lipase CC	75	120	99	13 000	2.8
DDL	Lipase PF	30	120	8	1300	1.2
DDL	Lipase PF	45	120	72	1600	1.8
DDL	Lipase PF	60	120	99	4000	2.5
DDL	Lipase PF	75	120	100	9600	3.3
PDL	Lipase CC	75	240	65	16 200	2.4
PDL	Lipase PF	75	120	96	7200	2.7
HDL	Lipase PC	75	120	100	5800	2.0
HDL	Lipase PF	60	120	99	2600	3.8

[a] Polymerization of lactone using lipase catalyst (50 mg per 1.0 mmol of lactone) in bulk.
[b] Determined by SEC.

In contrast to small or medium lactones that polymerized easily using chemical catalysts, the polymerization of macrolactones (m>10) is generally slow and gives low molecular weight (Duda, 2002). Kobayashi and co-workers reported that large lactones can be polymerized with a great efficiency using lipases as catalysts (Uyama, 1995b; Mee, 2006) and explained it by the stronger recognition of the macrolides by the lipase catalyst.

Among the large ring size lactones, **Pentadecanolide (PDL),** also called **Exaltolide®**, polymerizes in Poly(Pentadecanolide) (PPDL), a crystalline biodegradable polymer with good thermal stability (Focarete, 2001). Moreover, in a recent work, it was demonstrated that PPDL is nontoxic and due to its high crystallinity, it is not easily degraded by hydrolysis (Meulen, 2008). For these reasons, PPDL has shown great interest to replace the commonly used polyesters. In the following section, the different processes of polymerization and copolymerization of poly(Pentadecanolide) by eROP are described.

1.2.1.1. Enzymatic Ring-Opening Polymerization of Pentadecanolide: State of the art

PPDL was first synthesized by eROP in bulk (by simply mixing PDL with the catalyst in a dried tube) with lipases of different origins (CC, PF and PC)and at various reaction temperature. Allthough reactions were carried out at high temperature and high lipase concentrations, the reaction rates were extremely low (Uyama, 1996). Various alternatives, based on work done on other lactones were explored to make the reaction more ecofriendly. The most important reactions are summarized in Table 1.3.

Table 1.3 : Summary of the eROP of PDL.

Enzyme	Reaction media	T (°C)	Time (h)	Conv. (%)	M_n (g/mol)	M_w/M_n	Ref.
Lipase CC	Bulk	75	240	65	16200	2.4	Uyama,1996
Lipase PF	Bulk	75	120	96	7200	2.7	Uyama,1996
Lipase PS 30	Bulk	80	72	92	34400	2.4	Bisht, 1997
Novozym 435	Bulk	80	24	100	22100	3.3	Bisht, 1997
Lipase PS 30 imm.	0.2% water	70	24	100	62000	1.9	Bisht, 1997
Lipase PC	Water	60	72	79	500	1.2	Namekawa, 1998b
Novozym 435	Toluene	70	-	-	86400	-	Kumar, 2000

Bisht *et al.* investigated the use of immobilized lipase to increase the reaction rate. The immobilization of lipase was known to improve considerably the enzyme stability, recyclability and activity of esterification reaction (Bianchi, 1988; May, 1997). Two immobilized enzyme, lipase PS 30 and Novozym 435, were tested with PPDL and induced higher conversion rate and higher molecular weights, thus confirming the higher reactivity of immobilized lipase. In a second approach, the same authors described the effect of the addition of a nucleophile (water) on the conversion and molecular weight of PDL, using the immobilized lipase PS30 and demonstrated that high molecular weight (62 000g/mol) can be obtained in shorter time by adding a small amount of water (0.2%) (Bisht, 1997). These results demonstrated that the low molecular weight found in the earlier work of Uyama *et al.* (Uyama, 1996) is not a consequence of an intrinsic limitation of lipase catalyst systems. According to the previous study and within the aim to make the process more ecofriendly, Kobayashi *et al.* studied the polymerization of PDL in water using a lipase PC and showed high polymerization yield (79%) but low molecular weight (500g/mol) compared to bulk polymerization. In another approach, the polymerization of PDL was studied using the Novozym 435 in the presence of organic solvents and compared to the bulk polymerization, an increase in the monomer conversion (from 32 to 90%) and molecular weight (from 22 100 to 86 000 g/mol) was reported (Kumar, 2000). Moreover, a reduction of the polymerization temperature from 90 to 55 °C gave PPDL with higher molecular weight. The final PPDL polymer shows good thermal stability (degradation above 380ºC), a high melting point (97ºC) and a high crystallinity (Focarete, 2001). Its crystalline structure was determined as pseudo-orthorhombic monoclinic and presents similar properties to that of polyethylene with the advantage of biodegradability.

The enzymatic ring-opening polymerization of functionalized Pentadecanolide has been rarely reported. For instance, the eROP of substituted lactones such as α-Methyl-PDL was carried out in toluene at 45ºC and compared to the synthesis of PDL. Smaller reactivity has been reported for the substituted PDL than for PDL, suggesting that the enzymatic polymerizability is strongly depended on the presence of functional groups in the ring (Kikuchi, 2002).

An interesting work was carried out on the eROP of PDL and an unsaturated analog, Globalide (mixture of two constitutional isomers with the double bond at the 11 or 12 position of the PDL ring), using the lipase Novozym 435 and toluene at 60ºC (Meulen, 2008). In this case, even the functionalized PDL was polymerized conveniently to high molecular weights. The unsaturated polymer presented lower melting point (46.2ºC) than the saturated PPDL (97°C). It was also demonstrated that the polymers were non toxic and a degradation study revealed no hydrolytic or

enzymatic degradability of the polymers, due to the high crystallinity and hydrophobicity of the materials.

1.2.1.2. Enzymatic Ring-Opening Copolymerization of Pentadecanolide: State of the art

The copolymerization is a convenient method for the synthesis of copolymer with tuneable properties. The lipase-catalyzed copolymerization has been investigated with a wide range of co-monomers. In this section, exclusively copolymers containing PDL were described. In the first report on PDL obtained by eROP, Uyama *et al.* described its copolymerization with other lactones such as δ-VL, ε-CL, UDL and DDL using various types of lipase (PF and PC) and reaction temperatures. They obtained relatively low reaction rates and molecular weights (M_n<6000g/mol) but they confirmed the copolymerization by ^{13}C NMR spectroscopy (Uyama, 1996), as shown on Figure 1.7.

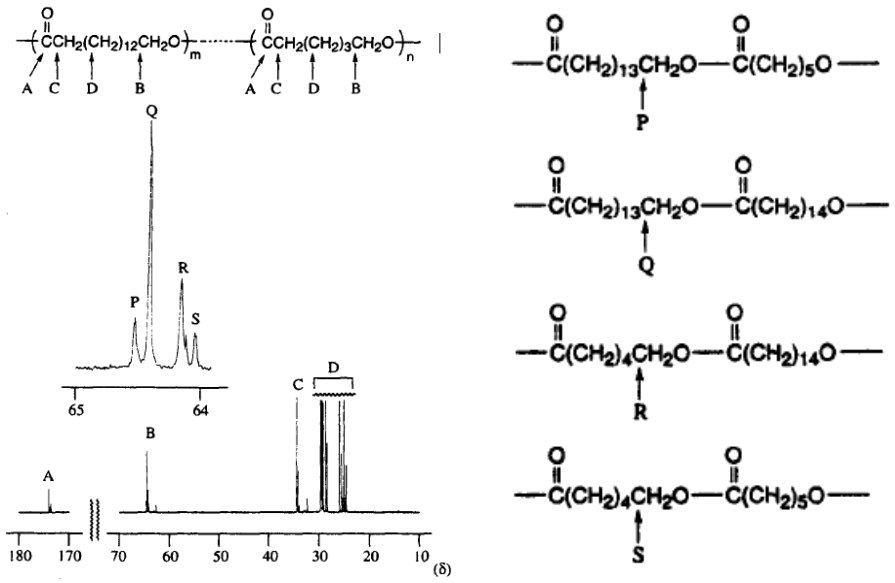

Figure 1.7 : 13C NMR spectrum of a PPDL-PCL copolymer and attribution of the peak of the expansion spectrum between 64 and 65 ppm (adapted from Uyama, 1996).

In the expansion of the spectrum between 64 and 65 ppm, the four peaks P,Q,R and S were attributed to the α-methylene carbon between PDL-CL, PDL- PDL, CL-PDL and CL-CL units, respectively (Uyama, 1996). Later, Kumar *et al.* described the copolymerization of PDL and ε-CL using Novozym 435 at 70ºC with small quantities of toluene. It is worth noting that unexpected fast rates were obtained and the polymerization of PDL was calculated to be 13 faster than that of CL (Kumar, 2000). The copolymers were prepared at various PDL/CL ratios and all the copolymers were obtained with a random structure, high crystallinity and high molecular

weight (up to 20 000g/mol). Moreover, a linear decrease of the melting temperature of the copolymers was reported with increasing the amount of CL monomer, between the melting point of PPDL (97°C) and that of PCL (59°C). The PCL and PPDL copolymers and homopolymers were characterized by SAXS/WAXS. The homopolymers presented a similar profile at wide angle but differed from the presence in PPDL of the (001) reflection at $2\theta = 4.5°$ that corresponds to the periodicity in the chain direction. The intensity of this reflection decreases in the copolymers with increasing the CL content, confirming the cocrystallization of the comonomer units (Ceccorulli, 2005).

PDL was also copolymerized with non cyclic monomers such as divinyl ester of adipic acid or sebastic acid and glycol using lipases CA and PC in diisopropyl ether at 60ºC for 72h. Relatively low yields (47% and 37%, respectively) and low molecular weight (10 000 g/mol) were reported. The copolymers, characterized by SAXS, presented lower crystallinity than their homopolymers (Namekawa, 2000).

Unusual copolymers were prepared by copolymerization of PDL with trimethylene carbonate (TMC) using the Novozym 435 as catalyst. As observed in previous studied (Focarete, 2001), the common behavior upon copolymerization of crystallizable polymers is a progressive decrease of crystallinity with increasing comonomer. Poly(PDL-TMC) presented a very remarkable feature: all copolymers were highly crystalline independently from the comonomer ratio. This result strongly suggests that some type of cocrystallization occurs in poly(PDL-TMC). Moreover, the X-ray diffraction patterns of poly(PDL-TMC) were practically identical to that of poly(PDL) in the range $10° < 2\delta < 80°$. Significant differences were observed in the low-angle region below 10°, indicating the presence of two crystal phases: the crystal of poly(PDL) and another crystal characterized by a larger fiber axis periodicity and possibly associated with crystallization of alternate PDL-TMC sequences (Focarete, 2002).

More recently, Jiang *et al.* described the copolymerization of PDL with a dialkyl ester and a diol (Jiang, 2008) or with dioxanone (Jiang, 2007) using the lipase catalyst Novozym 435 and toluene at 70ºC and showed the formation of semi crystalline, thermally stable polymers.

The Enzymatic Ring-Opening copolymerization of functionalized Pentadecanolide has been described once and deals with the enzymatic synthesis by ROP of Globalide with CL, 1,5-dioxepan-2-one and 4-methyl caprolactone in toluene at 60ºC for 24h (Meulen, 2011). The formation of random copolymers, with molecular weight of around 20 000 g/mol was confirmed

by ^{13}C NMR spectroscopy and thermal analysis revealed that the melting point lowered upon incorporating the co-monomers.

1.2.1.3. Mechanism of enzymatic Ring-Opening Polymerization

The mechanism of ROP of lactones by lipase is believed to proceed by the activated monomer mechanism (Figure 1.8) (Namekawa, 1999; Kobayashi, 2006).

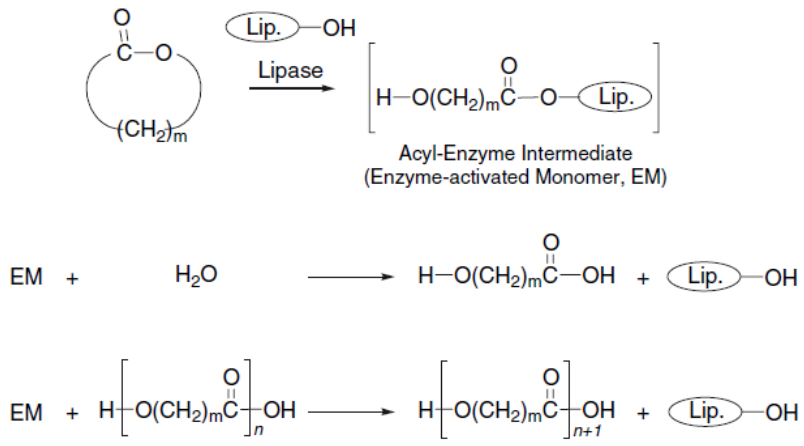

Figure 1.8 : Proposed mechanism of lipase-catalyzed ring opening polymerization (Kabayashi, 2006).

In the first step, the lactone is attacked by the catalytic site of the lipase, a serine residue, leading to the formation of the acyl-enzyme intermediate (Enzyme-activated Monomer, EM). Once the enzyme-activated monomer, EM, is formed, two processes might occur. The EM can be attacked by water to recover the free enzyme and the initial lactone or the monomer unit attacks the EM leading to the addition of one more unit to the polymer chains and regeneration of the enzyme.

1.2.2. Preparation of polyester nanoparticles in nano-emulsions

The preparation of nanoparticles, either inorganic (gold, silver or silica), solid lipid or polymeric, in confined media is generally performed in a two-step procedure. The first step consists in the preparation of the specific system while the second step is the generation of polymeric nanoparticles. Various confined systems have been used for the formation of nanoparticles, for instance, emulsions, nano-emulsions or microemulsions. Among these different systems, the use of nano-emulsions as template is often preferred over emulsions and microemulsions as it enables an efficient control of the nanoparticles size using low amount of surfactant. The nanoparticle generation is triggered either by precipitation of a preformed polymer or by in-situ polymerization of a monomer into nano-emulsion droplets (Schork, 2005; Antonietti, 2002; Asua, 2002).

1.2.2.1. Precipitation of a preformed polyester

In this process, the preformed polyester, for example polylactic acid (PLA), poly(lactic-co-glycolic acid) (PLGA) or polycaprolactone (PCL) is first dissolved in an organic solvent (generally a chlorinated solvent such as chloroform, methylene chloride) prior to emulsification. After formation of the nano-emulsion, the precipitation of the polymer is induced by removing the solvent which dissolves the polymer. Various methods have been used to remove the solvent (Anton, 2008; Soppimath, 2001; Vauthier, 2009):

- **The solvent-diffusion method** (Fessy, 1989) consists in preparing the nano-emulsion with water-saturated solvent or solvent saturated water to ensure the initial thermodynamic equilibrium of both liquids. After preparation, the nano-emulsion is diluted with an extensive amount of pure water, thus leading to the diffusion of the solvent toward the continuous phase. This method requires the use of high volume of water and non-volatile solvents like benzyl alcohol, benzyl acetate or propylene carbonate for their miscibility with water (Quintanar-Guerrero, 1997; Trimaille, 2003).

- **The solvent-evaporation method** consists in evaporating the solvent which first diffuses through the continuous phase of the nano-emulsion. The solvent is generally extracted under vacuum or by distillation. Volatile, partly water soluble solvents such as dichloromethane or chloroform have been widely used but for toxicity reason they have been replaced by ethyl acetate (Calderó, 2011).

- **The reverse salting-out/emulsification method** consists in formulating an emulsion with a solvent, dissolving the polymer and totally miscible with water, like acetone. A high concentration of salt is added to the water phase thus inducing a change of the solvent solubility in water and leading to emulsification. The precipitation of the polymer is triggered by a reverse salting-out effect produced by dilution of the emulsion with water, thus enhancing solvent diffusion (Allemann, 1992).

Generally, the size of the nanoparticles obtained by those methods is slightly smaller than the size of the nano-emulsion due to the elimination of the solvent contained in the nano-emulsion droplets and can be reduced by increasing the stirring, the surfactant concentration or by decreasing the polymer content.

1.2.2.2. In-situ polymerization

The in-situ polymerization of monomers in nano-emulsion, also called miniemulsion polymerization is a commonly used method for the formation of polymeric nanoparticles (Ugelstadt, 1973; Lovell, 1997; Landfester, 2000b, 2001, 2006, 2009; Crespy, 2010; Staff, 2012).

The principle of miniemulsion polymerization consists in forming a nano-emulsion containing a monomer as dispersed phase, a surfactant, and a hydrophobe (Ugelstadt, 1973; Landfester, 1999) and polymerizing the monomer inside the nano-emulsion droplets. The mechanism of miniemulsion polymerization has been widely investigated and is based on droplet nucleation, which occurs when the initiator enter into the monomer droplet. Particle grows directly in the monomer droplets leading to particles which ideally keep their size (Landfester, 2009).

Nano-emulsion polymerization was widely described for radical initiated polymerization (Ugelstadt, 1973) for polymers such as polystyrene or polyacrylate (Schork, 2005). Recently, new types of reactions were reported in nano-emulsions such as polyaddition to obtain epoxy (Landfester, 2000a) and polyurethane (Tiarks, 2001), anionic polymerization for the formation of phenyl glycidyl ether using didodecyldimethyl ammonium hydroxide as inisurf (initiator + surfactant) (Maitre, 2000), cationic polymerization for the formation of p-methoxystyrene (Cauvin, 2002) or metal-catalyzed polymerization of ethylene in aqueous nano-emulsion (Soula, 2001). It is worth noting that the formation of polyester was rarely described. Indeed, the synthesis of polyesters generally requires relatively high temperature to remove the water and displace the equilibrium; therefore, the formation of polyester is then compromised in the presence of large amount of water such as in O/W nano-emulsions. However, the locally high

hydrophobicity of the nano-emulsion droplets allows water to be expelled from the reaction locus, thus polyester synthesis in nano-emulsions can be expected.

As previously mentioned in this section and among the large variety of polyester, Pentadecanolide polymer presents a large interest for its high crystallinity, biodegradability and biocompatibility. Polypentadecanolide can be easily synthesized in bulk, water or organic solvent using mild conditions (See section 1.2.1.1), however its synthesis in nano-emulsion has been rarely described. The most significant results on Ring-Opening Polymerization of Pentadecanolide in nano-emulsions are reviewed below.

Barrère *et al.* described the **acid-catalyzed ring-opening polymerization of PDL** in nano-emulsion at 90ºC. They have shown the formation of PPDL with a relatively high yield and low molecular weight (1150g/mol) (Barrère, 2003).

The ROP of pentadecanolide was also extensively studied using lipase as catalyst. Knowing that an important feature of lipases is their ability to adsorb at interfaces (Reis, 2008) of confined media such as emulsions, nano-emulsions or micro-emulsions, Taden *et al.* reported the **enzymatic ring-opening polymerization of PDL** at 45ºC using very low enzyme concentrations (0.125%). Complete conversion was obtained in at least 24h and PPDL nanoparticles with extremely high molecular weight (200 000 g/mol) and size around 100 nm were reported. The authors proposed the following eROP mechanism of lactones in nano-emulsion (Taden, 2003) considering that the mechanism of eROP described in section 1.2.1.3 takes place at the interface of the nano-emulsion. As they also noted the presence of a bimodal molecular weight distribution, they proposed two possible growth reactions (Figure 1.9). The first approach suggests that lactone units are inserted in the enzyme-acyl monomer (EAM) until it detaches from the lipase by reaction with a water molecule (reaction 3). The second approach suggests that the enzyme-acyl monomer can be directly react directly with water (reaction 3) and the free hydroxyl group from either opened monomers or detached polymers attack another enzyme-activated monomer (reaction 4). The number of end groups is given by the equilibrium reaction with water (reaction 3), whereas the high molecular weight is explained by the relative reaction rates of each reaction pathway.

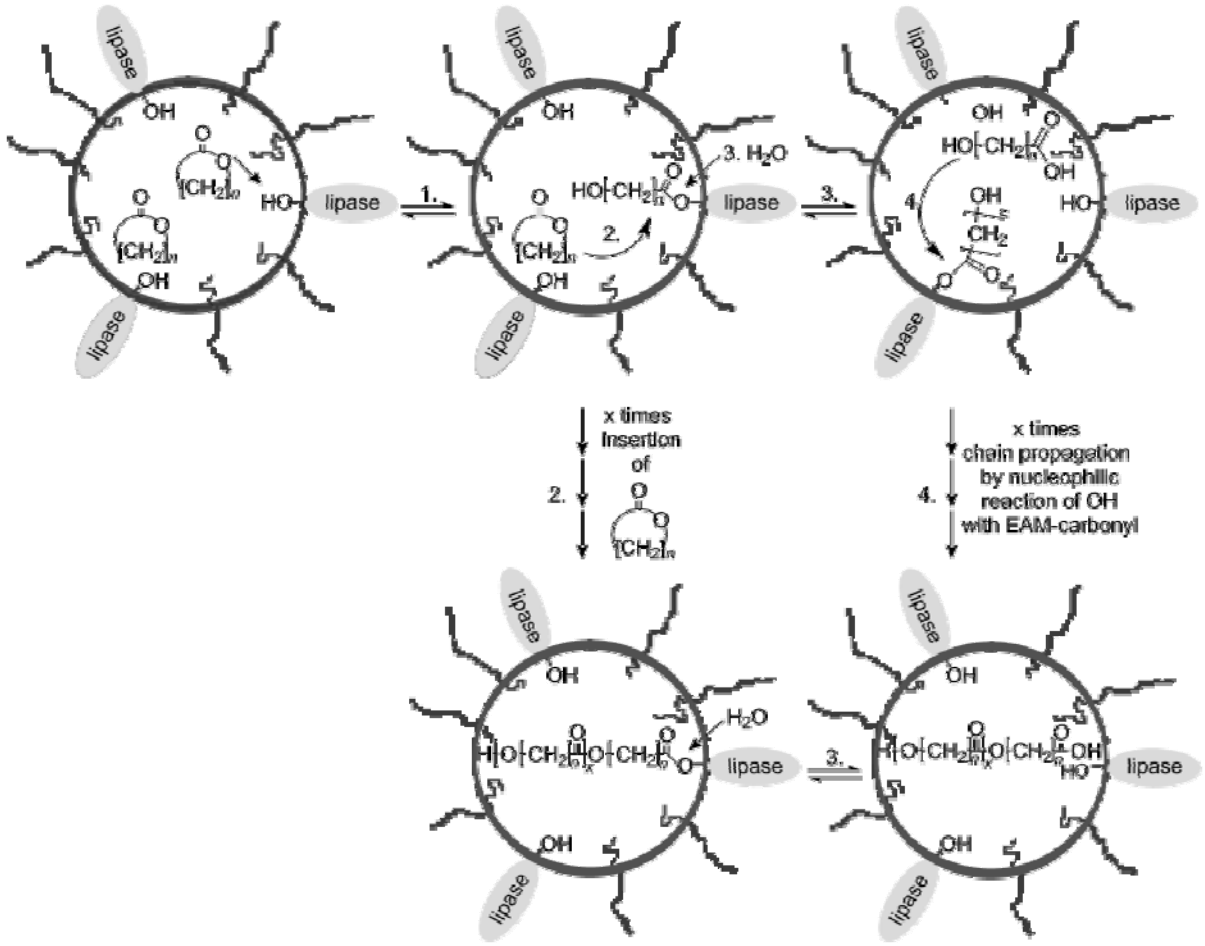

Figure 1.9 : Proposed mechanism of lipase-catalyzed ring opening polymerization in nano-emulsions (Taden, 2003) EAM = Enzyme-Acyl Monomer.

Recently, the previously described enzymatic ROP was carried out in pentadecanolide and hexadecanolide nano-emulsions stabilized by Brij®58 as surfactant (instead of Lutensol®AT50). Two types of lipase were tested (Lipase Amano AK and PS) and high conversions were reached in about 5h, independently on the amount of hydrophobe, surfactant or reaction time (Målberg, 2010). It is worth mentioning that the molecular weight obtained for polyHDL was low (1500g/mol) compared to the results previously obtained by Taden *et al.* (M_w > 200 000g/mol) but this difference was not discussed by the authors.

1.2.3. Applications

Polyester nanoparticles are interesting materials when looking at biodegradability and biocompatibility for their possible applications in medical fields such as drug delivery and tissue engineering since they have not only carbon-carbon but also hydrolytically degradable bonds in their backbone. Polyester nanoparticles can carry a wide range of surface functionalities and can encapsulate a large variety of materials such as drugs, dyes or inorganic materials, generally for pharmaceutical applications: (Pinto Reis, 2006 a-b; Guterres, 2007; Teixera, 2012)

Both hydrophilic and hydrophobic drugs have been encapsulated in polyester nanoparticles generally made of PLGA (Mundargi, 2008; Vrignaud, 2011). Among the large variety of compounds that have been incorporated in PLGA nanoparticles, proteins and peptides (Pinto-Reis, 2006a-b), Insulin or Ketoprofen (Barichello, 1999) can be cited as examples.

Polyester nanoparticles have also been used for the encapsulation of fluorescent dyes. During the preparation of the nano-emulsions, the fluorescent dye is incorporated in the dispersed phase. After precipitation of the preformed polymer (generally by solvent evaporation), fluorescent nanoparticles of PLGA, PLA or PCL have been obtained. The uptake tests of those nanoparticles on different cell lines have shown a faster uptake compared to that of polystyrene nanoparticles (Musyanovych, 2008).

The encapsulation of magnetic nanoparticles has attracted much interest for the so-called theranostic approach. The encapsulation of magnetic nanoparticles has been achieved successfully into PLGA (Astete, 2007; Okassa, 2007; Lee, 2004). First, the magnetic nanoparticles were coated with oleic acid or a mixture of oleic acid and oleyl amine. After incorporation into the dispersed phase of the nano-emulsion (PLGA + Ethyl acetate), the solvent is removed by solvent-evaporation leading to the formation of magnetic-polymeric nanocomposites. Since the magnetic nanoparticles are very small, each polymer particle was able to encapsulate many inorganic particles.

Apart from their applications as drug carriers, nanoparticles can be used to stabilize emulsions. This application will be described in details in section 1.3.

1.3. EMULSIONS STABILIZED BY NANOPARTICLES

Emulsions stabilized by nanoparticles were first mentioned by Ramsden (Ramsden, 1903) and first published by Pickering in 1907 (Pickering, 1907). So far, many types of solid particles (hydrophilic or hydrophobic silica, clay, barium sulfate, calcium carbonate, polystyrene, etc.) (Aveyard, 2003; Binks, 2000a and 2001; Simovic, 2003) have been used to stabilize emulsions; however the use of biodegradable polyester nanoparticles have been rarely described (Laredj-bourezg, 2012). In the following section, a general overview of solid stabilized emulsion will be presented.

1.3.1. Nanoparticles requirements

To stabilize an emulsion, the nanoparticles have to be partially wetted by the phases of the emulsion. Due to this characteristic, the nanoparticles attach at the interface O/W. Finkle *et al.* in 1923 demonstrated that nanoparticles had to be preferentially wetted by the continuous phase (Finkle, 1923) to form stable emulsions. Then, Schulman *et al.* described for the first time the effect of the wettability of the nanoparticles on the type of emulsion (Schulman, 1954). The wettability of the nanoparticles by a liquid is mainly defined by the contact angle θ between the aqueous or oil phase and the particles. The value of the contact angle determines the position of the nanoparticles at the interface (Figure 1.10).

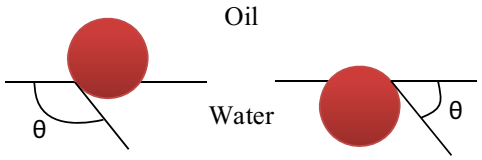

Figure 1.10 : Position of a small spherical particle at a planar fluid–water interface for a contact angle (measured through the aqueous phase) greater than 90° (left), and less than 90° (right) (Binks, 2002a-c)

The particles having a contact angle lower than 90º are considered as hydrophilic while those having a contact angle higher than 90º are said hydrophobic. It is worth noting that the contact angle is well defined for spherical nanoparticles but this notion is arbitrary when the particle shape is irregular. The wettability of the particles influences the quantity of energy needed to remove them from the interface (desorption). Assuming that the particles are spherical of submicron size and that the effect of the mass is negligible, the energy ΔE required to desorb the nanoparticles of radius r from the O/W interface is given by (Binks, 2002b):

$$\Delta E = \pi r^2 \gamma (1 - cos\,\theta)^2 \quad (1.9)$$

Where γ is the interfacial tension between oil and water, and θ is the contact angle between the nanoparticles and water. The desorption energy is low when the contact angle is high (θ> 160º) or low (θ < 20º) and the energy reaches a maximum for contact angle close to 90º (Binks, 2002b-c). In this case, the particles are strongly adsorbed at the interface (almost irreversibly) which might favor the stabilization of emulsions.

Binks *et al.* demonstrated experimentally how the wettability of the particles enables to predict the interface curvature, and thus the type of emulsions (Binks, 2000a). They stated that particles having a contact angle with water higher than 90° are hydrophobic and stabilize W/O emulsions while particles having a contact angle lower than 90° are hydrophilic and stabilize O/W emulsions (Figure 1.11).

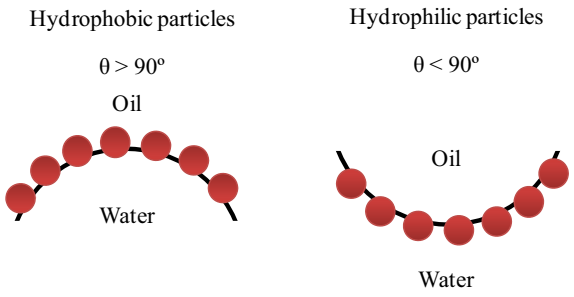

Figure 1.11 : Emulsion type as a function of the contact angle.

An optimal stabilization is expected at contact angle close to 90º while no stabilization was reported at extreme contact angle (close to 0 and 180°).

The value of the contact angle for particles can be assimilated to the HLB value for a surfactant as it enables to predict the type of emulsion. It is worth noting that nanoparticles do no stabilize emulsions by lowering the interfacial tension like surfactant do but by creating a mechanical and steric barrier that prevents destabilization.

1.3.2. Stabilization mechanisms and factor influencing the stability of Pickering emulsions

Different mechanisms were proposed to stabilize the O/W interface. Those mechanisms are represented in Figure 1.12. Solid particles can organize themselves as:

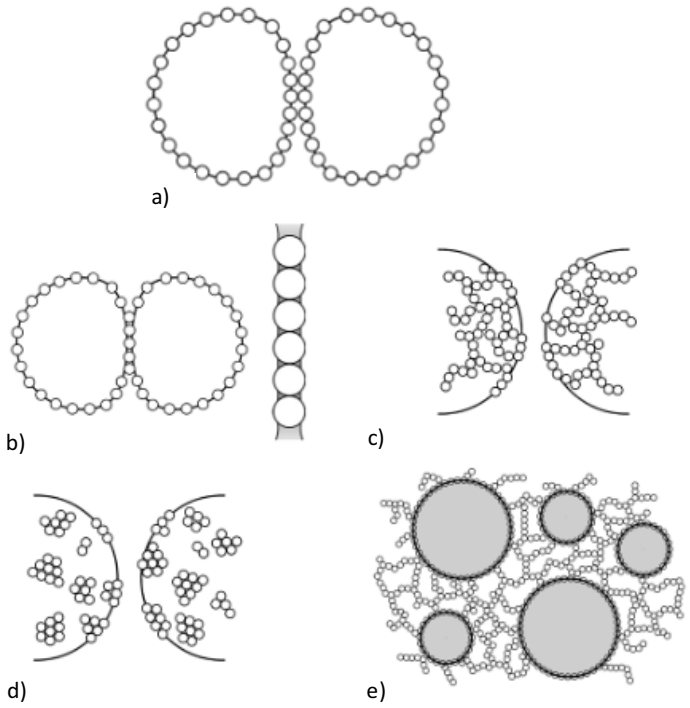

Figure 1.12 : Possible configurations of particles in solid-stabilized emulsions (Binks, 2006).

a) A mono- or multi- layer covering totally the interface. When two drops are in contact, two particle layers prevent coalescence. It is named bilayer stabilization (Figure 1.12.a).

b) A single layer between two drops. It is called stabilization by bridging of a single layer (Horozov, 2006) (Figure 1.12.b).

c) A 2D network of aggregates at the interface: partial covering (Yan, 1993; Vignati, 2003) (Figure 1.12.c).

d) Domains that sparsely covered the drop (Tarimala, 2004; Hassander, 1989, Binks, 1999) (Figure 1.12.d).

e) A 3D network in the continuous phase (Thieme, 1999) that increases the stability of emulsions by increasing the viscosity and preventing the contact between the drops (Binks, 1999) (Figure 1.12.e).

Several key factors are involved in the stabilization of solid stabilized emulsions (Leal-calderon, 2008) including the characteristics of the particles (wettability, location, concentration, size, and

shape) but also the oil type and of course the presence of additives (electrolytes, surfactant) in emulsion systems. In this section, a brief overview of the effects of those parameters is described.

- **Particle wettability**

Various techniques have been described in order to modify the wettability of the particle. Tambe *et al*, 1994, reported that the presence of stearic acid in the system modifies the wetting properties of the particles and enhance the formation of O/W and W/O emulsions depending on its concentration (Tambe, 1994). Since the beginning of the 2000, many systematic studies on the effect of the particle wettability to stabilize emulsions have been published. For instance, Binks *et al.* in 2000 chemically modified silica particles by changing the silanol content by hydrophobization of the silica. This chemical change affected the wettability of the particles and induced a phase inversion of the emulsion, transitional inversion (Binks, 2000a). Another way to produce the transitional inversion of the emulsion consists in using a mixture of hydrophilic and hydrophobic particles (Binks, 2000b).

- **Particle location**

Although it was demonstrated that the particle wettability generally determines the type of emulsions, it was also proved that to stabilize an emulsion, the particle have to be firstly dispersed in the continuous phase (Finkle, 1923). In fact, the change of the emulsion type was related to the contact angle hysteresis that occurs when the particles are placed in a liquid and migrate across an interface. This behavior was corroborated by Yan and Masliyah that managed to stabilize O/W emulsions by dispersing, prior to emulsification, hydrophobic particles in the aqueous phase (Yan, 1993).

- **Particle concentration**

The concentration of particles has also been reported as a major factor to stabilize emulsions. In fact, it was demonstrated that by increasing the particle concentration, the size of the emulsion droplet decreases, thus increasing the emulsion stability, up to a limit droplet size value is reached. Then, the excess of particle is present in the continuous phase (Tambe, 1994; Frelichowka, 2010). It was demonstrated that a high concentration of particle does not necessarily lead to a dense coverage. Stable solid stabilized emulsions have been observed without a dense coverage but with the presence of aggregates at the interface or a bi- or tri- dimensional structure

(Figure 1.12 c, d and e) which was responsible of the emulsions stability (Tarimala, 2004; Yan, 1993; Thieme, 1999).

- **Particle size and shape**

The size of the particles is also an important parameter as it determines their ability to stay in suspension and their mechanism of adsorption at the interface. Experimentally, it was demonstrated that the stability of emulsions increases with a decrease of the particle size to a critical particle size (Tambe, 1994, Binks 2001). Below this critical size, the Brownian movement is significant enough to affect the adsorption of the particles at the interface. Some studies have pointed out the effect of the polydispersity on the stability of emulsions. Tarimala and Daim demonstrated that the particle polydispersity reduces the stability of emulsions by disrupting the surface coverage of oil droplets (Tarimala, 2004). The shape of the particle is another factor that influences the stability of emulsions. In order to simplify analysis and calculations, particles are generally considered as spherical although it is rarely the case in practice. Vignati *et al.* showed that the size and roughness of the particles have a great influence on the stability of the emulsion as the particle roughness affects the contact angle and thus the emulsion stability (Vignati, 2003).

- **Oil phase**

The type of oil influences the interfacial tension, the contact angle with the solid particles, the chemical interaction between the surface of the particles and the liquid and the adsorption energy of the particles at the interface (Aveyard, 2003; Binks, 2000c). The effect of the type of oil has been widely studied with modified silica particles (hydrophobe particles) and it was observed that the particles stabilize preferentially O/W emulsions with non polar oil and W/O with polar oil.

- **O/W ratio**

Another factor, the O/W ratio shows to affect the type of emulsion. It was shown by Binks *et al.* that by increasing the O/W ratio, a catastrophic phase inversion was observed from O/W to W/O type with hydrophilic particles or from W/O to O/W with hydrophobic particles (Binks, 2000c-d). It was also reported that the emulsions are most stable at conditions near the inversion unlike surfactant-stabilized emulsions in the same conditions.

- **Electrolytes and pH**

As most of the particles contain charged group in aqueous solution, the addition of electrolytes is a key factor to reduce the surface potential and consequently promote flocculation (in agreement with the DLVO theory). It was reported that slightly flocculated particles were necessary to stabilize emulsions (Hasssander, 1989). In fact, non-flocculated particles shows higher mobility at the interface than flocculated particles (Tambe, 1994), thus inducing a lower stability of the emulsion. On the contrary, completely flocculated particle do not allow the stabilization of emulsions. Binks *et al.* in 1999 demonstrated that the flocculation of hydrophilic silica particles influence the creaming and coalescence of the emulsions (Binks, 1999). The structure of the particles at the interface was studied as a function of the electrolyte concentration as well as by changing the pH on polydimethylsiloxane particles (Simovic, 2003, 2004; Prestidge, 2004 and 2006). It was shown that an optimum of stability can be obtained at an optimal concentration of electrolytes which depends of course on the type of particles (Ashby, 2000). Binks *et al.* also showed that the wettability of silica particles can be varied by changing the pH of the aqueous solution. At high pH, the silanol groups are dissociated, thus increasing the wettability of the particles by water and enhancing the formation of O/W emulsions (Binks, 2000c).

- **Surfactants**

The stabilization of emulsions has also been reported using a combination of surfactant and solid particles. Due to the adsorption properties of surfactants, the latter can adsorb at the particle interface to modify their wettability but they can also adsorb more rapidly at the O/W interface and remove the particle (Vashisth, 2010). Systematic studies of the behavior and properties of emulsions stabilized by a combination of surfactants and nanoparticles have generated considerable research interest during the last five years (Binks, 2007a-c; Leal-Calderón, 2008).

1.3.3. Applications

In this section, some applications of the emulsions stabilized by nanoparticles will be described. In the **petroleum industry**, undesirable emulsion of water-in-petroleum, stabilized by fine particles (argile,wax, asphaltenes…) are one of the most important issues. For a better oil extraction, the destabilization of these emulsions is required and therefore a better understanding of their stabilization mechanism is necessary (Yan, 1999). It was reported that the destabilization of those emulsion requires the use of large quantities of surfactants to displace the particles from the interface.

In the **pharmaceutical industry**, Pickering emulsions are generally cited as carriers for the controlled release of actives. Nevertheless, in the literature there are few articles dealing with solid-stabilized emulsion as carrier for the release of actives. Simovic *et al.* have studied the release of a model hydrophobic molecule from the drop of an emulsion stabilized by silica particles. They demonstrated that the release kinetic can be controlled by controlling the density of particles at the interface. The lower the density of the particles, the higher the velocity of release is (Simovic, 2004, 2007). Recently, the permeation of testosterone through a membrane was studied from solid-stabilized emulsions (Binks, 2012).

In the **food and cosmetic industry,** Pickering emulsions have been used to eliminate the surfactants from the formulations (Dickinson, 2010). For example, emulsions stabilized by titanium dioxide particles have been developed to obtain solar protection without addition of surfactant (Gers-Barlag, 2004). Although Pickering emulsions have been claimed to improve the properties of cosmetic emulsions, only few reports described the effect of the Pickering emulsion on the skin. Frelichowska *et al.* in 2009 have reported the skin absorption of a lipophilic drug, all-trans retinol, in emulsions stabilized by silica nanoparticles on the skin and significant differences were observed compared to surfactant-stabilized emulsion of the same droplet size (Frelichowska, 2009).

In the **perfumery industry,** it has been demonstrated that Pickering emulsions reduces the evaporation of the emulsified oil phase which is an advantageous factor to reduce perfume or aroma evaporation (Binks, 2010a-b).

Solid stabilized emulsions have also been used as template for **the formation of new porous materials** by evaporating both emulsion phases. Such materials have been described with silica particles (Aveyard, 2003) and possess some characteristic features such as an important rigidity,

important absorption ability, high resistance to temperature and high specific surface. Porous materials of different pore size and structure can be tuned by adjusting the composition of the initial emulsion (Aranberri, 2009) and they can be used as support for catalysts, gas sensor or humidity sensor (Binks, 2002d; Arditty, 2003).

Within the aim to better control the liberation of an encapsulated compound, the formation of a rigid shell around the drop has been suggested. Pickering emulsions have been considered as a favorable **template for the formation of composites**: The inner drop can be used as reaction media for polymerization and the particles at the interface represent the shell of the composite. Various types of composites have been prepared: for example composites made of an inner core of polyaniline and a shell of iron oxide (Xiao, 2007) or silica (He, 2007) particles.

A particular application uses Pickering emulsions as template for **the formation of colloidosomes** (Dinsmore, 2002). Colloidosomes, firstly described by Velev *et al.* in 1996, are hollow core-shell microcapsules whose external shell is formed by colloidal particles (Velev, 1996). Colloidosomes are formed by locking the particles at the interface of a Pickering emulsions. One of the methods to lock the particles at the interface consists in the sintering of the particle together by heating them above the glass transition. Weitz and coworkers developed robust colloidosomes made of polystyrene particles by annealing at temperature around 105ºC (Kim, 2007). Later other types of particles, with lower glass-transition, such as poly(styrene-co-n-butylacrylate) have been used to form colloidosomes by sintering at temperature as low as 45ºC (Laib, 2008; Yow, 2009; Salari, 2010; Yuan, 2011). An alternative to form colloidosomes is to use an aqueous gelling agent to gellify the aqueous phase of a W/O emulsion (Cayre, 2004). Few papers described colloidosomes stabilized by covalently cross-linking the particles. For instance, Poly(divinylbenzene-alt-maleic anhydride) microspheres have been cross-linked from the aqueous continuous phase by addition of polyamine (Croll, 2003). Recently, the formation colloidosomes has been reported by covalently cross-linking the nanoparticles from the inner phase (Figure 1.13).

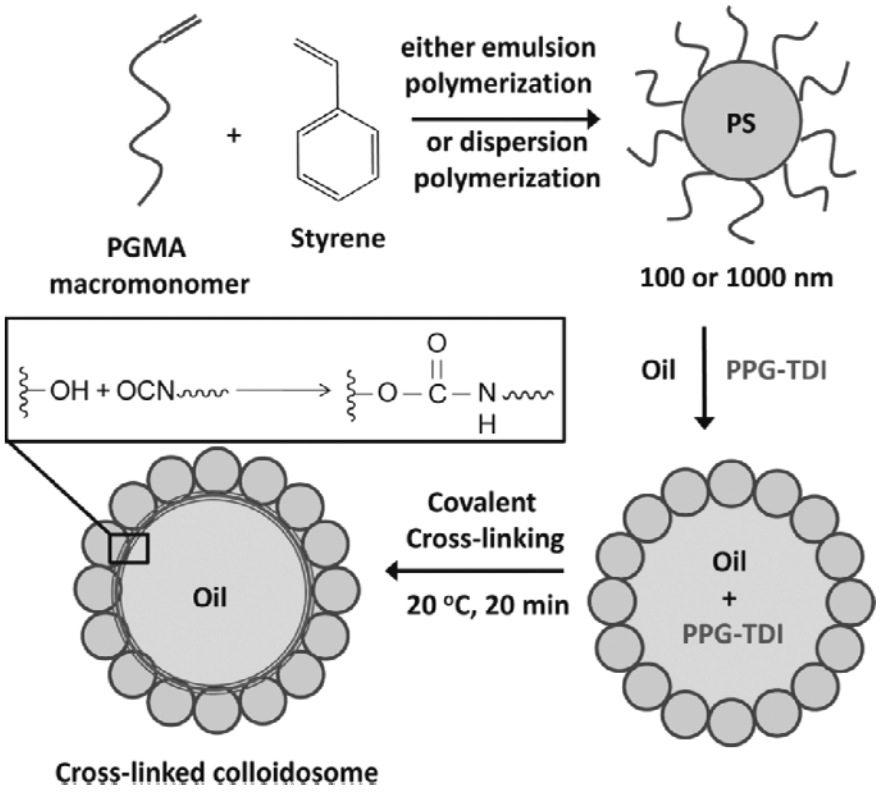

Figure 1.13 : Covalently cross-linked colloidosomes prepared by selfassembly of Polyglycidylmethacrylate50-Polystyrene (PGMA50-PS) latex particles around oil droplets in the presence of the oil-soluble PPG-TDI cross-linker (Thomson, 2010).

Colloidosomes were produced by covalent cross-linking of the hydroxyl group of sterically stabilized polystyrene nanoparticles and an oil soluble polymeric isocyanate in the oil phase of the emulsion.

OBJECTIVES

2. OBJECTIVES

The presence of volatile fragrant molecules is generally associated with a feeling of pleasantness or cleanness in consumer products. Because of their high volatilities, the perception of fragrances is quite limited over time. Therefore, various delivery systems have been developed by the industry to control and extend the release of volatile ingredients by diffusion and also to protect active molecules against degradation. A promising encapsulation technique which has seen a gain of academic interest is the formation of capsules with tunable permeability, so-called colloidosomes (Velev, 1996; Dinsmore, 2002). These are generally formed by locking the nanoparticles at the interface of a Pickering emulsion either by thermal annealing (Dinsmore, 2002; Laïb, 2008), polyelectrolyte adsorption, gel trapping (Cayre, 2004) or covalent cross-linking. However, there are very few articles concerning colloidosomes stabilized by covalent cross-linking and their efficiency shows some limitations (Thomson, 2010). In addition, although Pickering emulsions have been known for over a century, the range of nanoparticles used to stabilize emulsions has been limited to silica, clays, polystyrene, polyacrylate latexes or metallic nanoparticles (Aveyard, 2003; Binks, 2006). Within the aim to apply colloidosomes or Pickering emulsions as carriers for cosmetic or pharmaceutical application, the use of biodegradable and biocompatible polymeric nanoparticles such as polyester nanoparticles is of major interest.

Polyester nanoparticles are solid colloidal particles with sizes generally between 20 and 500 nm that can be prepared in colloidal systems either from a preformed polymer (Anton, 2008; Soppimath, 2001) or by polymerization of monomers (Schork, 2005; Asua, 2002; Antonietti, 2002). In the former method, polymeric nanoparticles can be obtained by solvent evaporation, spontaneous emulsification/ solvent diffusion or by salting out methods. These processes have been mainly used with polymers such as polylactic acid, polyglycolic acid and their copolymers (Fessy, 1989) and polycaprolactone (Cho, 2006). The main disadvantage of these processes is the use of toxic organic solvents (often chlorinated solvents) to dissolve the preformed polymer. On the other hand, a large variety of strategies have been developed to generate polymeric nanoparticles by polymerization of monomers in colloidal systems. These include microemulsion (Stoffer, 1980; Candau, 1984) and emulsion polymerization (Lovell, 1997) as well as polymerization in nano-emulsion (miniemulsion polymerization) (Ugelstadt, 1973; Asua, 2002, Antonietti, 2002). Compared to conventional emulsion polymerization where emulsion droplets

behave as monomer reservoirs, in nano-emulsion polymerization monomer droplets can be considered as nano-reactors; thus acting as template for the nanoparticle formation.

Nano-emulsions are emulsions with extremely small droplet size, typically in the range of 20-500 nm. Due to their small droplet size, nano-emulsions are transparent and present a better stability against gravitational separation than conventional emulsions. Nano-emulsions have been usually prepared by high-energy methods in which an external energy input is applied, by means of high pressure homogenization or ultrasonication, to achieve emulsification. However, nano-emulsions can also be prepared by low-energy methods taking advantage of the internal energy of the system components which is released during the emulsification process (McClemens, 2011; Solans, 2012). The most common low-energy methods are based on phase inversion, triggered by changing temperature at constant composition (Phase Inversion Temperature method, PIT method) or by changing composition at constant temperature (Phase Inversion Composition method, PIC method). Compared to high-energy methods where the droplet size of the nano-emulsion decreases by increasing the energy given to the system, emulsification by low-energy methods generally produces smaller and more uniform droplets when the physic-chemical properties of the system are optimized.

Apart from their use as drug delivery systems, nano-emulsions have been used as templates for nanoparticle formation. Despite the large number of articles describing the polymerization of monomers in nano-emulsions, only few articles refer to this process in nano-emulsions obtained by low-energy methods (Spernath, 2007). This can be explained by the fact that the emulsification by low-energy methods of rather polar oils, such as certain monomers, requires a finer selection of the system components. Therefore, studies on the preparation of polymeric nanoparticles from nano-emulsion droplets obtained by low-energy methods are of great interest.

Concerning in-situ polymerization of monomers in nano-emulsions, radical reactions have been mainly described since its first report in 1973 for polymers such as polystyrene or polyacrylate and their mechanism have been compared to emulsion polymerization (Ugelstadt, 1973; Schork, 2005). Recently, many new types of reactions such as anionic, cationic, or metal catalyzed polyaddition, polycondensation or ring-opening polymerization have been reported (Maitre, 2000; Cauvin, 2002; Soula, 2001; Barrère, 2003; Ruppert, 2010; Siebert, 2012). However, these reactions generally require the use of harsh conditions (low pH, toxic initiator, high temperature) to obtain polymers with acceptable yield and molecular weight. Only few articles have mentioned the use of biological compounds as catalysts for esterification (Aschenbrenner, 2009) and ring-

opening polymerization (Taden, 2003). In this context, a research effort is needed on the polymerization in nano-emulsion droplets under mild conditions.

The global objective of this research work was **to study the polymerization in mild conditions of monomer-in-water nano-emulsions obtained by low-energy methods, the characterization of the obtained nanoparticles and their applications for the delivery of volatile compounds.**

The main objective implies the following partial objectives:

1. Design of Oil-in-Water (O/W) nano-emulsions by low-energy methods using low toxicity monomers as oil components.
2. Synthesis of polyester nanoparticles, by polymerization in the nano-emulsion droplets, and their characterization.
3. Study of functional properties of the polyester nanoparticles for the delivery of volatile compounds.

The following working plan was established to achieve these objectives:

- Selection of the nano-emulsion components (monomers and surfactants) as well as catalysts.

- Formation of O/W nano-emulsions by low-energy methods

    - Study of the phase behavior of water/surfactant/monomer systems by means of phase diagram determinations.
    - Formation of O/W nano-emulsions by the PIT or PIC emulsification method.
    - Determination of the regions of nano-emulsion formation in the corresponding water/ surfactant/ monomer systems.
    - Effect of the preparation method (PIT or PIC method) on the properties of O/W nano-emulsions.

- Characterization of nano-emulsions, namely droplet size, by means of Dynamic Light Scattering (DLS) and Light BackScattering (LBS) measurements.

- Study of O/W nano-emulsions stability.

  - Assessments of the changes of droplet size with time.
  - Effect of the addition of a co-oil on the stabilization of O/W nano-emulsions.
  - Determination of the destabilization processes by data analysis of the changes of droplet size with time.

- Synthesis of polymeric nanoparticles in nano-emulsions by polymerization in the dispersed phase.
  - Influence of the reaction parameters on the polymerization rate by means of Nuclear Magnetic Resonance (NMR) spectroscopy.
  - Functionalization of polyester nanoparticles by copolymerization of two monomers in nano-emulsions.
  - Characterization of the obtained polymer by determination of the melting point by Differential Scanning Calorimetry (DSC), molecular weight by Gel Permeation Chromatography (GPC) and crystallinity by Small and Wide Angle X-ray Scattering (SAXS/WAXS).

- Characterization of size distribution and morphology of polyester nanoparticles by Transmission Electron Microscopy (TEM).

- Stability of aqueous polyester dispersions in water by means of Dynamic Light Scattering (DLS) and zeta potential measurements and influence of electrolytes.

- Study of functional properties of the polyester nanoparticles

  - Polyester nanoparticles for the controlled release of actives
  - Polyester nanoparticles as stabilizers for perfume-in-water emulsions. Study of the influence of nanoparticle concentration, O/W ratio and the type of nanoparticle on the formation and stability of Pickering emulsions.
  - Formation of microcapsules by cross-linking the nanoparticles at the interface of the O/W Pickering emulsions. Study of the cross-linking reaction over time and influence of the cross-linker concentration.
  - Study of perfume release from the cross-linked microcapsules.

EXPERIMENTAL

3. EXPERIMENTAL

The surfactant, oils and aqueous phases used in this work have been abbreviated as S, O and W respectively. Percentages and ratios are always expressed in weight unless otherwise stated.

3.1. MATERIALS

3.1.1. Oil Components

3.1.1.1. Macrocyclic lactones

Macrocyclic lactones, Exaltolide®, hydroxy-Exaltolide® and Habanolide®, supplied by Firmenich SA, were used as oil phases of nano-emulsions. The syntheses of these lactones have been described in the Patent EP 0512348A1 (Hopp, 1992).

Exaltolide®, Pentadecanolide (PDL) or Oxacyclohexadecan-2-one, ($C_{15}H_{28}O_2$) (Figure 3.1) has a molar mass of 240 g/mol and a melting point of 38ºC. This lactone is a white, slightly hygroscopic and crystalline solid at 25ºC. It is practically insoluble in water, freely soluble in alcohol and acetone. Its octanol/water partition coefficient, log P, is 6.1 and its vapour pressure is 0.09 Pa at 20ºC. Exaltolide® is one of the finest synthetic musk notes used in many applications like perfumery, cosmetics, detergency, etc.

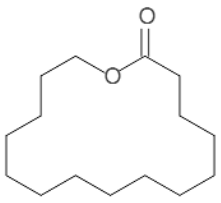

Figure 3.1 : Molecular structure of Exaltolide®.

Hydroxy-Exaltolide®, OH-Exaltolide®, 12-hydroxyl-Oxacyclohexadecan-2-one ($C_{15}H_{29}O_3$) is a hydroxyl functionalized Exaltolide® (Figure 3.2). It has a molar mass of 256 g/mol and a melting point of 59.5 ºC. Hydroxy-Exaltolide® is a white, slightly hygroscopic and crystalline solid at 25ºC. It is slightly soluble in water, freely soluble in alcohol and acetone.

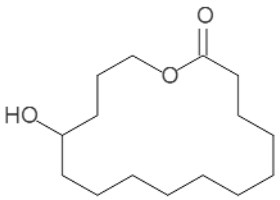

Figure 3.2 : Molecular structure of Hydroxy-Exaltolide®.

Habanolide®, Oxacyclohexadec-12-en-2-one, ($C_{15}H_{26}O_{2)}$ is a macrocyclic unsaturated lactone (Figure 3.3). This lactone has a molar mass of 238 g/mol, a density of 0.964 g/mL and a melting point lower than -20ºC. Habanolide®is a colourless to pale yellow liquid at 25ºC. It is practically insoluble in water (0.964 mg/L at 25ºC), freely soluble in alcohol and acetone. Its octanol/water partition coefficient, log P, is higher than 6.2 and its vapour pressure is lower than 0.1 Pa at 20ºC. Habanolide®is also one of the synthetic musk notes used like Exaltolide®in applications like perfumery, cosmetics, detergency, etc.

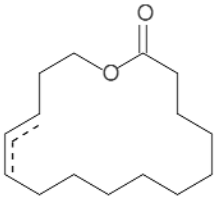

Figure 3.3 : Molecular structure of Habanolide®.

3.1.1.2. Aliphatic hydrocarbons

n-hexadecane is an alkane with the chemical formula $C_{16}H_{34}$. It has a molar mass of 226.44 g/mol. It is a colourless liquid with a melting point of 18ºC and a refractive index of 1.434. It is insoluble in water. Hexadecane was supplied by Sigma Aldrich with a purity ≥ 99%.

Squalane is a natural hydrocarbon with a formula $C_{30}H_{62}$ (Figure 3.4) with a molar mass of 422.81 g/mol. It is a colorless, transparent with a density of 810 mg. mL^{-1}, a melting point of -38 °C, a refractive index of 1.452. It is insoluble in water and its chemically inert nature makes it particularly useful in cosmetics application as emollient or moisturizer. Squalane was supplied by Sigma Aldrich with a purity of 99%.

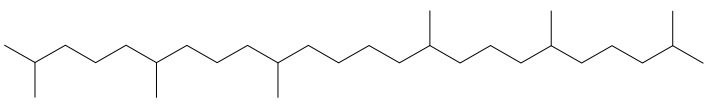

Figure 3.4 : Molecular structure of squalane.

3.1.1.3. Other oil components

Single oil compounds were used as dispersed phase of Pickering emulsions and were selected for their different polar properties.

Manzanate® (ethyl 2-methylpentanoate) was supplied from Givaudan International AG.

Benzyl acetate was purchased from Sigma-Aldrich

Limonene was purchased from Sigma-Aldrich.

Their main properties are summarized in Table 3.2.

A **model perfume** (**MP**), supplied by Firmenich was used for the preparation of Pickering emulsions. It is a mixture of five compounds in equivalent quantities (Composition in Table 3.1).

Table 3.1 : Composition of the model perfume (MP), commercial name, supplier and IUPAC name

Commercial name	Supplier	IUPAC name
Cyclamen Aldehyde extra®	Givaudan	(+-)-3-(4-isopropylphenyl)-2-methylpropanal
Romascone®	Firmenich	(+-)-methyl 2,2-dimethyl-6-methylene-1-cyclohexanecarboxylate
-	Givaudan Int.AG	(2Z)-2-phenyl-2-hexenenitrile
Verdox®	IFF inc	(+-)-2-ter-butyl-1-cyclohexylacetate
Vertenex®	Givaudan Int.AG	Trans and Cis-4-(1,1-dimethylethyl)-1-cyclohexylacetate

Some applications of the nanoparticles in the flavor and fragrance industry were investigated. The affinity of the nanoparticles with a mixture of eleven volatile fragrant molecules was studied. Its composition and characteristics are described in Table 3.2.

Table 3.2 : Composition, supplier and main characteristics of 11 volatile fragrant molecules.

Raw materials	Supplier	Log P	Vapor pressure (Pa at 20°C)	Volatility (µg/L)
Ethyl butyrate Natural	Firmenich SA	1.8	877.08	44093
(Z)-3-hexen-1-ol	Firmenich SA	1.5	283.00	4100
Manzanate®	Givaudan int.AG	2.7	344.19	351000
(Z)-3-hexenyl acetate	Firmenich SA	2.6	143.91	3400
Limonene		4.5	171.18	4293
Lymolene®	IFF Inc	3.3	60.40	1269
Triplal®	IFF Inc	2.7	50.00	935
Benzyl acetate		1.9	19.00	285
Romascone®	Firmenich SA	3.9	28.64	704
Citral (Geranial + Neral)		3.2	4.14	203
Pear ester	Robertet	4.7	2.21	37

Desmodur®N100 is a solvent-free, aliphatic polyisocyanate resin based on hexamethylene diisocyanate (Figure 3.5). The content of NCO group in the molecule is of 22 ± 0.3%. Desmodur®N100 is used primarily as the hardener component for lightfast two-pack polyurethane coatings with high resistance to chemicals and weathering, very good gloss retention and outstanding mechanical properties. Preferred co-reactants are polyacrylate or polyester polyols.

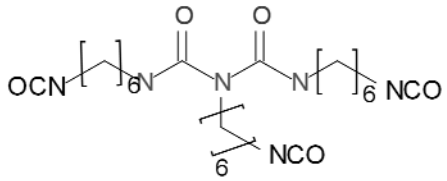

Figure 3.5 : Molecular structure of Desmodur®N100 .

3.1.2. Surfactants

Two surfactants have been mainly used: Brij®96V and Cremophor®EL. Their main characteristics are detailed below.

Brij®96V (or Brij®TM O10) is a polyoxyethylene 10 oleyl ether nonionic surfactant purchased from Sigma Aldrich. It is a yellow viscous inhomogeneous liquid at 25ºC (need to be warm up to 50ºC to be well homogenized). Its molar mass is approximately 700 g/mol; it has a density of 1.0 g/mL and a viscosity of 0.1 Pa.s at 25ºC. Its HLB number is of 12.4. Brij®96V is soluble in water, ethanol, propylene glycol and some mineral oil. The CMC value of 0.029% (v/w) is known from the provider and the surface area was found in the literature to be 0.454 nm^2 and this value was assumed to be constant at all O/S ratios (Warisnoicharoen, 2000). This surfactant is suitable for pharmaceutical applications. The topical usage level recommended is 0.5-10%.

Cremophor®EL is a nonionic surfactant provided by BASF. It is obtained from the reaction between one mole of castor oil and 35 moles of ethylene oxide (Figure 3.6). It is a yellow viscous liquid with a HLB number between 12 and 14. It has a density of 1.05-1.06 g/mL, a viscosity of 0.7-0.85 Pa.s at 25ºC and the calculated molecular weight is of 2473 g/mol. Cremophor®EL is soluble in water and various organic solvents such as ethanol, propanol, isopropanol, ethyl acetate or chloroform. This surfactant can be used in pharmaceutical (oral, intravenous or topical) or cosmetic applications.

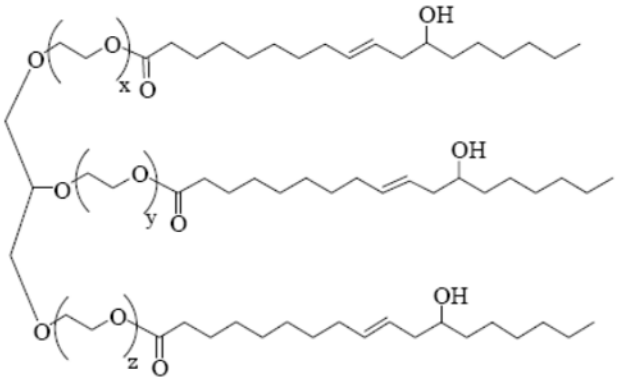

Figure 3.6 : Molecular structure of Cremophor®EL .

Other nonionic surfactants tested were Span®20, Tween®80 from Sigma Aldrich and Pluronic®types: P123, F127, L62, L 64, PE 6200, PE 6200, PE 6800, PE 10300, PE 10400, provided by BASF.

3.1.3. Aqueous components

Deionised water was used for all experiments.

Sodium hydroxide (purity ≥ 99.0% from Carlo Erba).

Sodium chloride (purity ≥ 99.0% from Carlo Erba).

3.1.4. Enzymes

Lipase PS "Amano" SD is a lipase from *Pseudomonas* origin developed by AMANO ENZYME INC. This lipase is manufactured by submerged culture of a selected strain belonging to Burkholderia cepacia. The obtained enzyme has a high lipolytic activity. This product is a slightly yellowish or white powder, soluble in water but insoluble in ethanol. This enzyme has a high activity in a wide range of pH (3.5-11.0) and temperature (25-60ºC). The maximum activity (≥ 33 000 U/g) is found at the optimum pH of 7.0 and temperature of 50ºC.

3.1.5. Other reagents

The following compounds were used for analysis:

Deuterated-chloroform (from Eurisotop) used for NMR measurements.
Tetrahydrofurane HPLC grade (from Merck) used as eluent for GPC measurements.
Phosphotungstic acid hydrate: $12WO_3$. H_3PO_4. xH_2O (from Fluka) for microscopy grade.
Uranyl acetate dehydrate: $(CH_3COO)_2$. UO^{2+}. H_2O (from Fluka) for microscopy grade.
Isooctane (2,2,4-Trimethylpentane, 99.5%, for analysis, from Acros Organics) for GC analysis.
Diethyl ether (for analysis, from Carlo Erba Reactifs SDS) for GC analysis.
1,4-dibromobenzene (from Sigma-Aldrich) as internal standard for GC analysis.

3.2. INSTRUMENTS

The instruments used for the research work have been classified by alphabetic order. A short description has been included for some techniques.

➢ Conductimeter

The conductimeter Crison model GLP-31 is equipped with a conductivity cell, model 52-92, made of a platinum electrode (cell constant =1 cm^{-1}) and a temperature sensor, model 55-31.

➢ Chromatographs

- **Gas Chromatograph (GC)**

The equipment of gas chromatography GC 7890A is composed of an auto-sampler 7683 series from Agilent Technologies and a UV detector. The column used is an apolar HP-5 of 30 cm, an inner diameter of 0.32 mm and a film thickness of 0.25 μm.

- **Gel Permeation Chromatograph (GPC)**

- A Shimadzu liquid chromatography instrument, composed of two pumps LC-10AT, an automatic system of sample injection SIL-10AD and a UV detector LC-10ATVP was used. The column used is a MZ-Gel SD plus linear filled with 5μm particles of cross-linked styrene/divinylbenzene high-performance copolymer. Measurements were analyzed with the Shimadzu Class-VP software. This equipment was used to determine molecular weights of poly(Exaltolide®) within ± 5% accuracy.

- A Viscotek GPC max VE 2001, composed of a solvent Sample Module, a vacuum online degasser, a LC pump and an autosampler was also used to determine molecular weights of poly(Exaltolide®) and poly(OH-Exaltolide®). It is combined with a Viscotek UV detector 2500, a Viscotek VE3580 RI detector and a Viscotek-270-Dual-Detector viscometer. The column used is a Macherey-Nagel VA 300/7.7 Nucleogel GPC 500-5 column. This equipment was used.

➢ Differential Scanning Calorimeter (DSC)

The DSC, model DSC 821 from Mettler Toledo, is equipped with a platinum temperature captor and measures the heat flow variation with temperature under nitrogen atmosphere. The temperature can vary from -150ºC up to 500ºC at a rate between 0.1 and 20ºC/min. The DSC 821 measures the heat differences between a sample and an inert reference.

➢ Light dispersion equipments

• Cross-corelation light scattering instrument

Cross-correlation light scattering instrument (LS Instruments, Fribourg, Switzerland) is equipped with a He-Ne laser (λ=632.8 nm) directed to the sample cell, which is placed in a thermostated bath. The beam intensity was adjusted for all the samples at 200 Kcounts/s. The scattered light was detected by a photomultiplier at an angle of 90º. After detection, the scattered light was analyzed by a correlator as indicated in Figure 3.7.

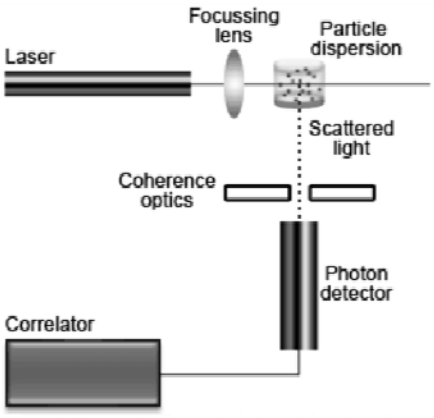

Figure 3.7 : Schematic representation of a conventional light scattering equipment (Malvern).

The Dynamic Light Scattering (DLS) technique is based on the assumption that all particles, droplets or molecules smaller than 1 micrometer present in suspension are in movement. This movement is called the Brownian movement and is due to the thermal energy induced by the interaction of each object with the solvent. When these objects are submitted to a monochromatic laser light, they scatter the light. The intensity of this scattered light is characteristic of the object but depends on several parameters like the particle size, the refractive indexes, the particles shape, etc. The fluctuation in the intensity of the scattered light is related to the Brownian motion by means of the diffusion coefficient of the particles with the solvent. The diffusion coefficient D is related to the hydrodynamic radius R_h of the object by the Stokes-Einstein equation:

$$D = \frac{k_B T}{6\pi\eta R_h} \quad 3.1$$

Where k_B is the Boltzmann's constant, T is the temperature and η is the viscosity of the continuous phase. The diffusion coefficient not only depends on the size of the particles but also on the surface structure as well as the type and concentration of ions that may be dissolved in the medium. Therefore, the particle size measured by the apparatus is the hydrodynamic radius and is generally larger than those obtained by other techniques such as microscopy image analysis

- **Light BackScattering (LBS)**

Turbiscan TM LaB is an apparatus from Formulaction made of a cell compartment that can contain a bottom flat cylindrical tube made of borosilicate in which the sample is introduced. The light source, a pulsed near infrared light emitting diode LED (λ = 880 nm) passes through the sample. The detectors consist in two synchronous optical sensors. The transmission sensor (T) receives the light transmitted through the sample at 180º from the incident beam while the backscattering sensor (BS) receives the light backscattered by the sample at 45º from the incident beam (Figure 3.8). The measurement performed allows the quantification of the physical processes involved: backscattered and transmitted light fluxes measured depend respectively on the mean path length of photon in the dispersion l and l*. These physical absolute parameters, depending on the particle diameter d and the volume fraction , give information on the real state of the dispersion.

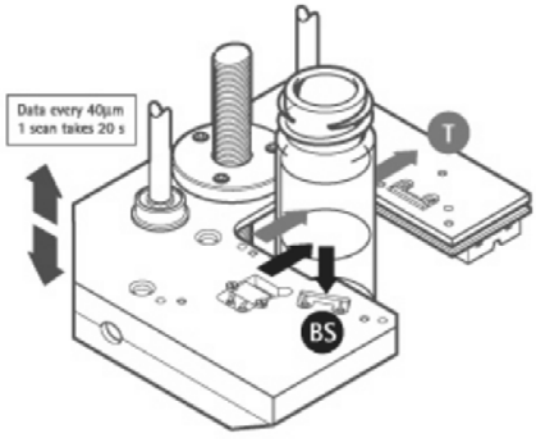

Figure 3.8 : Schematic representation of the Turbiscan equipment (Formulaction).

- **Laser diffraction analyzer**

The laser diffraction analyzer, model Mastersizer hydro 2000 from Malvern Instrument is equipped with a laser using a wavelength λ = 632.8 nm and a sample dispersion unit of approximately 200mL using an agitation which can be performed between 350 and 3500 rpm. The technique of laser diffraction enables the measure of particles size. It measures the intensity of light diffracted as a laser beam passes through a dispersed particulate sample. This data is then analyzed to calculate the size of the particles that created the scattering pattern. This instrument uses either the Mie theory or the Fraunhofer approximation for particle size calculation.

➢ Microscopes

- **Optical microscope**

The Optical microscope Reichert Polyvar 2 from Leica is equipped with four objectives, a light polarizer, a prism and a video camera (Sony CCD-Iris) connected to a PC with the software Leica IM 500 for the image capture.

- **Scanning Electron Microscope (SEM)**

The tabletop microscope TM-1000 from Hitachi Science uses a focused beam of electrons with a high kinetic energy (15 kV) to interact with the surface of a solid sample. The electrons are emitted from a heated filament of tungsten and focused by one condenser lenses to a spot. When electrons interact with the solid sample, a variety of elastic and inelastic collisions take place generating different signals. Those signals include secondary electrons, backscattered electrons (BSE), diffracted backscattered electrons (EBSD), X-ray, visible light or heat among others. TM1000 is provided with a detector of solid state backscattered electron. The distribution map of the signal intensity of those electrons generates an image with a three-dimensional appearance, which shows the morphology and topography of the sample. The magnification ranges from 20X to approximately 10 000X. For a conventional imaging by SEM, the sample must be electrically conductive. For non conductive samples (such as organic compounds), an ultrathin (thickness ca. 10nm) layer of electrically conducting material has to be deposited.

- **Transmission Electron Microscopes (TEM)**

- The transmission electron microscope JEOL 1010 from Jeol Ltd., Tokyo, Japan, operates with an accelerating voltage of 80kV. A Charge Coupled Device Megaview III (SIS) camera (Münster, Germany) was used for image capture.

- Tecnai F20 microscope (FEI) operates with a maximum accelerating voltage of 200 kV, at a temperature between −170°C and −175°C, under low-dose imaging conditions was used for cryo-TEM analysis.

The TEM technique consists of an electron beam passing through a series of lenses to form a magnified image of a sample that has been inserted in the area of the objective lens. An image is formed from the interaction of the electrons transmitted through the specimen. However, electron beams are easily scattered by air molecules. The TEM columns must be kept under high vacuum. In addition, electrons cannot be focused by glass lenses therefore electromagnetic lenses are used instead. Resolution of TEMs is far superior to that of optical microscopes due to the fact that electrons are used for the source of illumination rather than visible or ultra-violet light. Optical microscopes are limited to a resolution in the order of 100 nm whereas modern TEMs demonstrate resolutions approaching 0.1 nm. Organic compounds such as polymers do not conduct electrons, therefore negative staining have to be performed to enhance the electron density. The negative staining method consists of adding a heavy metal ion onto the sample deposited on the carbon grid. By this method, the organic compounds are not stained themselves but are surrounded by the dense stain layer of the heavy metal. Therefore, the specimen appears in negative contrast (Harris, 1999).

➢ Nuclear Magnetic Resonance (NMR) spectrometer

The spectrometer Varian VNMRS 400 MHz has a console with a Direct Digital receiver and an One NMR probe, which can be tuned automatically to any nucleus between 15N and 31P with ProTune autotuning. It also has an automated 100-sample changer (for standard 8” NMR tubes) and uses VnmrJ3.2 software. This spectrometer delivers routine, rapid heteronuclear-detect spectra like 19F, 31P, 13C, 11B, and 195Pt in automation.

A Bruker-DPX-400 spectrometer was used to obtain the ^{1}H and ^{13}C NMR spectra of copolymers; δ is expressed in parts per million (ppm) downfield from Me_4Si as internal standard.

➢ Small and wide angle X-Ray scattering instrument (SAXS/WAXS)

The diffractometer GRAZ *S3 MICRO* from Hecus X-RAY Systems GMBH is equipped with a generator Siemens model Kristalloflex K-760 and an anode Cu-K^{α} of 15.42 nm of wavelength. The system is composed of a light source Genix microfocus and a focalization system FOX 2D. It allows measuring at small angles (0.2º-8º) and wide angle (17º-28º). Measurements are analyzed with the 3DVIEW software.

A SAXS instrument consists of a monochromatic beam of X-rays brought to a sample from which some of the X-rays scatter, while most of them simply go through the sample without interacting with it. The scattered X-rays are then detected at a detector which is typically a 2-dimensional flat X-ray detector situated behind the sample perpendicular to the direction of the primary beam that initially hit the sample. The SAXS/WAXS technique gives information about the shape and size of macromolecules, characteristic distances of partially ordered materials, pore sizes, and other data.

➢ Spectrophotometers

- **Fourier Transformed Infra-red spectroscopy (FTIR)**

The Fourier Transform Infra-Red (FTIR) spectrometer Nicolet model 510 enables measurements of the transmission as a function of the wave number from 390 to 3900 cm^{-1}. Pellets of solid samples and KBr were prepared by pressing the mixture under 10 tons.

- **UV-Visible Spectrophotometer**

The spectrometer Cary 300 Bio UV-Visible from Varian Inc measures the absorbance of a sample compared to a reference in the wavelength range from 190 to 800 nm.

➢ Tensiometers

- The tensiometer Krüss model K 12 is used with a Wilhelmy plate with a length of 3.92 cm to measure the surface tension of oil phases.

- KSV Instrument model Sigma 700 is a high resolution electrobalance provided with a software for the control, the acquisition and the data treatment. It is used with a glass fiber bottom-tube for measurements of contact angle between a solid and a liquid.

➢ Thermogravimetric analysis equipment (TGA)

The thermogravimeter model TGA/SDTA 851e is used to measure the weight loss of a sample compared to a reference. The temperature can vary from -25ºC up to 800ºC at a rate between 1 and 20ºC/min. Sealed aluminum pans were used for temperature lower than 550ºC.

➢ Zetasizer

The zetasizer Nano-Z from Malvern consists of an electric field applied to a solution of molecules or a dispersion of particles, which move with a velocity related to their zeta potential. This velocity is measured using a patented laser interferometric technique called M3-PALS (Phase Analysis Light Scattering) and the electrophoretic mobility is calculated. Then the zeta potential is calculated using the Henry's equation:

$$\xi = \frac{3\mu\eta}{2\varepsilon\varepsilon_0 f(\kappa r)} \qquad 3.2$$

where μ is the electrophoretic mobility, η is the viscosity of the medium, ε and ε0 are the dielectric constants for water and vacuum respectively and f(κr) is the Henry's function that generally takes two values 1.5 or 1.0. f(κr) is fixed at 1.5, and is referred to as the Smoluchowski approximation. The Smoluchowski approximation considered that the particles are larger than about 200 nm dispersed in an aqueous solution containing more that 10^{-3}M of electrolytes. For smaller particles in low dielectric constant media, f(κr) is fixed at 1 and is referred to as the Hückel approximation. In this thesis, the Smoluchowski approximation was used for the determination of the zeta potential ξ. The Smoluchowski approximation is used for the folded capillary cell and the universal dip cell when used with aqueous samples.

3.3. METHODS

3.3.1. Phase Inversion Temperature (PIT) determination

The PIT of water/nonionic surfactant/oil mixture was determined by following the changes in conductivity with temperature. The samples were prepared in a round-bottom flask with two inlets for both electrodes. Measurements were started at 15ºC and the temperature was slowly increased up to 90ºC while conductivity values were recorded. Samples were prepared mixing the oil component and the surfactant and water or an aqueous solution of 10^{-2} M of NaCl was added to the above mixture. The addition of electrolytes at low concentrations enables a finer definition of the phase inversion temperature without any significant changes in the PIT values (Shinoda, 1969). When commercial surfactants are used, the addition of salt is not necessary as they might already contain salt residues from their synthesis.

3.3.2. Nano-emulsion preparation by low-energy methods

Phase Inversion Composition method (PIC): The nano-emulsions were prepared at a constant temperature of 25ºC by dropwise addition of water using a syringe, to the mixture of oil and surfactant (previously homogenized). The addition was performed under vortex stirring at approximately 3200 rpm.

Phase Inversion Temperature method (PIT): The nano-emulsions were obtained by quenching the sample from the corresponding Phase Inversion Temperature (PIT or a slightly higher temperature) to 25ºC. The quick decrease of temperature was performed under stirring using an ice bath.

Nano-emulsion region determination: The region of nano-emulsion formation was determined in water/nonionic surfactant/oil systems at 25ºC. Samples were prepared at various O/S ratio and water content. Bluish and transparent samples were named nano-emulsions. At high oil content, white but bluish samples were also considered as nano-emulsion.

3.3.3. Nano-emulsion characterization

Droplet size determination: The Dynamic Light Scattering (DLS) technique was used to determine the droplet size of O/W nano-emulsions. Nano-emulsions were not diluted prior to the measurements in order to keep the exact composition of the sample and turbid samples could not

be measured due to the detection limit of the equipment. Three measurements were performed at an angle of 90º and the thermostated bath was settled on 25ºC. The viscosity of the continuous phase (water) at 25ºC is 0.9 mPa.s and its refractive index is of 1.33.

Nano-emulsion theoretical diameter determination: The theoretical minimum droplet size that can be obtained for a certain concentration of surfactant is calculated considering an ideal system. The concentration of surfactant in the continuous phase is considered equal to the CMC meaning that there are no aggregates in the continuous phase, thus there is a fraction of the surfactant adsorbed at the interface (S_I) or present as free monomeric molecules in the continuous phase (S_M). The fraction of surfactant at the liquid-air interface is not taken into account. Therefore, the total concentration of surfactant, S, is:

$$S = S_M + S_I \tag{3.3}$$

The part of surfactant present as monomeric molecules in the aqueous phase are calculated by:

$$S_M = CMC \cdot V_T \cdot (1 - \phi_d) \cdot M_w \tag{3.4}$$

Where CMC is the Critical Micellar Concentration, V_T the total volume, ϕ the volume fraction of dispersed phase and M_w the molecular weight of the surfactant.

Knowing that the total area (A_T) and the total volume (V_T) of the nano-emulsion droplets are expresses as:

$$A_T = N \cdot 4\pi \cdot r^2 \tag{3.5}$$

$$\text{and } V_T = N \cdot \frac{4}{3} \cdot \pi r^3 \tag{3.6}$$

Where N represents the total number of droplets and r the average radius of a droplet. From this two equations, the ratio A_T/V_T is expressed by:

$$\frac{A_T}{V_T} = \frac{3}{r} \tag{3.7}$$

The volume fraction of surfactant adsorbed at the interface is calculated from the area of the drop ($A_T = \frac{3}{r} V_T$) and the area occupied by each molecule of surfactant (a_s):

$$S_I = A_T \cdot a_S = \frac{3 \cdot V_T \cdot \phi_d}{r} \cdot \frac{M_w}{a_S \cdot N_A} \quad 3.8$$

With N_A the Avogadro number. From equation 3.3, 3.4 and 3.8 minimum droplet radius r is expressed by:

$$r = \frac{3 \cdot \phi_d}{a_S \cdot N_A \cdot \left(\frac{[S]}{M_w} + CMC \cdot (\phi_d - 1)\right)} \quad 3.9$$

The equation does not take into account the thickness of the hydrophilic part of the surfactant that is inside the drop. This thickness is neglected compared to the diameter of the droplet.

Size and morphology determination: The nano-emulsion droplets were visualized by Cryo-TEM. A thin aqueous film was formed by dipping and withdrawing a bare specimen grid from the suspension. Glow-discharged Quantifoil® holey carbon coated grids were used. After withdrawal from suspension the grid was blotted against filter paper, leaving thin sample films spanning the grid holes. These films were vitrified by plunging the grid into ethane, which was kept at its melting point by liquid nitrogen, using a Vitrobot (FEI Company, Eindhoven, Netherlands) with the following options: blot offset 0 and blot time 2.5s, and keeping the sample before freezing at 100% humidity. The temperature at which the thin films and from which vitrification was initiated was room temperature. The vitreous sample films were transferred to a microscope Tecnai F20 (FEI Company, Eindhoven, Netherlands) using a Gatan cryo-holder (Gatan, Pleasanton, CA). Nano-emulsion droplet size d_n was determined by measuring approximately 100 nanoparticles by means of the image analysis software, Image J. The following equation was used to determine the average particle size.

$$d_n = \frac{\sum_i n_i d_i}{\sum_i n_i} \quad \text{number average diameter} \quad 3.10$$

3.3.4. Nano-emulsion stability

Macroscopic observation: The nano-emulsions were kept in a thermostated bath and the aspect was observed as a function of time. Some changes in the appearance are characteristic of the destabilization processes. For example, a white layer on top or at the bottom of the sample is characteristic of creaming or sedimentation, respectively. A loss of transparency is an indication of coalescence or Ostwald ripening.

Size evolution over time and temperature: The nano-emulsion stability was determined by measuring the droplet size as a function of time at 25ºC by means of a DLS. The measurements were performed without previous dilution of the nano-emulsion, at an angle of 90º and the thermostated bath was settled on 25ºC.

Evolution of the light backscattering over time: The stability of nano-emulsions was also assessed by measuring the transmission and/or the light backscattering by means of the Turbiscan^{TM} lab. The sample (15g) was introduced in a cylindrical tube and the transmission and backscattering data were collected every hour during 24h at 25ºC and 45ºC and expressed as a function of the sample height. The data analyses were performed by the lab expert software and provide the calculation of the droplet diameter by the Mie theory for droplet smaller than the wavelength of the laser.

3.3.5. Polymerization in nano-emulsions

Synthesis: The nano-emulsions were chosen regarding the maximum oil content, the lowest surfactant concentration (for biocompatibility reasons) and their stability at 25ºC and 45ºC. Nano-emulsions were prepared with 80% of water and then diluted to 90% of continuous phase with a solution of lipase Amano PS in water at 25ºC. The time t=0 is taken when the sample is placed at the desired reaction temperature under stirring. The evolution of the conversion rate over time was followed as a function of two reaction temperatures (25ºC and 45ºC) as well as three enzyme concentrations (0.1, 0.035, 0.01%).

Conversion rate: An aliquot of the reaction sample (300 µL) at different reaction time was added to deuterated chloroform (700 µL). The monomer and polymer dissolve in chloroform and separate from the water phase. The mixture was analyzed by ^{1}H NMR using a relaxation time of 1s and a pulse angle of 45º. The peaks corresponding to the monomer and the polymer were identified and the integration (*Int*) of the two peaks enables the calculation of the conversion rate using the following equation:

$$Conversion = \frac{Int(polymer)}{Int(monomer) + Int\ (polymer)} \qquad 3.11$$

3.3.6. Copolymerization in nano-emulsions

The O/W nano-emulsions containing Exaltolide® and a comonomer (either OH-Exaltolide® or Habanolide®) as oil phase were formed by the low-energy PIT method at 90% of water. The O/S ratio as well as the monomers/hexadecane ratio were fixed at 70/30 and 90/10 respectively. The ratios of Exaltolide®/comonomer studied were: 90/10; 75/25; 50/50; 0/100. The polymerization was initiated by addition of a lipase Amano PS at 0.1% and carried out for 24h at 45ºC under magnetic stirring

3.3.7. Characterization of polyester nanoparticles

Molecular weight measurements: The nanoparticle dispersion was washed three times with ethanol by centrifugation-redispersion cycles at 3000 rpm for 15 minutes in order to eliminate the surfactant. Nanoparticles were then lyophilized before characterization. The poly(Exaltolide®) nanoparticles were dissolved at 0.1% in THF.

First, a scan of the UV absorbtion of the polyester nanoparticles was performed from 200 to 800 nm to determine the maximum absorption wavelength of the polymer. It was found to be at λ=241 nm for poly(Exaltolide®). No absorption band were observed for poly(OH-Exaltolide®).

Molecular weights of poly(Exaltolide®) were determined by Gel Permeation Chromatography analysis using a UV detector adjusted at a wavelength of 241 nm using THF as eluent at a flow rate of 1 mL/min. 100 µL of the polymer solution were injected in the instrument. The molecular weights were calculated using a calibration relative to polystyrene standards. The calibration curve is presented in Figure 3.9 .

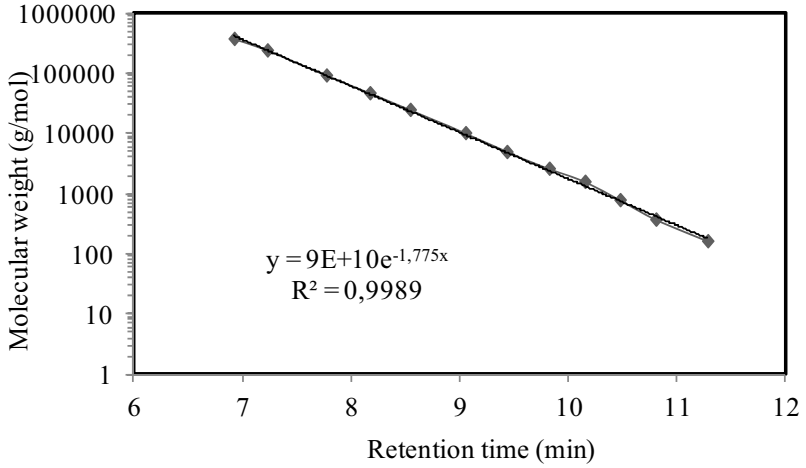

Figure 3.9 : Calibration curve of GPC measurements with polystyrene standards.

Molecular weights of poly(OH-Exaltolide®) were determined by Gel Permeation Chromatography analysis using a viscosimeter as detector, THF as eluent at a flow rate of 1 mL/min. The poly(OH-Exaltolide®) nanoparticles (ca. 40 mg) were accurately weighted and dissolved in THF (10 mL); 100 µL of the polymer solution were injected in the instrument.

Melting point and crystallinity degree: The latex dispersion was washed 6 times with water by centrifugation-redispersion cycles at 15000 rpm for 45 min in order to eliminate the maximum of surfactant. The nanoparticles were then redispersed in water and lyophilized before characterization. Measurements were carried out in three steps:

First heating scan: from 25ºC to120ºC at a rate of 10ºC/min.

Cooling scan: from 120ºC to 25ºC at a rate of 10ºC/min.

Second heating scan: from 25ºC to 120ºC at a rate of 10ºC/min.

Sample mass around 10 mg were weighted. From the DSC profiles, the melting and crystallization temperature were determined as the temperature corresponding to the higher heat flow value (in absolute value). The crystallization and melting enthalpies were determined by the area under each corresponding peak. Then, the degree of crystallinity of the polymer was calculated as the ratio of the melting enthalpy of the sample and the pure crystalline polymer.

Crystalline structure determination: The crystalline structure of the washed and dried polyester nanoparticles was determined by SAXS/WAXS measurements at 25ºC for 30 min. The dried polymer was placed in a sample holder between two films of Kallebrat® for measurements at room temperature.

Particle size distribution and morphology: The size and shape of the nanoparticles were determined by TEM. The sample were prepared as follow: A Formvar® carbon coated copper grid (200 mesh) was placed upside down on a drop of nanoparticle dispersion (0.01% of solid content) and left for 1 minute to enhance nanoparticle adsorption. Then, the grid was placed on a drop of phosphotungstic acid or uranyl acetate solution (2% in water) for 1 minute to negatively stain the sample. The excess of liquid was taken off touching a thin filter paper and the grid was dried before micrographs analysis.

The size of a minimum of 1000 randomly selected particles was measured from several TEM micrographs taken at different magnifications, by means of an image analysis software package

(Image J) in order to obtain the average size and size distribution. The following equations were used to determine the average particle sizes and the polydispersity index.

$$d_n = \frac{\sum_i n_i d_i}{\sum_i n_i} \quad \text{number average diameter} \qquad 3.10$$

$$d_w = \frac{\sum_i n_i {d_i}^4}{\sum_i n_i d_i^3} \quad \text{weight average diameter} \qquad 3.12$$

$$d_v = \left(\frac{\sum_i n_i d_i^3}{\sum_i n_i}\right)^{1/3} \quad \text{volume average diameter} \qquad 3.13$$

$$\text{PDI} = \frac{d_w}{d_n} \quad \text{polydispersity index} \qquad 3.14$$

Where n_i the number of particles with a diameter d_i. A dispersion of polymeric nanoparticle is considered monodispersed when the polydispersity index is lower than 1.05 (Tsaur, 1987).

Wetting properties: The contact angle between the nanoparticle powder and water was measured observing the capillarity of water through the powder. Nanoparticles were placed in a glass fiber-bottom tube and put in contact with water. While water goes up by capillarity through the powder, the mass of the sample was recorded over time using a tensiometer. The Washburn equation was used to calculate the contact angle, θ:

$$m^2 = \frac{c\rho^2\gamma_L \cos\theta}{\eta^2} t \qquad 3.15$$

Where m is the mass of the sample, c the Washburn constant, ρ, γ and η are the density, the interfacial tension and the viscosity of water, respectively. t is the time and θ the contact angle. Decane was considered as a solvent of zero contact angle and was used for the determination of the Washburn constant c.

3.3.8. Properties of polyester nanoparticles in dispersions

Macroscopic aspect: The nanoparticles were dispersed at 0.1% in water and different pure oil compounds. The visual aspect of the dispersions was observed after 24h at 25ºC. In order to study the effect of temperature on the nanoparticle dispersions, the temperature was increased in 10ºC

steps from 20ºC to 70ºC with the vials being hand shaken and left for one hour at each temperature.

Electrolyte solutions (10 g) at various concentrations from 10^{-4} to 10^{-1} M were prepared. 50 µL of the nanoparticles dispersion (1%) were added to the electrolyte solution and left in an ultrasound bath for 15 min (Salary, 2010).

Particle size: The nanoparticles size was determined by means of the DLS technique at a scattered angle of 90º. Sample temperature was maintained at 25ºC by a water bath.

Zeta potential measurements: The cell was filled with the nanoparticle dispersion using a plastic pipette to avoid the formation of bubbles in the thin tube. Three measurements of 20 scans were acquired for each sample. Electrophoretic mobilities were measured at 25°C (± 1ºC) using particle dispersion described above. The electrophoretic mobilities were converted to zeta potential using the approximation of Smoluchowski (Equation 3.2).

3.3.9. Study of the polyester nanoparticles affinity with volatile compounds

Polymeric nanoparticles were dispersed in a water/ethanol/volatile fragrant molecules mixture in order to look at their activity on the perfume evaporation over time. The method consists in following the evolution of the composition of a mixture of 11 volatile fragrant molecules (Table 3.2) over time at a fixed temperature (32°C) by GC analysis (Berthier, 2010).

Sample preparation: The samples were made of a mixture ethanol/water at a ratio of 9/1 and 10% of the mixture of volatile fragrant molecules. Samples were prepared in two steps: First, the polymer was mixed to the solution of ethanol/water and then the model perfume was added. A reference sample was prepared without polymer using the same ratio as in the sample.

Evaporation method: Aluminum crucibles from Mettler Toledo (small enough to fit in GC tubes) were placed on a plate heated to 32°C, the temperature of the skin. The plate was placed in a box in order to avoid air flow fluctuation. The crucibles were filled with 10 µL of the sample using a micropipette Rainin®Pos-D special for volatile compounds. The crucible at 45 min was first filled with the composition and the chronometer was started. The crucibles corresponding to the time 2,4,6,8,10,15,20,25 and 30 min were then filled and the injection time was added to the sample time. Measures were done after various evaporation times were performed.

Extraction and GC analysis: The aluminium crucible was transferred to a GC vial (capacity of 1.8mL, from VWR) filled with 1mL of a solution of isooctane (2,2,4-Trimethylpentane, 99.5%, for analysis, from Acros Organics) and diethyl ether (for analysis, from Carlo Erba Reactifs SDS) at 9/1 by volume; this solution was spiked with 1,4-dibromobenzene at 150 mg/L (Sigma-Aldrich) as the internal standard. The extract was analyzed by gas chromatography. The GC temperature profile was: 100ºC for 1 min, ramped to 170ºC at 10ºC/min for a total run time of 8 min. Helium was the mobile gas phase; the split ratio was 50:1. The retention times of ethyl butyrate and Romascone® were 1.43 and 3.70 min, respectively. A calibration curve was measured and used to quantify each molecule. Samples were measured in triplicate.

3.3.10. Pickering emulsion preparation, characterization and stability

Emulsion preparation: Nanoparticles were first dispersed in the water phase and the oil phase was added during emulsification with a Jankel and Kunkel ultra turrax T25 homogenizer with a 10 mm head operating at 13500 rpm for 2 min; time starting after the total addition of the oil phase. Emulsions were then transferred into 5 mL vials and stored in a water bath thermostated at 25ºC.

Emulsion type determination: The emulsion type was determined immediately after preparation by the drop test that consists in observing the behavior of a drop of emulsion on the water surface. O/W emulsions disperse in water and remain as drop on an oil surface while W/O emulsions disperse in oil and remain as drop at the water surface. The emulsion type was also determined by measuring the conductivity of the emulsion after preparation. O/W emulsion present high conductivity values corresponding to the conductivity of the water phase while W/O emulsion have conductivity values close to zero

Microscopic appearance and droplet size determination by optical microscopy: A drop of emulsion was placed between a glass slide and a cover slip. The samples were then observed under different magnifications by means of an optical microscope. The emulsion images were captured by a camera and analyzed using the software Image J. Average size and polydispersity indexes were obtained using the equations 3.10 to 3.14.

Droplet Size determination by laser diffraction: The mean droplet size and size distribution of emulsions were determined immediately after preparation and after 1 day. Few drops of emulsion were diluted in the 200 mL of water of the dispersion unit and a constant agitation of 2000 rpm was fixed. Three measurements were performed for each sample and the average size distribution

was obtained. The refractive index was fixed as the one of the continuous phase (RI = 1.33) and the absorption was fixed at 0.01 for emulsions.

Pickering emulsion theoretical diameter determination: The minimum theoretical diameter of Pickering emulsions was calculated for a certain composition. First, the number, *Np*, of the spherical particles of radius *a*, which are contained on the surface of a drop of radius r, at surface coverage φ_a is expressed by the following equation:

$$Np = \frac{4\pi r^2 \varphi_a}{\pi a^2} = 4\varphi_a \frac{r^2}{a^2} \quad 3.16$$

Where φ_a is the fraction of the surface area that is covered by adsorbed particles. The nanoparticles were considered as closely packed, $\varphi_a = \pi/(12)^{1/2} = 0.907$. Then, the total number of particles N is:

$$N = Np\, Nd \quad 3.17$$

Where N_d the number of drops is determined as:

$$N_d = \frac{V_d}{\frac{4}{3}\pi R^3} = \frac{3\phi_d V}{4\pi R^3} \quad 3.18$$

Where V_d and ϕ_d are the volume and volume fraction of the disperse phase in the emulsion, respectively, and *V* is the total volume of the emulsion. Likewise, for *N* we obtained:

$$N = \frac{\phi_p V_c}{\frac{4}{3}\,\pi a^3} = \frac{3\phi_p(1-\phi_d)V}{4\pi a^3} \quad 3.19$$

Where ϕ_p is the volume fraction of the particles in the continuous phase, whose volume is *V*c. Substituting the Equations 3.16, 3.18 and 3.19 in 3.17, the diameter of the smallest stable drop, is expressed by:

$$d = 2r = 8a\varphi_a \frac{\phi_d}{(1-\phi_d)} \frac{1}{\phi_p} \quad 3.20$$

This equation assumed that all particles (of bulk volume fraction ϕ_p) contained in the continuous phase are adsorbed on the drops, and that the surface coverage φ_a is high enough to protect the drops against coalescence during the collisions between them.

Stability: The stability of O/W emulsions to creaming or sedimentation was assessed by measuring the position of each phase (water, cream, oil) over time and temperature (from 25ºC to 60ºC) adapting the method described by Binks *et al.* (Binks, 2009). The emulsions were left in a water bath at a determined temperature and the volume of each phase was recorded for 1 hour.

3.3.11. Microcapsules synthesis, characterization and stability

Synthesis: Desmodur®N100 (isocyanate) was added to the oil phase of the Pickering emulsion prior to emulsification. The reaction temperature was fixed at 40ºC and the reaction was left under magnetic stirring for 2, 4 and 24 h to enable the cross-linking of the nanoparticles at the interface of the emulsion as represented in Figure 3.10.

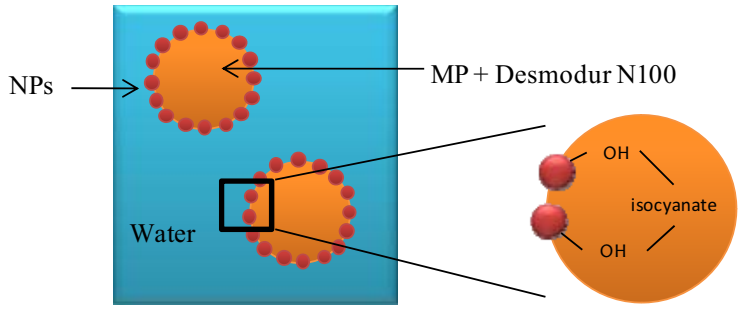

Figure 3.10 : Schematic representation of microcapsule formation.

Various ratios of $OH_{nanoparticle}/NCO_{DesmodurN100}$ were studied: 1/0, 5/1, 1/1 and 1/5. The calculation of the OH/NCO ratio considers that the reaction of hydroxyl group with alcohol is much faster than the reaction of isocyanate with water. Poly(Exaltolide®) has a molecular weight of 2647 g/ mol and contains one OH group per chain while poly(OH-Exaltolide®) has a molecular weight of 1554 g/ mol and 10 OH groups per molecules.

After reaction, microcapsules were washed three times with ethanol by redispersion-centrifugation cycles at 3000 rpm for 10 min before drying over night in an oven at 40ºC before characterization.

Evolution of the reaction: Microcapsules were analyzed by mean of an Infra-Red spectrophotometer, NICOLET model 510. A blank of KBr is analyzed and deduced from the measurements. Microcapsules were also characterized by measuring the mass loss while heating the sample by means of thermogravimetric analysis (TGA) between 25ºC and 550ºC with a rate of 10ºC/ min. Sample mass of around 10 mg were weighted.

Morphology and size determination: Microcapsule dispersions were placed between a microscope slide and a cover slip to be visualized by optical microscopy at different reaction times. The samples were gently pressed with a spatula to evidence the deformation of the capsules under pressure. Microcapsule shape and size were also determined by SEM analysis. A drop of microcapsules dispersion in ethanol was dried onto a SEM sticker. The samples were coated by an ultrathin layer of electrically conducting material (carbon), deposited on the sample by low-vacuum sputter coating. The samples were observed by means of a tabletop SEM.

3.3.12. Perfume release from microcapsules

Sample preparation: Microcapsules were introduced in a body wash formulation (composition in Table 3.3) to obtain a concentration of perfume (MP) of 0.2%. The samples were stored at room temperature before extraction after 6, 24 and 168 h.

Table 3.3 : Composition of a body wash formulation

Composition	%
water deionised	58.40
Polyacrylate-1 Crosspolymer (Noveon)	8.00
Citric Acid (40% aqueous solution)	0.50
Sodium C12-C15 Pareth Sulfate (Zschimmer & Schwarz)	25.00
Cocamidopropyl Betaine (Goldschmidt AG)	4.00
DMDM Hydantoin and Iodopropynyl Butylcarbamate (Lonza)	0.10
Sodium Chloride (20% aqueous solution)	4.00

Extraction and GC analysis: The samples at t = 6, 24 and 168 h (1 mL) were diluted in water (4 mL) and then extracted with isooctane (5 mL) containing 1,4-dibromobenzene (150 mg/L) as internal standard. The extract was analyzed by gas chromatography using a system GC 7890A equipped with an auto sampler 7683 series from Agilent Technologies (1 µL injected) and a HP-5 column of 30 m, an inner diameter of 0.32 mm and a film thickness of 0.25 µm. The GC temperature profile was: 100°C for 1 minute, ramped to 150°C at 10°C/min, ramped to 200°C at 25°C/min, 200°C for 1 minute for a total run time of 9 minutes. Helium was the mobile gas phase; the split ratio was 50/1. A calibration curve was measured and used to quantify each molecule. Samples were measured in triplicate.

RESULTS AND DISCUSSIONS

4. RESULTS AND DISCUSSIONS

4.1. SELECTION OF NANO-EMULSION COMPONENTS AND PRELIMINARY STUDIES

The first objective of this research work was the formation of monomer-in-water nano-emulsions by low-energy methods for their further use as templates for in-situ polymerization. One requirement was the use of non-toxic compounds and eco-friendly methods. In order to achieve these objectives, the first approach consisted in a literature search and a preliminary study to determine the appropriate components of the nano-emulsions. The results of these studies are presented in the following sections.

4.1.1. Selection of the monomers

As described in the introduction (section 1.2.1), lactones polymerize efficiently under mild conditions using enzymes as catalysts leading to the formation of biodegradable polyesters (Matsumura, 2006). Therefore, lactones were the candidate of choice for this research work. Moreover, lactones having a large ring have attracted much attention for their ability to polymerize easily due to their low ring strength (Uyama, 1995a-b).

Among the large ring lactones, **Exaltolide®**, also called pentadecanolide, a macrocyclic lactone containing 15 carbons in its ring, was selected for its ability to form biodegradable and biocompatible polymers with a high crystallinity and thermal stability by enzymatic Ring-Opening Polymerization (eROP) (Focarete, 2001; Gazzano, 2003). The polymerization reaction was expected to be the following (Figure 4.1):

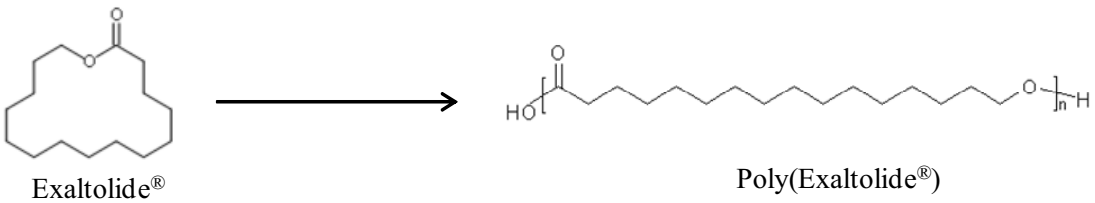

Figure 4.1 : Enzymatic ring-opening polymerization of Exaltolide® to poly(Exaltolide®).

For applications such as delivery systems in the pharmaceutical, textile, food or cosmetic fields, the functionalization of the polymeric nanoparticles surface is a key factor (Vrignaud, 2011;

Pinto-Reis, 2006a-b). Within this aim, the polymerization of a functionalized monomer was also considered. The **hydroxy-Exaltolide®** was selected for the presence of a hydroxyl group in the C12 position of the Exaltolide® ring and the following reaction was expected (Figure 4.2).

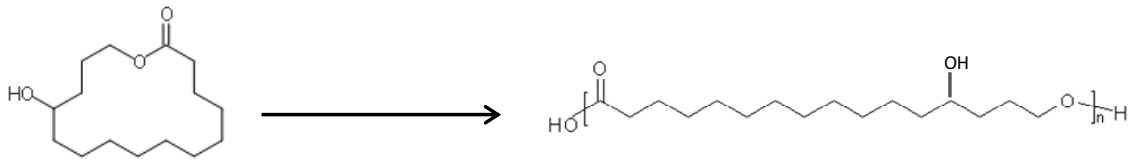

OH-Exaltolide® Poly(OH-Exaltolide®)

Figure 4.2 : Enzymatic ring-opening polymerization of OH-Exaltolide® to poly(OH-Exaltolide®).

Another monomer, **Habanolide**, was also selected for its double bond in the C12 position of the Exaltolide® ring and the following reaction was expected (Figure 4.3.

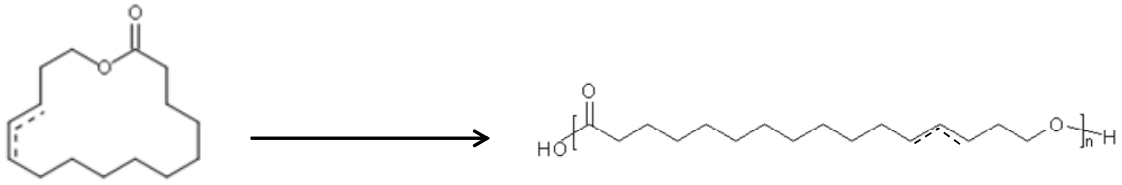

Habanolide ® Poly(Habanolide®)

Figure 4.3 : Enzymatic ring-opening polymerization of Habanolide® to poly(Habanolide®).

4.1.2. Selection of the surfactants

The nano-emulsification of monomers by low-energy methods has been rarely described (Spernath, 2007). This can be explained by the fact that the emulsification by low-energy methods of rather polar oils such as certain monomers requires a finer selection of the system components. Therefore, the selection of the right surfactant is a key factor for nano-emulsion formation by low-energy methods. Moreover, considering possible applications in the pharmaceutical or cosmetic field, non-toxic surfactants were required. Among the different types of surfactants, nonionics were preferred. They are generally considered as less toxic than charged surfactants. Due to their structure without charges, they are less sensitive to the electrolytes that can be present in the media. These surfactants also offer a high flexibility; the size of the hydrophilic and hydrophobic chains can be varied depending on the hydrophobicity required.

As first trial, the formation of nano-emulsion by the PIC method (section 3.3.2) at 25ºC was tested in the system water/Lutensol®AT50/Exaltolide®:hexadecane which had been reported to

form nano-emulsions by high-energy methods (Taden, 2003). Emulsification was attempted in samples with water contents between 80 and 95%, O/S ratio from 30/70 to 70/30 and an Exaltolide®/hexadecane ratio of 10/1. Nano-emulsions could not be obtained by the PIC method for this system. Therefore, a screening of different types of nonionic surfactants was carried out to form nano-emulsions of Exaltolide®-in-water.

Nonionic surfactants with a large range of HLB numbers and chemical structure were tested at an O/S ratio of 50/50 and 80% of water. The systems were evaluated after preparation by their visual aspect namely the appearance of a bluish color caused by the Tyndall effect. The results are summarized in Table 4.1.

Table 4.1 : Influence of surfactant structure and HLB on O/W nano-emulsion formation by the PIC method for the water/surfactant/Exaltolide®:hexadecane system with 90% water, an O/S ratio of 50/50 and a Exaltolide®/hexadecane ratio of 10/1.

Surfactant	HLB[a]	Nano-emulsion formation
Pluronic®L62	1-7	NO
Pluronic®P123	7-12	NO
Pluronic®PE 6200	10.5	NO
Cremophor®EL	12	**YES (Translucent)**
Brij®96V	12.4	**YES (Transparent)**
Tween®80	15	NO
Pluronic®L64	12-18	NO
Pluronic®F127	18-23	NO
Pluroni®PE 6800	30	NO
Pluronic®PE 10300		NO
Pluronic®PE 10400		NO

[a] HLB calculated by the provider.

O/W nano-emulsions were formed with Brij®96V and Cremophor®EL. Surfactants of low HLB such as Pluronic®L 62, P 123 or PE 6200 were too hydrophobic and were preferentially located in the oil phase while surfactants of high HLB (Pluronic®L 64, F 127) were too hydrophilic and were preferentially dissolved and/or aggregate in the water phase instead of adsorbing at the interface. This first screening revealed that surfactants with HLB around 12 were required for nano-emulsification by the PIC low-energy method of Exaltolide® in water. To confirm these conclusions, tests were also carried out with mixture of surfactants of low and high HLB such as

Span®20 and Tween®80 to reach a hydrophilic- lipophilic balance of approximately 12 and results are presented in Table 4.2.

Table 4.2 : Influence of the HLB of surfactant mixtures on O/W nano-emulsion formation by the PIC method for the water/surfactant/Exaltolide®:hexadecane system with 90% of water, an O/S ratio of 70/30 and Exaltolide®/hexadecane ratio of 10/1.

Surfactant Mixture S1/S2	S1/S2 ratio	HLB	Nano-emulsion formation
Span®20/Tween®80	30/70	13.1	**YES (Translucent)**
Span®20/Tween®80	50/50	11.8	**YES (Translucent)**
Span®20/Tween®80	70/30	10.52	NO

Table 4.2 shows that a mixture of sorbitan derivatives (Span®20/Tween®80) at mixing ratios of 30/70 and 50/50 and respective HLB values of 13.1 and 11.8 enable the formation of bluish translucent nano-emulsions. Lower HLB values did not permit nano-emulsion formation. For these two ratios, the calculated HLB values are 13.1 and 11.8 respectively. Among the various types of surfactants tested, those made of ethoxylated alcohol (Brij®96V), ethoxylated triglyceride (Cremophor®EL) and sorbitan derivatives (Span®20/Tween®80) favor the formation of Exaltolide®-in-water nano-emulsions, thus it can be concluded that the structure of the surfactant is not a key feature for nano-emulsion formation with Exaltolide® while the HLB number plays an important role. A HLB number close to 12 was required for nano-emulsification of the water/surfactant/Exaltolide®:hexadecane system.

Some additional experiments were carried out using the previously selected surfactants (Brij®96V, Cremophor®EL and Span®20/Tween®80) at 90% of water, an O/S ratio of 70/30 and an Exaltolide®/hexadecane ratio of 10/1 by the PIC method. Compared to Brij®96V and the mixture Span®20/Tween®80, Cremophor®EL does not form transparent nano-emulsions at this O/S ratio (70/30). Therefore, Cremophor®EL was not selected for further studies. Regarding stability, nano-emulsions with Span®20/Tween®80 destabilize by creaming in minutes while those using Brij®96V present better stability at 25ºC.

The water/Brij®96V/Exaltolide®:hexadecane system was chosen and its pseudo ternary phase diagram is described in Appendix 1.

Since nano-emulsification of Hydroxy-Exaltolide® (OH-Exaltolide®) in water had not been described in the literature, the system water/surfactant/OH-Exaltolide® was first studied without addition of co-oil. Following the results obtained with Exaltolide®, surfactants such as Tween®80,

Brij®96V and Cremophor®EL were first tested in samples with 90% of water and O/S ratios from 30/70 to 70/30 by the PIC method. The results are summarized in Table 4.3.

Table 4.3 : Summary of the surfactant screening for the nano-emulsion formation by the PIC method in the water/surfactant/OH-Exaltolide® system with 90% water.

Surfactant	HLB	O/S Ratio	Nano-emulsion formation
Tween®80	15	30/70	NO
		50/50	NO
		70/30	NO
Cremophor®EL	12	30/70	**YES (Transparent)**
		50/50	**YES (Transparent)**
		70/30	**YES (Transparent)**
Brij®96V	12.4	30/70	**YES (Transparent)**
		50/50	**YES (Translucent)**
		70/30	NO

Milky emulsions were obtained with Tween®80 while bluish transparent or translucent nano-emulsions were formed with Cremophor®EL and Brij®96V. Indeed, Tween®80, with a HLB number of 15, is too hydrophilic and mainly dissolves and/or aggregates in the water phase instead of adsorbing at the interface. Brij®96V and Cremophor®EL present similar HLB number; nevertheless, Cremophor®EL enables the formation of bluish transparent nano-emulsions in a larger range of O/S ratios than Brij®96V. Moreover, emulsions with Cremophor®EL showed good stability over time. These results can be explained by the fact that Cremophor®EL present more ethylene oxide units in its structure and is then preferred for the emulsification of OH-Exaltolide® as compared to the emulsification of Exaltolide®. In this case, the chemical structure of the surfactant is more important than the HLB number. Therefore, **the water/Cremophor®EL/OH-Exaltolide® system** was chosen for further experiments.

4.1.3. Determination of the co-oil type and concentration

The stability of nano-emulsions is a key factor to use them as templates for the in-situ polymerization of a monomer. Stability is then required at the polymerization temperature for the whole reaction time. It has been reported in an earlier work (Taden, 2003) that polymerization of Exaltolide® can be carried out in nano-emulsions at 45ºC for 24h and that the addition of hexadecane as “co-oil” was essential to decrease nano-emulsion Ostwald ripening (Landfester,

1999). For biocompatibility reasons and also to decrease in a higher extent Ostwald ripening, it was relevant to replace hexadecane by a more biocompatible and less soluble co-oil such as squalane. The co-oil type as well as the concentration was investigated in the system water/Brij®96V/Exaltolide®:co-oil. Three different oil/co-oil ratios were chosen and nano-emulsions with an O/S ratio of 50/50 and 90% water were prepared by the PIT method (see 4.2.1.2). The droplet sizes were measured by DLS immediately after preparation at 25ºC and after 24h at 25ºC and 45ºC and the results are summarized in Table 4.4.

Table 4.4 : Average droplet diameters and standard deviations of nano-emulsions of the water/Brij®96V/Exaltolide®:co-oil system prepared by the PIT method with 90% water and an O/S ratio of 50/50 as a function of co-oil type and concentration. Diameters measured after preparation at 25ºC and after 24h at 25ºC and 45ºC.

Average diameter ± standard deviation (nm)					
		Exaltolide®/hexadecane	Exaltolide®/squalane		
T (ºC)	Time (h)	90/10	90/10	95/5	98/2
25	0	20.5 ± 9.9	24.6 ± 8.0	76.6 ± 36.5	NM
25	24	24.8 ± 8.9	24.4 ± 7.8	88.5 ± 42.3	NM
45	24	121.9 ± 58.1	114.5 ± 62.5	NM	NM

NM = not measurable. Nano-emulsions were milky and too turbid and diameters > 200 nm were suspected.

When hexadecane was used in Exaltolide®/hexadecane ratio of 90/10, the system was stable at 25ºC for 24h but a slight increase of the droplet size at 45ºC was observed. This increase could be attributed to one or more destabilization mechanisms (section 1.1.2) but it could also be explained by the higher solubility of the surfactant molecules in the oil phase at high temperature and their lower availability for the interface that induced the formation of bigger drops and led to destabilization. When hexadecane is replaced by squalane in the same ratio, similar results were obtained. However, experiment with lower concentrations of squalane revealed that at least 5% of the squalane in the oil phase was necessary to maintain stability at 25ºC and 10% to maintain a reasonable stability at 45°C. Looking at these results and for biocompatibility reasons, hexadecane was replaced by squalane and an **Exaltolide®/squalane ratio of 90/10** was used for further experiments.

The effect of squalane on nano-emulsion stability was also investigated in the water/Cremophor®EL/OH-Exaltolide® system. Nano-emulsions with 90% water and an O/S ratio of 50/50 were prepared at various OH-Exaltolide®/squalane ratios and the average diameters measured by DLS at 25ºC after preparation and after 24h at 25ºC and 45°C. The results are summarized in Table 4.5.

Table 4.5 : Average droplet diameters and standard deviations of nano-emulsions of the water/Cremophor®EL/OH-Exaltolide®:squalane system prepared by the PIC method with 90% water and an O/S ratio of 50/50 as a function of co-oil type and concentration. Diameters measured after preparation at 25ºC and after 24h at 25ºC and 45ºC.

Average diameter ± standard deviation (nm)					
		OH-Exaltolide®/squalane			
T (ºC)	Time (h)	100/0	98/2	95/5	90/10
25	0	27.5 ± 10.6	25.7 ± 6.2	43.9 ± 21.4	NM
25	24	26.1 ± 8.2	26.1 ± 8.3	45.6 ± 22.6	NM
45	24	NM	31.3 ± 11.7	253.0 ± 123.7	NM

NM = not measurable. Nano-emulsions were turbid and diameters>200 nm were suspected.

When no co-oil was present in the system, nano-emulsions showed droplet size around 25 nm and good stability at 25°C. When the temperature is increased to 45°C, turbidity increases indicating an increase of the droplet sizes that could not be measured by DLS. At higher temperature, the surfactant molecules became more hydrophobic and as a result, bigger drops were formed. Moreover, the increase of the droplet size could be induced by some of the destabilization mechanisms described in the section 1.1.2. In the presence of squalane, it was observed that by increasing the oil/co-oil ratio from 98/2 to 90/10, the samples became more turbid and the droplet size increased at 25°C. It is worth noting that at oil/ co-oil ratio of 98/2, droplet sizes are similar to those obtained without co-oil at 25ºC and after 24h at 45ºC, the nano-emulsion showed droplet size around 30 nm, thus 2% of squalane in the dispersed phase is required to stabilize this system at 45ºC as well as 25ºC. In contrast, the presence of higher squalane concentration leads to higher droplets sizes and affects both the formation and stability of the nano-emulsions. Consequently, a ratio **OH-Exaltolide®:squalane of 98/2** was chosen for further experiments.

Summary:

Two lactones, Exaltolide® and OH-Exaltolide®, were selected for the study. From the screening of surfactants, Brij®96V and Cremophor®EL, commonly used in pharmaceutical applications, were chosen to emulsify Exaltolide® and OH-Exaltolide®, respectively. In order to maintain a sufficient stability of the nano-emulsions, co-oil was added to the system. Squalane was used to replace commonly used co-oils such as hexadecane. Finally, the preliminary study showed that an Exaltolide®/squalane ratio of 90/10 was necessary to stabilize the system water/Brij®96V/Exaltolide®:squalane while a OH-Exaltolide®/squalane ratio of 98/2 was required for the system water/Cremophor®EL/OH-Exaltolide®:squalane.

4.2. NANO-EMULSION FORMATION BY LOW-ENERGY METHODS

In this section, the formation of nano-emulsion by low-energy method (PIT or PIC) is described for two selected systems: **water/Brij®96V/Exaltolide®:squalane** and **water/Cremophor®EL /OH-Exaltolide®:squalane** systems. For each system, the phase inversion temperature was determined in order to investigate the preparation of nano-emulsions formation by the PIT method. Then, the influence of the composition (water content and O/S ratio) on the properties of the nano-emulsions was studied. Finally, the behavior of nano-emulsions under storage determined by their stability at 25°C and 45°C was investigated.

4.2.1. Water/Brij®96V/Exaltolide®: squalane system

4.2.1.1. Determination of Phase Inversion Temperature

The PIT was determined by conductivity measurements as a function of temperature, as described in section 3.3.1, for samples containing 90% water and O/S ratio of 40/60, 50/50 and 60/40. The results are plotted in Figure 4.4.

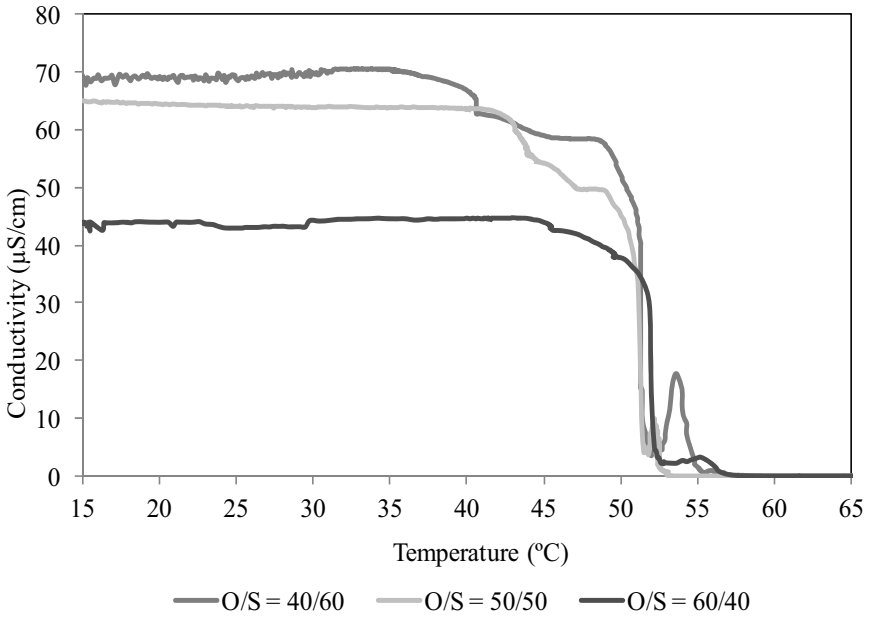

Figure 4.4 : Conductivity plotted against temperature for samples of the water/Brij®96V/Exaltolide®:squalane system with 90% water and at three O/S ratios.

At temperatures below 35ºC, the conductivity values are constant for each O/S ratios and the lower the O/S ratio, the higher the conductivity is. At temperatures above 35ºC, the conductivity

starts decreasing. First, it decreases slowly up to 45ºC and then, a sharp decrease of conductivity to values close to zero occurs, corresponding to the phase inversion from direct O/W to inverse W/O emulsions. At the O/S ratio of 40/60, conductivity decreases close to the 0 $\mu S/cm^{-1}$ at 52ºC and increases again to 60 $\mu S/cm^{-1}$ at 54ºC. This increase of conductivity can be explained by the high viscosity of the sample at this temperature suggesting the presence of liquid crystalline phases in the system (Izquierdo, 2005). Phase Inversion Temperature (PIT) values between 50 and 52ºC were estimated for samples with the three O/S ratios studied. It is worth mentioning that the PIT for pure ethoxylated nonionic surfactants is a system property while for technical grade surfactants it depends on composition.

4.2.1.2. Nano-emulsion formation and characterization

Nano-emulsions with 90% water and O/S ratios from 40/60 to 70/30 were prepared by three different methods. First, samples were prepared by simply mixing all the system components at 25°C but the formation of bluish transparent nano-emulsions was not achieved for any of the studied compositions. Nano-emulsions formation was then attempted by the PIC method (consisting in the slow addition of water to the oil-surfactant mixture) at 25°C. The visual aspect of the samples in Figure 4.5.a shows that transparent bluish, translucent or milky O/W nano-emulsions are formed. The turbidity of the nano-emulsions increases with the O/S ratio, indicating an increase of the droplet size.

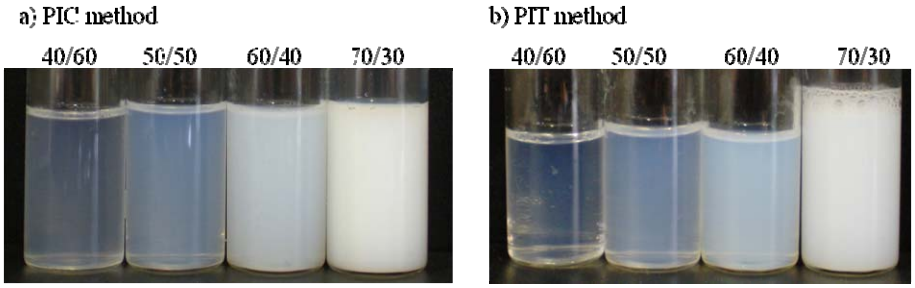

Figure 4.5 : Aspect of the nano-emulsions of the water/Brij®96V/Exaltolide®:squalane system with 90% of water and O/S ratio of 40/60, 50/50, 60/40 and 70/30 prepared by the a) PIC method and b) PIT method.

Nano-emulsion formation was also tested by the PIT method: all the components of the system were heated up to a temperature slightly higher than the PIT (60°C) and quenched to 25ºC. The visual appearance of the samples indicates that nano-emulsions were obtained by the PIT methods with 90% water and O/S ratios from 40/60 to 70/30 (Figure 4.5.b.). An increase of the O/S ratio also results in an increase of the turbidity. It is worth noting that O/W nano-emulsions prepared by the PIT method are slightly more transparent than those prepared by the PIC method.

Moreover, nano-emulsion formation with 95% water and the same O/S ratios were prepared by the PIT method to compare the results to those obtained at 90% water. The average drop diameters were measured by DLS for the nano-emulsions prepared at 90% water and O/S ratios of 40/60, 50/50 and 60/40 by the PIC and the PIT methods and at 95% water by the PIT method. The average droplet diameters, measured experimentally at 25ºC, are represented as a function of the O/S ratio in Figure 4.6. At the O/S ratio of 70/30, emulsions were bluish milky. These emulsions were too turbid to be measured by DLS without dilution but are probably in the nano scale with droplet size around 200 nm as suggested by the Tyndall effect. In addition, the theoretical minimum droplet size for samples with 90% water was calculated according to Equation 3.9 considering that all the surfactant is at the interface. The results are represented in Figure 4.6.

$$r = \frac{3 \times \phi}{a_s \times N_A \times \left(\frac{[S]}{M} + CMC(\phi\text{-}1)\right)} \qquad 3.9$$

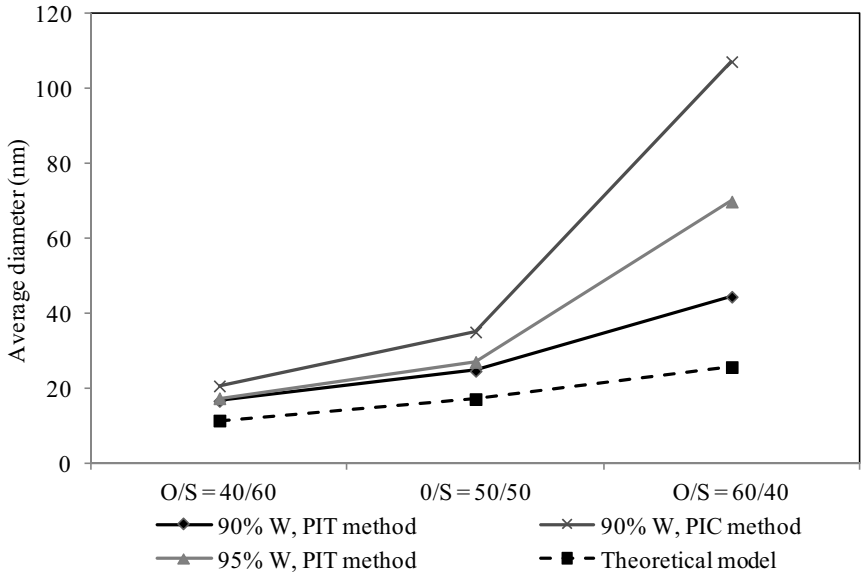

Figure 4.6 : Average droplet diameters as a function of the O/S ratio for nano-emulsions of the water/Brij®96V/Exaltolide®:squalane system with 90% water prepared by the PIC method and at 90% and 95% water prepared by the PIT method and the theoretical minimum diameter calculated by the Equation 3.9.

For the two emulsification methods and water contents studied, the average droplet size increases with the O/S ratio and follows the trend of the theoretical model, thus confirming the visual observations. This result also proves that the oil phase is the dispersed phase of the nano-emulsions, meaning that direct O/W nano-emulsions were formed.

At low O/S ratios, similar droplet sizes were obtained for nano-emulsions prepared with 90 and 95% water. Slightly higher droplet sizes were obtained with 90% water prepared by the PIC

method. Moreover all these values are similar to the theoretical values. At high O/S ratio, the experimental droplet size was higher than the theoretical values. Nevertheless, the nano-emulsions formed with 90% water by the PIT method were the closest to the theoretical values. The difference with the theoretical values, especially at high O/S ratios, means that some surfactant molecules might be free in the continuous phase and that the emulsification was not optimal. Regarding the preparation methods, droplet diameters between 20 and 120 nm were obtained by the PIC method while droplet sizes between 18 and 70 nm were obtained by the PIT method. The gap in the drop size, essentially observed at high O/S, between the PIT and the PIC method might be due to the higher polydispersity obtained by the PIC method. Therefore, the PIT method was selected for the rest of the study. As far as the water content is concerned, the higher droplet size obtained at higher percentage of water was explained by a dilution effect inducing a lack of sufficient surfactant to stabilize smaller drops. It can be concluded that by changing the composition of the system (water content or O/S ratio) or the preparation method, O/W nano-emulsion droplet sizes can be tuned easily to values between 10 and 200 nm.

To confirm the results obtained by DLS, a nano-emulsion with 90% water and an O/S ratio of 50/50 prepared by the PIT method was characterized by Cryo-TEM technique (Klang, 2012). An example of the images obtained is shown in Figure 4.7.

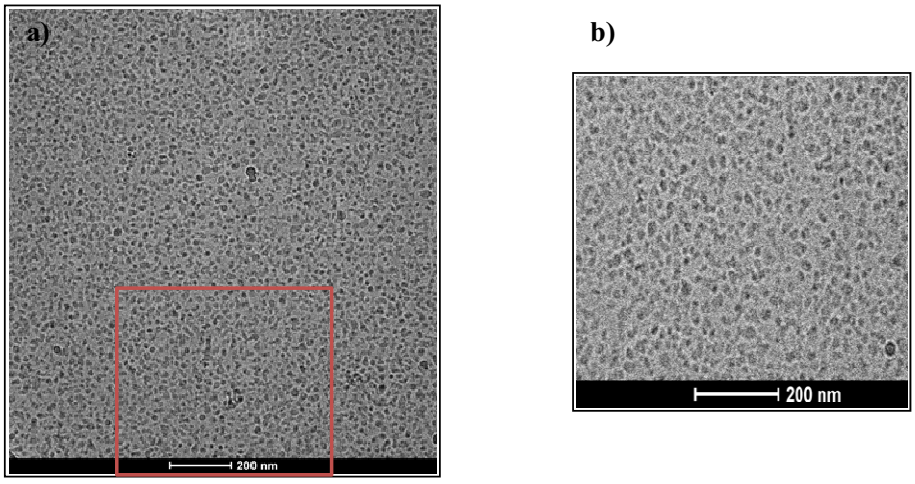

Figure 4.7 : a) Cryo-TEM micrographs of a nano-emulsion for the water/Brij®96V/Exaltolide®:squalane system with 90% water and an O/S ratio of 50/50, prepared by the PIT method and b) the red square enlargement.

The droplets of nano-emulsions as well as high sample homogeneity were observed readily on the TEM micrograph. The size of the droplets was determined by the Image J software for 100 drops and the mean droplet size was found to be 16.7 ± 3.6 nm. The droplet diameter obtained by Cryo-TEM image analysis was smaller than that provided by dynamic light scattering measurements

(24.6 ± 8 nm), as the former provides the hard sphere diameter while the latter the hydrodynamic diameter, meaning the size of the droplets surrounded by the water shell that moves with the droplet.

The region of nano-emulsion formation prepared by the PIT method is represented in the ternary diagram as the shadowed grey area (Figure 4.8).

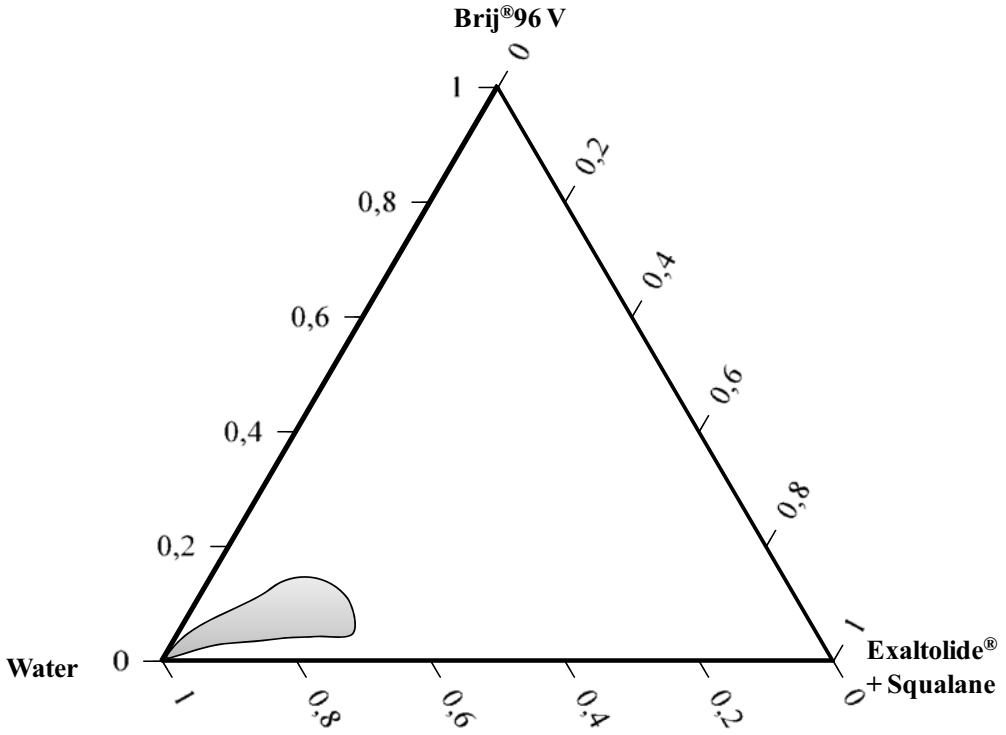

Figure 4.8 : Region of O/W nano-emulsion formation for the water/Brij®96V/ Exaltolide®:squalane system, prepared by the PIT method.

Bluish transparent nano-emulsions were formed starting from approximately 70% of water and at O/S ratio from 30/70 to 70/30.

4.2.1.3. Kinetic stability

In order to evaluate the behavior of nano-emulsions under storage, their stability at 25°C was first studied. As described in the introduction, nano-emulsions, due to their small droplet size, are stable against sedimentation and creaming but can destabilize irreversibly by Ostwald ripening and/or coalescence. Nano-emulsions with 90% water and three O/S ratios (40/60, 50/50 and 60/40) were prepared by the PIT method. The stability was determined by measuring the changes in droplet size with time at 25°C by means of DLS. The results are shown in Figure 4.9.

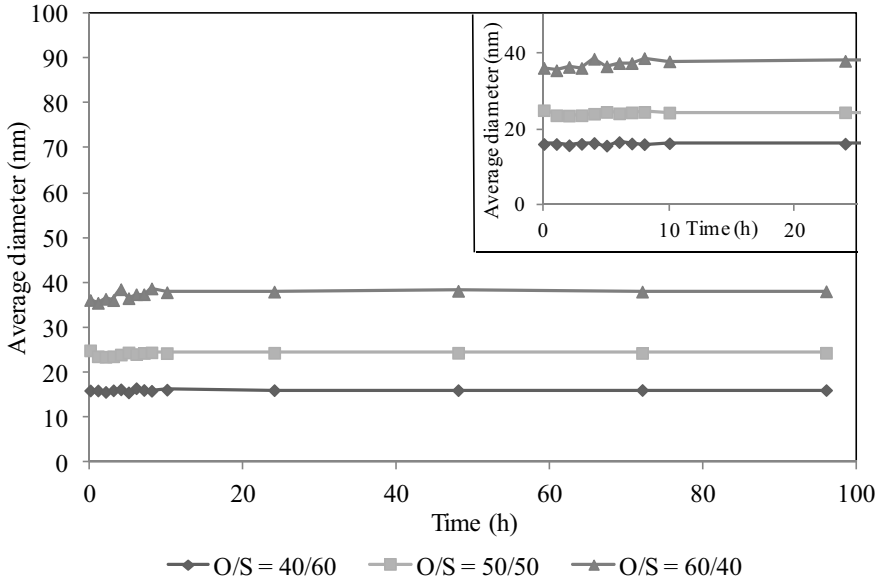

Figure 4.9 : Average diameters of nano-emulsions for the water/Brij®96V /Exaltolide®:squalane system with 90% water and O/S ratios of 40/60, 50/50 and 60/40, prepared by the PIT method and stored at 25ºC. Inset: magnification of the graph at short time experiment.

The droplet size does not vary during the experimental time (4 days) for any of the O/S ratios studied. The magnification of the graph at short experiment times shows that the droplet size is constant for all the O/S studied. Moreover, it should be noted that the higher the O/S ratio, the higher the droplet size is as evidenced by the turbidity of the samples showed in Figure 4.5.b. The above observations reveal that nano-emulsions are stable for at least a storage time of 4 days at 25ºC.

When nano-emulsions are used as template for in-situ polymerization, their stability at the reaction temperature and for the reaction time is primordial. As mentioned in the introduction, the polymerization of Exaltolide® has been performed by enzymatic-Ring Opening Polymerization at 45ºC for 24h to reach complete conversion. Knowing this data, the stability of the nano-emulsions was also studied at 45ºC during 24h. When measuring droplet size by DLS at this temperature, evaporation of water occurs, due to the small volume of sample. It may have a great effect on the results. Therefore, the study of nano-emulsion stability at 45ºC by DLS was considered not accurate. The stability of nano-emulsions was then assessed by light transmission (in which sample with higher volume are used) as a function of time at 25ºC and 45ºC for the nano-emulsion with 90% water and an O/S ratio of 50/50. Those experiments are also considered as accelerated stability test and give an idea of the long-term stability of samples. Figure 4.10 shows the transmission data (expressed in percentage compared to internal standards) as a

function of the sample height and time and the average diameter calculated from the transmission values between sample height of 10 and 30 mm as a function of time at 25ºC and 45ºC.

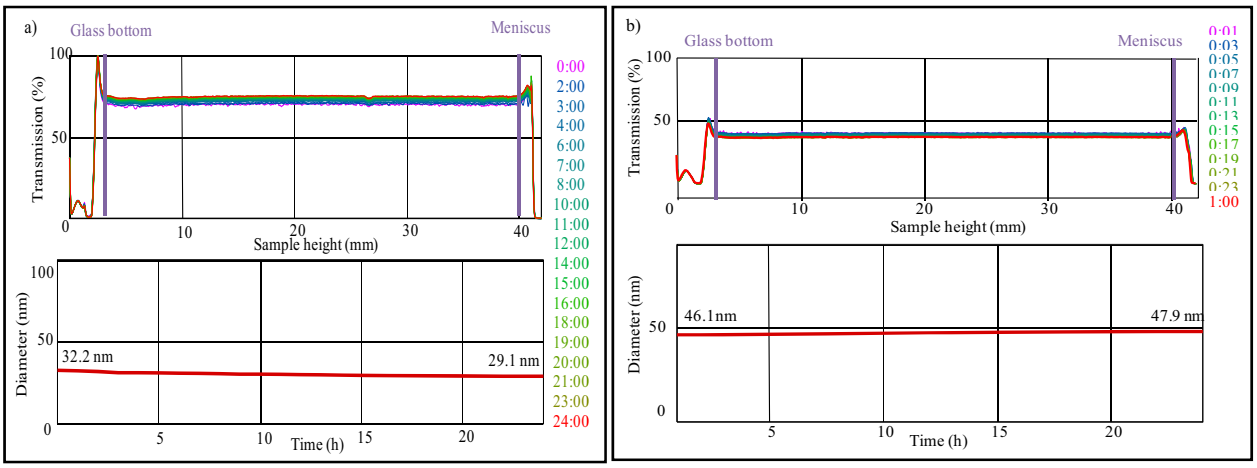

Figure 4.10 : Transmission along the sample height as a function of time for a nano-emulsion for the water/Brij®96V/Exaltolide®:squalane system with 90% water and an O/S ratio of 50/50 prepared by the PIT method (upper graph) and the average diameter calculated from the transmission values between sample height of 10 and 30 mm as a function of time (lower graph) at a) 25ºC and b) 45ºC.

For both studied temperatures, the transmission values are constant in the whole sample height and during the experimental time of 24h, indicating that the sample is homogeneous and no destabilization processes such as sedimentation or creaming occurs. It should be noted that at the meniscus and the bottom of the cell, an increase of transmission is observed which is due to the multiple light diffractions but has no physical meaning. Moreover, the curves are overlapped for the time period studied meaning that there is no evolution of the droplet size with time thus, neither coalescence nor Ostwald ripening occur. The constant transmission values over time demonstrate that the nano-emulsion is stable at 25ºC (confirming previous results obtained by DLS) and at 45ºC. The nano-emulsion at 25ºC shows higher transmission (70%) than the nano-emulsion at 45ºC (40%) due to its higher transparency and smaller droplet sizes. From the transmission values, the diameters at each time t were calculated using the Mie theory and the average of the diameters obtained at sample height between 10 and 30 mm are represented as a function of time at 25ºC and 45ºC in Figure 4.10.a and Figure 4.10.b (lower graphs), respectively. The droplet diameter is constant over time at both temperatures. At 25ºC, it ranges between 32 nm at t= 0 and 29.1 nm at t= 24 h while at 45ºC, values between 46.1 nm at t=0 and 47.9 nm at t=24h were obtained. Diameter values obtained at 25ºC are similar to the values obtained by DLS. The slight difference might be explained by the limitation of the Mie theory for particles bigger than the laser wavelength and by the polydispersity.

4.2.2. Water/Cremophor®EL/OH-Exaltolide®:squalane system

4.2.2.1. Determination of Phase Inversion Temperature

The Phase Inversion Temperature (PIT) of the water/Cremophor®EL/OH-Exaltolide®:squalane system was determined by conductivity measurements as a function of temperature for a sample with 90% water, an O/S ratio of 70/30 and an OH-Exaltolide®/squalane ratio of 98/2. In order to increase the conductivity values and better define the inversion region, an aqueous solution of NaCl at 10^{-2} M was used instead of water, as mentioned in the section 3.3.1. The results are plotted in Figure 4.11.

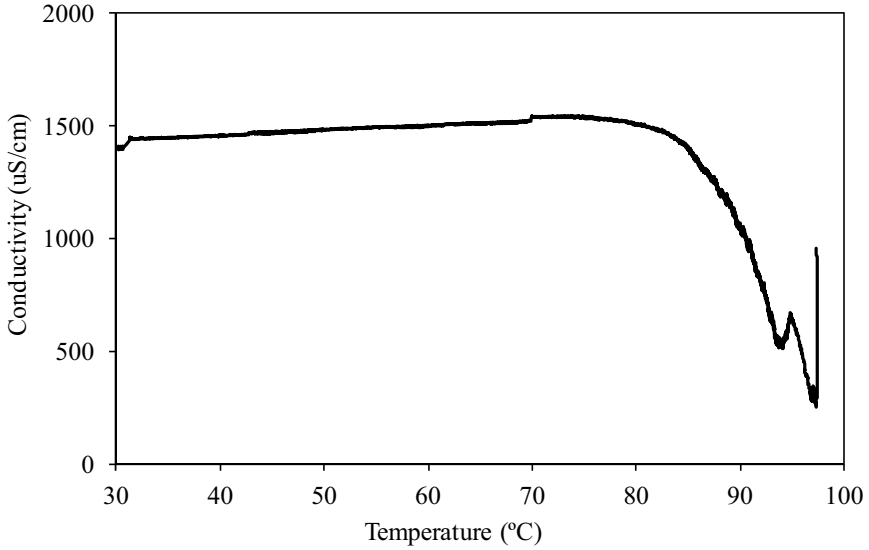

Figure 4.11 : Conductivity plotted against temperature for the sample of the water /Cremophor®EL/OH-Exaltolide®:squalane system at 90% of water and an O/S ratio of 70/30.

Conductivity values increase slowly up to 80ºC and a sharp decrease is then observed. The zero conductivity corresponding to the inverse W/O structure is not reached. The decrease of temperature at 85ºC might correspond to the PIT but it can also be due to sample components evaporation, namely water, during the heating process leading to some changes in the composition of the system. Moreover, at such high temperature, the control of the heating was not accurate. This fact could interfere in the accuracy of the conductivity values. As a consequence, the phase inversion is not properly defined by conductivity measurements for this system. Moreover, the PIT would be at temperature higher than 80ºC. Therefore, the use of the PIT method for nano-emulsion formation was not considered appropriate for this system.

4.2.2.2. Nano-emulsion formation and characterization

Nano-emulsions of the water/Cremophor®EL/OH-Exaltolide®:squalane system were then prepared at four O/S ratios (40/60, 50/50, 60/40 and 70/30) by dropwise addition of water to the oil–surfactant mixtures at 25ºC. The water was added in steps of 10% up to 90% water and the aspect of the samples was assessed visually.

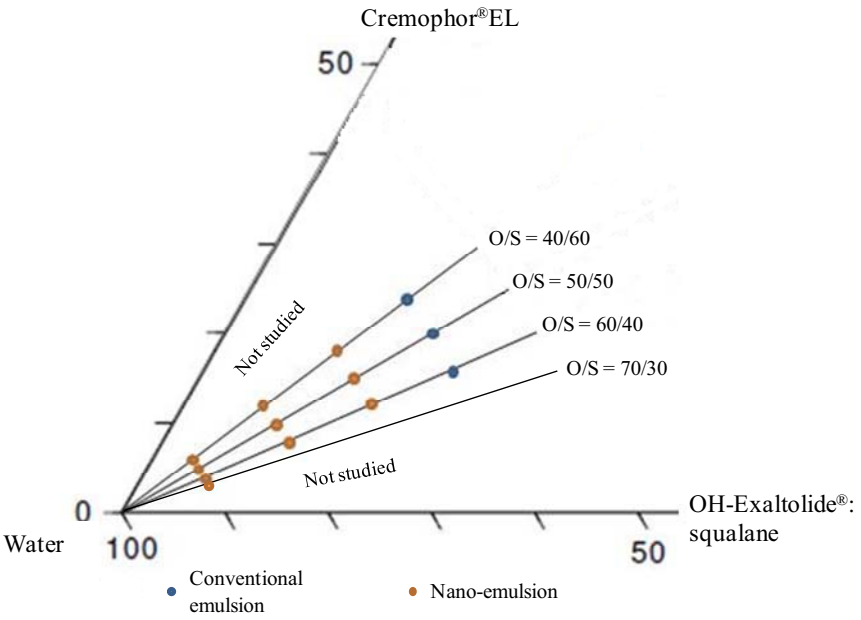

Figure 4.12: Representation of the nano-emulsion region of the water/Cremophor®EL/Hydroxy-Exaltolide®:squalane system prepared by the PIC method at 25°C.

Transparent bluish nano-emulsions were obtained from approximately 65% of water and for all the O/S ratios studied (40/60 to 70/30), as indicated in Figure 4.12. It is worth noting that this system allows the formation of nano-emulsions at a higher O/S ratio than systems previously reported using the same surfactant (Sadurni, 2005), thus making this system interesting for applications where the trend is to reduce the surfactant content such as pharmaceutical or cosmetic formulation.

The visual aspect of nano-emulsions with 90% water and various O/S ratios after formation is shown in Figure 4.13.a.

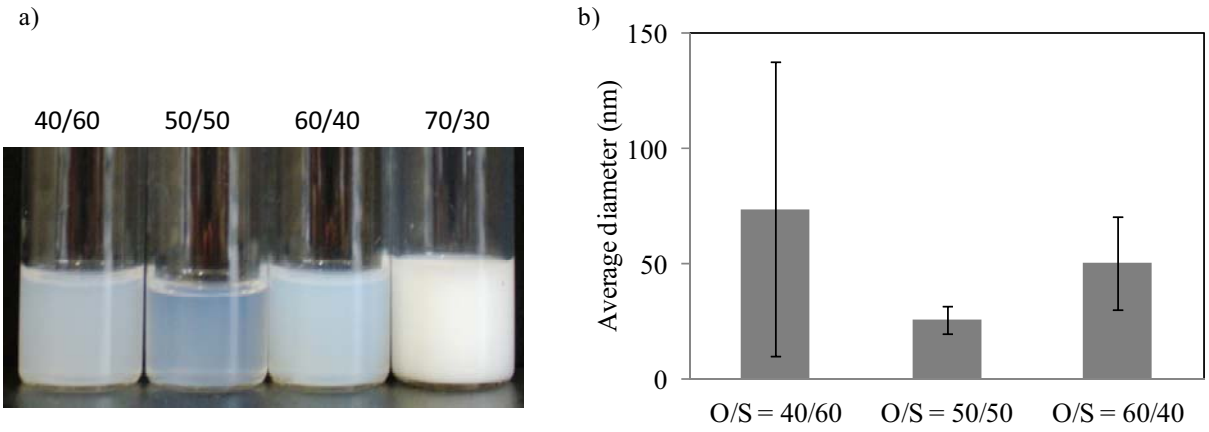

Figure 4.13 : Nano-emulsions of the water/Cremophor®EL/OH-Exaltolide®:squalane system with 90% water at four O/S ratios, prepared by the PIC method at 25°C and a) Visual aspects and b) Average diameters and standard deviations obtained by DLS.

The sample with an O/S ratio of 50/50 presents the lowest turbidity after preparation. When the O/S increases, the turbidity increases due to the higher volume of dispersed phase in the system. Nevertheless, the sample with an O/S ratio of 40/60 is more turbid than the sample with the O/S ratio of 50/50. In order to confirm this behavior, the droplet sizes were measured by DLS at 25°C and the average diameters and the standard deviations were plotted as a function of O/S ratios in Figure 4.13.b. The droplet diameters after preparation range between 26 and 75 nm and exhibit a minimum for the composition with O/S ratio of 50/50. The droplet sizes obtained by DLS confirm the visual observations (the sample with an O/S ratio of 70/30 could not be measured by DLS due to its high turbidity). The behavior obtained at low O/S could be explained by a lack of homogeneity during the preparation method. In fact, during the slow addition of water, the presence of highly viscous liquid crystalline phases was observed and the homogenization appeared to be critical.

The nano-emulsion with 90% of water and an O/S ratio of 50/50, prepared by the PIC method was also characterized by cryo-TEM and micrographs are shown on Figure 4.14.

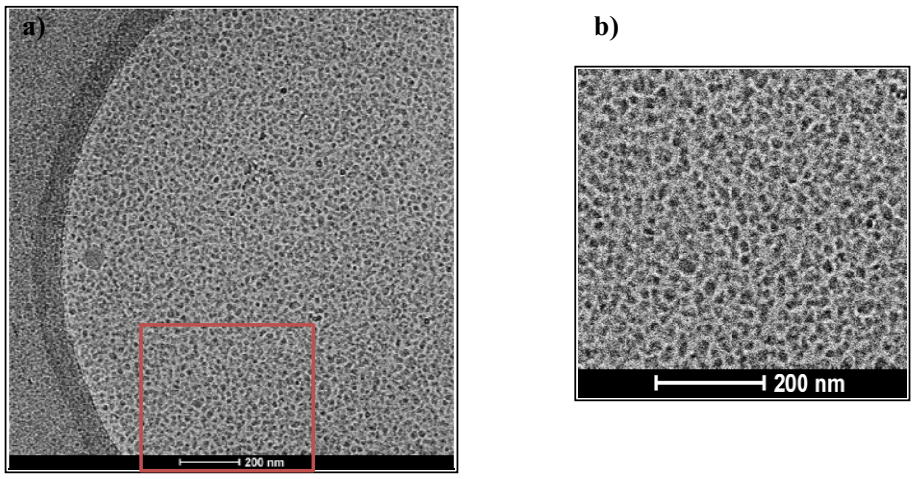

Figure 4.14 : a) Cryo-TEM micrographs of nano-emulsions of the water/Cremophor®EL/OH-Exaltolide®:squalane system with 90% water and an O/S ratio of 50/50, after preparation by the PIC method at 25°C and b) the red square enlargement.

The average droplet size, calculated from 100 drops, was found to be approximately 15.9 ± 3.6 nm. The droplet size measured by Cryo-TEM analysis is smaller than that obtained by DLS measurements (25 ± 6.2 nm). The difference, as mentioned previously, is attributed to the measurement of the hydrodynamic radius (droplet surrounded by the water shell that moves with it) by DLS and the measurement of the hard sphere by cryo-TEM. The size of the droplet of this system is similar to that of the water/Brij®96V/Exaltolide®:squalane system.

4.2.2.3. Kinetic stability

The stability was studied for nano-emulsions with 90% water and three O/S ratios (40/60, 50/50, 60/40) at 25ºC by measuring the changes of droplet size by DLS over 4 days. Neither creaming nor sedimentation was visually observed. The results at 25°C are plotted in Figure 4.15.

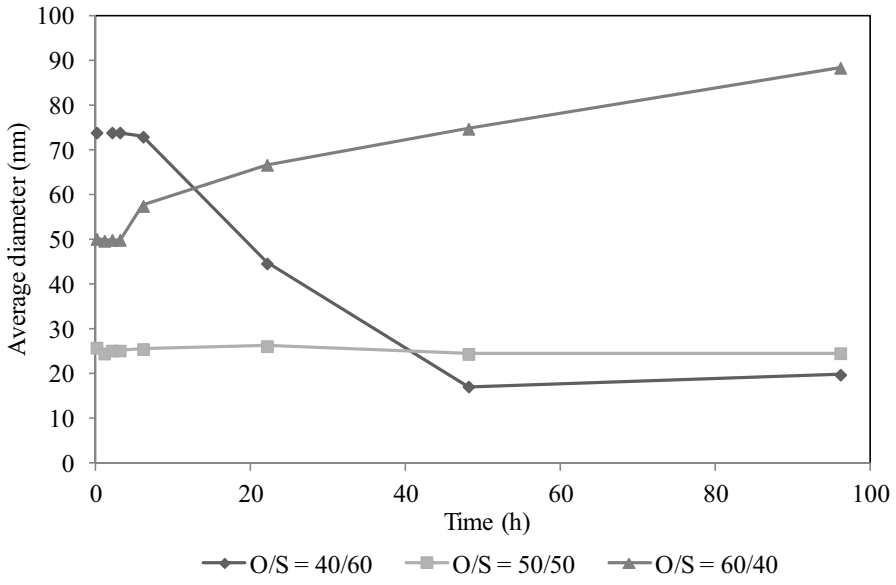

Figure 4.15 : Average diameters of nano-emulsions of the water/Cremophor®EL/OH-Exaltolide®:squalane system prepared by the PIC method at 25°C with 90% water and three different O/S ratios.

For the sample with an O/S ratio of 40/60, a large decrease of the droplet size occurred after 10 hours of preparation and a plateau was reached around 16 nm after 48 h. Then, droplet size was constant for the rest of the experimental time. This behavior could be explained considering that during the addition of water, a liquid crystalline phase of high viscosity is formed that might be responsible for the slow kinetics of this sample. At an O/S ratio of 50/50, the nano-emulsion droplet size is constant over time indicating nano-emulsion stability at 25ºC for the time period studied while at higher O/S (60/40), the droplet size increases slowly with time from 50 to 90 nm indicating destabilization of the nano-emulsion. Neither sedimentation nor creaming was observed visually for this sample thus, irreversible phenomena such as coalescence or Ostwald ripening were suspected. Within the aim to determine the mechanism of destabilization of this nano-emulsion, the LSW theory (to assess Ostwald ripening) and the Deminière theory (to assess coalescence), as described in introduction, were applied (Lifshitz, 1961; Deminière, 1998). The LSW theory predicts a linear relation between r^3 and time and the Deminière theory predicts a linear relation between $1/r^2$ and time when Ostwald ripening or coalescence are the predominant destabilization mechanisms, respectively. Thus, r^3 and $1/r^2$ were plotted against time in Figure 4.16 .

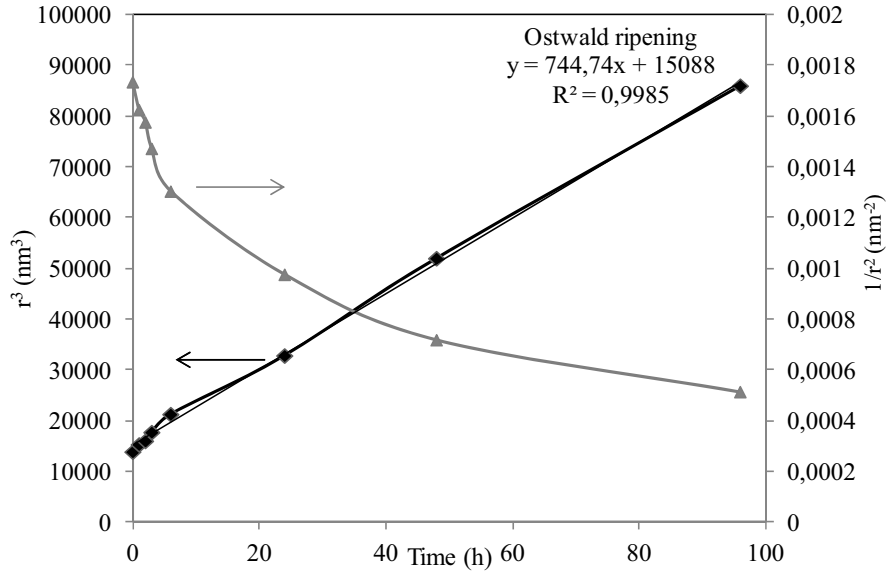

Figure 4.16 : r^3 and $1/r^2$ plotted versus time of nano-emulsions of the water/Cremophor®EL/OH-Exaltolide®:squalane system prepared by the PIC method at 25ºC with 90% water and an O/S ratio of 60/40.

The values of $1/r^2$ decrease with time but the slope is not linear thus coalescence was not considered as the main destabilization mechanism of this nano-emulsion. The values of r^3 increases with time during the experimental time of 96 h and a linear regression do fit well the experimental results. The linear regression shows a determination coefficient higher than 0.99, thus suggesting that Ostwald ripening is the main destabilization process for this nano-emulsion. The Ostwald ripening rate ω_{OR} obtained, according to Equation 1.7, from the slope of the straight line of Figure 4.16, is $0.21 \times 10^{-27} m^3/s$. This value is in agreement with low Ostwald ripening rates found in the literature for nano-emulsions with aliphatic hydrocarbons (Izquierdo, 2005).

The stability of the nano-emulsions containing 90% of water and an O/S ratio of 50/50 was also assessed from light transmission spectra at 25ºC and 45ºC. Figure 4.17 shows the transmission data (expressed in percentage compared to internal standards) as a function of the sample height at different times (upper graph) and the evolution of the average droplet diameter as a function time calculated as the average of the diameter between a sample height of 10 and 30 mm (lower graph).

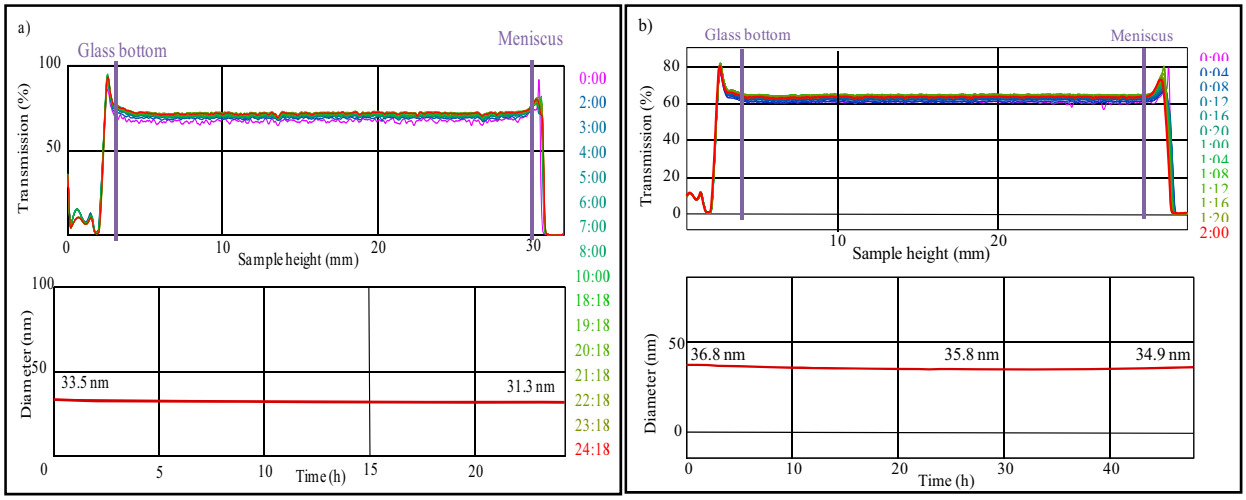

Figure 4.17 : Transmission as a function of the sample height at various times obtained for the nano-emulsions of the water/Cremophor®EL/OH-Exaltolide®:squalane system prepared by the PIC method at 25°C with 90% water and an O/S of 50/50 (upper graph) and the average diameter calculated from the transmission values between sample height of 10 and 30 mm (lower graph) at a) 25ºC and b) 45ºC.

The transmission values are constant on the whole height of the sample and a variation of less than 2% occurs over the time studied of 24h, indicating respectively that the sample is homogeneous (no sedimentation nor creaming) and that there is no increase in the droplet size (no coalescence nor Ostwald ripening). The constant transmission values over time demonstrate that the nano-emulsion at an O/S ratio of 50/50 is stable at 25ºC as well as 45ºC in the period of time studied and confirm previous results obtained by DLS at 25ºC. It is worth noting that the transmission data are slightly higher at 45ºC indicating higher droplet sizes. The diameters at each time t, calculated using the Mie theory as the average of the diameters obtained at each sample height between 10 and 30 mm, shown in Figure 4.17 (lower graphs), confirm this assumption. The droplet diameter is constant over time at both 25ºC and 45ºC. At 25ºC, it ranges between 33.5 nm at t = 0 and 31.3 nm at t= 24 h while at 45ºC, values between 36.8 nm at t=0 and 35.8 nm at t=24h were obtained. Diameter values obtained at 25ºC are similar to the values obtained by DLS. The slight differences might be explained, as mentioned earlier by the limitation of the Mie theory for particles bigger than the laser wavelength and by the polydispersity.

Summary:

A systematic study on nano-emulsion formation was carried out with two selected systems. Bluish transparent nano-emulsions with diameter between 10 and 100nm were formed with the water/Brij®96V/Exaltolide®:squalane system using both the PIT and the PIC methods. The nano-emulsions were obtained in the region of O/S ratios from 30/70 to 90/10 and water content up to 70%. The water/Cremophor®EL/OH-Exaltolide®:squalane system enable the formation of bluish transparent emulsion by the PIC method. The nano-emulsions were obtained in the region of O/S ratios from 40/60 to 70/30 and water content up to 70% which is a large region compare to system described in the literature for the same surfactant. The PIT of this system is higher than 80ºC and is considered too high for emulsification in the frame of this work.

Since nano-emulsions can be used as template for the polymerization of the monomer, their stability at 25°C and 45°C is a key factor. For the studied systems, the nano-emulsions with 90% water and an O/S ratio of 50/50 are stable for at least 4 days at 25ºC and one day at 45ºC indicating a sufficient stability at 25ºC and 45ºC to carry out the polymerization in the droplet of the nano-emulsions.

4.3. POLYESTER NANOPARTICLES FROM NANO-EMULSION TEMPLATES

In this section, the generation of polyester nanoparticles, performed by enzymatic ring-opening polymerization (eROP) in nano-emulsion is described. The influence of the polymerization parameters and nano-emulsion properties on the final polymeric nanoparticles was investigated. In addition, the synthesis of functionalized nanoparticles was studied by eROP of a hydroxy-functionalized monomer in nano-emulsions. Moreover, copolymerization in nano-emulsions between various lactone-type monomers is also described.

4.3.1. Selection of the template

From the previous section, nano-emulsions of the water/Brij®96V/Exaltolide®:squalane and water/Cremophor®EL/OH-Exaltolide®:squalane systems were selected for their good stability over time and temperature. The composition and the main characteristics of the nano-emulsion templates used for the following experiments are detailed in Table 4.6.

Table 4.6 : Summary of the nano-emulsion template compositions

Monomer	Exaltolide®	OH-Exaltolide®
Surfactant	Brij®96V	Cremophor®EL
Water content (%)	90	90
O/S ratio	50/50	50/50
Monomer/squalane ratio	90/10	98/2
Preparation method	PIT	PIC at 25°C
Droplet size[a] at 25°C	29.1 nm	31.3 nm
Droplet size[a] at 45°C	47.9 nm	35.8 nm

[a] Diameters determined by Light BackScattering (LBS) measurements after 24h.

4.3.2. Selection of the catalyst

A general requirement of this research work was the use of non-toxic compounds and eco-friendly processes. Within this aim, a bibliographic research was done in order to define the appropriate conditions for the ring-opening polymerization (ROP) of macrocyclic lactones (See Introduction section 1.2.1). The ring opening polymerization of macrocyclic lactones generally required the use of catalysts. Among the large variety of catalysts that have been used for this reaction, lipases were selected for their properties to accelerate hydrolysis of ester bond needed for the reaction of ring-opening polymerization and for their interfacial properties that make them suitable for reaction in nano-emulsion. A lipase from *pseudomonias cepacia,* Lipase Amano PS was previously used for eROP of macrocyclic lactones in nano-emulsions obtained by high-energy method (Taden, 2003). Compared to bulk reactions that require more than 10% enzyme, at 70°C for several days, complete conversion was obtained in nano-emulsion at low enzyme concentration (0.125%) and low temperature (45°C) Therefore, the latter lipase, AMANO PS, was selected for this study.

4.3.3. Synthesis and characterization of poly(Exaltolide®) nanoparticles by eROP

As described in the introduction, many parameters such as pH, temperature, reaction media, enzyme concentration or enzyme origin can influence the rate of enzymatic ring-opening polymerization (Namekawa, 1998 and 1999; Bisht, 1997; Mei, 2002). In this study, the reaction media consists in the nano-emulsion droplets and the pH is fixed at the pH of the external phase, pH_{water} = 6-7, which is considered as the optimum value for the lipase Amano PS activity. In this study, the effect of temperature as well as enzyme concentration on the reaction kinetics was investigated and the obtained poly(Exaltolide®) nanoparticles were characterized by their molecular weight, melting point, crystallinity and size. Then, the effect of the nano-emulsion template was also taken into account. The experiments performed in this study are summarized in Table 4.7.

Table 4.7 : Summary of the polymerization experiments performed in nano-emulsions.

Exp.	Water content (%)	O/S ratio	Enzyme concentration (%)	Temperature (ºC)
1	90	50/50	0.1	25
2	90	50/50	0.1	45
3	90	50/50	0.035	45
4	90	50/50	0.01	45
5	90	40/60	0.1	45
6	90	60/40	0.1	45

4.3.3.1. Influence of temperature

The eROP of Exaltolide® was carried out in a nano-emulsion initiated by 0.1% of lipase at two temperatures: 25ºC and 45ºC, Exp.1 and Exp. 2 respectively. The nanoparticle dispersion obtained at 25ºC looks flocculated after 24h while the dispersion at 45ºC is homogeneous and milky. The conversion rate of both reactions was followed for 24h by ^{1}H NMR spectroscopy (Appendices 4 and 5). A typical ^{1}H NMR spectrum of a sample after one hour of reaction is presented in Figure 4.18.a.

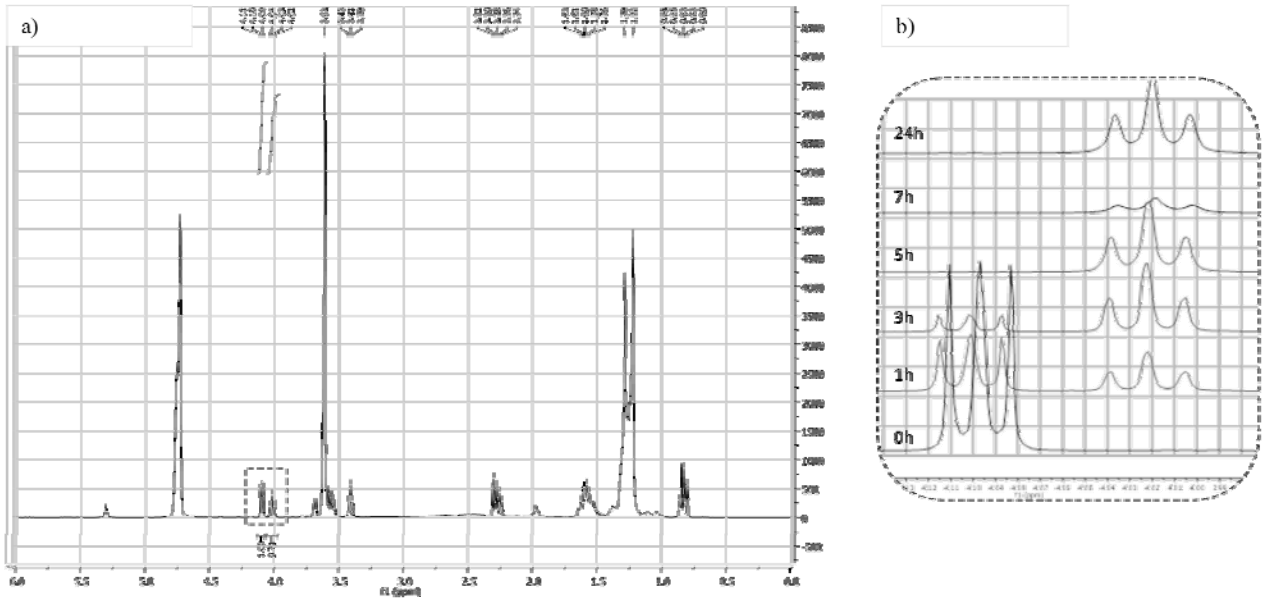

Figure 4.18: a) Typical ^{1}H NMR spectrum of a poly(Exaltolide®) nanoparticle dispersion after 1h eROP at 45°C with 0.1% lipase in nano-emulsion with 90% water and an O/S ratio of 50/50 (Exp. 2) and b) Evolution of the monomer and polymer characteristic peaks over time.

The sample after one hour of polymerization is composed of a mixture of Exaltolide® monomer, surfactant and squalane but also opened monomer, oligomer and polymer. The ^{1}H NMR spectra shows a signal at 3.62 (m) which can be assigned to the α-methylene protons of the terminal hydroxyl group (-C$\underline{H}_2$-O-H) of the polymer and the surfactant. The signal at δ 2.3 ppm corresponds to the α-methylene protons of the terminal carboxylic group. Monomer conversion was determined from the relative peak areas of signal corresponding to the ester methylene (-C$\underline{H}_2$-O-C=O) of the polymer (t, 4.02 ppm) and the ester methylene (-C$\underline{H}_2$-O-C=O) of the monomer (t, 4.10 ppm) (Uyama, 1996). The evolution of the monomer and polymer peaks over time is plotted in Figure 4.18.b and the ratio of the integration of each peaks (Equation 3.11) enable the calculation of the conversion rate at both temperatures, represented as a function of time in Figure 4.19.

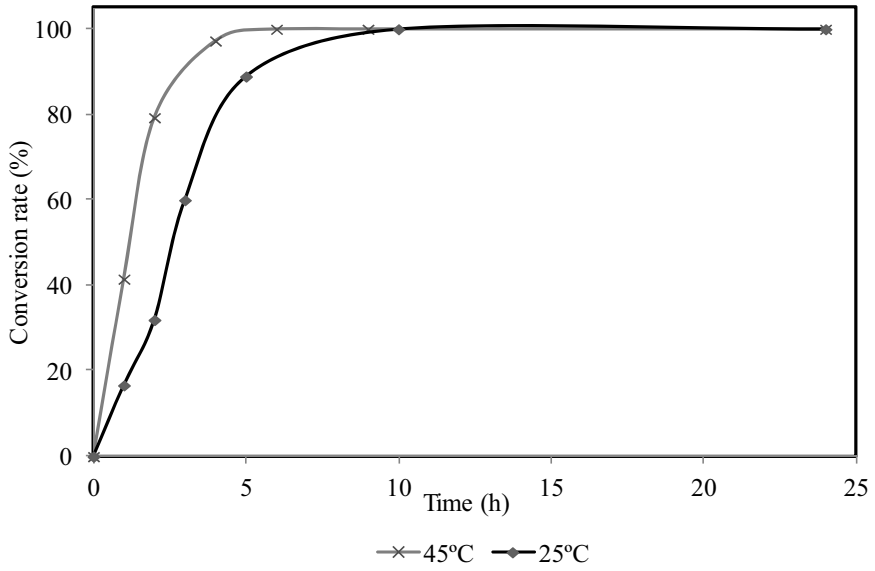

Figure 4.19 : Monomer conversion plotted as a function of time for the synthesis of poly(Exaltolide®) nanoparticles by eROP (0.1% lipase) at a) 25ºC (Exp. 1) and b) 45ºC (Exp. 2) in nano-emulsion with 90% water and an O/S of 50/50.

The conversion increases rapidly during the first hours, at both studied temperatures. Complete conversion is reached in 4 hours at 45ºC while at 25ºC 10 hours were needed to reach a conversion superior to 90%. Indeed, when the reaction temperature increases, the number of collisions between the monomer and the lipase increases as well as the energy of the collisions; thus increasing the polymerization rate (Lovell, 1997). Moreover, lipases initiate the ROP by forming an acyl-enzyme intermediate between the monomer and an activated serine residue (obtained by deprotonation of serine by histidine and aspartate). An increase of the temperature leads to a faster deprotonation of the serine residues, forming thus more active sites and leading to a quicker reaction. The optimum temperature for the lipase Amano PS is known to be around

50°C thus explaining the fast conversion at 45°C. Knowing the value of the optimum enzyme temperature and considering the probable instability of nano-emulsions at temperature closer to the PIT (52ºC), higher reaction temperatures were not investigated. Moreover, in the studied conditions, short reaction times were needed to obtain complete conversion compared to enzyme-catalyzed reactions in organic solvents. The latter were reported to last at least several days (Uyama, 1996) at 75ºC. Compared to bulk reaction, nano-emulsions present a larger interfacial area where the lipase can adsorb (Taden, 2003) and initiate a large number of active site for polymerization thus increasing the conversion rate. Moreover, in confined media such as nano-emulsion droplets, the entropy is reduced and the collisions between the monomer and the active site are increased thus speeding up the reaction (Schork, 2005). Although the reaction temperature accelerates considerably the conversion rate, its effect on the molecular weight of the final polymer was also demonstrated (Namekawa, 1999).

Poly(Exaltolide®) molecular weights were measured by Gel Permeation Chromatography following two methods of detection described in section 3.3.7. The obtained molecular weights and polymerization degree are summarized in the Table 4.8.

Table 4.8 : Retention times and molecular weights obtained for poly(Exaltolide®) nanoparticles obtained by eROP (0.1% lipase) at a) 25ºC (Exp. 1) and b) 45ºC (Exp. 2) in nano-emulsion with 90% water and an O/S of 50/50. M_n is the number average molecular weight and M_w is the weight average molecular weight, PDI is the polydispersity index and DP the degree of polymerization.

Exp.	T (ºC)	M_n[a] (g/mol)	M_n[b] (g/mol)	M_w[b] (g/mol)	PDI[b]	DP_n
1	25	425 1234 2647	1050	1190	1.13	4.3
2	45	2647	1070	1170	1.09	4.4

[a] Molecular weight measured by GPC, detection UV using polystyrene standards for calibration, [b] Molecular weight measured by GPC, detection viscosity.

The molecular weights were determined by two GPC methods using either UV or viscosity detection. It is worth mentioning that GPC measurement by UV detection is based on the separation of the polymers by the hydrodynamic volume and requires the use of a calibration by polystyrene standards while the viscosity detection is based on universal calibration. Results obtained by viscosity detection might be more accurate as they do not depend on the structure of the molecules (difference of molecular structure between polystyrene and poly(Exaltolide®)).

When the measurement is based on a calibration by polystyrene standards, polymers obtained at either 25 or 45ºC present a major molecular weight of 2647 g/mol. However, the polymer obtained at 25ºC reveal the presence of oligomers with low molecular weights (425, 1234 g/mol) when detected by UV. When using a Universal calibration, no changes in the polymer molecular weight (1050 g/mol) were obtained. Nevertheless, in both cases, the low molecular weights measured are at the limit of the exclusion volume of the GPC column, thus making the results inaccurate.

Nevertheless, it can be concluded that an increase of the reaction temperature does not allow the formation of poly(Exaltolide®) with higher molecular weight but might improve the polydispersity. Molecular weight values of the same order of magnitude have been reported when polymerization is carried out in the presence of water (Namekawa, 1998b). Curiously, the two research groups that have described the formation of poly(Exaltolide®) in nano-emulsion reports different values of molecular weight. Taden *et al.* in 2003 described the formation of poly(Exaltolide®) nanoparticles with a high molecular weight of 200 000g/mol while Målberg *et al.* obtained molecular weight of 1100 g/mol. In both cases, these results concern the formation of nanoparticles of size around 200 nm (Taden, 2003; Målberg, 2010) but in the latter study, the authors also showed that the molecular weight do not depend on the size of the nanoparticle but on the concentration of co-oil. Moreover, in both studies, different surfactant have been used but it was assumed that the surfactant do not alter the reaction. In this study, the low molecular weights are obtained by eROP in nano-emulsion droplets with size as low as 20 nm. The low molecular weight obtained was attributed to the reaction mechanism. Due to the higher surface area in nano-emulsions, the number of lipase molecules at the interfase is high thus including the large number of initiated chains that can lead to the formation of low molecular weight polymers

It should be mentioned that, in general, relatively low molecular weight polymers organize themselves into crystalline structures more readily than longer molecules (Sperling, 2005). As a high crystallinity is a key feature for the applications foreseen in this work, the molecular weights obtained were considered appropriate.

Knowing that poly(Exaltolide®) is a crystalline polymer when obtained in bulk, a study of the crystalline properties of the poly(Exaltolide®) nanoparticles obtained was carried out. The final polymers were characterized by their melting and crystallization temperature as well as enthalpy by DSC, thus permitting the calculation of the crystallinity degree. Figure 4.20 represents the

DSC profile of poly(Exaltolide®) obtained by eROP in nano-emulsion at 45°C by addition of 0.1% enzymes.

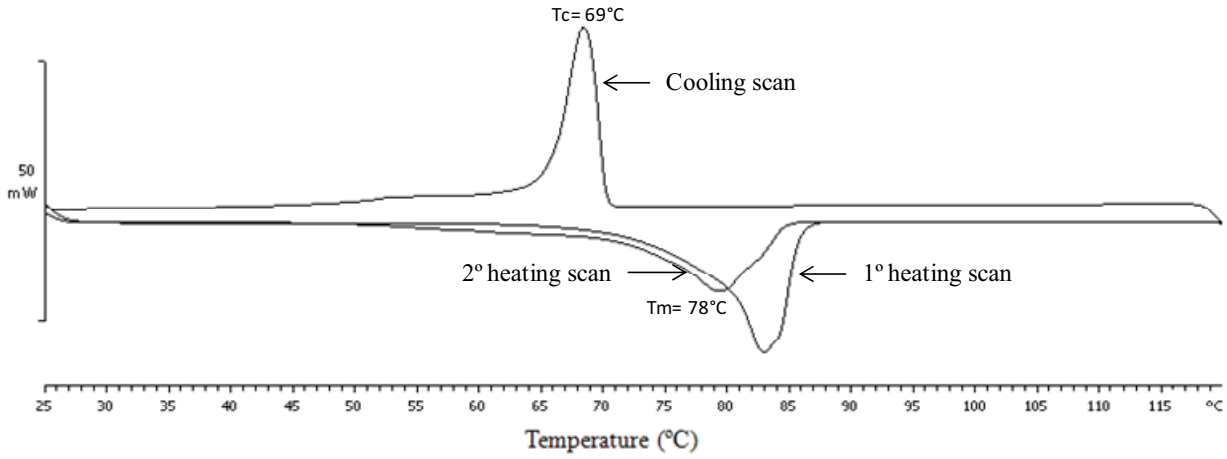

Figure 4.20 : DSC profile of poly(Exaltolide®) nanoparticles obtained by eROP (0.1% lipase) at 45ºC (Exp. 2) in nano-emulsion with 90% water and an O/S of 50/50: cooling and second heating runs.

During the first heating scan, a single endothermic peak corresponding to the fusion of the polyester nanoparticles is observed. During cooling from the melt, a crystallization exothermic peak at 69°C of high enthalpy appears. The low undercooling (Tm–Tc = 10ºC) clearly indicates a strong ability of poly(Exaltolide®) chains to crystallize. In the second heating run, a single endotherm is observed corresponding to the melting of the polymer. The absence of a cold crystallization shows that the polymer completely crystallizes during the cooling run. This observation is also confirmed by the concordance of enthalpy values of crystallization and melting (Table 4.9). The glass-transition temperature (T_g) of Poly(Exaltolide®) is not observed in the range of temperature studied and was not observed even at temperature as low as -100°C. Those results are in agreement with earlier published data on Poly(Exaltolide®) (Focarete, 2001) showing that the need to use dynamic mechanical analysis for Tg determination. The values of melting and crystallization temperature and enthalpy of the poly(Exaltolide®) nanoparticles synthesized at 25ºC and 45ºC are summarized in Table 4.9 and compared to the values for the polymer obtained in bulk (Focarete, 2001) (DSC profiles in Appendix 4).

Table 4.9 : Summary of the calorimetric properties of the poly(Exaltolide®) nanoparticles obtained by eROP (0.1% lipase) at 25ºC (Exp. 1) and 45ºC (Exp. 2) in nano-emulsion with 90% water and an O/S of 50/50 and comparison with the polymer obtained in bulk. T and ΔH are the temperature and the difference of enthalpy, respectively. The sub indices m and c correspond to melting and crystallization respectively. χ is the crystallinity degree.

Exp.	Temperature (ºC)	Tm (ºC)[a]	ΔHm (J/g)[a]	Tc (ºC)	ΔHc (J/g)	Tm (ºC)[b]	ΔHm (J/g)[b]	χ^c
1	25	82.12	-187.52	69.38	160.32	76.68	-162.69	69.8
2	45	82.13	-208.22	69.85	172.53	78.16	-175.84	75.5
Bulk[d]	70	78	-134	78	134	97	149	64

[a] From the first heat; [b] From the second heat; [c] Determined from DSC considering ΔH^0_m = 233 J/g for 100% crystalline polymer (Lebedev, 1984); [d] The bulk reaction was carried out with Novozym 435 at 70ºC in toluene (Focarete, 2001).

During the first heating scan, a single endothermic peak is observed centered on a temperature of approximately 82ºC. The second heating scan, after cooling to 25ºC, shows a larger endothermic peak with a maximum value at 76.7 and 78.2ºC for the polymer obtained at 25 and 45ºC respectively. The single peak in the first heating scan is shifted to lower temperature in the second scan indicating that different crystalline structures coexist after the cooling and melting process. Considering the second heating scan, it can be observed that the melting temperature decreases by approximately 20 ºC from bulk poly(Exaltolide®) to nanoparticles. This decrease is explained by the difference in the crystalline structure between the bulk and the nanoparticles. It is worth noting that the melting point of crystalline nanoparticles is size-dependent. Some reports have shown that the melting temperature lowers as the particle diameter decreases (Bunjes, 2000; Cho, 2006). In a simulation study, Jiang *et al.* found that the melting point of semi-crystalline nanoparticles of polyethylene decreases sharply when the nanoparticle diameter is less than 30 nm (Jiang, 2003). The difference in the melting temperature between bulk and nanoparticle of around 20ºC would suggest that poly(Exaltolide®) nanoparticles prepared in this work have a size below 50 nm, Indeed, if polymerization occurs as expected in nano-emulsion droplets, the droplet acts as template and the nanoparticle size is then expected in the range of the nano-emulsion droplet size meaning between 20 and 50 nm. Thus the results of calorimetric measurements confirms the formation of poly(Exaltolide®) nanoparticles with size below 50nm.

Moreover, the crystallinity degree of poly(Exaltolide®) nanoparticles was calculated from the second heating scan as the difference between the melting enthalpy of the sample and pure crystalline poly(Exaltolide®) for both reaction temperatures. The crystallinity degree increases by increasing the reaction temperature and higher crystallinity values were obtained in nano-emulsion compared to bulk reaction (Table 4.9). The crystallinity can be hardly related to the

molecular weight (Cai, 2010) but in the present study, some assumption were proposed. The fact that poly(Exaltolide®) prepared at 25ºC shows lower crystallinity than that of the polymer prepared at 45ºC, that presents a single molecular weight distribution, can be explained by the presence of some oligomers of low molecular weight. The crystallinity of the polymer is explained by the mobility of the chains and as the polydispersity increases, the chain are more mobile resulting in the decrease of crystallinity observed in this study.

The crystalline structure of the polymers was also analyzed by SAXS/ WAXS measurements and the X-ray diffraction patterns at 25 and 45ºC are presented in Figure 4.21.

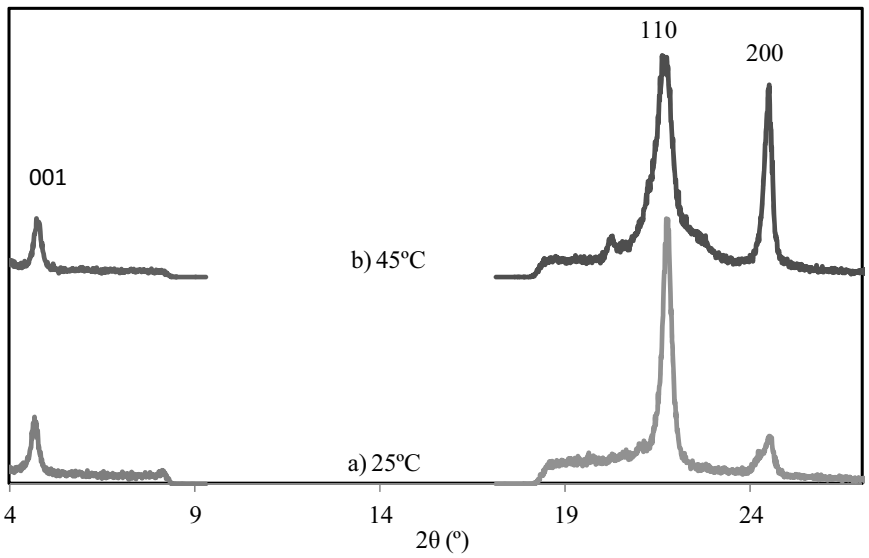

Figure 4.21: X-ray diffraction pattern of poly(Exaltolide®) nanoparticles obtained by eROP (0.1% lipase) at a) 25ºC (Exp. 1) and b) 45ºC (Exp. 2) in nano-emulsion with 90% water and an O/S of 50/50.

For both studied temperatures, the poly(Exaltolide®) diffraction pattern is characterized at wide angles by two strong reflections at 2θ = 21.6º and 2θ = 24.5º corresponding to a distance of 0.411 and 0.363 nm, respectively. These two strong reflections are associated to the lateral packing distance between the polymer chains. At small angle, one small reflection was observed for both diffraction patterns at 2θ = 4.7º corresponding to a distance of 2.0 nm. Similar profiles are obtained for the poly(Exaltolide®) at 25ºC and 45ºC, nevertheless, the profile of the polymer obtained at 25ºC shows a loss of intensity at 2θ = 24.5º, suggesting that the crystal grows preferentially along the (110) axis when reaction occurs at 25ºC. This can be explained by the loss of crystallinity previously observed by DSC (χ = 69.8% at 25ºC and 75% at 45ºC).

The reflections obtained for both spectra were compared with data from the literature and they were found to be characteristic of polypentadecanolide (poly(Exaltolide®) (Gazzano, 2003).

Polypentadecanolide has been described as an orthorhombic crystal structure characterized by its reflection at small angle corresponding to the dimension of the lattice. This distance is also compatible with the length of the Exaltolide® monomer unit in a planar zigzag conformation.

The samples were visualized by Transmission Electron Microscopy, in order to confirm the formation of nanoparticles and determine their size and morphology. Representative micrographs of the poly(Exaltolide®) nanoparticles prepared at 25 and 45ºC are shown in Figure 4.22.

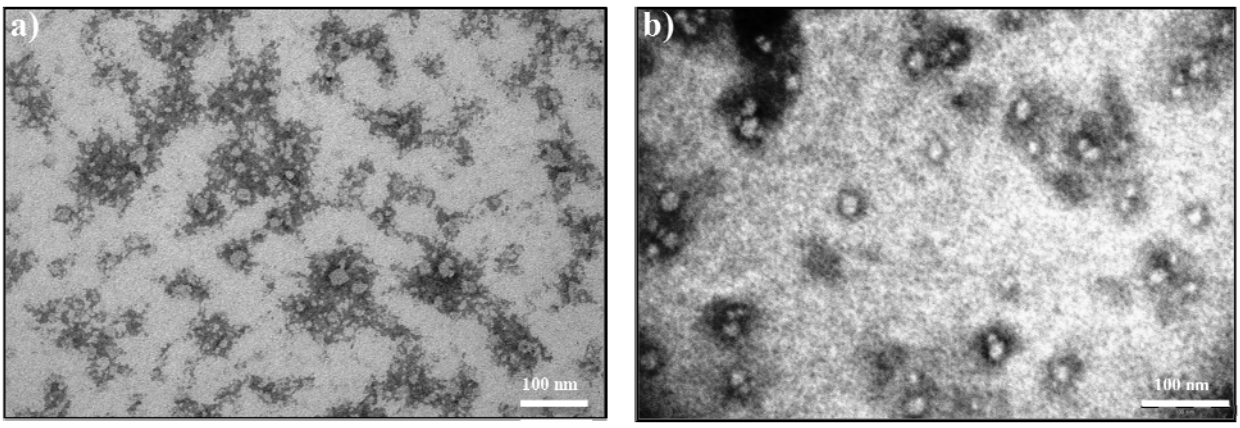

Figure 4.22 : TEM micrographs of poly(Exaltolide®) nanoparticles obtained by eROP (0.1% lipase) in nano-emulsion with 90% water and an O/S of 50/50 at a) 25ºC (Exp. 1) and b) 45ºC (Exp. 2).

As poly(Exaltolide®) is a non conductive material, samples were stained by phosphotungstic acid (PTA), as described in the experimental section 3.3.7 and are therefore observed as white dots surrounded by a black layer of PTA (Harris, 1999). Nanoparticles present a rounded shape and the nanoparticles obtained at 45ºC shows a larger size than those obtained at 25ºC. It is worth noting that the nanoparticles appear slightly aggregated.

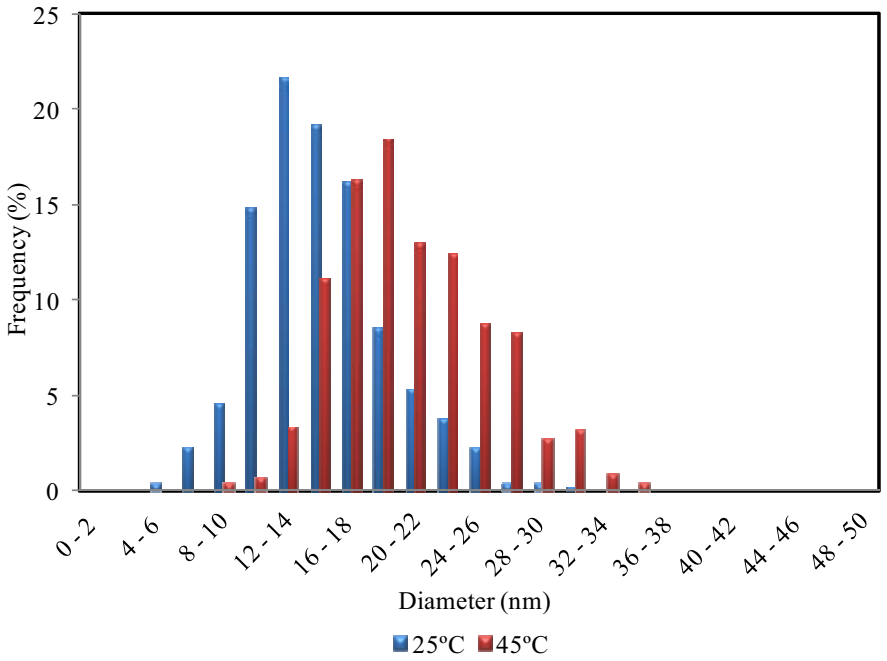

Figure 4.23 : Particle size distribution of poly(Exaltolide®) nanoparticles obtained by eROP (0.1% lipase) at 25ºC and 45ºC in nano-emulsion with 90% water and an O/S of 50/50.

The size distribution of poly(Exaltolide®) nanoparticles obtained at 25ºC and 45ºC (Figure 4.23) shows a unimodal distribution. Poly(Exaltolide®) nanoparticles prepared at 25ºC present smaller number average diameter (15.1 ± 4.0 nm) than the nanoparticles prepared at 45ºC (20.7 ± 4.71 nm). It was shown in section 4.2.1.3 that nano-emulsions present a bigger droplet size at 45ºC than at 25ºC. These results would confirm that nano-emulsion droplet act as templates. Table 4.10 shows the number average diameter of nanoparticles obtained by TEM and, for comparison purposes, that of the nano-emulsion droplets assessed by Cryo-TEM and LBS.

Table 4.10 : Mean diameters of nano-emulsion droplets measured by cryo-TEM and LBS and poly(Exaltolide®) nanoparticles obtained by eROP at 25ºC and 45ºC and 0.1% lipase in nano-emulsion with 90% water and an O/S of 50/50, measured by TEM.

Temperature	25ºC	45ºC
Nano-emulsion diameter by Cryo-TEM	16.7 ± 3.6 nm	-
Nano-emulsion diameter by LBS (24h)	29.1 nm	47.9 nm
Nanoparticles diameter by TEM	15.1 ± 4.0 nm	20.7 ± 4.71 nm
PDI	1.21	1.15

At 25ºC, the mean particle size of poly(Exaltolide®) nanoparticles (15.1 ± 4.0 nm) was similar to the size of the nano-emulsion droplets (16.7 ± 3.6 nm) determined by Cryo-TEM. This result confirms that the nano-emulsion droplet acts as template. Knowing from the section 4.2.1.3 that the nano-emulsion droplet size increases at 45ºC to values of approximately 48 nm (assessed by

LBS), nanoparticle size around 30 nm (measured by TEM) was expected when synthesized at 45ºC. However, at 45ºC, nanoparticles present a lower size (20.7 ± 4.71 nm) than the nano-emulsion droplet.

This difference can be explained by two factors. On one hand, it was shown that the polymerization starts within the first minutes after the lipase addition at 25ºC (Figure 4.19), thus making the interface less flexible, less permeable and preventing the increase of the droplets size that was observed for nano-emulsions left at 45ºC (Figure 4.17). On the second hand, lipases are well known for their property to adsorb at interfaces (Reis, 2009), it is then suggested that the lipase acts as nano-emulsion stabilizer and prevent the increase of droplet size when the sample is left under reaction at 45ºC. The polydispersity index calculated for the nanoparticles obtained at both temperature are relatively high (>1.05), indicating that the nanoparticle dispersions are not monodispersed.

4.3.3.2. Influence of enzyme concentration

Another parameter that affects polymerization is the enzyme concentration. In order to study this parameter, the reaction was carried out at 45ºC for 24h with 0.1, 0.035 and 0.01% lipase. The evolution of the conversion, followed over time by ^{1}H NMR spectroscopy, is plotted as a function of time in Figure 4.24. The NMR spectra are given in Appendices 2 and 3.

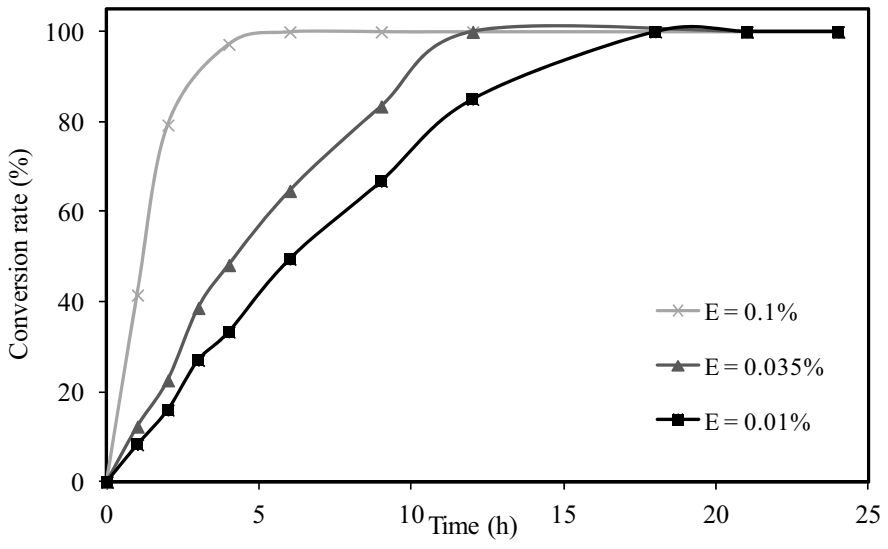

Figure 4.24 : Monomer conversion vs. time for the synthesis of poly(Exaltolide®) nanoparticles obtained by eROP at 45ºC with 0.1% (Exp. 2), 0.035% (Exp. 3) and 0.01% (Exp. 4) in nano-emulsion with 90% water and an O/S of 50/50.

The monomer conversion rate increases linearly until a plateau is reached at 100% of monomer conversion after 4, 10, and 15 hours for the respective enzyme concentration of 0.1, 0.035 and 0.01%. In the range of concentrations studied, the higher the enzyme concentration, the faster the reaction is. Nevertheless, even at a really low enzyme concentration (0.01%), the reaction is completed after 24h. Compared to eROP in organic solvent that requires several days to reach good conversion rate (Uyama, 1996; Bisht, 1997), the reaction in nano-emulsion enables faster polymerization of lactone. This observation agrees with results reported on reactions in confined media such as nano-emulsions (Taden, 2003; Shork, 2005; Målberg, 2010).

The influence of lipase concentration on poly(Exaltolide®) molecular weight and crystallinity was determined by GPC and DSC measurements. The DSC profiles are shown in Appendix 4. Data are gathered in Table 4.11.

Table 4.11 : Molecular weight and calorimetric properties for poly(Exaltolide®) nanoparticles obtained by eROP at 45ºC and 0.1% (Exp. 2), 0.035% (Exp. 3) and 0.01% (Exp. 4) in nano-emulsion with 90% water and an O/S of 50/50. Mn is the average number molecular weight, T and ΔH are the temperature and the difference of enthalpy, respectively. The sub indices m and c correspond to melting and crystallization respectively. χ is the crystallinity degree.

Exp.	Lipase (%)	Mn[a] (g/mol)	Tm (ºC)[b]	ΔHm (J/g)[b]	Tc (ºC)	ΔHc (J/g)	Tm (ºC)[c]	ΔHm (J/g)[c]	X[d]
2	0.1	1070	82.13	-208.22	69.85	172.53	78.16	-175.84	75.5
3	0.035	1060	81.62	-203.65	69.16 56.14	122.79 44.16	84.62 76.80 59.25	-3.48 -132.68 -25.09	69.2
4	0.01	1050	82.41	-213.56	72.15	169.99	81.48 76.68 60.31	-15.57 -127.03 -24.5	71.7

[a] Molecular weight measured by GPC universal calibration; [b] From the first heat; [c] From the second heat; [d] Determined from DSC considering ΔH^0_m = 233 J/g for 100% crystalline polymer (Lebedev, 1984).

The measured molecular weight was equivalent whatever the enzyme concentration indicating that the latter does not influence the size of the polymer chain. Looking at the calorimetric data, melting temperature and crystallization temperature from the first heating scan and cooling scan do not show major differences by changing the enzyme concentration. These results confirm that all samples underwent similar thermal history. Looking then at the second heating scan, the

presence of new melting peaks are observed by decreasing the enzyme concentration. This result is explained by a decrease in the number of initiated chain at lower enzyme concentration; the reaction takes then longer and leads to the formation of a mixture of polymer of different crystallinity.

SAXS measurements were performed in order to find out any changes in the crystalline structure and X-ray diffraction patterns. The results are presented in Figure 4.25.

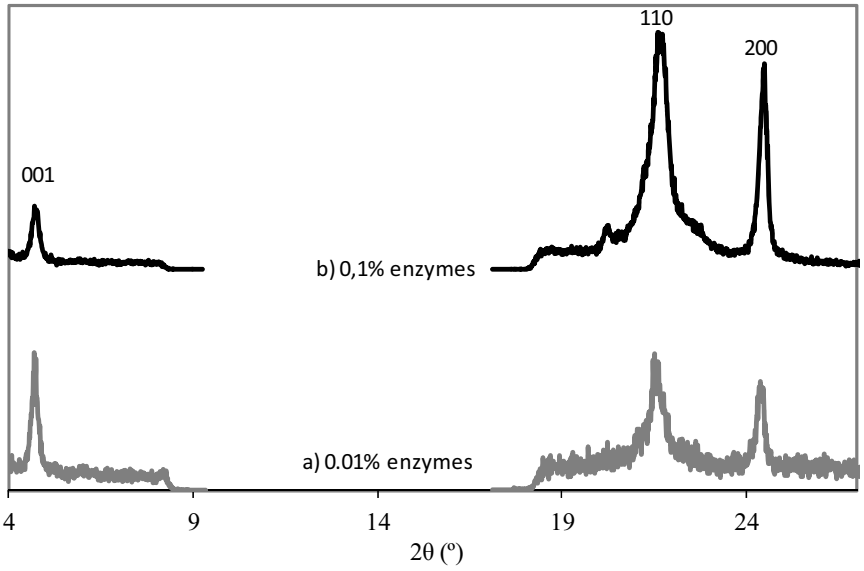

Figure 4.25 : X-ray diffraction pattern of poly(Exaltolide®) nanoparticles obtained by eROP at 45ºC and 0.1% (Exp. 2) and 0.01% (Exp. 4) lipase in nano-emulsion with 90% water and an O/S of 50/50.

No differences were observed from the diffraction patterns by varying the enzyme concentration. At low concentration of enzyme, the different melting temperature obtained (Table 4.11) can be explained by the presence of oligomers with lower molecular weight but identical crystalline structure. The oligomers were not detected by GPC due to the limit of the exclusion volume of the column. As described previously, a pseudo-orthorhombic crystalline structure was attributed to the poly(Exaltolide®) nanoparticles (Gazzano, 2003).

4.3.3.3. Influence of nano-emulsion template

Nano-emulsions with O/S ratios of 40/60 (Exp. 5), 50/50 (Exp. 2) and 60/40 (Exp. 6) were studied. All polymerizations were left to react for 24h under stirring at a fixed temperature of 45ºC and enzyme concentration of 0.1%. Reactions were followed over time by ^{1}H NMR spectroscopy and GPC. Complete conversion of Exaltolide® was confirmed by ^{1}H NMR (Appendices 2 and 3) and no variation of molecular weight (2647 g/mol) was observed. Samples

were visualized by TEM and the image data analysis allows the determination of the particle size distribution (PSD) presented in Figure 4.26 for the three nano-emulsions studied.

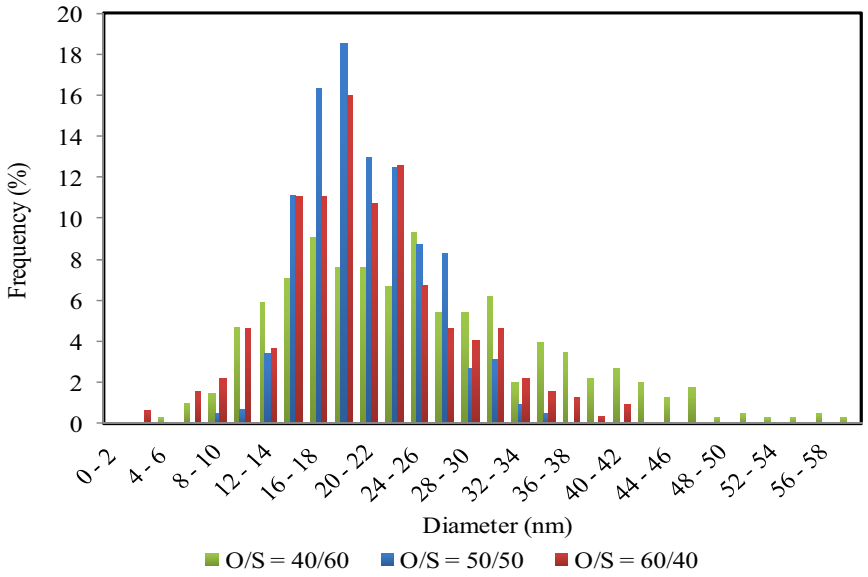

Figure 4.26 : Particle size distribution of poly(Exaltolide®) nanoparticles obtained by eROP at 45ºC and 0.1% lipase in nano-emulsion with 90% water and an O/S of 40/60 (Exp. 5), 50/50 (Exp. 2) and 60/40 (Exp. 6).

All nanoparticle dispersions show unimodal distributions centered on a value between 16 and 22 nm. Only small deviation in the PSD was observed between the three O/S ratios. It is worth noting that at the lowest O/S ratio, the PSD is slightly larger. Table 4.12 summarizes the values of the mean diameter calculated by TEM image analysis as well as the calorimetric data obtained by DSC (Appendix 4).

Table 4.12 : Average diameters, standard deviations and calorimetric data of poly(Exaltolide®) nanoparticles obtained by eROP at 45ºC and 0.1% lipase in nano-emulsion with 90% water and an O/S of 40/60 (Exp. 5), 50/50 (Exp. 2) and 60/40 (Exp. 6). d is the diameter. NEM and NP correspond to nano-emulsion and nanoparticle, respectively. T and ΔH are the temperature and the difference of enthalpy, respectively. The sub indices m and c correspond to melting and crystallization respectively. χ is the crystallinity degree.

Exp	O/S	d_{NEM}(nm)	d_{NP}(nm)	PDI	Tm (ºC)[a]	ΔHm (J/g)[a]	Tc (ºC)	ΔHc (J/g)	Tm (ºC)[b]	ΔHm (J/g)[b]	χ^c
5	40/60	16.0 ±5.1	25.4±11.4	1.65	85.9	-181.4	76.7	154.5	78.9	-158.6	68.1
2	50/50	24.9 ±8.0	20.7±4.7	1.15	82.1	-208.2	69.9	172.5	78.2	-175.8	75.5
6	60/40	36.1 ±11.3	22.7±6.7	1.25	80.0	-197.9	69.8	165.8	77.3	-166.5	71.5

[a] From the first heat; [b] From the first heat; [c] Determined from DSC considering ΔH^0_m = 233 J/g for 100% crystalline polymer (Lebedev, 1984).

The size of the nano-emulsion template increases by increasing the O/S ratio while no clear tendency was observed for the nanoparticles. The size of the nanoparticles cannot be correlated to the average droplet diameter of the nano-emulsion template. One hypothesis to this observation is that the addition of lipase, with interfacial properties, modifies the size of the template (Reis, 2009). Looking at the calorimetric data, melting and crystallization events for the three polymers follows the same tendency as previously detailed in section 4.3.3.1. It should be noted that the crystallinity (**χ**) of the polymer decreases by increasing the size and polydispersity of the particles (Cho, 2006).

4.3.4. Synthesis and characterization of poly(OH-Exaltolide®) nanoparticles by eROP

Within the aim to synthesize functionalized poly(Exaltolide®) nanoparticles, a monomer containing a functional hydroxyl group, OH-Exaltolide®, was polymerized in nano-emulsion. Nano-emulsions of the water/Cremophor®EL/OH-Exaltolide®:squalane system, described in section 4.2.2, were used as template. The concentration of water was fixed at 90%, the O/S ratio at 50/50 and the OH-Exaltolide®/squalane ratio at 98/2. The nano-emulsions were prepared by the PIC method. Due to the similarity in structures of the two monomers, the reaction parameters previously determined for Exaltolide® (Exp. 2) were fixed. The reaction was then carried out with 0.1% lipase at 45ºC for 24h and followed by ^{1}H NMR spectroscopy.

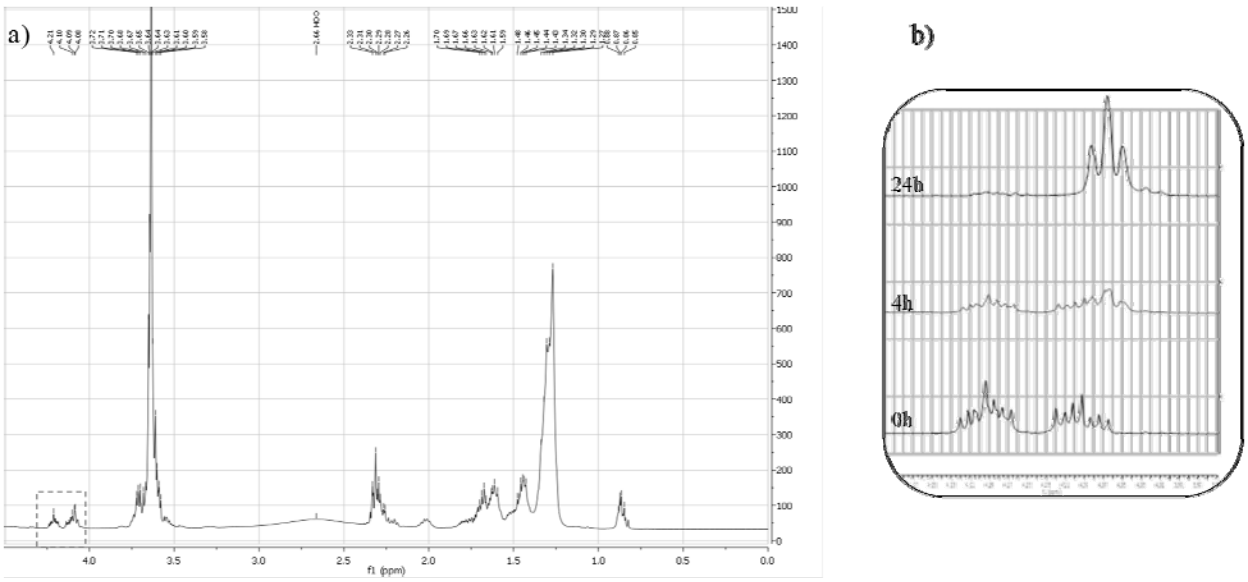

Figure 4.27: a) Typical ^{1}H NMR spectrum of a poly(OH-Exaltolide®) nanoparticle dispersion after 4h of eROP at 45°C and 0.1% lipase in nano-emulsion with 90% water and an O/S ratio of 50/50 and b) Evolution of the monomer and polymer characteristic peaks over time.

Figure 4.27 shows a typical spectrum obtained during the polymerization of poly(OH-Exaltolide®). The identification of each peak is similar to that of poly(Exaltolide®) described in section 4.3.3.1. The region of the spectrum between δ = 4.0 and 4.2 ppm (Figure 4.27.b) is the region of interest to follow the reaction over time as it shows the characteristic peaks of the monomer and the polymer. First it should be noted that compared to Exaltolide®, OH-Exaltolide® monomer do not present a triplet but a multiplet explained by the presence of the OH group in the 11 and 12 position of the macrocycle. Moreover, Cremophor®EL present in the system shows a multiplet in this region of the spectrum (Appendix 2). After 4h of reaction, the presence of a triplet centered on 4.09 ppm corresponding to the ester methylene (-C$\underline{H_2}$-O-C=O) of the polymer appears. The exact conversion cannot be calculated by means of NMR spectroscopy as the monomer and the polymer do not present distinct peaks in this region and their respective integrations cannot be determined. Nevertheless, after 24h of reaction, a single triplet is observed in this region of the NMR spectra thus, suggesting the final conversion of the monomer. The final poly(OH-Exaltolide®) was then characterized by its molecular weight (GPC) and thermal behavior (DSC) and compared to poly(Exaltolide®) and OH-Exaltolide® monomer. The results are shown in Table 4.13.

Table 4.13 : Molecular weight and Calorimetric data of OH-Exaltolide®, poly(OH-Exaltolide®) and poly(Exaltolide®) obtained by eROP at 45°C and 0.1% lipase in nano-emulsion with 90% water and an O/S ratio of 50/50. Mn is the average number molecular weight, T and ΔH are the temperature and the difference of enthalpy, respectively. The sub indices m and c correspond to melting and crystallization respectively. χ is the crystallinity degree.

Sample	Mn[a] (g/mol)	Tm (°C)[b]	ΔHm (J/g)[b]	Tc (°C)	ΔHc (J/g)	Tm (°C)[c]	ΔHm (J/g)[c]	χ[d]
OH-Exaltolide®	256	56.2 60.0	-7.9 -10.3	-	-	-	-	°-
Poly(Exaltolide®)	1070	82.1	-208.2	69.9	172.5	78.2	-175.8	75.5
Poly(OH-Exaltolide®)	1554	79.2 84.5	-239.3 -66.2	74.9	135.9	73.9 85.2	-73.7 -56.8	-

[a] Measurement by GPC universal calibration; [b] From the first heat; [c] From the second heat; [d] Determined from DSC considering ΔH0m = 233 J/g for 100% crystalline polymer (Lebedev, 1984).

The average molecular weight value of poly(OH Exaltolide®) was 1554 g/mol and corresponds to a polymerization degree of 6. The average molecular weight is similar to that of poly(Exaltolide®), indicating that the presence of the hydroxyl group do not interfere in the polymerization. Looking at the calorimetric data, two melting peaks were observed for OH-Exaltolide® and poly(OH-Exaltolide®) while only one peak was described for poly(Exaltolide®).

The monomer OH-Exaltolide® presents a melting temperature of 60ºC (confirmed by the literature) and a shoulder (56ºC) to the main peak reveals the presence of impurities which might come from the synthesis (presence of the OH-group on the C11 position of the Exaltolide® ring). This result might also explain the presence of multiplet observed by 1H NMR spectroscopy but this aspect was not further studied. As far as poly(OH-Exaltolide®) is concerned, two endothermic peaks at 74 and 85ºC were observed before and after cooling to 25ºC, thus indicating the presence of polymers with either two molecular weights or two crystallinities. Moreover, considering the structure of Cremophor®EL (presence of ester groups), its possible insertion in the polymer structure can be considered. It should be mentioned that the activity of the Lipase is higher for eROP than for the hydrolysis of aliphatic esters such as Cremophor®EL, thus suggesting a preferential polymerization of the lactone than with Cremophor®EL.

Table 4.14 : Distances of the main reflections of the X-ray diffraction pattern of poly(OH-Exaltolide®) and poly(Exaltolide®) obtained by eROP at 45°C and 0.1% lipase in nano-emulsion with 90% water and an O/S ratio of 50/50.

Polymer	x(001) (nm)	x(110) (nm)	x(200) (nm)
Poly(Exaltolide®)	2.0	0.411	0.363
Poly(OH-Exaltolide®)	2.11	0.418	0.386

Similar reflection bands than those observed for poly(Exaltolide®) were measured by SAXS and the interpretation of each band was described in section 4.3.3.1. The distances of the main reflection bands of poly(Exaltolide®) and poly(OH-Exaltolide®) are presented in Table 4.14. Slightly higher distances were observed for poly(OH-Exaltolide®). The differences might be due to the presence of the OH groups in poly(OH-Exaltolide®) that increases the space between the polymer chains. The presence of two structured crystalline polymers was not observed by SAXS thus confirming the hypothesis emitted with the DSC results that the same polymer having various molecular weight but the same crystalline structure is evidenced. Poly(OH-Exaltolide®) nanoparticles were visualized on TEM micrographs (Figure 4.28).

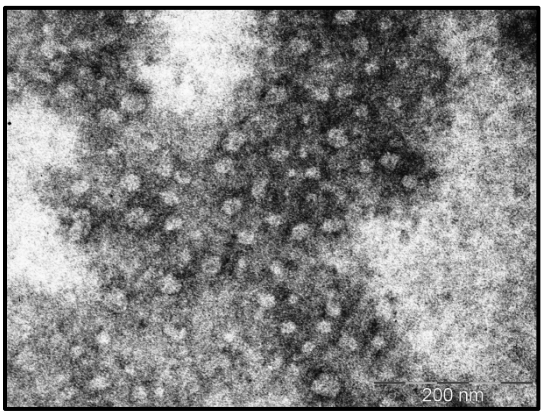

Figure 4.28 : TEM micrograph of poly(OH-Exaltolide®) of poly(OH-Exaltolide®) and poly(Exaltolide®) obtained by eROP at 45°C and 0.1% lipase in nano-emulsion with 90% water and an O/S ratio of 50/50.

The average diameter, calculated over few nanoparticles, was around 21.3 ± 5.4 nm. The size of the nanoparticle is similar to the size of the nano-emulsion template (15.9 nm measured by Cryo-TEM analysis) and comparable to that of poly(Exaltolide®).

4.3.5. Copolymerization by eROP

In order to show whether the degree of functionalization can be controlled, copolymerization of Exaltolide® with OH-Exaltolide® was studied. Another lactone Habanolide, an unsaturated Exaltolide®, was also used as comonomer with Exaltolide® for polymerization in nano-emulsion. Three ratios of Exaltolide®/co-monomer were studied: 50/50; 75/25; 90/10 and the copolymers were compared to the homopolymers of poly(Exaltolide®), poly(OH-Exaltolide®) and poly(Habanolide®). Nano-emulsions of the water/Brij®96V/Exaltolide®:comonomer:hexadecane system with 90% water, an O/S ratio of 70/30 and a monomer: hexadecane ratio of 90/10 were used. The use of hexadecane instead of squalane was proved not to affect the properties of the polymer. The co-monomer was incorporated to the oil phase of the nano-emulsion which was formed by the PIT method. White bluish nano-emulsions were formed at the studied O/S ratio. The polymerization was carried out at 45ºC for 24h under stirring and complete conversion was assumed. The NMR spectra of the final copolymers are plotted in Figure 4.29. The entire spectra do not present much interest for this study and as described in section 4.3.2.1, only the region of the NMR spectra between $\delta = 4$ and $\delta = 4.15$ ppm is of interest and shown in Figure 4.29.

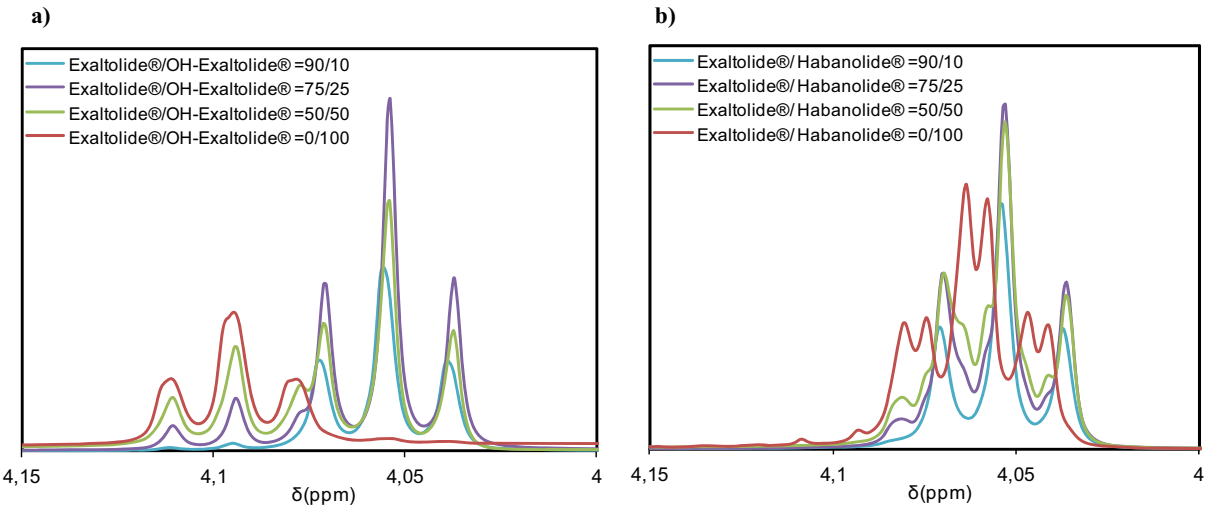

Figure 4.29 : Ester methylene -C$\underline{H}_2$-O-C=O region of the ^{1}H NMR spectrum of a) Exaltolide®/OH-Exaltolide® copolymers and b) Exaltolide®/Habanolide® copolymers obtained by eROP at 45°C and 0.1% lipase in nano-emulsion with 90% water and an O/S ratio of 70/30.

As commented previously, the monomers Exaltolide® and OH-Exaltolide® present chemical shift at δ = 4.10 (triplet) and δ = 4.05 - 4.23 (multiplet) respectively. It is worth noting that those peaks are not observed on the Figure 4.29.a, thus confirming the complete conversion of the comonomers. Figure 4.29.a shows the presence of two triplets. The first triplet centered on δ = 4.05 ppm was attributed to the ester methylene proton (-C$\underline{H}_2$-O-C=O) between two Exaltolide® units while the second triplet, centered on δ = 4.09 ppm was attributed to the ester methylene proton between two OH-Exaltolide® units, as characterized previously in section 4.3.3.1 and 4.3.4. The ratios of one triplet to the other, calculated from the ratio of the integration of each peak, are in agreement with the initial ratios of the comonomers in the oil droplet (Table 4.15). In order to find out whether copolymerization occurs, ^{13}C NMR spectroscopy was performed.

As far as the copolymerization with Habanolide® is concerned, a multiplet is observed in the region 4.0-4.2 ppm (Figure 4.29.b). When the polymerization is carried out using only Habanolide as monomer (Exaltolide®/Habanolide® = 0/100), two overlapped triplet were observed centered on δ = 4.06 and 4.07 ppm. Those two triplets were attributed to the ester methylene proton between two Habanolide® units (the double bond in C11 and C12 implies the presence of 2 triplets). Then, a triplet centered on a δ = 4.09 ppm was observed corresponding to the ester methylene proton between two Exaltolide® units. By polymerizing simultaneously both monomers in the oil droplets, the two triplets of the ester methylene proton between two Habanolide® units were overlapped with the triplet of the ester methylene proton between the two Exaltolide® units. ^{1}H NMR spectroscopy confirms the polymerization of both monomers but do not permit to conclude on the copolymerization. Therefore, ^{13}C NMR was performed within the

aim to determine the copolymerization. Figure 4.30.a shows the ^{13}C NMR spectra of the copolymer from Exaltolide® and OH-Exaltolide® at a ratio 50/50. In order to confirm the copolymer structure, the expanded peak region between δ = 64.2 and 64.6 ppm, attributed to the carbon -$\underline{C}H_2$-O-C=O was examined (Figure 4.30.b).

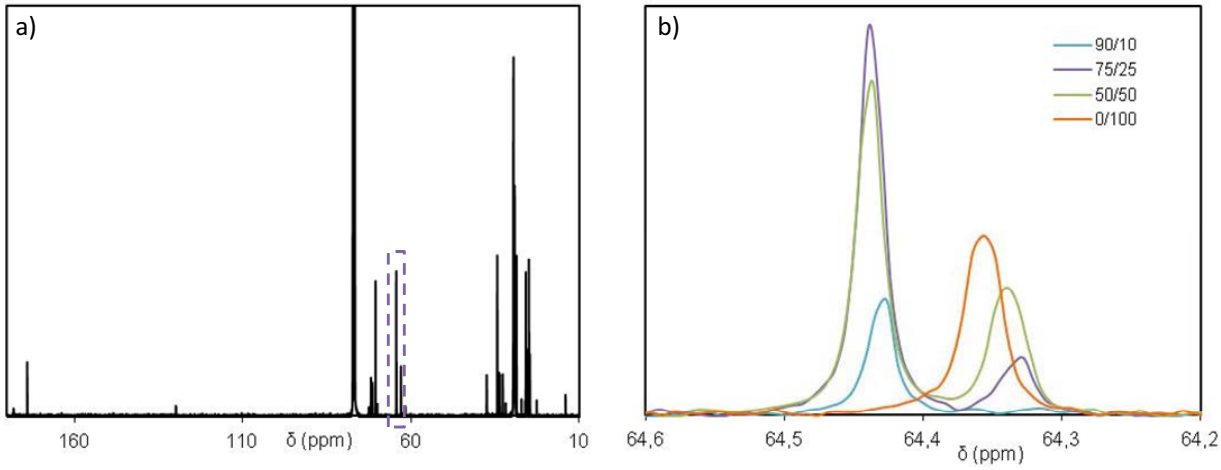

Figure 4.30 : a) Typical ^{13}C spectrum of a copolymer of Exaltolide® and OH-Exaltolide®(50/50) and b) Ester methylene -$\underline{C}H_2$-O-C=O region of the ^{13}C NMR spectrum of copolymers obtained by eROP at 45°C and 0.1% lipase in nano-emulsion with 90% water and an O/S ratio of 70/30 at various Exaltolide®/OH-Exaltolide® ratios.

By polymerizing both monomers simultaneously in the oil droplets of the nano-emulsions, random copolymerization of the comonomers was expected. By NMR, peaks corresponding to the ester methylene carbon between an Exaltolide® and a comonomer unit (OH-Exaltolide®) were expected (Figure 4.31).

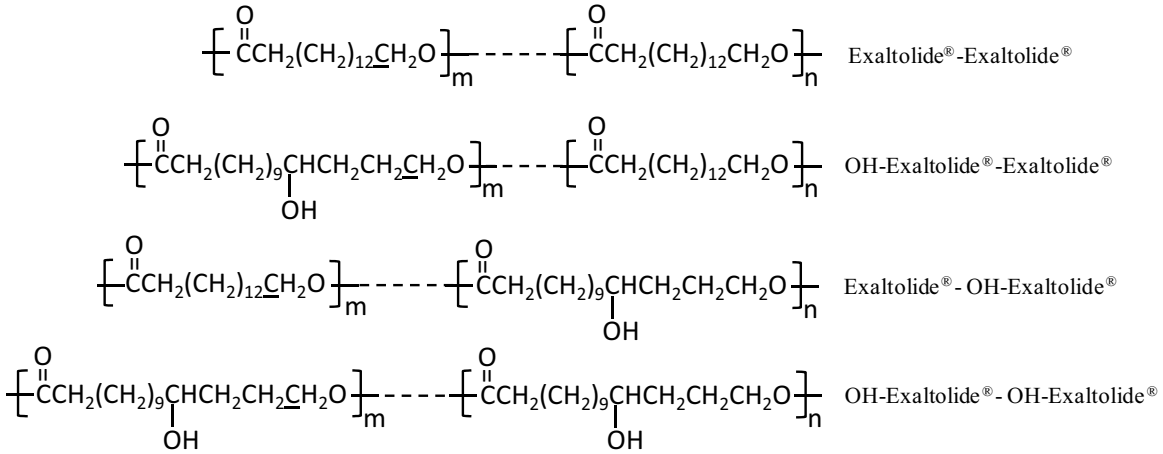

Figure 4.31 : Possible bonds in the copolymer of Exaltolide® and OH-Exaltolide® (based on the work of Uyama, 1996).

Unfortunately, the peaks corresponding to the OH-Exaltolide®-Exaltolide® or Exaltolide®-OH-Exaltolide® bonds were not observed and this behavior was explained by the extremely low effect

of the OH in the C12 position on the ester methylene in the C15 position. The NMR spectra confirms the conversion of each monomer but do not permit to conclude on copolymerization. Nevertheless, the probability that each monomer polymerize with itself and not with the comonomer while they are both present in the droplet of the nano-emulsion is low. Therefore, in order to confirm the copolymerization, the DSC profile of the homopolymers and copolymers were plotted on Figure 4.32.

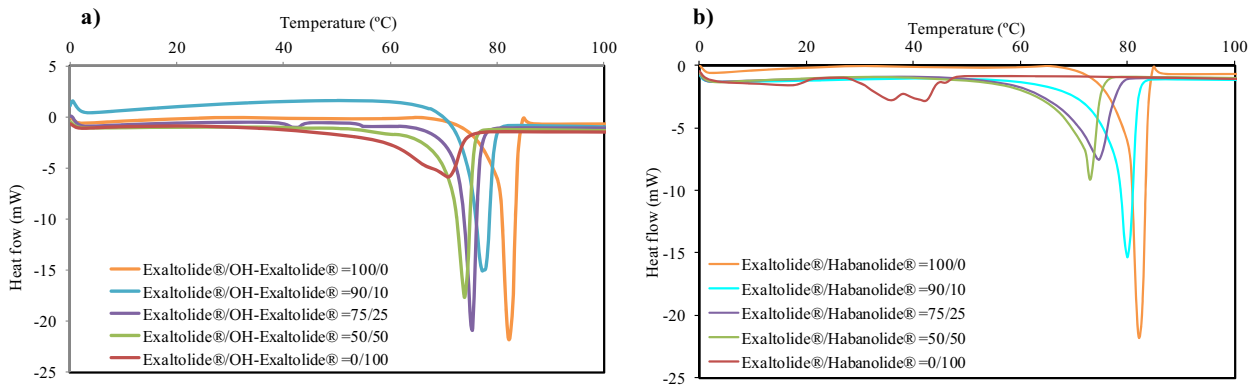

Figure 4.32 : DSC heating curves of homopolymers and copolymers of a) Exaltolide®/OH-Exaltolide® and b) Exaltolide®/Habanolide obtained by eROP at 45°C and 0.1% lipase in nano-emulsion with 90% water and an O/S ratio of 70/30.

The homopolymers poly(Exaltolide®) shows a single endothermic peak at the highest melting temperature (82ºC) as described in section 4.3.3. Poly(OH-Exaltolide®) and poly(Habanolide®) present a large endothermic peak at a melting temperature of 71ºC (slightly lower than determined in section 4.3.4 due to the different conditions of the template) and 43ºC respectively. All copolymers show a single melting process at temperatures intermediate to those of the reference homopolymers (Table 4.15).

Table 4.15 : Calculated ratio of each comonomer unit and calorimetric data of the Exaltolide®/ OH-Exaltolide® and Exaltolide®/ Habanolide® copolymers obtained by eROP at 45°C and 0.1% lipase in nano-emulsion with 90% water and an O/S ratio of 70/30. T_m and ΔH_m are the temperature and difference of enthalpy of melting.

Comonomer	Ratio Exaltolide®/comonomer	Ratio Exaltolide®/comonomer[a]	T_m (°C)[b]	ΔH_m (J/g)[b]
OH-Exaltolide®	0/100	-	70.5	132.8
	50/50	57/43	73.26	137.2
	75/25	82/18	74.65	150.7
	90/10	94/6	76.67	165.4
	100/0	-	82.1	208.2
Habanolide®	0/100	-	41.9 (large)	58.0
	50/50	-	72.7	130.1
	75/25	-	74.4	139.9
	90/10	-	79.5	164.6
	100/0	-	82.1	208.2

[a] Ratio of Exaltolide® to comonomer unit in the final copolymer calculated from the ratio of NMR peak integrations [b] From the first heat.

The presence of a single peak suggests the formation of a copolymer instead of a mixture of two homopolymers. The melting transition systematically shifts to lower temperatures with increasing the content of co-monomer (OH-Exaltolide® or Habanolide®) units in the copolymer. The homopolymers of OH-Exaltolide® and Habanolide® show lower crystallinity than poly(Exaltolide®) thus by increasing the amount of the comonomer, the melting point of the copolymers decreases, for example from 82 to 73ºC when 50% of Exaltolide® was replaced by OH-Exaltolide®. Similar behaviors were described in the literature for random copolymers (Kumar, 2000; Meulen, 2011). Moreover, Ceccorulli *et al.* in 2005 described the cocrystallization of random copolymers of PDL and PCL suggested by the high values of melting enthalpy. Considering the large melting enthalpy values in Table 4.15, it can be said that the comonomer units cocrystallize, giving rise to a conspicuous crystal phase (Ceccorulli, 2005). The combination of various techniques such as NMR and calorimetry permit to conclude that copolymerization of comonomers occurs by eROP.

Summary:

Poly(Exaltolide®) nanoparticles were synthesized successfully by eROP initiated by the addition of 0.1% lipase at 45ºC for 24h. The effect of reaction parameters such as temperature and enzyme concentration on poly(Exaltolide®) formation have been investigated. An increase of temperature and enzyme concentration has revealed an increase of the reaction kinetics without significant changes in the molecular weight and crystallinity. Poly(Exaltolide®) nanoparticles have been observed by TEM thus, confirming the template effect of nano-emulsions. The reaction conditions for poly(Exaltolide®) formation have been applied to the hydroxy functionalized Exaltolide® and the formation of crystalline poly(OH-Exaltolide®) nanoparticles have been confirmed by means of GPC, DSC, SAXS/WAXS and TEM. Finally, the copolymerization of two lactone monomers has been carried out and the results allow concluding that the degree of functionalization can be controlled by the ratio of the two comonomers. The functionalization degree permits a regulation of the hydrophobicity of the nanoparticles by the number of OH-group present at the interface.

4.4. POTENTIAL APPLICATIONS OF POLYESTER NANOPARTICLES FOR THE DELIVERY OF VOLATILE COMPOUNDS

The perfumery industry deals with a large variety of volatile fragrant molecules, generally associated with a pleasant feeling in consumer products. Because of their high volatilities, the stability and long lasting perception of those molecules is quite limited. Thereby the perfumery industry is interested in delivery systems that permit a control of the fragrant smell. Nanoparticles and especially polymeric nanoparticles can be used in various applications for the pharmaceutical, food or cosmetic fields. In this work, the use of selected polymeric nanoparticles for the controlled release of volatile compounds was studied. In a first approach, the affinity of poly(Exaltolide®) and poly(OH-Exaltolide®) nanoparticles with volatile fragrant molecules was investigated. In another approach, the use of the polyester nanoparticles to stabilize emulsions containing volatile fragrant molecules as dispersed phase (Pickering emulsions) and, in a second step, to cross-link the nanoparticles at the interface of the Pickering emulsions to form permeable microcapsules was investigated. Finally, the release of the volatile fragrant molecules from the previously formed microcapsules was described.

4.4.1. Polyester nanoparticle affinity to volatile compounds

The affinity of polyester nanoparticles with volatile fragrant molecule was studied by adding the nanoparticles to a solution of water, ethanol and a mixture of 11 volatile fragrant molecules. The evaporation of the volatile compounds was followed over time by gas chromatography and compared to a reference without nanoparticles. Gas chromatography enables the determination of the evaporation over time of each compound of a perfume mixture.

In the case of poly(Exaltolide®) nanoparticles, two concentrations were studied: 1.5 and 3%. Among the 11 volatile fragrant molecules, Manzanate®, Ethyl butyrate natural, Limonene, (Z)-3-hexen-1.ol, (Z)-3-hexenyl acetate and Zestover present the same mass loss in the presence of nanoparticle as in the reference indicating that the nanoparticles do not have any affinity with those molecules and do not permit to control their release. Moreover, an increase of the nanoparticle concentration in the mixture (3%) does not reduce the mass loss over time. On the other hand, the release of certain compounds such as Lymolene®, Benzyl acetate, Romascone®, citral and pear ester was slowed down by the addition of increasing amount of poly(Exaltolide®)

nanoparticles in the mixture. As an example, Figure 4.33 shows the mass loss of Ethyl butyrate natural and Romascone® as a function of time for the reference and the two nanoparticle concentrations studied.

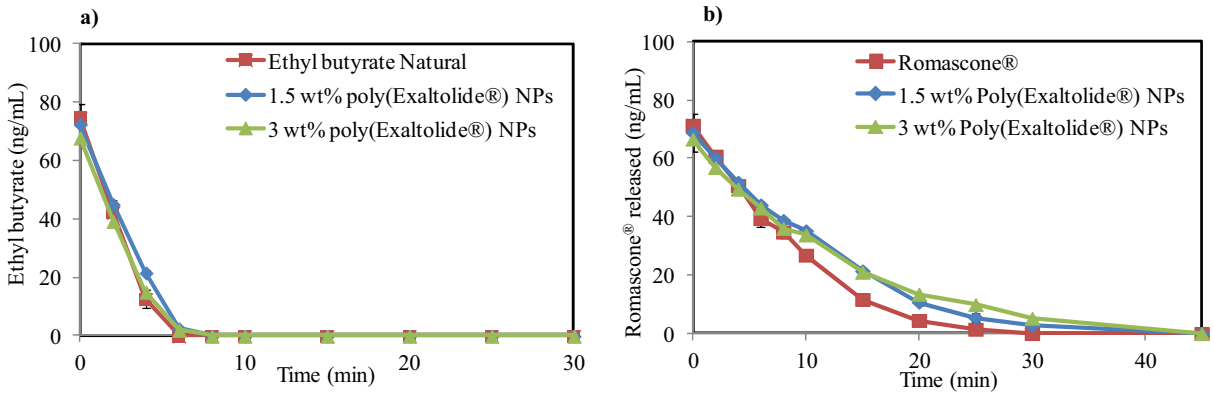

Figure 4.33 : Mass loss of a) Ethyl butyrate natural and b) Romascone® as a function of time from a mixture of water/ethanol/poly(Exaltolide®) nanoparticles at concentrations of 1.5 and 3% and comparison with a reference solution.

Concerning poly(OH-Exaltolide®) nanoparticles, one concentration was studied at 4.5% and no effect was observed on the mass loss over time for Manzanate®, Ethyl butyrate natural, Limonene, (Z)-3-hexen-1.ol, (Z)-3-hexenyl acetate and Zestover. Figure 4.34.a. shows that the mass loss of Ethyl butyrate in presence of poly(OH-Exaltolide®) nanoparticles is merged with the reference sample, meaning no association between ethyl butyrate and poly(OH-Exaltolide®) nanoparticles . As well as for poly(Exaltolide®) nanoparticles, some retention was observed on raw materials such as Lymolene®, Benzyl acetate, Romascone®, citral and pear ester. An example of the retention of Romascone® is presented in Figure 4.34.b. Comparing with the results of Figure 4.33.b, poly(Exaltolide®) in lower concentration (3%) enable a better control release of the Romascone®.

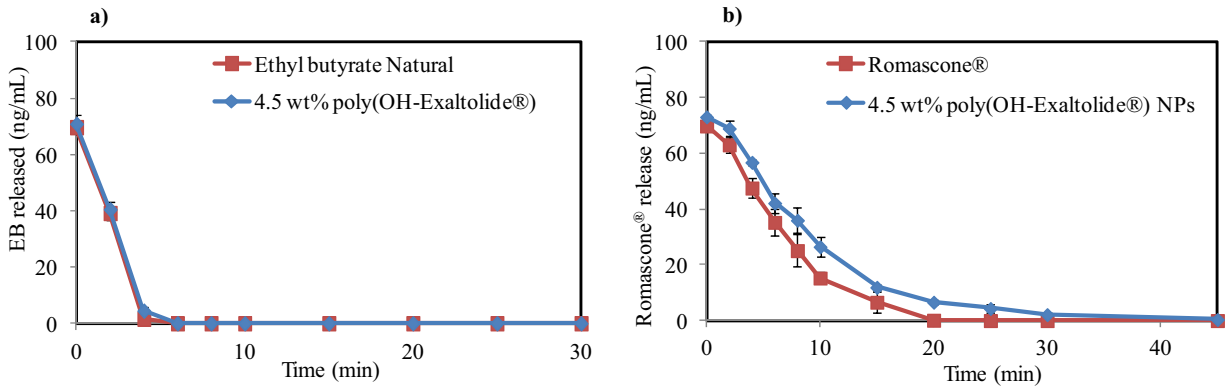

Figure 4.34 : Mass loss of a) Ethyl butyrate natural and b) Romascone® as a function of time from a mixture water/ ethanol/poly(OH-Exaltolide®) nanoparticles at a concentration of 4.5% and comparison with a reference.

First, it should be noted that the profiles of evaporation are not linear because a mixture of volatile fragrant molecules that interact between each other, is analyzed. Moreover, it is known from previous studies that after 5 minutes of experiment, the total amount of ethanol was evaporated. Thus, this experiment enables the study of the affinity of the nanoparticles with the volatile fragrant molecules without interference of the solvent. According to the volatility values presented in Table 3.2, poly(Exaltolide®) and poly(OH-Exaltolide®) nanoparticles show some effect on the mass loss of low volatile compounds but do not enable any control release of compounds having high volatilities. This behavior was reported in the article of Berthier *et al.* in 2010 using Pluronic® polymers. The authors also reported that ethyl butyrate which is soluble (40-60%) in ethanol do not form any aggregate with Pluronic® polymers while Romascone® which is insoluble forms aggregates such as micelles (Berthier, 2010). A similar behavior was suggested with the poly(Exaltolide®) and poly(OH-Exaltolide®) nanoparticles. The suggested aggregation of volatile fragrant molecules with polymeric nanoparticles may decrease the concentration of volatiles in the solvent phase and therefore its chemical potential. The reduction of the chemical potential may decrease its vapor pressure under these conditions and thus decreasing its evaporation.

Summary:

The affinity of the poly(Exaltolide®) and poly(OH-Exaltolide®) nanoparticles with volatile fragrant compounds was pointed out by a reduction of the evaporation of certain volatile fragrant molecules, suggesting the formation of aggregates of polymer and volatile compounds.

4.4.2. Pickering emulsions stabilized by polyester nanoparticles

This section deals with the results on the formation of Pickering emulsions containing volatile fragrant molecules as dispersed phase and stabilized by the polyester nanoparticles described in section 4.3. As a first step, the components of those emulsions were selected and the behavior of the nanoparticles in the different phases of the emulsion was investigated. Then, single oil-in-water emulsions stabilized by poly(Exaltolide®) nanoparticles were studied as a proof of concept. Finally, a systematic study of model perfume-in-water emulsions was carried out.

4.4.2.1. Selection of the emulsion components and preliminary study

- **Oil components**

Among the large number of volatile fragrant molecules used in the perfumery industry, three single oil compounds (Benzyl acetate, Manzanate® and Limonene) were chosen for their respectively high, medium and low polarity and volatiliies. Nevertheless, knowing that a commercial perfume might contain more than 50 compounds, its behavior in solution can be very different from that of single oils. As a compromise between a single oil and a commercial product, a model perfume (MP), made of 5 volatile fragrant molecules was selected for a systematic study. Considering that another purpose of this thesis was to carry out a cross-linking reaction between the nanoparticles at the interface of the emulsion and isocyanate, the oil phase of the emulsion should not contain any OH- group that might react with isocyanate. Therefore, the MP was designed within this aim. The main characteristics of these oils (log P, density, and volatility) are gathered in Table 4.16 and the measured values of the surface tension are also indicated.

Table 4.16 : Main characteristics and measured surface tension of the oil components.

Liquid phase	Log P	Density	Volatility (µg/L)	Surface tension (mN/m)
Benzyl acetate	1.6	1.054	285	35.9
Manzanate®	2.8	0.864	351000	26.3
Limonene	4.45	0.84	4293	25
Model Perfume	3-4	0.9484	-	26.9

- **Polymeric nanoparticles:**

Polyester nanoparticles, described in section 4.3, made of poly(Exaltolide®) and poly(OH-Exaltolide®) were selected for the preparation of Pickering emulsions. A summary of their main characteristics is presented in Table 4.17.

Table 4.17 : Main characteristics of poly(Exaltolide®) and poly(OH-Exaltolide®) nanoparticles used in this section.

Nanoparticle types	Poly(Exaltolide®)	Poly(OH-Exaltolide®)
nanoparticle mean diameter [a] (nm)	20.7 ± 4.7	21.3 ± 5.4
Molecular weight [b] (g/mol)	2647	1554
Melting point [c] (ºC)	78.2	79.8
Crystallinity degree [c]	75.5	-

[a] by TEM image analysis [b] by GPC measurements [c] by DSC measurements.

- **Preliminary study**

The ability of the nanoparticles to adsorb at the O/W interface is primarily dependent on the wettability of the particles (Binks, 2000a). The wettability of both poly(Exaltolide®) and poly(OH-Exaltolide®) nanoparticles was first characterized by measurements of the contact angle by capillarity of water in a tube filled with nanoparticles (method described in section 3.3.7). The values of the measured contact angles are summarized in Table 4.18.

Table 4.18: Contact angle between poly(Exaltolide®) and poly(OH-Exaltolide®) nanoparticles and water.

nanoparticle type	Contact angle (º)
Poly(Exaltolide®)	86.3
Poly(OH-Exaltolide®)	68.3

The contact angle between the poly(Exaltolide®) nanoparticles and water is 86.3º, close to 90º indicating that these nanoparticles are preferentially wetted by polar liquids such as water. The latter is higher than that of poly(OH-Exaltolide®) nanoparticles (68.3º) indicating that poly(OH-Exaltolide®) nanoparticles are better wetted by water than poly(Exaltolide®) nanoparticles. Indeed, due to the higher hydroxyl group content in the poly(OH-exaltolide®) nanoparticles structure, their affinity for polar solvent is higher, as confirmed by the value of contact angle.

Binks *et al.* reported that to obtain O/W emulsions, the nanoparticles have to be better wetted by the continuous phase of the emulsion (water) with a contact angle with water lower than 90º and preferentially close to this value (Binks, 2000a). Looking at the values obtained for poly(Exaltolide®) and poly(OH-Exaltolide®) nanoparticles, the formation of O/W Pickering emulsion can be considered as feasible and nanoparticles should be dispersed in the water continuous phase prior to emulsification. Therefore, the dispersion of the nanoparticles in water was studied. First, the effect of the ionic strength and the pH was reported to be a key factor for the dispersion of many types of nanoparticles and the latter formation of Pickering emulsions (Binks, 1999; Simovic 2003 and 2004; Salary, 2010). Those two parameters were investigated by varying NaCl and NaOH concentrations, respectively, in poly(Exaltolide®) and poly(OH-Exaltolide®) dispersions. Figure 4.35 shows the variation of the zeta potential and hydrodynamic radius of poly(Exaltolide®) nanoparticle in water as a function of ionic strength (NaCl concentration) and pH (NaOH concentration).

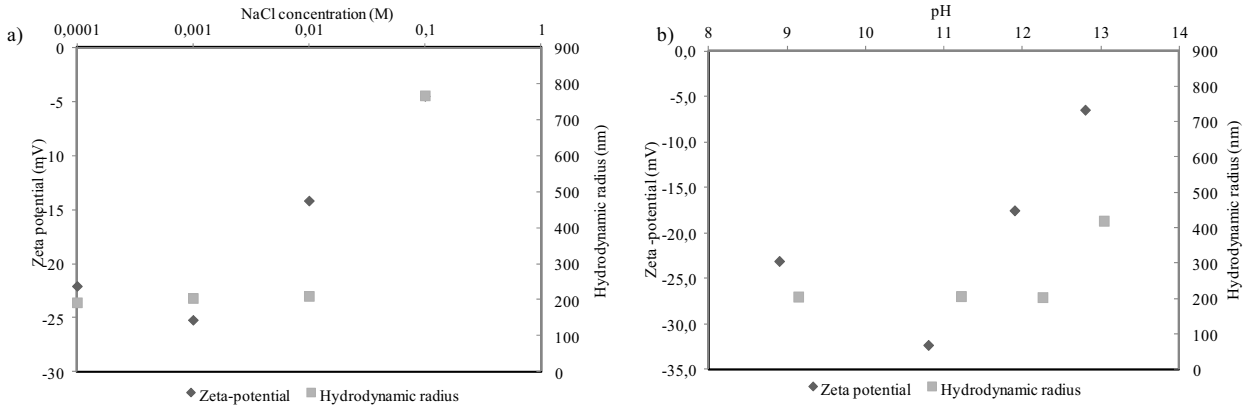

Figure 4.35 : Variation of the zeta-potential and hydrodynamic radius of poly(Exaltolide®) nanoparticles in water as a function of a) the ionic strength (NaCl concentration) and b) pH (NaOH concentration).

Both graphs reveal that the zeta potential and the hydrodynamic radius are constant up to a certain concentration of NaCl and NaOH (pH), the critical concentration of coagulation, after which a pronounced increase occurs caused by the aggregation of the poly(Exaltolide®) nanoparticles. The critical concentration of coagulation (CCC) is observed at a concentration of NaCl or NaOH between 10^{-2} and 10^{-1} M corresponding for the latter to a pH of around 12.

At low electrolyte concentration, the values of zeta potential (in absolute values) are high (>20mV) which suggest that the dispersion of nanoparticles is stable. By increasing the electrolyte concentration, the zeta potential increases to values close to zero. The charges of the nanoparticle tend to zero due to either a screening of the charged by the electrolytes or to the

nanoparticle aggregation. The evolution of the hydrodynamic radius shows the same behavior but the increase is observed at slightly higher electrolyte concentrations. This behavior suggests that the electrolytes first screen the charges of the nanoparticles (increase the zeta potential) which latter lead to nanoparticle aggregation. It is worth noting that the measured hydrodynamic radius by DLS, even at low electrolyte concentration, are high (200-400 nm), when compared to the size of nanoparticles measured by TEM image analysis. The difference can be explained by two factors. First, the DLS measures the hydrodynamic radius while the TEM give the diameter of the hard spheres and secondly, the nanoparticles might be already aggregated in non spherical aggregates which clearly influence the value of the hydrodynamic radius.

Same experiments were carried out for dispersion of poly(OH-Exaltolide®) in water (Appendix 5) and similar results were obtained.

For further purposes of the polyester nanoparticles, their stability at high temperature is a key factor. Therefore, as a preliminary study, poly(Exaltolide®) nanoparticle dispersions in water and in single oils were subjected to an increase of temperature from 20ºC to 60ºC in 10ºC steps and their behavior after one hour at each temperature step was shown in Figure 4.36.a.

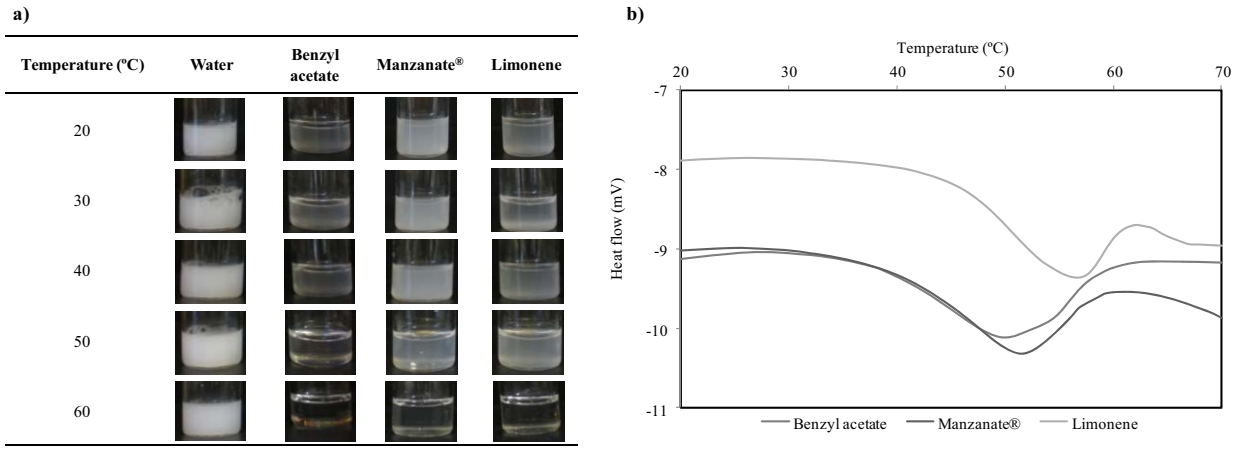

Figure 4.36 : a) Photographs of the poly(Exaltolide®) nanoparticles dispersion at 0.1% in water, Benzyl acetate, Manzanate®, and limonene after 1h at each temperature and b) DSC profiles of the nanoparticles dispersion in the three oils.

At 20ºC, dispersion of poly(Exaltolide®) nanoparticles in water shows a white bluish aspect and as the polarity of the liquid decreases (Benzyl acetate > Manzanate®> Limonene), sedimentation of the nanoparticles increases over night indicating a decrease in the stability of the dispersion (not observed on these pictures). When the temperature increases from 20°C to 60ºC, the dispersion of nanoparticles in water do not show any changes whereas the dispersions in the oils became translucent from 50ºC and completely transparent at 60ºC. This might be explained by

the solubility of the nanoparticles in the oil phase above 50ºC. In order to confirm these results, the dispersions were analyzed by DSC and profiles are shown in Figure 4.36.b. Between 20 and 70°C, only one endothermic peak was observed at 48ºC, 50ºC and 56ºC for the dispersion of poly(Exaltolide®) nanoparticles in Benzyl acetate, Manzanate® and Limonene respectively. These endothermic peaks correspond to the melting of the nanoparticles in the different oils. The melting temperatures measured are in agreement with the previous results obtained visually showing the solubilization of the nanoparticles in oils. The solubility of the nanoparticles at 50ºC in commonly used fragrance such as Benzyl acetate, Manzanate® and Limonene suggest the possible instability of the emulsion containing these fragrances as dispersed phase.

4.4.2.2. Oil-in-water emulsions stabilized by poly(Exaltolide®) nanoparticles

The formation of O/W type Pickering emulsion stabilized by poly(Exaltolide®) nanoparticles was, from the basis of the knowledge, expected for low O/W ratios and concentration of nanoparticles between 0.2 and 10% (Frelichowska, 2010; Juarez, 2012). This section reports the results on the formation of single oil-in-water Pickering emulsions stabilized by poly(Exaltolide®) nanoparticles as a function of the oil type, O/W ratio and nanoparticle concentration. The effect of the temperature on the Pickering emulsion stability is also reported.

- **Effect of the type of oil and poly(Exaltolide®) nanoparticle concentration**

In order to form O/W emulsions, poly(Exaltolide®) nanoparticles were first dispersed in the aqueous phase (Binks, 2000a). Emulsions with an O/W ratio of 30/70 were prepared by addition of the oil phase during emulsification by ultra turrax homogenizer at 13500 rpm for 2 min. Three single oils were compared: Benzyl acetate, Manzanate® and Limonene and 3 concentrations of nanoparticles were studied: 0.35, 0.7 and 1%. All emulsions showed a homogeneous milky appearance after preparation. Their visual aspect after 24h at 25ºC was that of separated, creamed and flocculated emulsions (Figure 4.37).

Oil type	Benzyl acetate			Manzanate®			Limonene		
%NP in aqueous dispersion	0.5	1	1.5	0.5	1	1.5	0.5	1	1.5
%NP in emulsion	0.35	0.7	1.0	0.35	0.7	1.0	0.35	0.7	1.0
Emulsions after 24h									

Figure 4.37: Photographs of the Pickering emulsions with an O/W ratio of 30/70 after 24h at 25ºC as a function of the type of oil and the poly(Exaltolide®) nanoparticle concentration.

O/W emulsions were formed with Limonene and Manzanate® while with benzyl acetate the emulsion was of the W/O type. It means that nanoparticles adsorb preferentially at the water side of the limonene- or Manzanate®-water interface and preferred the formation of O/W emulsions. At the polar oil-water interface such as the one between water and benzyl acetate, nanoparticles are preferentially located at the oil side of the interface and favor the formation of W/O emulsions. The study reveals that O/W emulsions can be easily obtained for non polar oil-water systems. However, the O/W emulsions show creaming and flocculation (Figure 4.37).

In the system water/ Benzyl acetate/ nanoparticles system, the increase of the nanoparticle concentration do not allow the formation of O/W emulsion due to their high affinity for the oil phase. In the water/Manzanate®/poly(Exaltolide®) nanoparticles system, only creaming is observed for the nanoparticle concentrations studied. It is worth noting that increasing the nanoparticles contents leads to more turbid separated aqueous phase and the percentage of separated water decreases slightly by increasing the nanoparticles concentration. The water/Limonene/poly(Exaltolide®) nanoparticle systems show phase separation at low nanoparticles concentration while creaming was observed at higher nanoparticle concentrations. This study reveals that to stabilize O/W emulsions with poly(Exaltolide®) nanoparticles, an oil phase with a log P > 2 is required as well as a minimum concentration of nanoparticles. The higher the log P of the oil compound, the more hydrophobic is the oil and the higher is the concentration of poly(Exaltolide®) nanoparticles required to avoid separation. Creaming can be reduced by increasing the concentration of nanoparticles but flocculation is observed whatever the nanoparticle concentration studied. It is worth mentioning that the turbidity of the aqueous phase implies the presence of nanoparticles in the continuous phase.

- **Effect of the O/W ratio**

Emulsions of Manzanate®-in-water were prepared at constant nanoparticle concentration of 0.7% and the O/W ratio was varied from 50/50 to 10/90. The type of emulsion was determined by means of conductivity measurements (Figure 4.38.a) and the visual aspect of the emulsions is presented on in Figure 4.38.b.

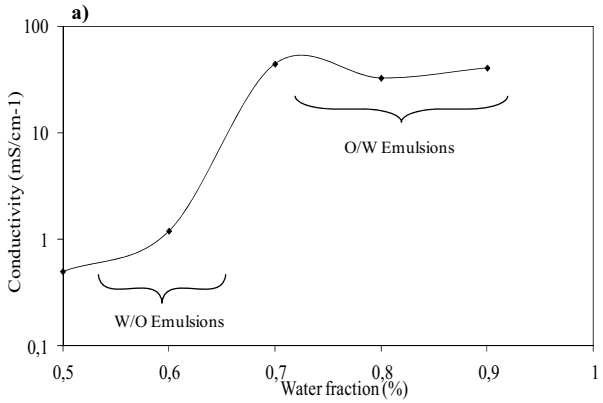

b)

Manzanate®/ Water	50/50	40/60	30/70	20/80	10/90
Water fraction	0.5	0.6	0.7	0.8	0.9
Emulsion type after preparation	W/O	-	O/W	O/W	O/W
Emulsions after 24h					

Figure 4.38 : a) Conductivity of the emulsions stabilized by 1% poly(Exaltolide®) nanoparticles at various O/W ratios as a function of the water fraction at 25ºCand b) Photographs of the emulsions after 24h at 25ºC.

Figure 4.38.a shows that the conductivity increases gradually on increasing the water fraction ϕ_w from conductivity values close to zero to values of around 50mS/cm^{-1}. The increase is more pronounced between 0.6 and 0.7% indicating that the emulsions invert from W/O to O/W at a volume of aqueous phase ϕ_w of around 0.6. This observation is confirmed by the visual aspect of the emulsion observed in Figure 4.38.a. All the emulsions show stability against coalescence, W/O emulsion at ϕ_w = 0.5 sediments while O/W emulsions cream. The emulsion with ϕ_w = 0.6 shows low values of conductivity but do not present sedimentation, thus the type of emulsion could not be clearly determined. This phenomenon of inversion of the type of emulsions is called catastrophic inversion. It was also reported that the emulsions close to the inversion are the more stable (Binks, 2000c-d) which explain the stability of the emulsion with the O/W ratio of 40/60. By studying the effect of the O/W ratio, it was shown that both types of emulsions can be obtained. As far as O/W emulsions are concerned, creaming and flocculation are the main destabilization mechanism observed.

- **Effect of the Temperature**

Another purpose of this thesis concerns the use of Pickering emulsions as template for the formation of microcapsules (Rossier-Miranda, 2009). Microcapsules can be obtained by various methods but generally thermal treatments are required to render more rigid the shell of the capsules (Laib, 2008; Thompson, 2010). Therefore, it is important to know the stability of the emulsions at temperature (Binks, 2003; Binks, 2009). A Manzanate®-in-water emulsion with an O/W ratio of 30/70 and 0.7% of poly(Exaltolide®) nanoparticles was prepared. The aspect of the emulsion after one hour at each temperature, from 20 to 70ºC (10ºC step), is presented in Figure 4.39.

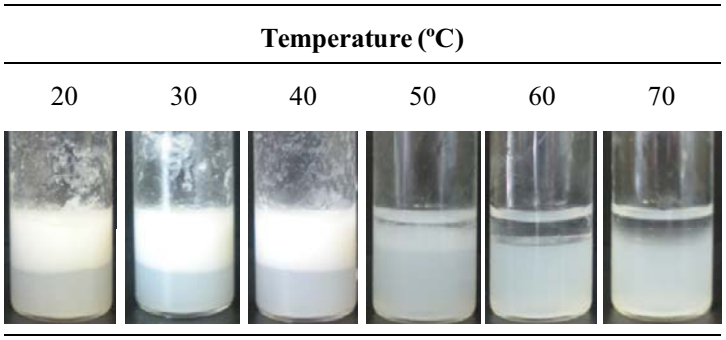

Figure 4.39 : Photographs of an Manzanate®-in-water emulsion with an O/W ratio of 30/70 and 1% poly(Exaltolide®) nanoparticles left for 1h at each temperatures from 20 to 70ºC.

At temperature below 50ºC, O/W emulsions cream and flocculate. At 50ºC, two liquid phases are observed as well as a layer of nanoparticles at the interface between Manzanate® and water. At temperature higher than 50ºC, emulsions separate in two liquid phases. The oil phase is transparent meaning that no nanoparticles are in dispersion while the water phase turbidity decreases by increasing temperature. These results are due to the solubility of the nanoparticles in Manzanate® at temperature close to 50ºC (results described in section 4.4.2.1).

4.4.2.3. Model Perfume-in-water emulsions stabilized by polyester nanoparticles

This section deals with the formation of emulsions of a Model Perfume (MP) in water stabilized by the two types of polyester nanoparticles. As a first step, the formation of MP-in-water emulsion was attempted with the conditions found previously to form O/W emulsion with Manzanate® as oil phase. Accordingly, the O/W ratio was 10/90 and the concentration of poly(Exaltolide®) and poly(OH-Exaltolide®) nanoparticles was 0.9%. Formation of an O/W emulsion was confirmed. As in Manzanate®-in-water emulsions, the main destabilization processes observed visually were creaming and flocculation. Within the aim to improve the stability of this system, the effect of the ionic strength, the pH, the preparation method, the nanoparticles concentration, the O/W ratio and the temperature were studied.

- **Influence of the ionic strength and pH**

Many articles reported the influence of the ionic strength or pH on the stabilization of Pickering emulsions (Binks, 1999; Simovic 2003 and 2004; Salary, 2010). Moreover, it was shown that the stabilization of Pickering emulsions depends on the aggregation of the nanoparticles at the interface (Binks, 2006). It was demonstrated in the preliminary study that a change in the ionic strength and the pH influences considerably the aggregation of the nanoparticles in an aqueous dispersion. In order to determine the degree of nanoparticles aggregation needed for the stabilization of emulsions, the influence of the ionic strength on emulsion formation and stability was investigated. Pickering emulsions stabilized by poly(Exaltolide®) nanoparticles were prepared at four NaCl concentrations as illustrated in Figure 4.40.

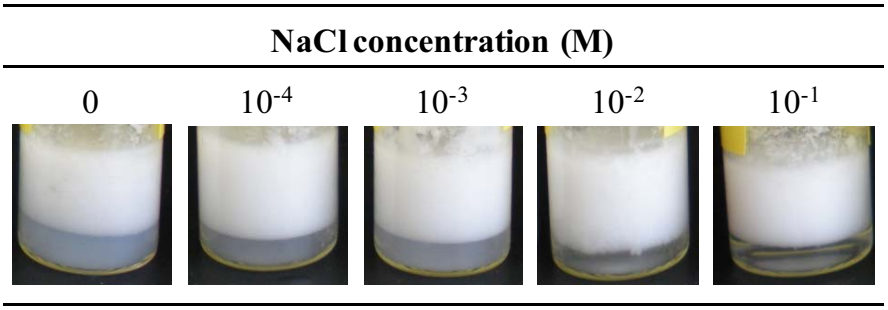

Figure 4.40 : Photographs of MP-in-water emulsions with O/W ratio of 90/10 and stabilized by 0.9% poly(Exaltolide®) nanoparticles at various NaCl concentrations.

At all the NaCl concentrations studied, O/W emulsions were formed but creaming and flocculation still appear as the main destabilization process. By increasing the NaCl concentration, the separated aqueous phase changes from a turbid aqueous dispersion to clear

water indicating a complete adsorption of the nanoparticles at the MP-water interface which occur at a NaCl concentration of 10^{-1} M. From this observation and from the results obtained in section 4.4.2.1, it can be concluded that the emulsions formed are stabilized by the poly(ester) nanoparticles which are slightly aggregated for a better adsorption on the drop interfaces. However, emulsions still flocculate whatever the concentration of NaCl. The flocculation of particle-stabilized drops may occur due to attractive interactions between particles adsorbed on different drops or when the adsorbed particles act as bridges between drops. Similar behavior were found when MP-in-water emulsions were stabilized by poly(OH-Exaltolide®). In order to find out if this interaction (flocculation) can be limited (Binks, 2005), emulsions stabilized by both poly(Exaltolide®) and poly(OH-Exaltolide®) nanoparticles were prepared at 10^{-1} M of NaCl and NaOH (pH≈12) and observed by optical microscopy (Figure 4.41).

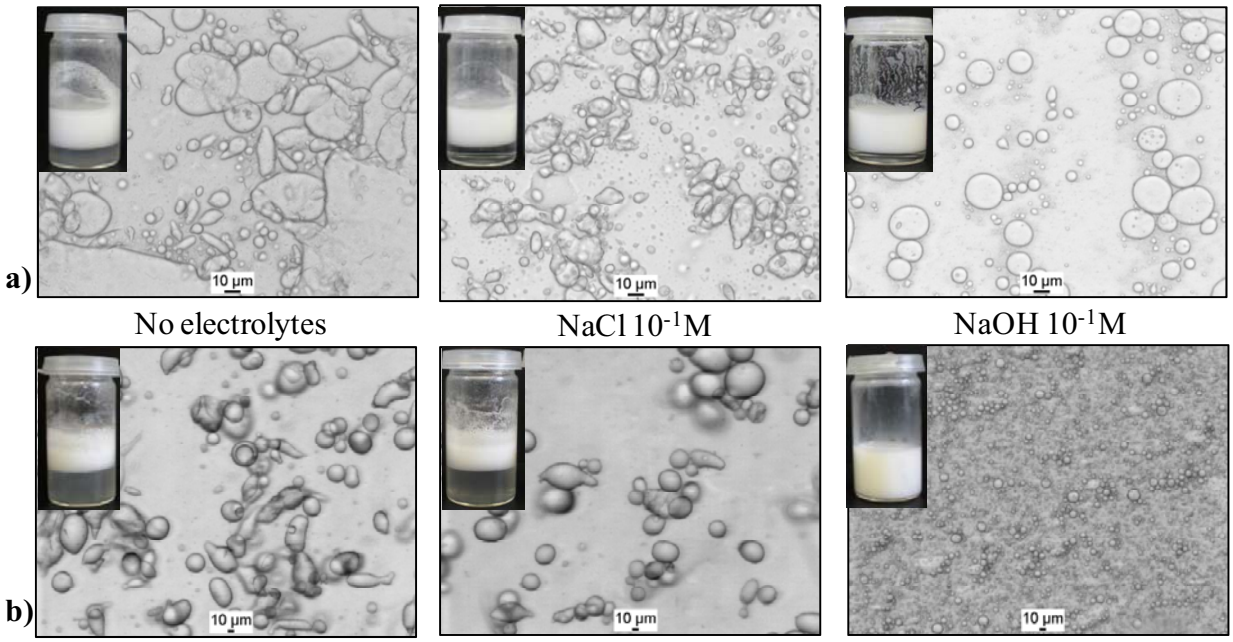

Figure 4.41 : Optical micrographs of the emulsions of Model Perfume-in-water with O/W ratio of 90/10 and stabilized by 0.9% of a) Poly(Exaltolide®) nanoparticles and b) poly(OH-Exaltolide®) nanoparticles using different types of electrolytes at 10^{-1} M. Insets show the emulsions after 24h at 25°C.

Optical micrographs of the emulsions prepared without addition of electrolytes reveals that the drops are not spherical, flocculate and coalesce by simple pressure of the cover slip. These emulsions are formed from nanoparticle dispersion in a low flocculation state as previously observed in section 4.4.2.1 and show low stability. The addition of NaCl electrolytes at 10^{-1} M shows the presence of non spherical drops slightly aggregated while a change of pH by the addition of NaOH enables the formation of spherical drops. The visual aspect of the emulsions (insets in Figure 4.41) shows creaming in the three conditions studied. It is worth noting that the separated aqueous phase changes from turbid to transparent by addition of both salt indicating

complete adsorption of the nanoparticle at the interface. Moreover, flocculation was observed only without addition of electrolytes and with addition of NaCl. Aggregation of the particle-stabilized drops (flocculation) is reduced by changing the pH through the addition of NaOH. The changes in pH of the aqueous continuous phase allows the decrease of the attractive forces between two particle-stabilized drops by increasing the number of negatively charged groups at the interface of the nanoparticles. Another way to explain the effect of pH versus the ionic strength is to consider the size of the nanoparticle aggregates at 10^{-1} M. As observed in Figure 4.35, the aggregates with NaCl are much bigger in size than those with NaOH. These aggregates might be too big and strong and thus, less favorable for the stabilization of emulsion as too strongly aggregated particle might be poor emulsifiers (Binks, 1999).

- **Location of the particles**

In order to confirm the presence of the nanoparticles at the interface of the emulsion, their location was assessed by addition of a fluorescent probe (Rhodamine 6G) (Whitby, 2011; Juarez, 2012). The emulsion was visualized by fluorescence optical microscopy after its dilution in a solution of Rhodamine 6G and pictures are presented in Figure 4.42. The Rhodamine 6G is a fluorescent hydrophilic dye but at the low concentration used (10^{-7} M), it is expected to adsorb completely on the polyester nanoparticles.

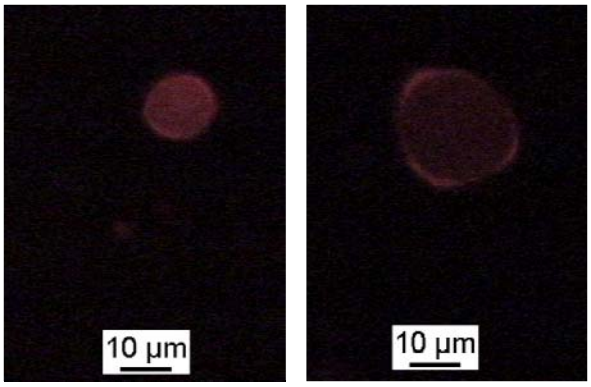

Figure 4.42 : Fluorescent optical micrographs of the diluted MP-in-water emulsion with an O/W ratio of 30/70 and stabilized by 0.7% poly(Exaltolide®) nanoparticles.

Micrographs show the presence of the dye at the interface of the drop and not in the continuous phase of the emulsion. As this dye is highly hydrophilic, its presence at the interface confirms its complete adsorption on the nanoparticles as well as the localization of the nanoparticles at the interface of the emulsion.

In the following experiment, Pickering emulsions were prepared by adjusting the pH of the nanoparticle dispersion to 12 with a solution of NaOH (1%) to ensure better stability against flocculation. As many parameters can affect the formation and stability of Pickering emulsions, the influence of the preparation method and the system composition was studied systematically for the water/ Poly(Exaltolide®)nanoparticle/ MP and water/ Poly(OH-Exaltolide®)nanoparticle/ MP systems .

- **Influence of the preparation method**

High energy homogenizers have been intensively used and permit a good control of the droplet sizes. Nevertheless, it also increases the collisions between the drops which favor the destabilization by coalescence. Therefore, emulsification using a low shear method (vortex stirring) was attempted and compared to a high shear method (ultra turrax) for the formation of Pickering emulsions with an O/W ratio of 90/10, 0.9% poly(Exaltolide®) or poly(OH-Exaltolide®) nanoparticles and pH adjusted to 12 with NaOH solution. The time of emulsification was fixed to 2 minutes for all experiments as Whitby *et al.* showed that at least 2 min of homogenization were required to reach the final drop size. (Binks, 2004; Whitby, 2011). The visual appearance showed that emulsions were not properly formed by a vortex stirring and quick destabilization of the emulsion by creaming occurred immediately after agitation was stopped. When agitation was performed by the high-energy homogenizer, emulsions were homogeneous and destabilized slowly by creaming. The microscopic images of the emulsions are presented in Figure 4.43.

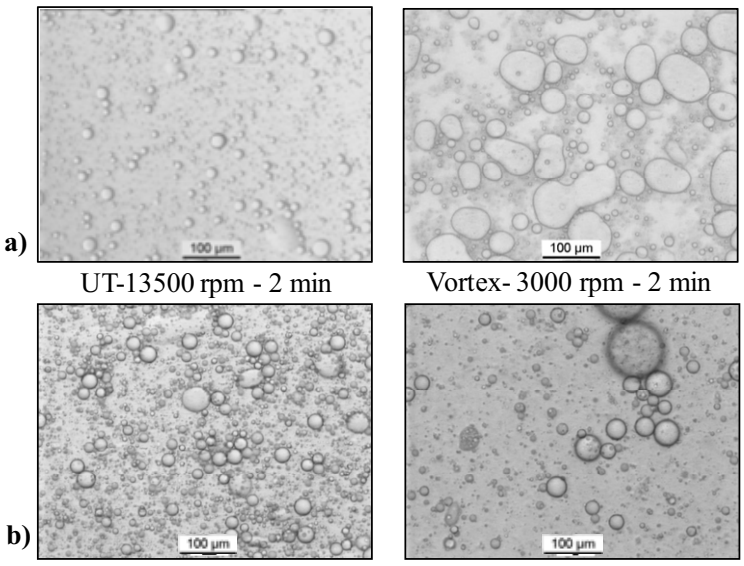

Figure 4.43 : Optical micrographs of MP-in-water emulsions with O/W ratio of 10/90 and 0.9% of a) Poly(Exaltolide®) nanoparticles and b) poly(OH-Exaltolide®) nanoparticles using two emulsification methods: ultra-turrax (UT) and vortex mixer.

The formation of spherical drops was observed by both methods and for both types of nanoparticles. High polydispersity is obtained for emulsions prepared by vortex stirring and instability through coalescence confirmed the visual appearance of the sample. Therefore, for the rest of the study, systems were emulsified by a high-energy homogenizer ultra turrax fixed at 13500 rpm for 2 min after the addition of the total volume of oil phase.

- **Influence of nanoparticle concentration**

In this study, emulsions were prepared with an O/W ratio of 30/70 and stabilized by poly(Exaltolide®) or poly(OH-Exaltolide®) nanoparticles. Other parameters were fixed from the previous studies (pH of the emulsion was adjusted to 12 with an aqueous solution of 1% NaOH and emulsification was performed using an ultra turrax at 13500 rpm for 2 min after the addition of the total oil volume). All emulsions formed were of the O/W type. The samples were characterized by optical microscopy (Figure 4.44).

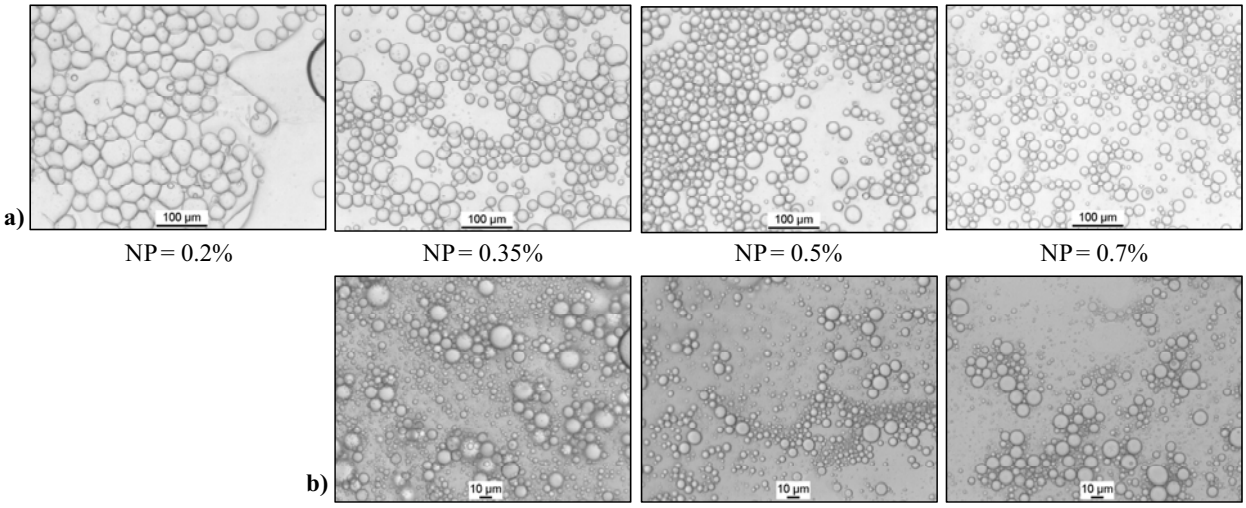

Figure 4.44 : Optical micrographs of MP-in-water emulsions with an O/W ratio of 70/30 stabilized by a) poly(Exaltolide®) nanoparticles and b) poly(OH-Exaltolide®) at 0.2, 0.35, 0.5, and 0.7% of nanoparticles (NP). Observation were made just after emulsification.

The pictures show that low nanoparticle concentration (0.2%) did not lead to the formation of stable emulsions. The quantity of nanoparticles was not sufficient and the emulsion destabilized quickly by simple addition of the cover slip. By increasing the concentration of poly(Exaltolide®) nanoparticles (Figure 4.44.a), the size of the emulsions drops decreased and became less polydisperse. For poly(OH-Exaltolide®) nanoparticles, the droplet size obtained was constant in the range of nanoparticles concentration studied and diameters were smaller than those observed for poly(Exaltolide®). This difference of diameter obtained for emulsion stabilized by poly(Exaltolide®) and poly(OH-Exaltolide®) is explained by the presence of more OH group at

the surface of poly(OH-Exaltolide®) nanoparticle that enhance their ability to reside at the interface and thus increase their stability by decreasing their droplet size. The study reveals that a minimum of poly(Exaltolide®) nanoparticles is necessary to stabilize the emulsions of MP-in-water. This minimum concentration was not observed for poly(OH-Exaltolide®) in the range of concentrations studied.

The image analysis of the optical micrographs of the water/ poly/Exaltolide®) nanoparticle/ MP system (Figure 4.44.a) enables the determination of the experimental mean weight diameter and polydispersity. The experimental values were plotted as a function of the poly(Exaltolide®) nanoparticles concentration in Figure 4.45 and compared to the theoretical values calculated by the Equation 3.20 described in the introduction.

$$d = 2r = 8a\varphi_a \frac{\phi}{(1-\phi)} \frac{1}{\phi_p} \qquad 3.20$$

In this equation, it is assumed that all particles (of bulk volume fraction ϕ_p) were in the continuous phase and adsorbed on the drops, and that the drops were covered by a monolayer of nanoparticles meaning a high surface coverage φ_a to protect the drops against coalescence during the collisions between them.

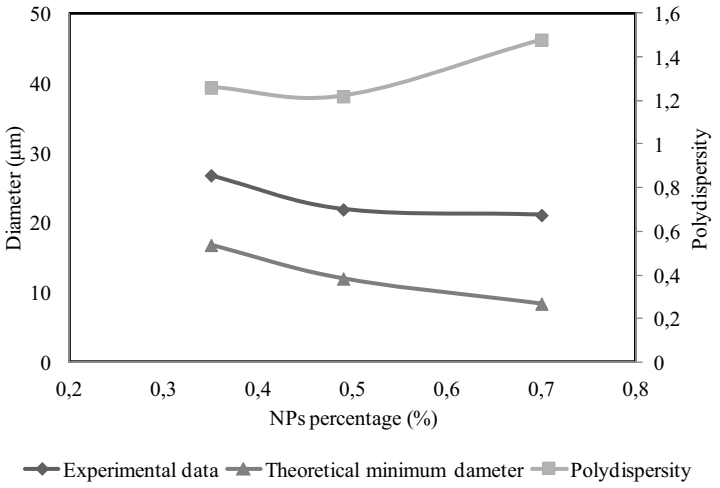

Figure 4.45 : Measured diameters and polydispersity of the MP-in-water Pickering emulsions with an O/W ratio of 30/70 stabilized by poly(Exaltolide®) nanoparticles as a function of the nanoparticles concentration and comparison with the theoretical minimum diameter.

Drop diameters between 22 and 28 µm and polydispersity indices between 1.2 and 1.5 were obtained. Figure 4.45 shows that the drop size decreases slightly by increasing the nanoparticle concentration and the experimental diameters are twice higher than the theoretical ones. For the

calculation of the theoretical values, it was assumed that all the particles are closely packed as a monolayer at the O/W interface. The gap between the calculated and theoretical diameters can be explained by the fact that nanoparticles are adsorbed as aggregates at the interface and not as a single monolayer. Moreover, the calculation considers that the entire surface of the drops is covered but this is rarely the case. The size of the emulsions was also characterized by means of drop laser diffraction after preparation at 25ºC. In Figure 4.46, the size distributions at three nanoparticle concentrations are presented.

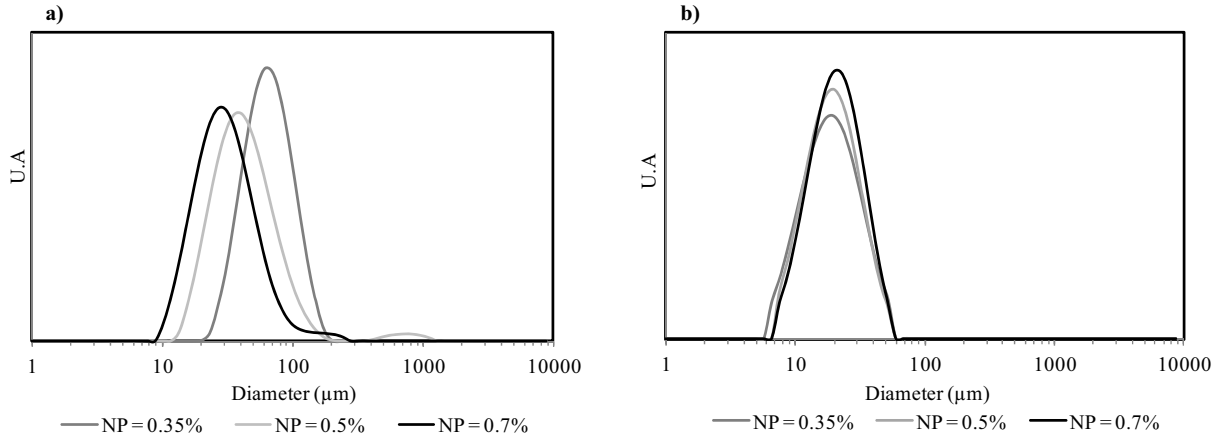

Figure 4.46 : Size distributions of MP-in-water emulsion with an O/W ratio of 30/70 stabilized by a) poly(Exaltolide®) nanoparticles and b) poly(OH-Exaltolide®) nanoparticles at 0.35, 0.5, and 0.7% of nanoparticles. Measurements done just after emulsification.

At the studied nanoparticle concentrations, a log normal drop size distribution was observed for the emulsions stabilized by both types of nanoparticles. The size distributions showed a single population centered on average diameters of 63.7, 54.3 and 32.7µm for poly(Exaltolide®) nanoparticle concentrations of 0.35, 0.5 and 0.7% respectively. The size distributions of emulsions stabilized by poly(Exaltolide®) nanoparticles were shifted to lower diameter values when the concentration of nanoparticles increases. The decrease of drop size with the increase of nanoparticles concentration confirms the results observed by optical microscopy. Similar results were reported in previous works on Pickering emulsions (Tambe, 1994) by an increase of the interface covering when the nanoparticle concentration increases. Emulsions stabilized by poly(OH-Exaltolide®) nanoparticles showed similar size distribution at all nanoparticle concentrations studied and average drop size was measured around 20µm. No changes in the droplet size might suggest that the maximum coverage of the interface by the poly(OH-Exaltolide®) nanoparticles was achieved at lower nanoparticle concentration and in the range of nanoparticle concentrations studied, droplet size reached a plateau. Nevertheless, it is worth noting that the values obtained by laser diffraction are significantly higher than those obtained by

microscopy image analysis and this gap can be explained by the dilution made in the dispersion unit of the equipment compared to optical microscopy that do not require dilution.

Among all the destabilization mechanisms that affect O/W Pickering emulsion, creaming (or sedimentation) can be visually observed. The stability of the emulsions stabilized by poly(Exaltolide®) was studied over time. For the experimental time studied, no detectable oil phase separation was observed. The creaming of the emulsion was then followed for 24h at 25ºC and the percentage of separated water phase is plotted as a function of time in Figure 4.47.a.

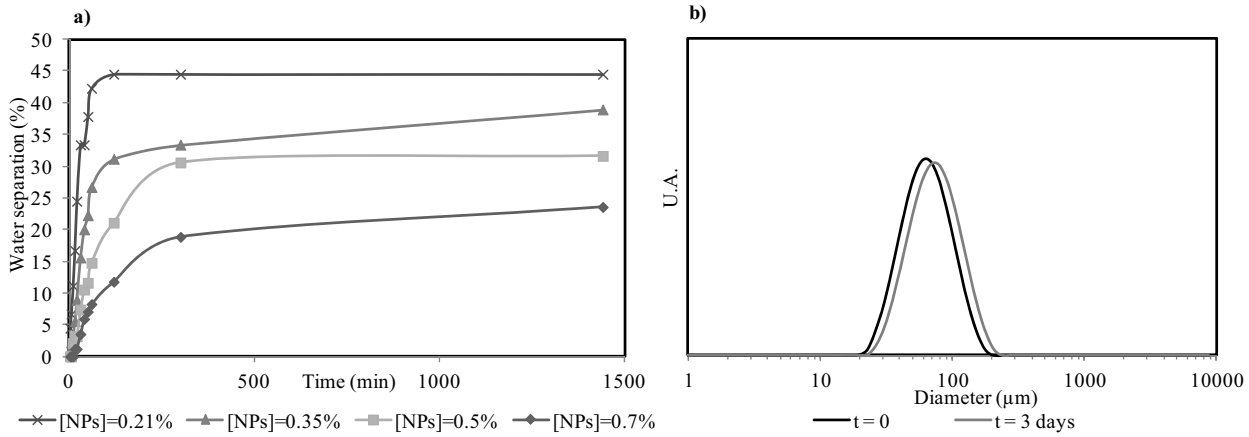

Figure 4.47 : a) Evolution over time of separated water from MP-in-water emulsion with O/W ratio of 70/30 and stabilized by poly(Exaltolide®) nanoparticles at 0.21, 0.35, 0.5, 0.7%, b) Size distributions of the MP-in-water emulsion with an O/W of 70/30 and stabilized by 0.7% poly(Exaltolide®) nanoparticles after preparation t=0 and three days. Samples were handshaken prior to measurements.

At low nanoparticles concentration (0.21%), almost half of the water separates after 2h. As the nanoparticle concentration increases, the extent of creaming decreases and the velocity of creaming is reduced. At 0.7% of nanoparticles, only 20% of the water is released after 24h. The rate of creaming of the emulsions depends on the drop diameter and the viscosity of the continuous phase. We considered that at the studied nanoparticle concentration, the viscosity of the aqueous phase is constant and therefore, the increase of stability against creaming is essentially due to the decrease in average diameter observed in Figure 4.46.a. The changes of droplet size associated to coalescence and/or Ostwald ripening were studied by measuring the droplet size at t=0 and after t=3 days. The two size distributions were plotted on Figure 4.47.b for the MP/W Pickering emulsion with an O/W ratio of 70/30 and 0.7% poly(Exaltolide®) nanoparticles. The size distribution of the emulsion after 3 days at 25ºC is slightly shifted to higher diameter values from 63.7 µm to 79.9 µm, thus indicating a destabilization of the emulsion either by coalescence of the drops or Ostwald ripening (Figure 4.46.b).

- **Influence of the O/W ratio**

The O/W ratio is another important key factor for the formation and stability of O/W emulsions (Binks, 2000c-d). As observed previously for Manzanate®-in-water emulsions, a catastrophic inversion can take place by increasing the O/W ratio. Emulsions with an O/W ratio of 50/50, 30/70 and 10/90 and different concentration of poly(Exaltolide®) nanoparticles were prepared following the conditions of preparation previously described in this section. First, it is worth mentioning that at the three O/W ratios studied, the droplet size decreases by increasing nanoparticle concentration but a minimum of nanoparticles concentration is needed to stabilize the Pickering emulsions. This minimum concentration is highly dependent on the O/W ratio and, as indicated in Table 4.19, it decreases by decreasing the oil content as fewer nanoparticles are needed to cover the O/W interface.

Table 4.19 : Minimum poly(Exaltolide®) nanoparticle concentration needed to obtain stable MP-in-water emulsion as a function of the O/W ratio.

O/W ratio	50/50	30/70	10/90
Minimum [NP] (%)	0.7	0.35	0.07

From these results, the concentration of nanoparticles was fixed at 0.7% and the emulsions were formed at the three O/W ratios. All emulsions were of O/W type. No catastrophic inversion was observed. The samples were then compared by optical microscopy (Figure 4.48) and droplet size measurements by laser diffraction (Figure 4.49).

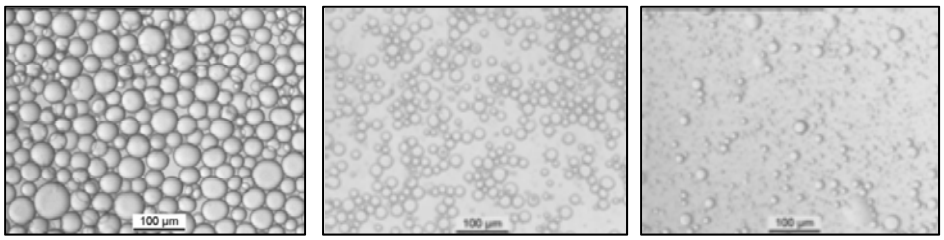

O/W = 50/50 O/W = 30/70 O/W = 10/90

Figure 4.48 : Optical micrographs of MP-in-water emulsions stabilized by 0.7% poly(Exaltolide®) nanoparticles at O/W ratio 50/50; 30/70 and 10/90.

The droplet size as well as the concentration of drop decreased significantly by decreasing the O/W ratio. It should be noted that the polydispersity increases at lower O/W ratios. Similar results were obtained by laser diffraction (Figure 4.49).

a)

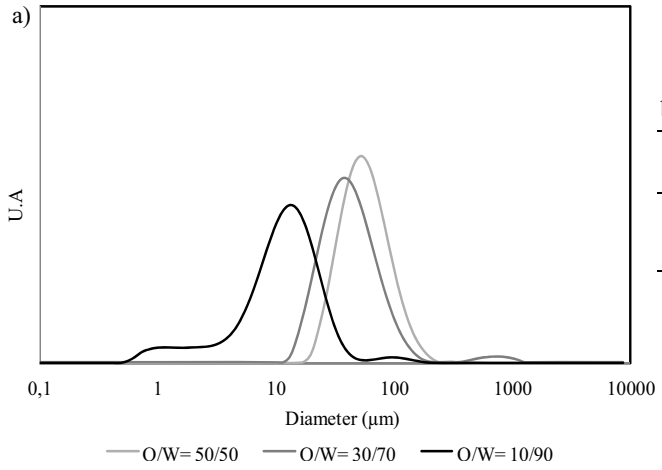

b)

O/W ratio	50/50	30/70	10/90
Creaming velocity 10^4 (m/s)	1.9	0.8	0.2

Figure 4.49 : a) Size distribution of MP-in-water emulsions stabilized by 0.7% poly(Exaltolide®) nanoparticles at O/W ratios 50/50; 30/70 and 10/90 and b) Creaming velocity as a function of the O/W ratio.

As the O/W ratio increases from 10/90 to 50/50, the average drop diameter increases by a factor of approximately 4. The distribution changes from a single log normal distribution at an O/W ratio of 50/50 to a slightly bimodal distribution at an O/W of 10/90. The less polydisperse emulsion is the one possessing the larger droplet size. The stability of those emulsions was recorded for 24h at 25ºC and quick creaming was observed. The creaming velocity was calculated using the Stokes equation described in section 1.1.2 and summarized in Figure 4.49.b. The creaming velocity decreases by a factor of 10 by reducing the O/W ratio.

- **Effect of temperature**

In order to study the effect of temperature on the emulsions formed in the previous section, the temperature was increased in 10ºC steps from 30ºC to 70ºC with the vials being hand shaken and left for one hour at each temperature (Binks, 2003; Binks, 2009). Visually, emulsions at O/W ratios (50/50; 30/70 and 50/50) showed creaming at low temperature and separated in two clear liquid phases at 70ºC. At this temperature, nanoparticles are located in the aqueous phase. The percentage of separated water is plotted against temperature in Figure 4.50.

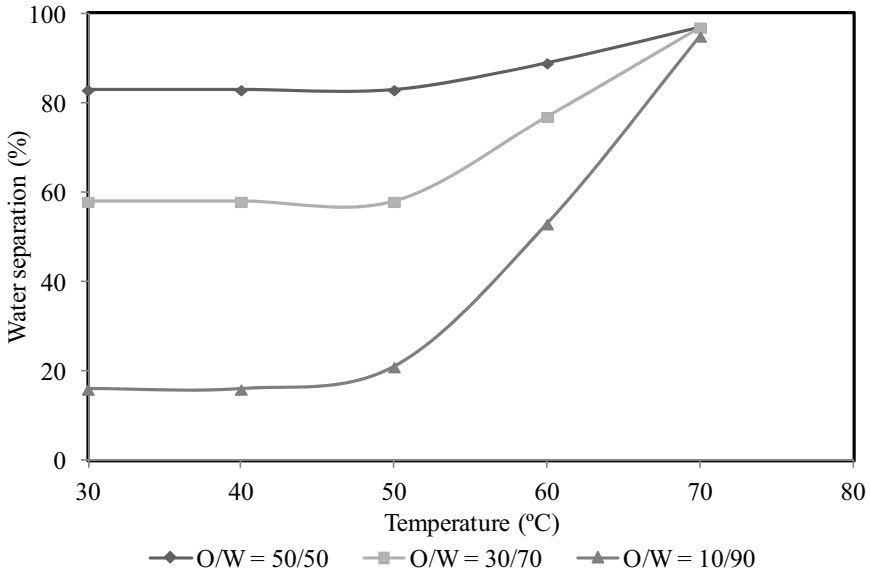

Figure 4.50 : Stability of MP-in-water emulsions stabilized by 0.7% poly(Exaltolide®) nanoparticles at three O/W ratios (50/50; 30/70 and 10/90) after standing 1h at each temperature.

The trend of all curves shows that the creaming increases with temperature from a temperature of 50°C and complete destabilization occurred at 70ºC. Complete destabilization can be explained by the earlier results described in 4.4.2.1 where it was demonstrated that the poly(Exaltolide®) nanoparticles melts around 50ºC in most of the oil phases studied. It was then assumed that those nanoparticles also melt around this temperature in MP and as the nanoparticles starts to melt, molecular species desorbs from the oil-water interface and dissolves in the oil phase. The droplets lose their rigid interface, coalesce between them and results in two clear liquid phases. Therefore, the use of MP-in-water emulsions stabilized by polyester nanoparticles should be limited to temperature lower than 50ºC.

Summary: The formation of perfume-in-water Pickering emulsions were stabilized successfully by either poly(Exaltolide®) and poly(OH-Exaltolide®) nanoparticles. A study of the influence of the ionic strength and pH has evidenced a change of the nanoparticle wettability and thus stabilization of the emulsions by aggregates of nanoparticles (obtained by addition of electrolytes in a concentration of 10^{-1} M). It was also demonstrated that changes in the O/W ratio or oil type lead to the formation of either O/W or W/O emulsions. The droplet size of the Perfume-in-water emulsions can be tuned by either changing the nanoparticle wettability (Poly(Exaltolide®) or poly(OH-Exaltolide®)), the nanoparticle concentration or the O/W ratio. A decrease of the droplet size generally leads to a better stability against creaming. The stability of the formed emulsions was studied at temperature and good stability was observed at temperature lower than 50ºC.

4.4.3. Synthesis and characterization of microcapsules

This section reports the formation of microcapsules via cross-linking of polyester nanoparticles at the interface of perfume-in-water Pickering emulsions stabilized by poly(Exaltolide®) and poly(OH-Exaltolide®) nanoparticles. The cross-linking, induced by chemical reaction between the hydroxyl group of the polyester nanoparticles and an oil-soluble polymeric diisocyanate at the interface of the droplets, was studied over time at various concentration of isocyanate and compared to a reference without isocyanate. Finally, the release of the perfume from the core of the microcapsules to a commercial formulation was determined as a function of time.

- **Selection of the template**

From the previous study described in section 4.3.2, Pickering emulsions stabilized by polyester nanoparticles were fully characterized. The composition of the template Pickering emulsion was fixed at an MP/W ratio of 10/90 and 0.9% of polyester nanoparticles. For the two types of nanoparticles studied, poly(Exaltolide®) and poly(OH-Exaltolide®), the emulsions present a unimodal size distribution with an average diameter of 32.7 and 19.9 μm, respectively measured by means of light diffraction. Size of around 20 and 10 μm were observed by optical microscopy.

- **Selection of the isocyanate**

Among the large variety of isocyanate cross-linkers, an oil-soluble one was chosen in order to confine the cross-linking reaction at the inner side of the interface (Scheme in Figure 3.10). Thus, cross-linking only occurs inside individual microcapsules rather than between them. The cross-linker selected is an aliphatic polyisocyanate, Desmodur®N100, which readily reacts with the hydroxyl groups from the polyester nanoparticles to form urethane bonds with no small molecule by-products. The following reaction was expected (Figure 4.51).

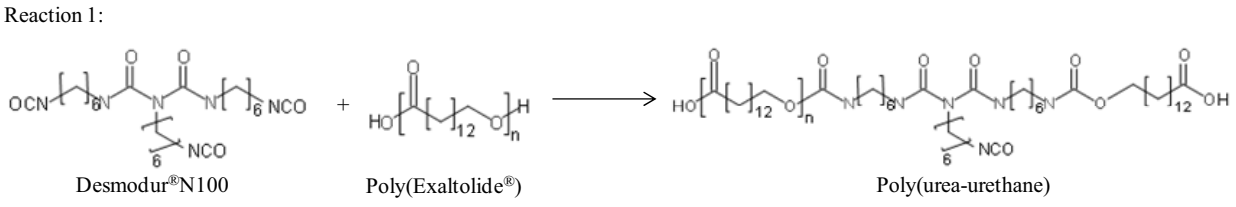

Figure 4.51 : Expected reaction between Desmodur®N100 and poly(Exaltolide®) nanoparticles for the formation of a poly(urea-urethane).

This commercially available polymeric cross-linker is significantly less toxic than small diisocyanates because it is non volatile. Moreover, its insolubility in water prevents partitioning between the oil droplets and the aqueous continuous phase.

4.4.3.1. Microcapsules from poly(Exaltolide®) stabilized emulsions

First, it is worth mentioning that, in principle, the cross-linking can occur between OH groups on the same poly(Exaltolide®) nanoparticle as well as between neighboring nanoparticles. However, calculation of the effective $OH_{poly(Exaltolide®)}/NCO_{Desmodur®N100}$ ratio can be problematic, since the ratio depends on adsorption of the nanoparticles at the interface. It was assumed that all the nanoparticles were adsorbed at the interface and that all the hydroxyl groups of the nanoparticles can react with the isocyanate which is an overestimation. This suggests that the Desmodur®N100 can be used for intraparticle cross-linking while still allowing efficient interparticle cross-linking to be achieved. The $OH_{poly(Exaltolide®)}/NCO_{Desmodur®N100}$ molar ratio was calculated for the poly(Exaltolide®) nanoparticles employed at a concentration of 1% assuming that all the nanoparticles are adsorbed at the interface and that poly(Exaltolide®) has a molecular weight of 2647 g/mol and contain one OH-group per chain. The reaction with the $OH_{poly(Exaltolide®)}/NCO_{Desmodur®N100}$ of 1/1 was first studied as an ideal case where the NCO groups reacts with every single hydroxyl group of the nanoparticles.

The cross-linker, Desmodur®N100, was dissolved in the oil phase of the Pickering emulsions prior to emulsification. The sample was then left to react at 40ºC under stirring. Two concentrations of isocyanate were studied and compared to the Pickering emulsion without addition of Desmodur®N100 subjected to the same reaction conditions. The reaction was followed over time (after 2, 4 and 20 h of reaction) by optical microscopy, infra-red spectroscopy and thermogravimetric analysis. The optical micrographs obtained for each $OH_{poly(Exaltolide®)}/NCO_{Desmodur®N100}$ ratio after 0, 2, 4 and 20h of reaction are presented in Figure 4.52.

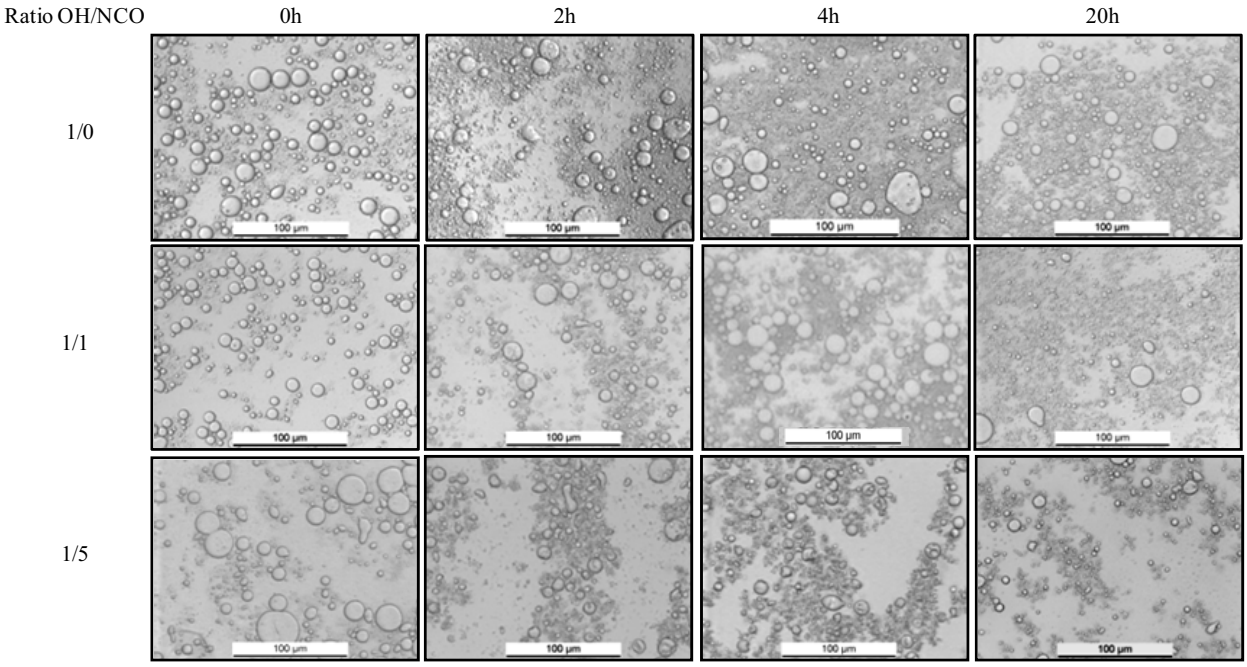

Figure 4.52 : Optical micrographs showing the evolution over time of the formation of microcapsules obtained from poly(Exaltolide®) nanoparticles stabilized emulsions with a MP/W ratio of 10/90 at three $OH_{poly(Exaltolide®)}/NCO_{Desmodur®N100}$ ratios at 40ºC.

At t=0, O/W Pickering emulsions were obtained at the three $OH_{poly(Exaltolide®)}/NCO_{Desmodur®N100}$ ratios. An increase of the droplet size was observed at the lower $OH_{poly(Exaltolide®)}/NCO_{Desmodur®N100}$ of 1/5, indicating a destabilization of the emulsion by addition of the cross-linker. It was known that Desmodur®N100 adsorbs at interfaces and can displace the nanoparticles from the Interface thus destabilizing the emulsion. When the reaction took place in the absence of cross-linker, the shape and roughness of the drop do not present significant changes which indicate that the reaction did not occur. Nevertheless, the polydispersity increased at such high temperature probably due to destabilization mechanisms such as coalescence or Ostwald ripening. A reaction of sintering of the nanoparticles at the interface was expected but did not seem to take place at such low temperature. After 2h of reaction at 40ºC, some changes in the shape and roughness of the drops was observed in the presence of cross-linker at $OH_{poly(Exaltolide®)}/NCO_{Desmodur®N100}$ ratios of 1/1 and 1/5. The drop became non spherical with a rough surface due to the formation of a rigid layer at the interface. After 4h of reaction, the effect of rigidity at the surface intensified and most of the drops were non spherical. This effect is increased by increasing the cross-linker concentration meaning by decreasing the $OH_{poly(Exaltolide®)}/NCO_{Desmodur®N100}$ ratio. After 20h of reaction, a significant decrease of the droplet size was observed explained by the diffusion of the oil phase at 40ºC. A reaction of 4h was then considered suitable for the formation of capsules.

The evolution of the reaction was confirmed by infra-red spectroscopy (Figure 4.53) by comparing the spectra with those of the poly(Exaltolide®) nanoparticles and Desmodur®N100.

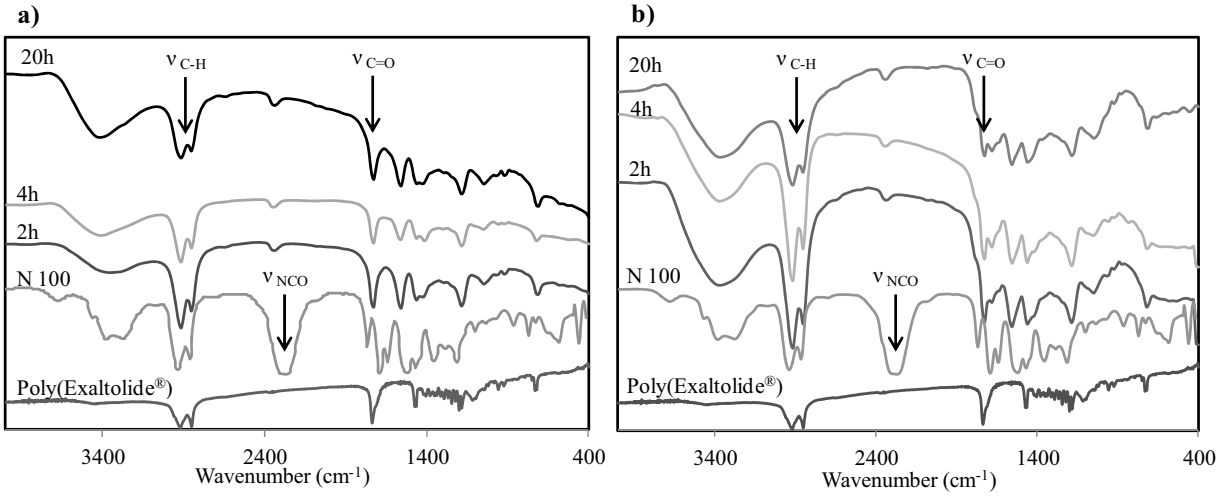

Figure 4.53 : FTIR spectra of poly(Exaltolide®) nanoparticles, Desmodur®N100 and microcapsules obtained at three reaction times (2, 4, 20h) for a ratio of a) $OH_{poly(Exaltolide®)}/NCO_{Desmodur®N100}$ = 1/1 and b) $OH_{poly(Exaltolide®)}/NCO_{Desmodur®N100}$ = 1/5.

The characteristic band of the carbonyl group of the poly(Exaltolide®) at 1730 cm^{-1} as well as the two bands at 2930 and 2850 cm^{-1}, attributed to symmetric and non symmetric stretching of the C-H bond of the poly(Exaltolide®), were observed in the spectra of the microcapsules, thus confirming the presence of poly(Exaltolide®) in the microcapsules. The chemical reaction between the OH groups of the nanoparticles and the NCO of Desmodur®N100 lead to the formation of a urethane bond (Reaction 1). Unfortunately, the presence of new urethane bond was not observed since this band is overlapped with the ester band of the carbonyl group of the poly(Exaltolide®). Moreover, the characteristic band of NCO at 2270 cm^{-1} was not observed in the spectra of the microcapsules since the unreacted Desmodur®N100 was removed by washing with ethanol. However, the bands of Desmodur®N100 at 1200, 1640, 1680 cm^{-1}, corresponding respectively to C-N stretch, N-H bending and C=O stretch were observed for the $OH_{poly(Exaltolide®)}/NCO_{Desmodur®N100}$ ratios of 1/5 (Figure 4.53.b), thus confirming the presence of Desmodur in the system and thus the reaction between the OH-group of poly(Exaltolide®) with the cross-linker. The latter bands were not observed on the spectra of microcapsules obtained at $OH_{poly(Exaltolide®)}/NCO_{Desmodur®N100}$ = 1/1 due to the low concentration of cross-linker present in the system but the reaction might also take place in these conditions. Moreover, it should be noticed that by increasing the reaction time, no changes were observed on the FTIR spectra of microcapsules, suggesting that the reaction of polyurethane formation lasts less than 2h (Trovati, 2010).

Then, it should be mentioned that the secondary reaction, the hydrolysis of the isocyanate in the presence of water (Figure 4.54: Reaction 2), can take place when Desmodur®N100 is in presence of water, such as the interface of a Pickering emulsion. This secondary reaction leads to the formation of an amine which can also react with another isocyanate group to form a polyurea (Figure 4.54: Reaction 3).

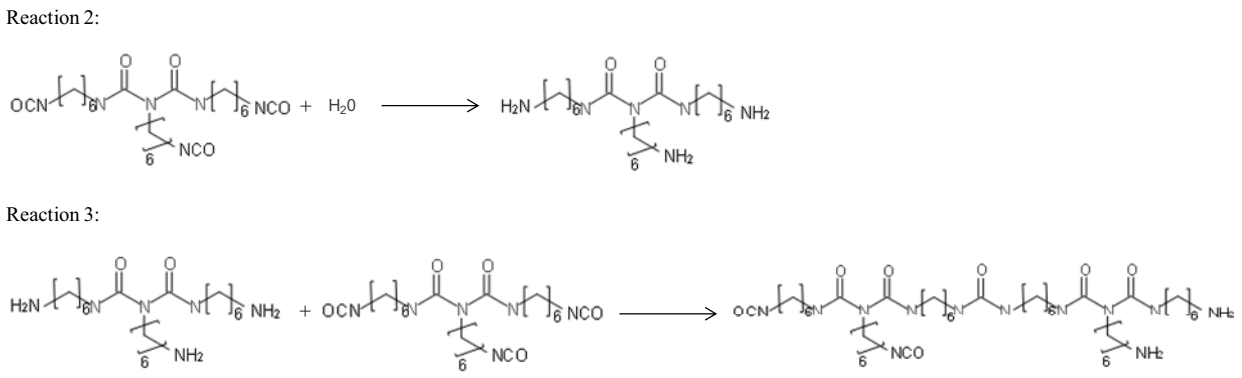

Figure 4.54 : Possible secondary reaction of Desmodur®N100 in the presence of water.

As Desmodur®N100 contains urea groups, the urea band at 1640 cm^{-1} in the FTIR is already observed in the microcapsules spectra and do not permit to conclude on the side reactions could not be confirmed but were assumed. Nevertheless, this secondary reaction might not block the polymerization as the side product can be incorporated in the polymer chain to form a polyurethane-polyurea. So, the side reaction is not a problematic issue in this context.

The spectra of the microcapsules at $OH_{poly(Exaltolide®)}/NCO_{Desmodur®N100}$ ratios of 1/1 and 1/5 suggest that the reaction between the OH groups of the nanoparticles and the cross-linker takes place in less than 2 h but do not permit to conclude on the efficacy of the cross-linking reaction. Therefore, to confirm the cross-linking reaction, the decomposition of microcapsules with temperature was analyzed by thermogravimetric analysis. The Derivative of the ThermoGravimetric (DTG) profile of the microcapsules obtained at the two isocyanate concentrations are plotted as a function of time and compared to the profile of poly(Exaltolide®) on Figure 4.55.

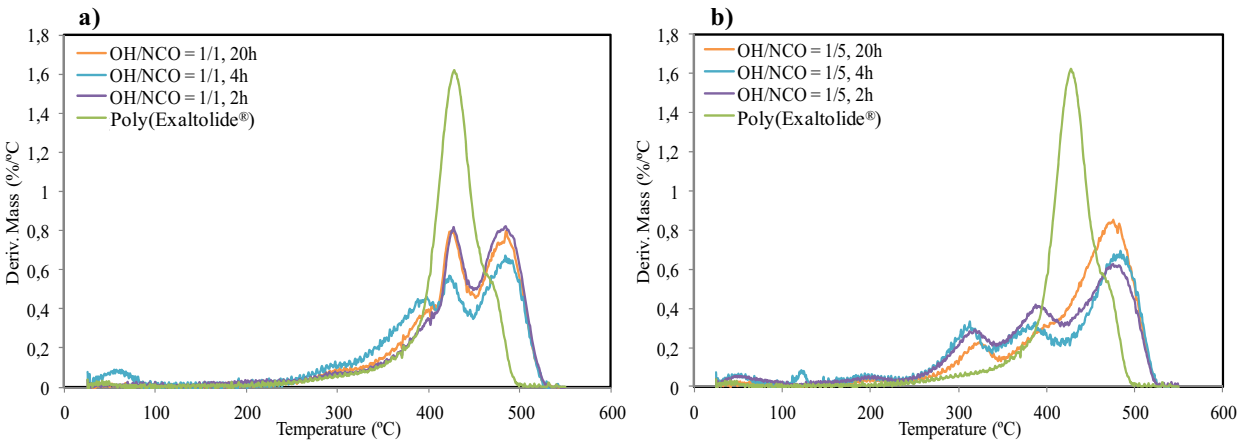

Figure 4.55 : DTG profiles of poly(Exaltolide®) nanoparticles, Desmodur®N100 and microcapsules obtained at three reaction times (2, 4, 20h) for a ratio of a) $OH_{poly(Exaltolide®)}/NCO_{Desmodur®N100}$ = 1/1 and b) $OH_{poly(Exaltolide®)}/NCO_{Desmodur®N100}$ = 1/5.

The DTG profile of the poly(Exaltolide®) nanoparticles shows that its thermal degradation occured above 350 °C and is composed of a main step followed by a minor loss, appearing as a shoulder in the derivative curve. The two decomposition steps were centered at 426 and 460 °C, respectively and no solid residue remained above 500 °C. From the literature (Focarete, 2001), the first degradation step was attributed to the degradation of the polymer into carbon dioxide, whereas the second step, to the degradation of the hydrocarbon part of poly(Exaltolide®) chain into poly(ethylene). This analysis confirms the fact that poly(Exaltolide®) is a stable polymer to temperature and can be processed at high temperature. When the process of microcapsule formation occurred at the $OH_{poly(Exaltolide®)}/NCO_{Desmodur®N100}$ ratio of 1/1, three degradation steps were observed centered on 391, 426 and 483ºC. These decomposition steps were attributed to the decomposition of the polyester nanoparticles after being used as emulsifier of MP/W emulsions at pH12. The Desmodur®N100 also decomposes in three peaks centered on 266, 361 and 457ºC (Appendix 6) which do not appear in the microcapsule decomposition meaning that there are no residue of Desmodur®N100. Moreover, a small peak was observed centered at 300ºC corresponding to the degradation of polyurethane and indicating that the cross-linking reaction proceeded properly (Trovati, 2010). By increasing the reaction time, no significant changes in the curves were observed meaning that reaction of polyurethane formation occurs in less than two hours, thus confirming the results obtained by FTIR spectroscopy.

When the process of microcapsule formation occurred at the $OH_{poly(Exaltolide®)}/NCO_{Desmodur®N100}$ ratio of 1/5 (Figure 4.55.b), three degradation steps were observed centered on 307, 383 and 483ºC The new peak at 307ºC was attributed to the decomposition of the polyurethane. By increasing the reaction time, no significant changes were observed in the curves at t= 2 and 4h

while after 20h of reaction, the decomposition at 383ºC seems to disappear. It should be noted that the peak at 426ºC, attributed to the decomposition of the polyester in CO_2 do not appear.

In order to better identify the influence of the $OH_{poly(Exaltolide®)}/NCO_{Desmodur®N100}$ ratio, the FTIR spectra and DTG profile for the microcapsules after 4h of reaction were plotted and compared to the FTIR spectra of poly(Exaltolide®) nanoparticles and Desmodur®N100 (Figure 4.56).

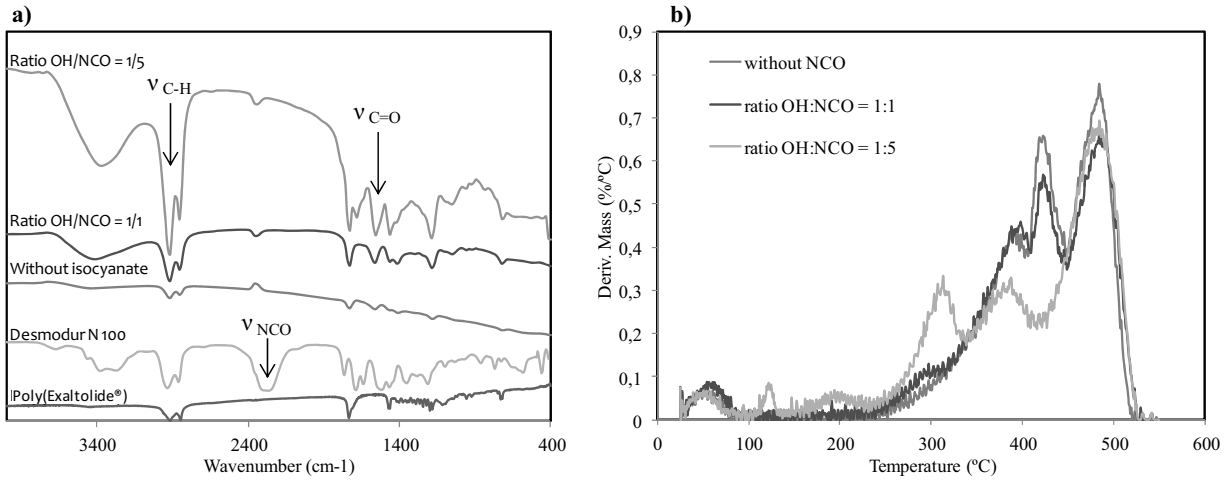

Figure 4.56 : a) FTIR spectra of poly(Exaltolide®) nanoparticles, Desmodur®N100 and microcapsules obtained at three $OH_{poly(Exaltolide®)}/NCO_{Desmodur®N100}$ ratios and b) the DTG profiles of the three microcapsules.

By increasing the isocyanate content in the oil phase of the emulsions, the intensity of the bands of the IR spectra corresponding to the Desmodur®N100 increases in the spectra of the microcapsules indicating an increase of the isocyanate unit in the polymer. Significant differences were observed by increasing the cross-linker concentration, in the DTG profiles. First, by adding more Isocyanate group in the system, the peak between 250 and 350ºC corresponding to the decomposition of polyurethane increases, thus referring to an increase of polyurethane function in the polymer. Moreover, by increasing the $OH_{poly(Exaltolide®)}/NCO_{Desmodur®N100}$ ratio, the peaks centered on 426ºC tend to disappear. This effect is attributed to an increase of the microcapsule rigidity (Trovati, 2010).

The microcapsules at the three $OH_{poly(Exaltolide®)}/NCO_{Desmodur®N100}$ ratios were observed by means of optical microscopy (Figure 4.57.a), after 4h of reaction.

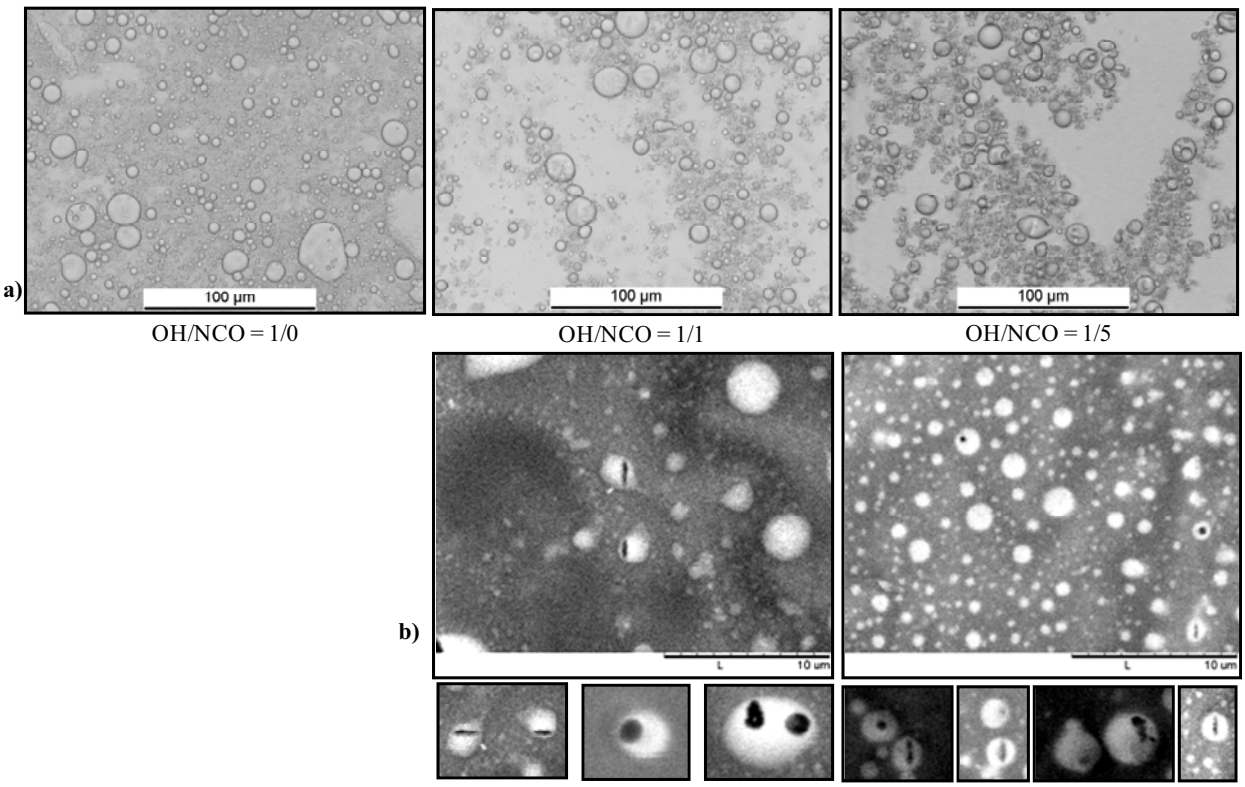

Figure 4.57 : a) Optical micrographs of poly(Exaltolide®) nanoparticles cross-linked microcapsules with a MP/W ratio of 10/90 after preparation at three $OH_{poly(Exaltolide®)}/NCO_{Desmodur®N100}$ ratios and b) SEM micrographs of poly(Exaltolide®) nanoparticles cross-linked microcapsules after washing with Ethanol. Insets: micrographs of selected microcapsules.

The addition of Desmodur®N100 to the oil phase of the emulsions enhance the cross-linking reaction and lead to the formation of microcapsules distinguished on the micrograph by the presence of non-spherical drops with roughness on their surface. When the concentration of isocyanate increases, the roughness at the surface of the drop is more evident which is also attributed to the higher rigidity of the capsules. In order to confirm the formation of microcapsules, the samples were washed three times with ethanol before visualization by SEM (Figure 4.57.b) and compared to the picture obtained by optical microscopy. Covalently cross-linked microcapsules obtained for both $OH_{poly(Exaltolide®)}/NCO_{Desmodur®N100}$ ratios were observed by SEM. Some opened capsules were identified as shown by the black holes on the capsule surface, thus confirming the formation of core-shell microcapsules. Unfortunately, the structure of the shell cannot be properly observed due to the limited resolution of the tabletop SEM.

Nevertheless, it should be noted that the size of the microcapsules is between 0.5 and 5 µm which is slightly smaller than the droplet size of the initial Pickering emulsion (diameter around 10 µm in Figure 4.52). This difference in size can be explained by shrinking of the capsules during the process (elimination of the perfume by evaporation and washing process).

4.4.3.2. Microcapsules from poly(OH-Exaltolide®) stabilized emulsions

In this section, an emulsion with an MP/W ratio of 10/90 and 0.9% of poly(OH-Exaltolide®) nanoparticles was selected for the subsequent formation of capsules by chemical cross-linking. In the previous section, the cross-linking reaction was achieved in 4h at 40ºC using an $OH_{poly(Exaltolide®)}/NCO_{Desmodur®N100}$ ratio of 1/1. The conditions were then applied to the poly(OH-Exaltolide®) system. The formed microcapsules were observed by optical microscopy (Figure 4.58).

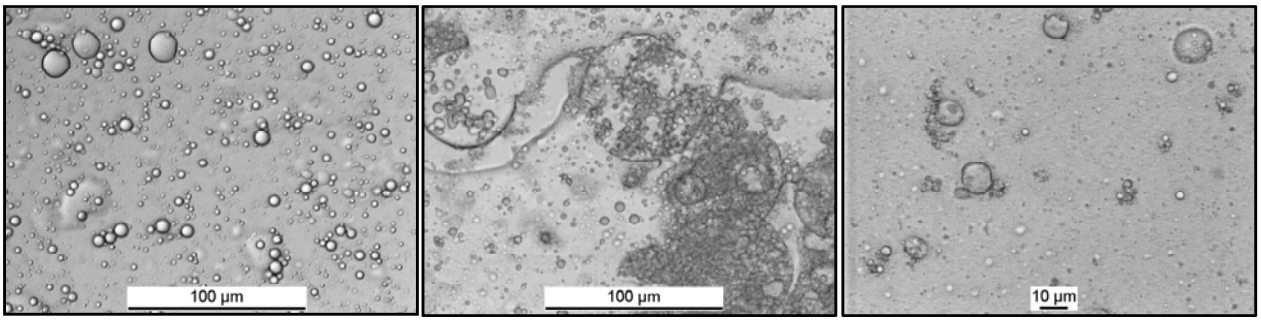

Figure 4.58 : Optical micrographs of microcapsules obtained from poly(OH-Exaltolide®) nanoparticles stabilized emulsions with a MP/W ratio of 10/90 at three $OH_{poly(OH-Exaltolide®)}/NCO_{Desmodur®N100}$ ratios at 40ºC.

Without addition of Desmodur N100, an O/W emulsion was formed with size around 20 µm. The cross-linking reaction did not occur after 4h at 40ºC as shown by the smooth surface and spherical shape of the drops. In contrast, by adding Desmodur®N100 in a $OH_{poly(OH-Exaltolide®)}/NCO_{Desmodur®N100}$ ratio of 1/1, A decrease in the size of the drops as well as changes in the shape (non spherical capsules) implied that the cross-linking reaction took place. Nevertheless, the droplet size was considerably smaller than that obtained with poly(Exaltolide®) nanoparticles, although the roughness at the surface was hard to distinguish. Moreover, cross-linking reaction between the OH groups of two different microcapsules was also suggested by the agglomeration of the drops (Figure 4.58). In fact as poly(OH-Exaltolide®) nanoparticles contains more OH-group in their structure, the reaction of polyurethane formation is faster at such high $OH_{poly(OH-Exaltolide®)}/NCO_{Desmodur®N100}$ ratio and can lead to inter-microcapsule reactions. In order to avoid inter microcapsules reaction and thus agglomeration, the $OH_{poly(OH-Exaltolide®)}/NCO_{Desmodur®N100}$ ratio was then increased from 1/1 to 5/1. The optical micrograph at this $OH_{poly(OH-Exaltolide®)}/NCO_{Desmodur®N100}$ ratio reveals the presence of microcapsules with rough surface and non spherical shape. It is worth noting that the polydispersity was considerably increased by addition of Desmodur N100 for this system compared to the system with

poly(Exaltolide®) nanoparticles. In order to confirm the cross-linking reaction, the final microcapsules were characterized by FTIR spectroscopy and SEM (Figure 4.59).

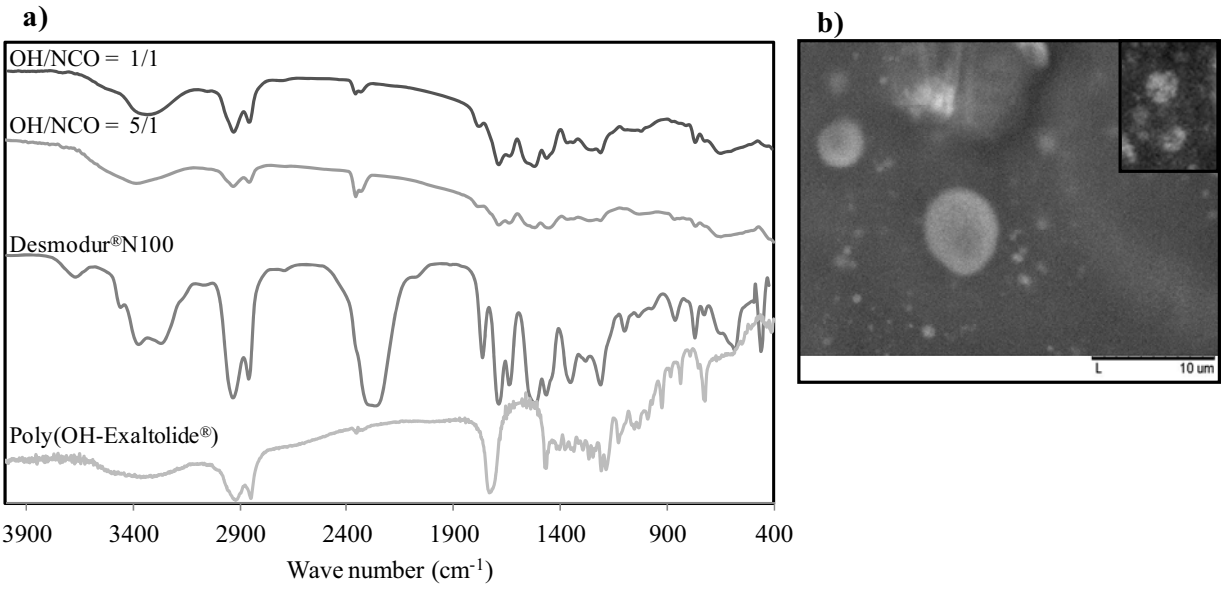

Figure 4.59 : a) FTIR spectra of poly(OH-Exaltolide®) nanoparticles, Desmodur®N100 and microcapsules obtained at two $OH_{poly(OH\text{-}Exaltolide®)}/NCO_{DesmodurN100}$ ratios and b) SEM micrographs and inset of poly(OH-Exaltolide®) nanoparticles cross-linked microcapsules obtained at a $OH_{poly(OH\text{-}Exaltolide®)}/NCO_{Desmodur®N100}$ ratio of 5/1 and inset of selected microcapsules.

The FTIR spectra show the presence of the isocyanate bands at 1200, 1640, 1680 cm^{-1} in the microcapsules but do not present the band at 2270 cm^{-1} corresponding to the NCO group. Moreover, characteristic bands of poly(OH-Exaltolide®) are present in the microcapsules spectra, thus indicating that Desmodur®N100 might have reacted with the nanoparticles. Moreover, it should be noted that the bands corresponding to the Desmodur®N100 are more intense when its concentration in the microcapsules increased. IR spectroscopy suggests the formation of covalently cross-linked microcapsules. The formed microcapsules were then visualized by SEM. The presence of capsules with size of less than 5 µm was observed. Due to their really small size, the microcapsules could not be viewed precisely but the roughness of the surface can be observed.

4.4.3.3. Application of the microcapsules to the release of the Model Perfume

The release of the Model Perfume from the microcapsules was studied when incorporated in a body wash formulation. The percentage of perfume released over time was measured for the microcapsules obtained by cross-linking at various OH/NCO ratios of poly(Exaltolide®) (Figure 4.60.a) and poly(OH-Exaltolide®) (Figure 4.60.b).

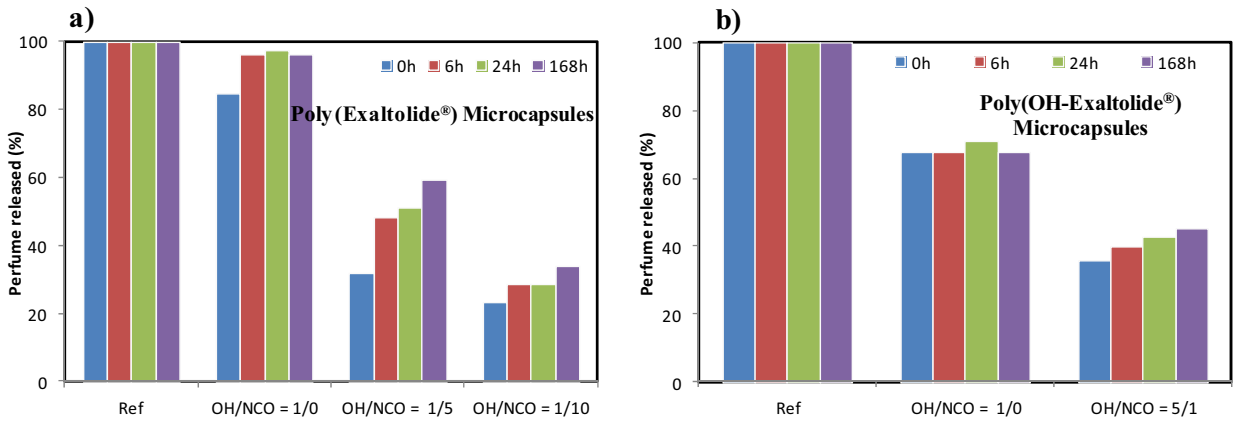

Figure 4.60 : Perfume released from the microcapsules obtained from a) poly(Exaltolide®) nanoparticles cross-linked emulsions at three $OH_{poly(Exaltolide®)}/NCO_{Desmodur®N100}$ ratios: 1/0; 1/5; 1/10 and b) poly(OH-Exaltolide®) nanoparticles cross-linked emulsions at two $OH_{poly(OH-Exaltolide®)}/NCO_{Desmodur®N100}$ ratios 1/0 and 5/1

First, it should be noted that, for a fixed OH/NCO ratio, the perfume release increases over time which is in agreement with diffusion profiles of volatile fragrant molecules. For the microcapsules made of poly(Exaltolide®), at OH/NCO ratio of 1/0, the cross-linking reaction did not occur and almost 90% of the perfume was released after 6h of experiment. The barrier made only by the poly(Exaltolide®) nanoparticles at the interface of the Pickering emulsion is highly permeable and do not retain the perfume in the core of the emulsion. When the isocyanate concentration increases, ($OH_{poly(Exaltolide®)}/NCO_{Desmodur®N100}$ ratio from 1/0 to 1/5), the perfume release is reduced from 90 to about 50%. The further increase of Desmodur®N100 concentration in the system ($OH_{poly(Exaltolide®)}/NCO_{Desmodur®N100}$ ratio of 1/10) allows to limit the perfume release to 35% approximately. As demonstrated in the previous section, the increase of isocyanate concentration induces a higher cross-linking of the nanoparticles at the interface of the Pickering emulsion and as a result, the microcapsules are more rigid and present a lower permeability to the model perfume.

For the microcapsules containing poly(OH-Exaltolide®), the release of MP at OH/NCO = 1/0 was around 70%, lower than the reference sample and the poly(Exaltolide®) microcapsules (Figure 4.60.a). It can be conclude that the poly(OH-Exaltolide®) nanoparticles at the interface of an emulsion (without cross-linking) play the role of barrier to the perfume better than poly(Exaltolide®) nanoparticles. The addition of Desmodur®N100 in a $OH_{poly(OH-Exaltolide®)}/NCO_{Desmodur®N100}$ ratio of 5/1 induces the formation of core-shell microcapsules (as demonstrated in the previous section) and enable a significant decrease of the released perfume from 70 to 40%. The encapsulation of the MP in the poly(OH-Exaltolide®) microcapsules tends to limit the release of the perfume compared to the initial emulsion. Comparable results to

poly(Exaltolide®) microcapsules were obtained when increasing the NCO concentration. This observation confirms the expectation concerning the formation of more rigid microcapsules.

The MP release from the microcapsules containing poly(Exaltolide®) and poly(OH-Exaltolide®) were compared at the same OH/NCO ratio of 5/1 and results are presented in Figure 4.61.

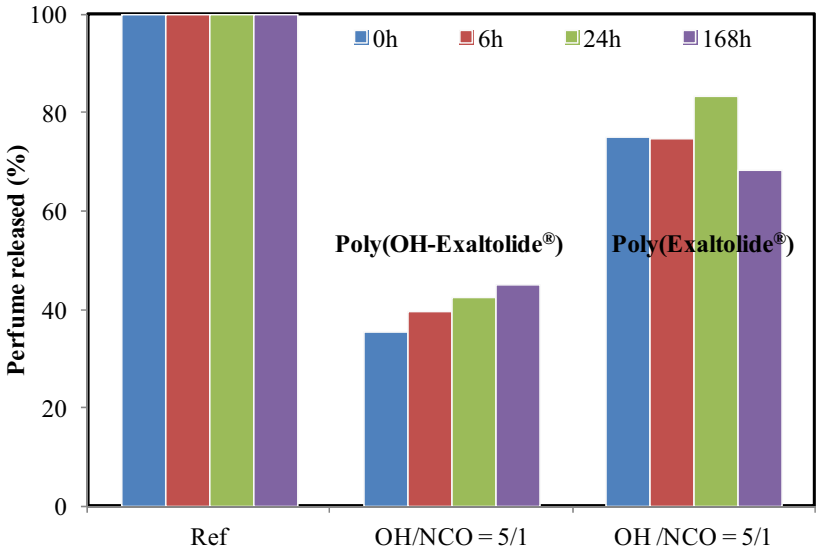

Figure 4.61 : Comparison of the perfume released from the microcapsules obtained from poly(OH-Exaltolide®) and Poly(Exaltolide®) nanoparticles cross-linked emulsions at the OH/NCO ratio 5/1.

Approximately 80% of perfume was release in the first 6 hours with poly(Exaltolide®) microcapsules while only 40% was released from poly(OH-Exaltolide®) microcapsules. The presence a higher content of OH-group in the structure of poly(OH-Exaltolide®), compared to poly(Exaltolide®), enable a better cross-linking at the interface with lower isocyanate concentration, thus creating a less permeable membrane and reducing the release of the MP.

Summary:

Microcapsules were formed by reaction at the interface of Model Perfume-in-water Pickering emulsions between the polyester nanoparticles and an Isocyanate cross-linker, Desmodur N100. The reaction takes place in less than 4h at 40ºC and an increase of the isocyanate concentration induces the formation of more rigid microcapsules. To conclude, studies of the perfume release over time have evidenced the formation of microcapsules with tuneable permeability. The release of perfume from the core of the capsules, followed over time, can be controlled by using poly(OH-Exaltolide®) nanoparticles instead of poly(Exaltolide®)nanoparticles or by controlling the rigidity of the capsules by increasing the isocyanate concentration.

CONCLUSIONS

5. CONCLUSIONS AND FUTURE WORK

Biodegradable polymeric nanoparticles have been obtained by polymerization in mild conditions of monomer-in-water nano-emulsions obtained by low-energy method. The properties of the polymeric nanoparticles have been determined and potential applications for the delivery of volatile compounds have been explored. The most important conclusions are the following.

Formation of O/W nano-emulsion by low-energy methods

Nano-emulsification of Exaltolide® and OH-Exaltolide® has been achieved successfully by low-energy methods using Brij®96Vand Cremophor®EL, respectively, as surfactant and squalane as co-oil.

The study on nano-emulsion formation in the water/Brij®96V/Exaltolide®:squalane system demonstrated that:

- Bluish transparent nano-emulsions are formed using both the PIT and the PIC methods at O/S ratios from 30/70 to 90/10 and water content from 70 to 95%.
- Nano-emulsions with 90% water showed droplet diameters between 10 and 200 nm depending on the O/S ratio and the preparation method. As expected, he the value of the droplet diameter, obtained by DLS is slightly higher than that obtained by TEM image analysis.
- The calculated theoretical diameters are slightly lower than the droplet diameters measured by DLS and are similar to those obtained by TEM analysis, indicating that emulsification is close to the optimum.

In addition, the study of nano-emulsion formation in the water/Cremophor®EL/OH-Exaltolide®:squalane system shows that:

- The formation of bluish transparent emulsions is achieved by the PIC method as the PIT of this system is too high to carry out properly the emulsification without changes in the composition. The nano-emulsions were obtained at O/S ratios from 40/60 to 70/30 and water content from 70 to 95%. Nano-emulsions with higher oil content are obtained in this system as compared to systems described in the literature with the same surfactant.
- Droplet diameters of nano-emulsion with 90% water are between 20 and 200 nm depending on the O/S ratio.

A study of the nano-emulsions stability, by following changes of the droplet size showed that:

- nano-emulsions of both systems containing 90% of water and an O/S ratio of 50/50 are stable for at least 4 days at 25ºC and one day at 45ºC indicating a good stability at room temperature and a sufficient stability at 45ºC to carry out the polymerization in the droplet of the nano-emulsions which takes place in 24hours.

Synthesis of polyester nanoparticles by polymerization in the nano-emulsion droplets and their characterization.

The study of the polymerization parameters (temperature and enzyme concentration), carried out in the water/Brij®96V/Exaltolide®:squalane system, demonstrated that:

- Complete conversion of the monomer is achieved in 7 h by addition of 0.1% enzyme at 45ºC. The reaction in confined media such as in nano-emulsion allows decreasing significantly the enzyme concentration, the reaction time and temperature as compared to the enzymatic ring-opening polymerization in bulk or organic solvents.
- Poly(Exaltolide®) with a molecular weight of around 2600 g/mol was obtained which is of the same order of magnitude as that obtained in bulk polymerization.
- Poly(Exaltolide®) nanoparticles present a melting point of 80ºC, slightly lower than that obtained for bulk polymer. This difference is explained by the melting point depression that occurs in the presence of small particles. This result suggests the formation of small size (<50 nm) poly(Exaltolide®) nanoparticles.
- Their size, as detected by TEM image analysis, was small (20nm) and in the range of the nano-emulsion droplet templates.
- Poly(Exaltolide®) presents a pseudo orthorhombic crystalline structure, which is in agreement with data found in the literature. The high crystallinity of the polymer (75%), determined by calorimetric analysis, is appropriate for further applications.

The study of polymerization of the functionalized Exaltolide®, OH-Exaltolide®, in nano-emulsions of the water/Cremophor®EL/OH-Exaltolide®:squalane system showed that:

- Complete conversion was achieved using the same reaction conditions as those used for Exaltolide® polymerization (0.1% enzyme, 45ºC and 24h).
- The molecular weight of the resulting poly(OH-Exaltolide®) was of the same order as that of poly(Exaltolide®).
- Poly(OH-Exaltolide®) present a high melting point and is a crystalline polymer with a similar structure to that of poly(Exaltolide®). This feature was not necessarily obvious as

the presence of the OH group in the Exaltolide® molecule might have altered the order of the crystalline structure.

- Spherical poly(OH-Exaltolide®) nanoparticles with sizes around 20nm were formed.
- Functionalization of polyester nanoparticles by mild polymerization in nano-emulsion had not been reported previously.

The study of simultaneous polymerization of two monomers (Exaltolide®/OH-Exaltolide® and Exaltolide®/Habanolide) in the nano-emulsion droplets of the water/Brij®96V/Exaltolide®: comonomer:hexadecane system demonstrated that:

- The copolymerization of the monomers was achieved and confirmed by ^{1}H and ^{13}C NMR spectroscopy. Complete conversion was observed after 24 h at 45ºC and the ratio of each monomer in the final polymer corresponds to that initially present in the nano-emulsion.
- The melting point of the resulting polymers decreases by increasing the co-monomer content.
- Mild copolymerization in nano-emulsions allows a possible control of the content of functional group in the polyester nanoparticles.

Potential applications of the polymeric nanoparticles for the delivery of volatile compounds.

Affinity of polyester nanoparticles with volatile fragrant molecules.

Affinity of the nanoparticles with volatile fragrant compounds was pointed out by a reduction of the evaporation in presence of nanoparticles, suggesting the formation of aggregates of polymer and volatile compounds. This study shows that the formed polyester nanoparticles can be used for the retention of volatile compounds.

Emulsions stabilized by polyester nanoparticles.

The formation and stability of nanoparticle-stabilized emulsions have been investigated as a function of various parameters and the main conclusions are the following:

- O/W emulsions have been formed with pure oil compounds and typical perfume formulation.
- Nanoparticle-stabilized emulsions has been stabilized successfully with poly(Exaltolide®) and poly(OH-Exaltolide®) nanoparticles. In general, smaller droplet sizes were observed with poly(OH-Exaltolide®) nanoparticles. By varying parameters such as the

nanoparticles concentration and the O/W ratio, the stability of Pickering emulsions is affected by modifying the emulsion drop size.

- Nanoparticles dispersed in water aggregate in the presence of 10^{-1}M of NaCl and at pH higher than 12. The optimal stabilization of O/W emulsions by nanoparticles has been achieved at pH 12, indicating that the emulsions are stabilized by aggregated nanoparticles.
- Nanoparticles melt in most of the oils studied at temperatures around 50ºC. As a consequence, the stability of the emulsions is limited to temperature below the melting of the particles at 50ºC.
- In this study, perfume-in-water emulsions with different O/W ratios have been successfully stabilized by biodegradable polyester nanoparticles in quantities as low as 1%. Moreover, the emulsion drop size can be controlled by varying parameters such as the nanoparticles wettability, the nanoparticles concentration, the O/W ratio.

Formation of microcapsules by cross-linking the nanoparticles at the interface of O/W Pickering emulsions.

- Formation of microcapsules has been achieved by covalent cross-linking of the nanoparticles at the interface of a perfume-in-water emulsion by addition of isocyanate at 40ºC for 4h. An increase of the isocyanate concentration results in the formation of more rigid polyurethane interface.
- The release of perfume from the core of the capsules, followed over time, can be controlled by using poly(OH-Exaltolide®) nanoparticles instead of poly(Exaltolide®)nanoparticles.
- A faster release was observed at low concentration of isocyanate, indicating the permeability of the O/W interface when covered by these polyester nanoparticles.

FUTURE WORK

Although the main objectives of this thesis have been reached in achieving the formation of core-shell microcapsules made of biodegradable polyester nanoparticles, more investigations are needed to improve each step of the study. For each step, some suggestions are listed below:

- Formation of nano-emulsions by low-energy methods:
    - Study in details of the phase diagrams of the studied system in order to understand better the mechanisms of nano-emulsion formation.
    - Study of the nano-emulsion stability at various O/S ratios, time and temperature.

- Synthesis of polyester nanoparticles from nano-emulsion templates
    - Study of the composition of the nano-emulsion template on the size of the obtained nanoparticles.
    - Further study on the functionalization and copolymerization kinetics and its relation with the functionalization degree.

- Formation of Pickering emulsions stabilized by polyester nanoparticles
    - Study of the functionalization degree of the nanoparticles (wettability) on the stabilization of perfume-in-water emulsions.
    - Study of the perfume release from Pickering emulsions stabilized by nanoparticles of various wettabilities.

- Formation of microcapsules from Pickering emulsion templates
    - Study of the reaction and composition parameters (temperature, size of emulsion, type of nanoparticles) on the final microcapsules.
    - Study of the microcapsules surface by SEM, TEM or Atomic Force Microcopy.
    - Another approach for the synthesis of microcapsules could be the cross-linking of the interface from the water phase using an hydrophilic isocyanate.

SUMMARY IN SPANISH

6. SUMMARY IN SPANISH

1. INTRODUCCIÓN

Las nano-emulsiones se definen como emulsiones que poseen un tamaño de gota en el rango nanométrico y típicamente inferior a 200 nm, (Solans, 2005; Mason, 2006; McClemens, 2011) presentando por ello una apariencia translucida o transparente (Figure 6.1).

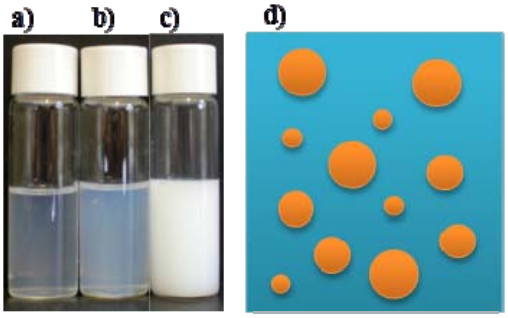

Figure 6.1 : Ejemplos de emulsiones: a) y b) nano-emulsiones, c) emulsión convencional. d) Representación esquemática de una dispersión liquido-liquido.

Las nano-emulsiones se han designado también como miniemulsiones, emulsiones submicrométricas, emulsiones ultrafinas, etc. No obstante, el término nano-emulsión ha sido adoptado en los últimos años, debido a que da una idea de que el tamaño de gota se halla en el rango nanométrico y que se trata de emulsiones, evitando confusiones con el término microemulsión (McClemens, 2012; Anton, 2011). Las emulsiones son sistemas termodinámicamente inestables que tienden a la separación en dos (o más) fases. Los principales procesos de desestabilización de las emulsiones son: cremado/sedimentación, floculación, coalescencia y maduración de Ostwald (Figure 6.2).

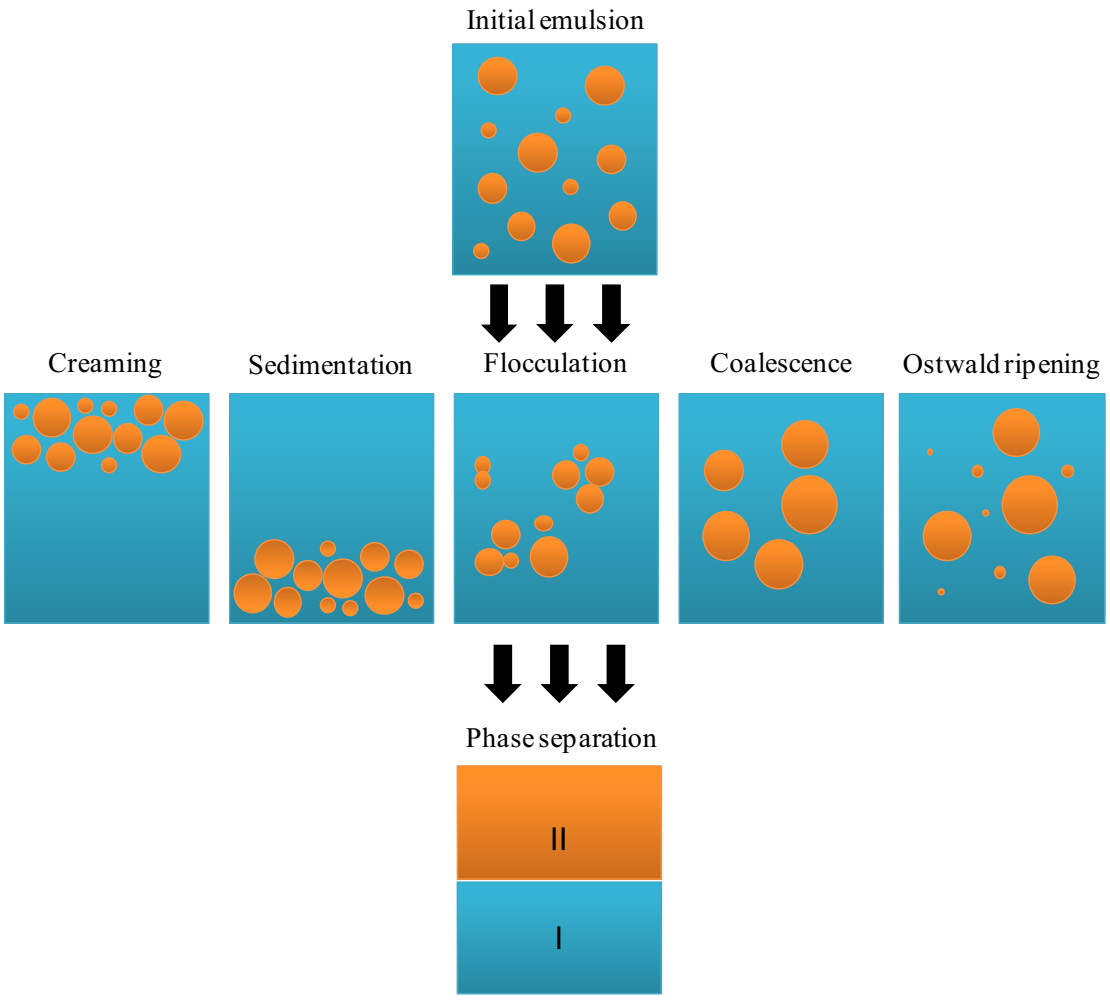

Figure 6.2 : Mecanismos de desestabilización de las emulsiones.

No obstante, las nano-emulsiones, debido a su pequeño tamaño de gota, son estables frente a la separación gravitacional (cremado/sedimentación). Por ello, las nano-emulsiones, convenientemente estabilizadas frente a los otros mecanismos de desestabilización, pueden presentar una estabilidad cinética elevada (Tadros, 2004; Izquierdo, 2002). Para prevenir los mecanismos de desestabilización previamente citados, las emulsiones se estabilizan mediante la adición de tensioactivos, los cuales tienen la propiedad de adsorberse en la interfase aceite/agua disminuyendo la tensión interfacial entre las dos fases, favoreciendo así su formación y estabilidad. Las nano-emulsiones se preparan generalmente por métodos de alta energía, en los cuales la energía para formar las gotas pequeñas proviene de una fuente externa como los homogeneizadores de alta presión o ultrasonidos. Sin embargo, también se pueden preparar por métodos de baja energía, aprovechando la energía interna de los componentes del sistema que se libera durante el proceso de emulsificación (Solans, 2012). Entre los métodos de baja energía

destacan los de inversión de fases que se basan en la inversión de la curvatura espontánea del tensioactivo, provocada por cambios de temperatura a composición constante (PIT) o por cambios en la composición a temperatura constante (PIC) durante el proceso de emulsificación. En comparación con los métodos de alta energía, donde el tamaño de las gotas de la nano-emulsión disminuye al aumentar la energía aportada al sistema, los métodos de baja energía generalmente producen gotas más pequeñas y más uniformes cuando las propiedades físico-químicas del sistema están optimizadas (Izquierdo, 2002; Morales, 2003 and 2006; Roger, 2011; Solé, 2012). Debido a sus pequeños tamaños de gota y a la posibilidad de conseguir una elevada estabilidad cinética, las nano-emulsiones se usan en una multitud de aplicaciones, por ejemplo como sistemas de liberación de fármacos (Gutiérrez, 2008; McClemens, 2011; Sonneville-Auburn, 2004) o como plantilla para la preparación de nanopartículas (Ugelstadt, 1973; Fessi, 1989; Anton, 2008), etc.

Las nanopartículas son partículas sólidas coloidales con tamaños generalmente entre 20 y 500 nm, que han despertado un gran interés en las últimas décadas, principalmente para la encapsulación de principios activos farmacéuticos, cosméticos (Vauthier, 2003; Vrignaud, 2011) o alimentarios. Se ha descrito extensamente en la literatura la preparación de nanopartículas generalmente inorgánicas (de oro, plata o sílice), lípidicas sólidas o poliméricas. La formación de nanopartículas poliméricas y especialmente las nanopartículas de poliésteres han despertado mucho interés en los últimos años por sus posible biodegradabilidad y biocompatibilidad (Meulen, 2008). La preparación de nanopartículas de poliésteres se ha descrito de varias maneras en la literatura consistiendo generalmente en un proceso en dos etapas. La primera etapa consiste en la preparación de un sistema coloidal como por ejemplo emulsiones, nano-emulsión, microemulsiones o cristales líquidos. Mientras que la segunda etapa consiste en la generación de nanopartículas poliméricas por precipitación de un polímero preformado o por polimerización de monómeros presentes en la fase dispersa del sistema coloidal. En el primer método, las nanopartículas poliméricas se obtienen por evaporación o difusión del disolvente o por “salting out” (Quintanar-guerrero, 1997; Anton, 2008; Vauthier, 2009). Estos procesos se han utilizado principalmente con polímeros tales como ácido poliláctico, ácido poliglicólico y sus copolímeros (Fessy, 1989), policaprolactona (Cho, 2006). La principal desventaja de este proceso es el uso de disolventes orgánicos tóxicos (generalmente clorados) para disolver el polímero preformado. La otra estrategia consiste en preparar nanopartículas poliméricas mediante la polimerización de un monómero (disuelto en la fase dispersa de nano-emulsiones) (Ugelstadt, 1973; Asua, 2002; Antonietti, 2002; Schork, 2005). A pesar del gran número de artículos que describen la formación

de nanopartículas poliméricas en nano-emulsiones, sólo algunos artículos se refieren a este proceso en nano-emulsiones obtenidas por métodos de baja energía (Spernath, 2007). Esto se explica por el hecho de que la emulsificación por métodos de baja energía de aceites polares, como ciertos monómeros, requiere un mayor esfuerzo en la selección apropiada de los componentes del sistema. Por lo tanto, se considero de interés estudiar la preparación de nanopartículas poliméricas a partir de nano-emulsiones obtenidas por métodos de baja energía.

La polimerización "in-situ" de monómeros en nano-emulsiones ha sido ampliamente estudiada desde que apareció la primera publicación sobre el tema en 1973 (Ugelstadt, 1973). Se describieron principalmente reacciones iniciadas por radicales libres para formar polímeros tales como el poliestireno o los poliacrilatos. Recientemente, se han descrito nuevos tipos de reacciones en nano-emulsiones como por ejemplo poliadición, policondensación o polimerización por apertura de anillo, catalizados por agentes aniónicos, catiónicos, ácidos o metálicos (Maitre, 2000; Cauvin, 2002; Soula, 2001; Barrère, 2003; Ruppert, 2010; Siebert, 2012; Antonietti, 2002). Sin embargo, estas reacciones requieren generalmente el uso de condiciones extremas (pH bajo, iniciadores tóxicos, alta temperaturas) para la obtención de polímeros con un rendimiento y un peso molecular aceptables. Sabiendo que la formación de poliésteres por apertura de lactonas se había realizado con éxito en "bulk" usando compuestos biológicos como enzimas, Taden *et al.* describieron in 2003 dicha reacción en nano-emulsiones usando una pentadecanolactona como monómero y una lipasa como catalizador (Taden, 2003) (Figure 6.3).

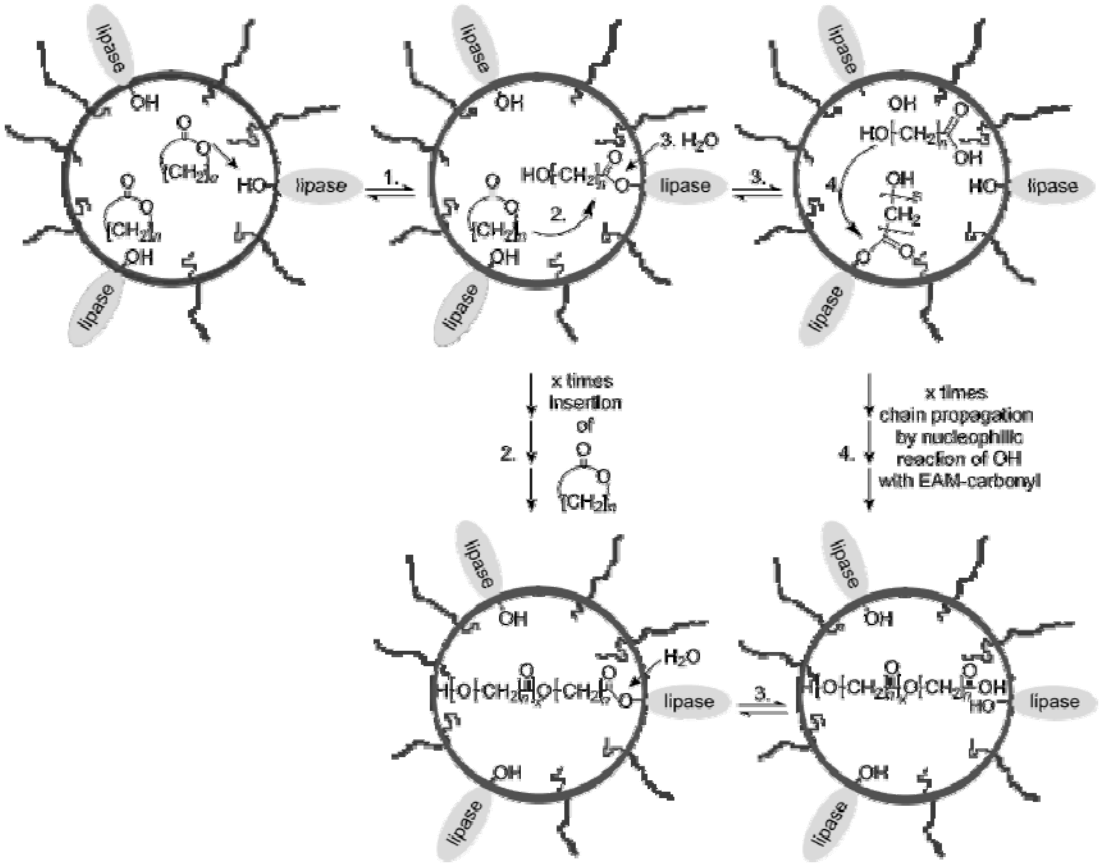

Figure 6.3 : Mecanismo de la polimerización por apertura de anillo de una lactona catalizada por lipasa en miniemulsion (Taden, 2003).

No obstante, el número de artículos describiendo este tipo de reacción en nano-emulsiones es limitado (Målberg, 2010). En este contexto, es necesario llevar a cabo una investigación más exhaustiva sobre la obtención de nanopartículas de poliéster por polimerización en nano-emulsión y en condiciones suaves.

Las nanopartículas se han utilizado ampliamente para la encapsulación y la posterior liberación controlada de compuestos activos (Pinto Reis, 2006a-b; Guterres, 2007; Vrignaud, 2011), pero también se pueden usar para la estabilización de emulsiones (Aveyard, 2003; Binks, 2006; Leal-Calderon, 2008). Aunque, generalmente, las emulsiones se estabilizan mediante moléculas de compuestos tensioactivos, también se pueden preparar y estabilizar mediante partículas sólidas (Figure 6.4).

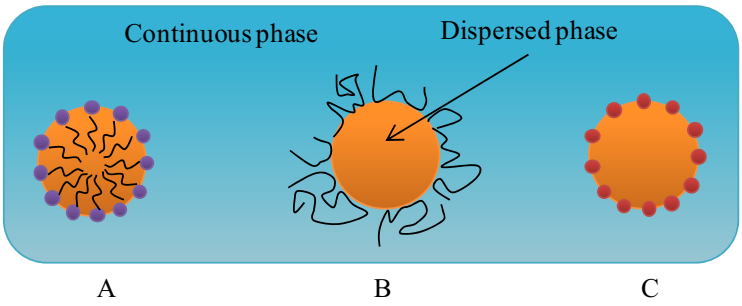

Figure 6.4 : Mecanismo de estabilización de las emulsiones aceite-en-agua : A – por tensioactivo, B- por polímeros, C- por partículas.

Estos sistemas reciben el nombre de emulsiones de Pickering (Ramsden, 1903; Pickering, 1907). Las nanopartículas sólidas, con un ángulo de contacto apropiado, tienden a adsorberse en la interfase agua/aceite de las emulsiones, proporcionando así una elevada estabilidad. Es importante señalar que las propiedades coloidales, tal como el ángulo de contacto (Binks, 2002a-c) de las nanopartículas sólidas, pueden variar dependiendo de determinados parámetros de composición (Tambe, 1994; Binks, 2001, Binks, 2007a-c), como el pH y la concentración de electrolitos (Hassander, 1989; Binks, 1999; Prestidge, 2004), influyendo así en el comportamiento de las emulsiones. Otros factores como la concentración de nanopartículas, su tamaño y su forma o la composición general del sistema pueden afectar también considerablemente el comportamiento de las emulsiones de Pickering. Aunque dichas emulsiones se conocen desde hace más de un siglo, la gama de nanopartículas que se usan para estabilizar dichas emulsiones se ha limitado a nanopartículas de sílica, arcilla, poliestireno, poliacrilato (Aveyard, 2002; Binks, 2006) o metálicas (Binks, 2012). Las emulsiones de Pickering se estabilizan debido a la formación de la barrera estérica y mecánica que forman las nanopartículas en la interfase, por lo tanto también se han descrito como posibles sistemas para controlar la liberación de compuestos volátiles (Binks, 2010a-b). No obstante, estos sistemas generalmente presentan una alta permeabilidad y por lo tanto una rápida liberación del compuesto encapsulado. Con el objetivo de mejorar su permeabilidad, se ha descrito la formación de cápsulas con permeabilidad modulable, denominadas coloidosomas (Velev, 1996; Dinsmore, 2002). Los coloidosomas se forman generalmente por reacciones térmicas (Dinsmore, 2012; Laïb, 2008), por adsorción de polielectrolitos, por captura de gel (Cayre, 2012) o reticulación covalente (Thomson, 2010) en la interfase de las emulsiones de Pickering.

2. OBJECTIVOS

El objetivo principal de este proyecto es estudiar la polimerización, en condiciones suaves, de monómeros que constituyen la fase dispersa de nano-emulsiones obtenidas por métodos de baja energía, la caracterización de las nanopartículas poliméricas resultantes y el estudio de sus posibles aplicaciones como sistemas de liberación controlada de compuestos volátiles. Este objetivo incluye los siguientes objetivos parciales:

1. Preparación de nano-emulsiones aceite-en-agua por métodos de baja energía usando monómeros no tóxicos como fase oleosa.
2. Síntesis de nanopartículas poliméricas mediante la polimerización en las gotas de nano-emulsión y su caracterización.
3. Estudio de propiedades funcionales de las nanopartículas poliméricas para la liberación de compuestos volátiles.

3. RESULTADOS Y DISCUSIÓN

En primer lugar, se seleccionaron los componentes de la nano-emulsión (monómeros y agentes tensioactivos). Una vez seleccionados los componentes de la nano-emulsión, se estudió la formación de nano-emulsiones aceite-en-agua por métodos de baja energía y su estabilidad. En segundo lugar, se estudió la síntesis de nanopartículas de poliésteres en nano-emulsiones. Además, se estudió la síntesis de nanopartículas de poliésteres funcionalizadas y a posteriori, la funcionalización de las nanopartículas poliméricas por copolimerización de dos monómeros en nano-emulsión. Por último, se estudió la posible aplicación de dichas nanopartículas para la estabilización de emulsiones de compuestos volátiles en agua.

3.1. SELECCIÓN DE LOS COMPONENTES DE LAS NANO-EMULSIONES.

Primeramente, se seleccionaron monómeros polimerizables a bajas temperaturas y un catalizador no tóxico, con el fin de llevar a cabo una polimerización en condiciones suaves. Esta selección se basó en trabajos anteriormente descritos.

Dentro de la gran variedad de monómeros (estireno, acrilato...) que se han utilizado para la polimerización en nano-emulsiones, se ha descrito que las lactonas polimerizan fácilmente

mediante polimerización por apertura de anillo a baja temperatura, mediante una reacción enzimática catalizada por una lipasa. Se seleccionó la lactona, **Exaltolide®**, (pentadecanolide) la cual presenta un gran anillo de 15 átomos de carbono (Figura 6.5). Además, puede llegar a formar un poliéster cristalino, característica requerida para la formación de membranas de baja permeabilidad a los compuestos volátiles (Focarete, 2001; Gazzano, 2003). Por otra parte, este monómero presenta una baja toxicidad y da lugar a un poliéster biocompatible y biodegradable, lo cual presenta un gran interés para los objetivos de esta investigación.

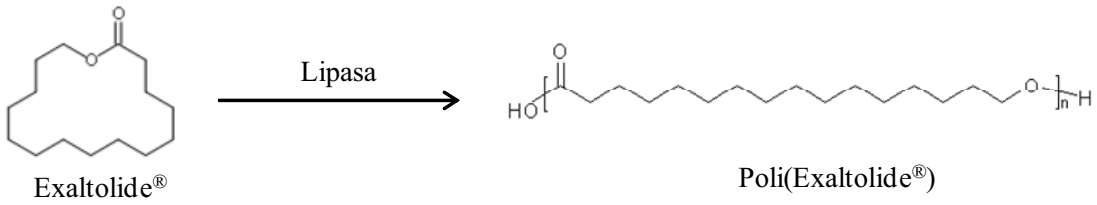

Figura 6.5 : Reacción de polimerización del monómero Exaltolide® en poli(Exaltolide®).

En segundo lugar, se seleccionó el monómero, **hidroxi-Exaltolide®**, el cual presenta un grupo funcional hidroxilo en el macrociclo de la Exaltolide®. Posibilitando así la obtención de un polímero funcionalizado por grupos OH (Figura 6.6).

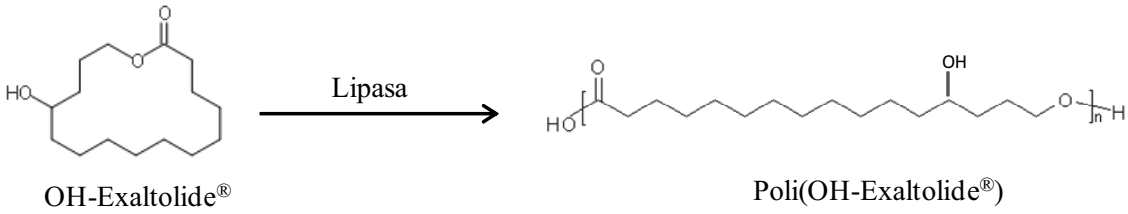

Figura 6.6 : Posible reacción de polimerización del monómero OH-Exaltolide® en poli(OH-Exaltolide®).

Dichas lactonas macrocíclicas puede polimerizar mediante la reacción de apertura de anillo y generalmente requiere el uso de catalizadores. Entre la gran variedad de catalizadores ya usados para esta reacción (generalmente organometálicos), las enzimas han atraído mucha atención en los últimos 20 años. Las mejores enzimas para este tipo de reacción son las lipasas, por su capacidad de hidrolizar enlaces ester. En base a un estudio bibliográfico, se seleccionó la **lipasa *pseudomonias cepacia*, Amano PS.**

3.2. FORMACIÓN DE NANO-EMULSIÓNES ACEITE-EN-AGUA POR METODOS DE BAJA ENERGIA

El primer objetivo de esta tesis consistió en la preparación de nano-emulsiones de un monómero-en-agua para su posterior uso como plantilla para la formación de nanopartículas ("miniemulsion polymerization"). Taden *et al.* describieron en 2003 la formación de nano-emulsiones Exaltolide®-en-agua utilizando un método de alta energía (Taden, 2003; Målberg, 2010). Con el objetivo de mejorar este proceso, en el presente trabajo, se estudió la formación de nano-emulsiones de Exaltolide®-en-agua y OH-Exaltolide®-en-agua, estabilizadas por tensioactivos no-iónicos, mediante un método de baja energía, es decir usando la energía liberada por el sistema durante el proceso de emulsificación. Entre los métodos de emulsificación de baja energía, destacan los de inversión de fase. La inversión de fase se puede llevar a cabo mediante cambios de temperatura (a composición constante, PIT) o de composición (a temperatura constante, PIC).

A partir de un estudio preliminar, se seleccionaron los tensioactivos no iónicos y co-solventes para cada uno de los monómeros elegidos. Se seleccionaron los sistemas **agua/Brij® 96V/Exaltolide®: escualano** y **agua/Cremophor®EL/OH-Exaltolide®: escualano** para la formación de nano-emulsiones. Las nano-emulsiones formadas se caracterizaron mediante técnicas tales como dispersión dinámica de luz (DLS), retrodiffusión de luz (LBS) y microscopía electrónica de transmisión (Crio-TEM), preparando las muestras mediante vitrificación. Es muy importante conocer la estabilidad de estas nano-emulsiones para su utilización como plantilla para la polimerización de los monómeros. Por ello, se estudió de manera sistemática la estabilidad de las nano-emulsiones formadas con los dos sistemas y se determinaron los mecanismos de desestabilización.

Se observó la formación de nano-emulsiones azuladas transparentes con el sistema **agua/Brij® 96V/Exaltolide®:escualano** utilizando tanto el método PIT como el método PIC. Se determinó la región de formación de nano-emulsiones por el método PIT y se observó una amplia región para relaciones de aceite/tensioactivo entre 30/70 y 90/10 con un contenido de agua superior a 70% (Figura 6.7.a-b). Los tamaños de gota de las nano-emulsiones con un contenido de agua del 90% y a varias relaciones aceite/tensioactivo se caracterizaron mediante DLS y se mostró la formación de nano-emulsiones con diámetros entre 16 y 100 nm dependiendo de las relaciones aceite/tensioactivo y el método de preparación. Por Crio-TEM se caracterizó una nano-emulsión conteniendo 90% de agua y una relación aceite/tensioactivo 50/50, resultando en un tamaño de gota medio de 16.7 ± 3.6 nm (Figura 6.7.c). Como era de esperar, el valor del diámetro de la gota

obtenido por DLS fue ligeramente mayor que el tamaño obtenido analizando las imágenes de Crio-TEM. En efecto, la técnica DLS mide el radio hidrodinámico (el tamaño de la gotas rodeadas por la capa de agua que se mueve con ellas), siempre mayor que el tamaño de las gotas medido por TEM. Por otra parte, se compararon los tamaños experimentales con los teóricos que se pueden obtener para una cierta composición, asumiendo que todo el tensioactivo se halla en la interfase. Se obtuvieron diámetros mínimos ligeramente inferiores a los diámetros medidos por DLS y similares a los obtenidos por análisis de las imágenes de Crio-TEM. Este resultado indicó que la emulsificación se acerca a la emulsificación óptima. En cuanto a la estabilidad, se estudiaron los cambios de diámetro de gota con el tiempo (24h) por DLS a 25ºC y por retrodiffusión de luz láser a 25ºC y a 45ºC para nano-emulsiones con 90% de agua y diversas relaciones aceite/tensioactivo. No se observaron cambios de tamaños de gotas durante al menos 1 día a 25ºC (Figura 6.7.d) y a 45ºC. Esto indicó que las nano-emulsiones presentaban una estabilidad suficiente para llevar a cabo la reacción de polimerización enzimática dentro de las gotas, tanto a temperatura ambiente como a 45ºC.

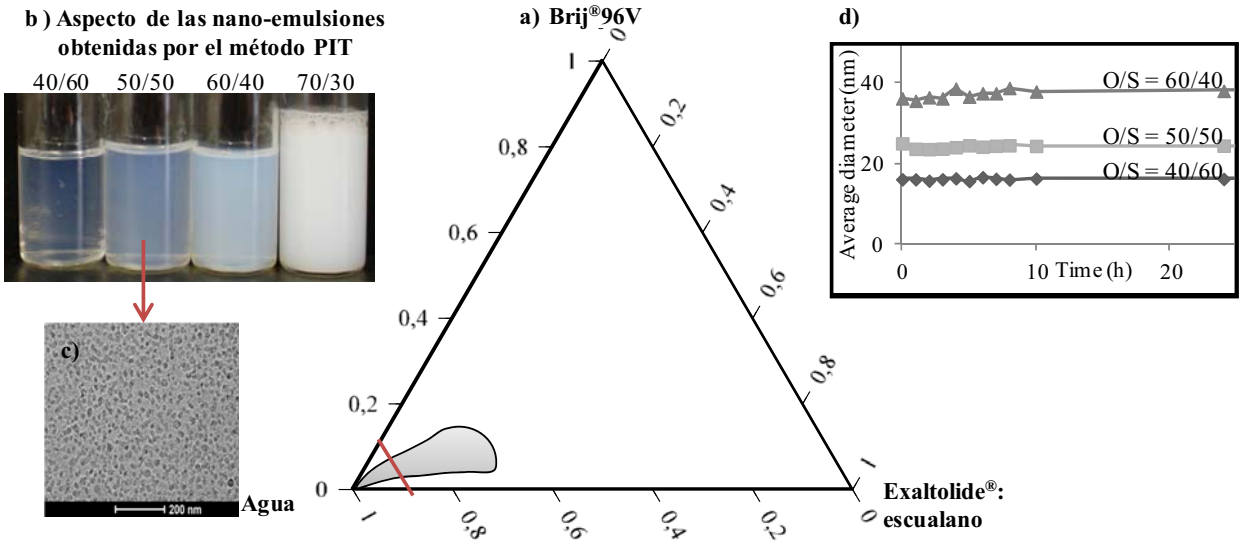

Figura 6.7 : Resumen de los resultados obtenidos con el sistema agua/Brij96V/Exaltolide®:escualano a) Región (gris) de formación de nano-emulsiones, b) Aspecto de las nano-emulsiones formadas por el método PIT con 90% de agua a varias relaciones aceite/tensioactivo (O/S), c) Imagen por Crio-TEM de la nano-emulsión con 90% de agua y la relación aceite/tensioactivo (O/S) 50/50, d) Evolución del tamaño de gota medidos por DLS con el tiempo a 25ºC.

También se formaron nano-emulsiones transparentes azuladas con el sistema **agua/Cremophor® EL/OH-Exaltolide®:escualano** usando el método PIC. Se determinó la región de formación de nano-emulsiones por este método para relaciones O/S entre 40/60 y 70/30 y se obtuvieron nano-emulsiones en composiciones entre 40/60 y 70/30 y con un contenido de agua del 70% o superior. Se comparó la región determinada por el sistema agua/Cremophor EL/OH-

Exaltolide®:escualano con la región obtenida por un sistema descrito en la literatura con el mismo tensioactivo pero distinto componente oleoso (Sadurni, 2005). Se observó que en los sistemas con Exaltolide® y OH-Exaltolide® se forman nano-emulsiones en una región más amplia pudiendo así emulsionar cantidades de aceite mayores con menos concentración de tensioactivo, lo cual permite una reducción del consumo de tensioactivo. Las nano-emulsiones conteniendo 90% de agua y a varias relaciones aceite/tensioactivo se caracterizaron por DLS y Crio-TEM y se obtuvieron tamaños de gota entre 25 y 200 nm dependiendo de la proporción aceite/tensioactivo (Figura 6.8.d). En cuanto a la estabilidad, se determinó el tamaño de gota de una nano-emulsión con 90% de agua y una proporción aceite/tensioactivo del 50/50 por DLS a 25ºC y por retrodiffusión de luz laser a 25ºC y 45ºC. En ningún caso se observaron cambios de tamaño de gota, indicando así que el sistema tiene una estabilidad suficiente a ambas temperaturas para llevar a cabo el proceso de polimerización.

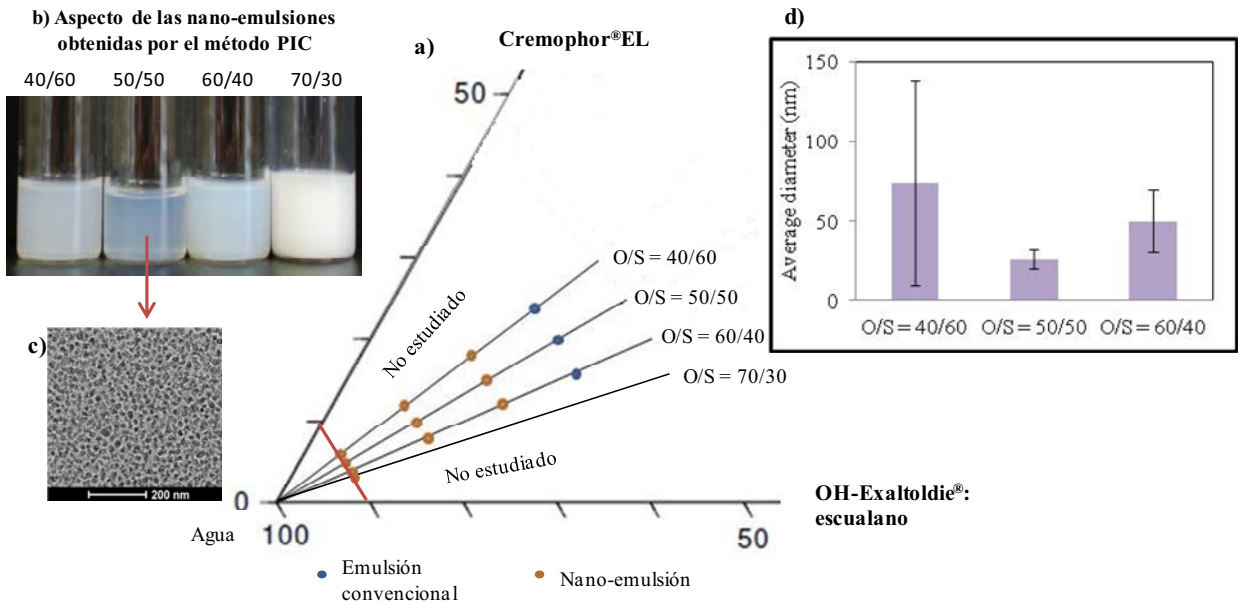

Figura 6.8 : Resumen de los resultados obtenidos con el sistema Agua/Cremophor EL/OH-Exaltolide®:escualano a) Región de formación de nano-emulsiones , b) Aspecto de las nano-emulsiones formadas por el método PIC con 90% de agua a varias relaciones aceite/tensioactivo (O/S), c) Imagen de Crio-TEM de la nano-emulsión con 90% de agua y relación aceite/tensioactivo (O/S) 50/50, d) Tamaños de gota medidos por DLS a varias relaciones aceite/tensioactivo.

A partir de los resultados anteriores, se concluyó que las nano-emulsiones de Exaltolide®- o OH-Exaltolide®-en-agua se pueden formar con éxito por métodos de baja energía, a partir de una cuidadosa selección de los tensioactivos y de co-solventes. En general, el tamaño de gota de las nano-emulsiones varió entre 10 y 200 nm. Las nano-emulsiones formadas presentaron una buena estabilidad tanto a 25ºC como a 45ºC durante un tiempo suficiente para llevar a cabo la polimerización enzimática. A partir de este primer estudio, nano-emulsiones del sistema

agua/Brij®96V/Exaltolide®:escualano en una relación **90/5/4.5:0.5** y del sistema **agua/Cremophor®EL/OH-Exaltolide®:escualano** en una relación de **90/5/4.9:0.1** fueron seleccionadas para posteriores estudios.

3.3. SÍNTESIS DE NANOPARTÍCULAS DE POLIÉSTER MEDIANTE POLIMERIZACIÓN EN NANO-EMULSIÓN Y SU CARACTERIZACIÓN.

Se llevó a cabo la polimerización de lactonas presentes en las gotas de las nano-emulsiones mediante la adición de un catalizador biológico del tipo lipasa. Se estudiaron los parámetros que influyen en la polimerización por abertura de anillo (eROP) tales como la temperatura, el tiempo y la concentración de lipasa. Su influencia en la conversión se estudió mediante Resonancia Magnética Nuclear (RMN). Los polímeros obtenidos se caracterizaron determinando el punto de fusión mediante Calorimetría Diferencial de barrido (DSC), el peso molecular mediante cromatografía de permeación de gel (GPC) y la estructura cristalina por difracción de rayos X a ángulo pequeño (SAXS). Las distribuciones de tamaño y la morfología de las nanopartículas poliméricas se determinaron por Microscopia Electrónica de Transmisión (TEM). Además, se compararon los tamaños de nanopartículas obtenidas con el tamaño de gotas de las nano-emulsiones.

En primer lugar, se estudió la influencia de los parámetros de reacción (temperatura y concentración de enzima) en la polimerización del Exaltolide® en nano-emulsiones del sistema agua/Brij®96V/Exaltolide®:escualano. Se siguió la conversión del monómero con el tiempo por RMN a dos temperaturas (25ºC y 45ºC) y para tres concentraciones de enzima (0.1; 0.035 y 0.01%). Se observó una conversión completa a poli(Exaltolide®), en todas las condiciones estudiada, en menos de 24h. Se caracterizaron los polímeros finales mediante la determinación del punto de fusión, de la cristalinidad, del peso molecular y de la estructura cristalina. Se concluyó que la formación de nanopartículas tenía lugar al cabo de 7h a 45ºC usando 0,1% de lipasa (Figura 6.9.a-b). Cabe destacar que la reacción en medios confinados, como en nano-emulsión, permitió disminuir significativamente la concentración de enzima, el tiempo de reacción y la temperatura respecto a la misma reacción de polimerización enzimática en disolventes orgánicos o en "bulk". El poli(Exaltolide®) resultante presentó un peso molecular alrededor de 2600 g/mol, del mismo orden de magnitud que el obtenido en la polimerización en "bulk" (Uyama, 1995; Namekawa, 1998b). Un resultado muy importante para las siguientes aplicaciones es que las nanopartículas de poli(Exaltolide®) obtenidas presentaron un punto de fusión T_m alto (80ºC) y una cristalinidad χ elevada (75%) (Figura 6.9.c). El punto de fusión obtenido fue menor y la cristalinidad mayor que los valores obtenidos para el polímero en "bulk"

(Focarete, 2001). La reducción del punto de fusión se explica por la disminución del tamaño de particula (Bunjes, 2000; Cho, 2006). Dicha reducción confirma la formación de nanopartículas de poli(Exaltolide®) con tamaños pequeños (<50 nm) (Jiang, 2003). Posteriormente, se determinó el tamaño de la nanopartículas de poli(Exaltolide®) por TEM. Se obtuvieron tamaños pequeños (20 nm), similares a los diámetros de las gotas de la nano-emulsión (Figura 6.9.c-e), confirmando así el efecto plantilla de la nano-emulsión. Los estudios sobre la estructura cristalina del polímero pusieron de manifiesto que se trata de una estructura pseudo ortorrómbica, en total acuerdo con los datos encontrados en la literatura (Gazzano, 2003).

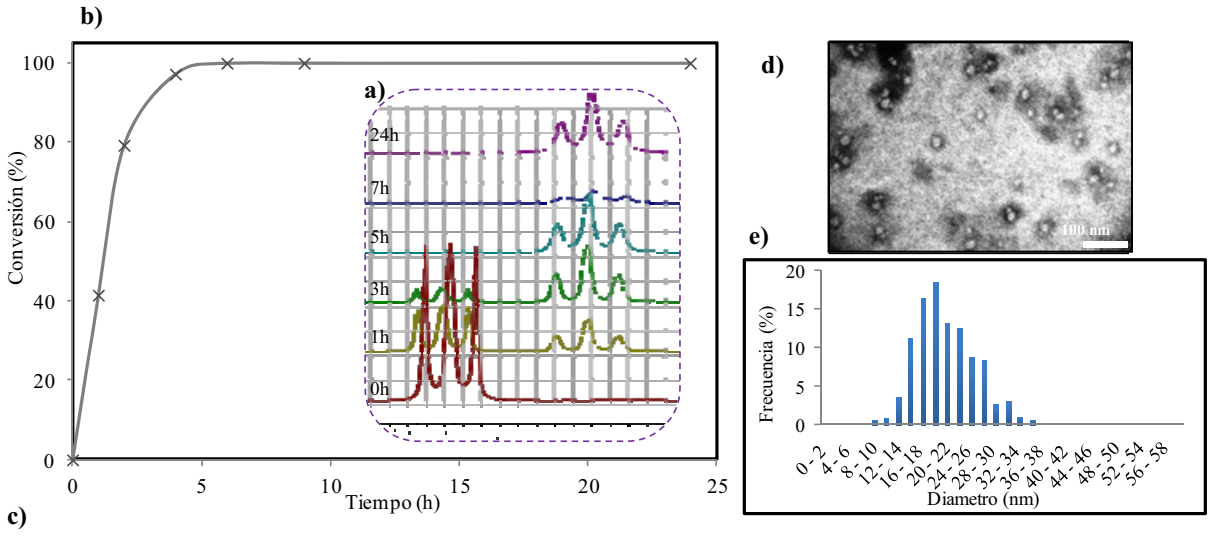

Exp	O/S	Mw (g/mol)	d_{nem} (nm)		d_{NP} (nm)		Tm (ºC)	ΔHm (J/g)	Tc (ºC)	ΔHc (J/g)	Tm (ºC)	ΔHm (J/g)	χ
2	50/50	2647	24.9	8.0	20.7	4.7	82.1	-208.2	69.9	172.5	78.2	-175.8	75.5

Figura 6.9 : Resumen de los resultados obtenidos para las nanopartículas obtenidas en nano-emulsión con el sistema agua/Brij 96V/Exaltolide®:escualano con 90% de agua y una relación aceite/tensioactivo 50/50. La reacción se llevo a cabo con 0.1% de lipasa, a 45ºC durante 24h. a) Evolución de los picos correspondiendo a los protones α-metileno del éster del monómero y del polímero con el tiempo por RMN, b) Evolución de la conversión de la polimerización con el tiempo, c) Resumen de los datos de peso molecular, tamaño de gota de nano-emulsión y de las nanopartículas y de calorimetría d) Imagen de TEM de las nanopartículas y e) distribución de tamaño de las nanopartículas de poli(Exaltolide®).

Este estudio confirmó la formación de nanopartículas de poliéster lineales por polimerización en nano-emulsión y permitió también optimizar las condiciones de reacción. A continuación, se aplicaron los mismos parámetros de reacción, determinados previamente, para las reacciones en nano-emulsiones del sistema agua/Cremophor®EL/OH-Exaltolide®: escualano. Se obtuvó la conversión completa en menos de 24h para este monómero. Se caracterizó el polímero poli(OH-Exaltolide®) mediante GPC y se determinó un peso molecular del mismo orden que el de poli(Exaltolide®). Se caracterizó también el poli(OH-Exaltolide®) mediante DSC, SAXS y TEM (Table 6.1).

Table 6.1 : Resumen de los datos de peso molecular, tamaño de gota y de calorimetría de las nanopartículas de poli(OH-Exaltolide®)

Sample	Mn (g/mol)	Dn (nm)	Tm (ºC)	ΔHm (J/g)	Tc (ºC)	ΔHc (J/g)	Tm (ºC)[c]	ΔHm (J/g)	X[d]
Poly(OH-Exaltolide®)	1554	21.3±5.4	79.2 84.5	-239.3 -66.2	74.9	135.9	73.9 85.2	-73.7 -56.8	-

El poli(OH-Exaltolide®) presentó un punto de fusión alto (85ºC) y una estructure cristalina similar al poli(Exaltolide®). Estos resultados sugirieron que la presencia del grupo OH en la molécula de Exaltolide® no altera significativamente la estructura del polímero final. Por otra parte, se observaron nanopartículas esféricas de poli(OH-Exaltolide®) por TEM con tamaños alrededor de 20 nm. Este estudio mostró la posibilidad de formar nanopartículas de poliéster funcionalizadas en condiciones suaves de polimerización en gotas de nano-emulsión. Cabe destacar que esta estrategia no se había descrito anteriormente.

Por último, se estudió la polimerización simultánea de dos monómeros (Exaltolide®/OH-Exaltolide® y Exaltolide®/Habanolide) en las gotas de nano-emulsión del sistema agua/Brij96V/Exaltolide®: comonómero:hexadecano. La copolimerización completa de los monómeros se confirmó por espectroscopia de ^{1}H (Figura 6.10.a) y ^{13}C NMR y se llevó a cabo en menos de 24 horas a 45ºC. Además, se calculó la relación de cada monómero en el polímero final y se observó que correspondía a la relación inicial de la nano-emulsión (Uyama, 1996; Kumar, 2000). Se caracterizaron los copolímeros obtenidos mediante medidas de puntos de fusión por DSC y se observó una disminución del punto de fusión al aumentar el contenido de comonómero (Figura 6.10.b). Los resultados obtenidos son similares a los descritos en la literatura, confirmando así, la formación de copolímeros (Ceccorulli, 2005; Meulen, 2011).

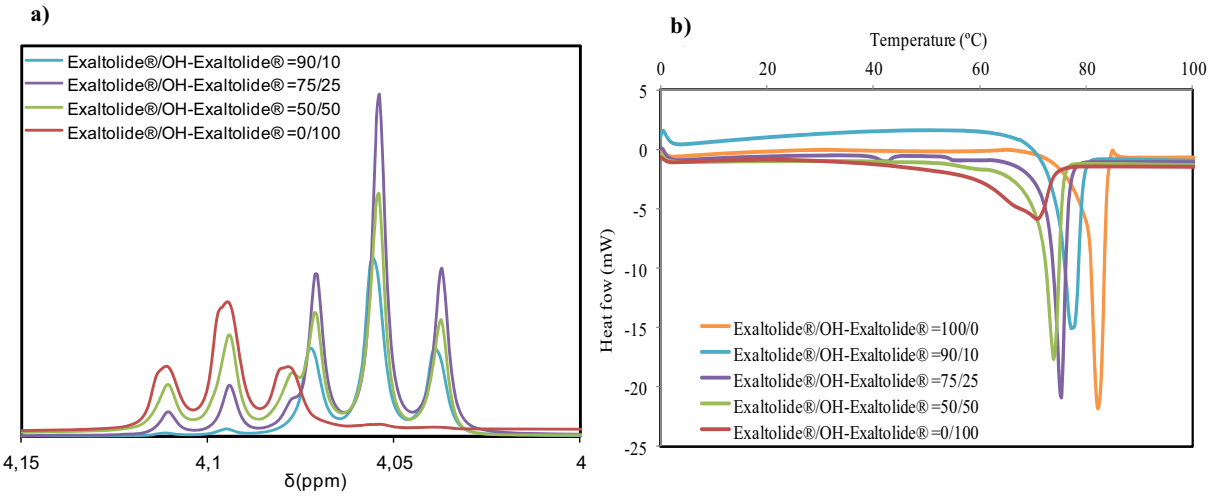

Figura 6.10 : Reacción de copolimerización entre Exaltolide® y OH-Exaltolide® usando 0.1% de lipasa, a 45ºC durante 24h en nano-emulsiones obtenidas por el método PIT con el sistema agua/Brij96V/Exaltolide®:OH-Exaltolide®:hexadecano con 90% de agua, una relación aceite/tensioactivo 70/30 y varias relaciones Exaltolide®/OH:Exaltolide®. a) Expansión del espectro de RMN entre 4.0 y 4.15 ppm representando el pico del protón α-metileno del ester de los homopolímeros y copolímeros y b) Perfil de DSC de homopolímeros y copolímeros.

A partir de todos los resultados anteriores, se puede concluir que la obtención de nanopartículas de poli(Exaltolide®) es posible por polimerización en condiciones suaves (temperatura y concentración de enzima bajas) en nano-emulsiones obtenidas por métodos de baja energía. Este proceso también permitió la obtención de nanopartículas funcionalizadas por grupos OH así como un control del grado de funcionalización de la superficie de las nanopartículas por copolimerización en nano-emulsiones.

3.4. POTENCIALES APLICACIONES DE LAS NANOPARTÍCULAS POLIMÉRICAS PARA LA LIBERACIÓN DE COMPUESTOS VOLÁTILES.

El último objetivo de este trabajo de investigación se refiere a la utilización de las nanopartículas de poliéster previamente sintetizadas para la liberación controlada de compuestos volátiles utilizados en las industrias de fragancias.

- **Afinidad de las nanopartículas de poliéster con componentes volátiles**

En primer lugar, se estudió la afinidad de las nanopartículas con varios compuestos volátiles midiendo su evaporación con el tiempo de una solución agua/etanol/perfume con nanoparticulas dispersas comparando con un sistema referencia sin nanopartículas. Se observó una disminución de la velocidad de evaporación de algunos compuestos volátiles en el sistema con nanopartículas, confirmando así la existencia de interacciones entre los compuestos volátiles y el polímero (Berthier, 2010). Por lo tanto, este estudio mostró que tanto las nanopartículas de

poli(Exaltolide®) como las de poli(OH-Exaltolide®), tienden a reducir la evaporación de compuestos volátiles y sugiriendo así que sería posible su aplicación para la retención de compuestos volátiles en formulaciones de la industria cosmética.

- **Emulsiones estabilizadas por nanopartículas de poliéster.**

En un segundo enfoque, se estudió el uso de las nanopartículas de poliéster para la estabilización de emulsiones de un perfume-en-agua.

En este contexto, se estudio primero el comportamiento de las nanopartículas de poli(Exaltolide®) y poli(OH-Exaltolide®) en agua mediante medidas de ángulo de contacto, de tamaño de partícula (DLS) y de potencial zeta. Se determinaron valores de ángulo de contacto inferiores a 90º para los dos tipos de nanopartículas (Figura 6.11.a) indicando así que las nanopartículas son hidrofilicas, característica que favorece la formación de emulsiones del tipo aceite-en-agua (Binks, 2000a) deseadas para la presente aplicación. Se estudió también el efecto de los cambios de la fuerza iónica y del pH sobre el comportamiento de las nanopartículas en dispersión acuosa mediante medidas de potencial zeta y de dispersión de luz laser. Se puso de manifiesto que tanto la presencia de electrolitos a una concentración de 10^{-1} M como el uso de un pH alto (pH≈12) conducen a la agregación de la nanopartículas (Figura 6.11.b) (Binks, 1999; Simovic, 2003, Prestidge, 2004; Salary, 2010). Por otra parte, se estudió el efecto de la temperatura en las dispersiones de nanopartículas con distintos componentes oleosos como limoneno, acetato de benzilo y Manzanate®, usados a posteriori como fase oleosa de las emulsiones. Se observó que las nanopartículas funden en la mayoría de los aceites a una temperatura alrededor de 50ºC (Figura 6.11.c).

a)

Tipo de nanopartículas	Angulo de contacto (º)
Poly(Exaltolide®)	86.3
Poly(OH-Exaltolide®)	68.3

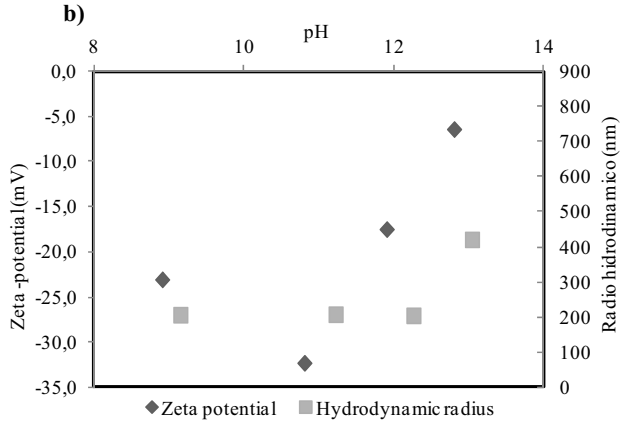

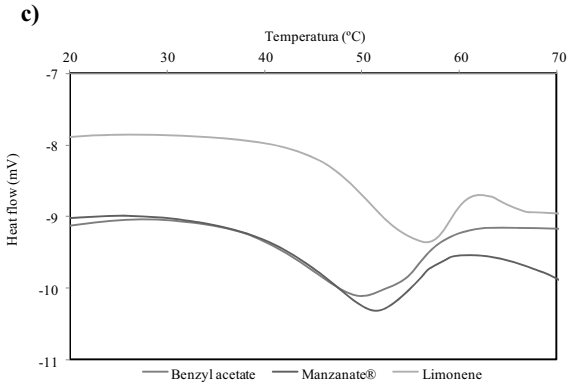

Figura 6.11 : a) Angulo de contacto entre las nanopartículas de poliéster y el agua medidos por el método de Washburn. b) Evolución del tamaño de gota y del potencial zeta de una dispersión de nanopartículas de poli(Exaltolide®) en función del pH y c) DSC perfil de las dispersión de nanopartículas de poli(Exaltolide®) en tres aceites: acetato de benzilo, Limoneno y Manzanate®.

A continuación, se utilizaron dichas dispersiones de nanopartículas en agua para estabilizar emulsiones aceite-en-agua mediante un método de alta energía (ultra-turrax). En primer lugar, se estudiaron emulsiones con un solo componente oleoso. Como caso intermedio entre un componente oleoso y un producto comercial, se utilizó un perfume modelo (MP), el cual contiene 5 compuestos volátiles.

Se estudió el efecto de varios factores tales como la adición de electrolitos, el método de preparación, la concentración de nanopartículas y la relación aceite/agua sobre la formación de emulsiones de MP-en-agua estabilizadas con las nanopartículas de poliésteres. Se estudió la presencia de electrolitos a una concentración de 10^{-1}M en la formación de emulsiones estabilizadas por nanopartículas de poli(Exaltolide®) y poli(OH-Exaltolide®) (Figure 6.12).

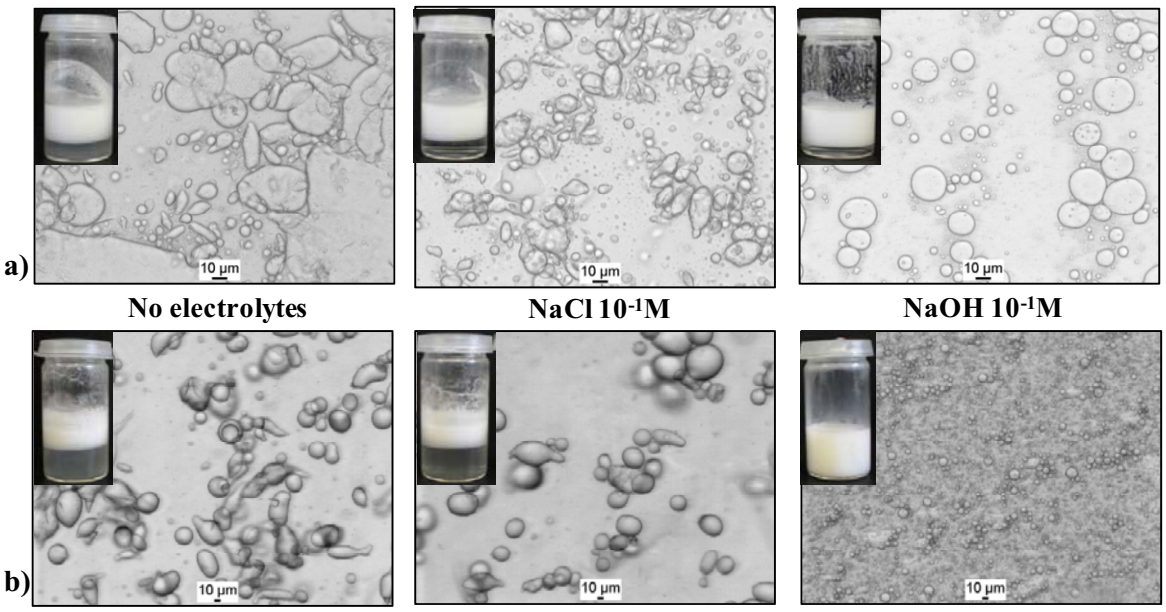

Figure 6.12 : Optical micrographs of the emulsions of Model Perfume-in-water with O/W ratio of 90/10 and stabilized by 0.9% of a) Poly(Exaltolide®) nanoparticles and b) poly(OH-Exaltolide®) nanoparticles using different types of electrolytes at 10^{-1} M. Insets show the emulsions after 24h at 25°C.

De acuerdo con los resultados de los estudios preliminares, fue necesaria la presencia de 10^{-1} M de NaOH y pH≈12 para obtener gotas de emulsiones esféricas y estabilizar las emulsiones, lo cual es indicativo de que las emulsiones se estabilizan por agregados de nanopartículas.

Asimismo, se evaluó la adsorción de las nanopartículas en la superficie de las gotas de emulsión, mediante la utilización de marcadores fluorescentes (Rhodamine 6G) (Vashisth, 2010; Whitby, 2011; Juarez, 2012). También, se puso de manifiesto que un aumento de la concentración de partículas o una disminución de la proporción aceite/agua daba lugar a tamaños de gota más pequeños, entre 10 y 100 µm, observando tamaños de gota más pequeños con las nanopartículas de poli(OH-Exaltolide®) (Figura 6.13).

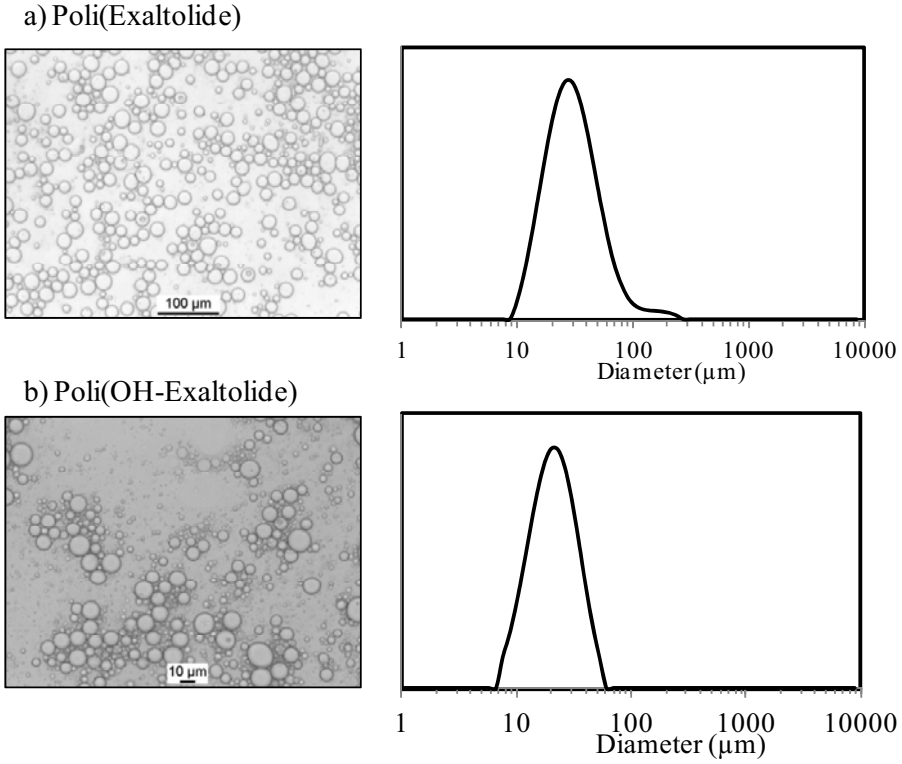

Figura 6.13 : Imagen de microscopia óptica y distribución de tamaño obtenido por difracción de luz laser de las emulsiones de MP-en-agua con una relación aceite/agua del 30/70 y estabilizadas por nanopartículas de a) poli(Exaltolide®) y b) poli(OH-Exaltolide®).

Finalmente, se estudió la estabilidad de dichas emulsiones a temperaturas altas y se observó una pérdida de estabilidad a temperaturas superiores a 50ºC debido a la fusión de las partículas a dicha temperatura, tal como se había observado en los estudios preliminares (Binks, 2003 y 2009) (Figure 6.14).

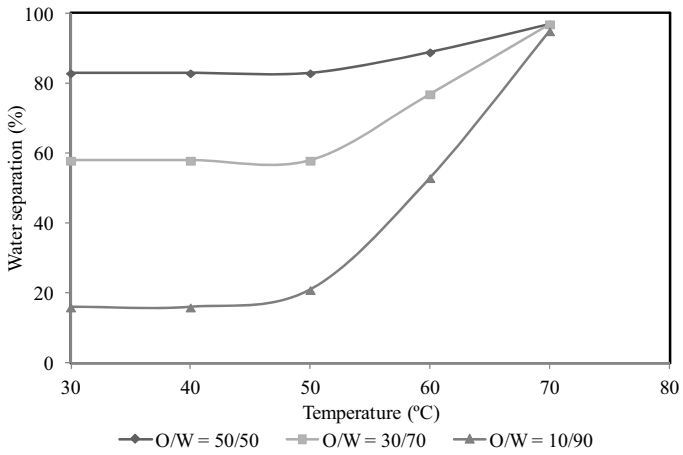

Figure 6.14 : Estabilidad de las emulsiones de MP-en-agua estabilizadas por 0.7% de nanopartículas de poli(Exaltolide®) a tres relaciones O/W (50/50; 30/70 and 10/90) después de 1h a cada temperatura.

Para concluir este estudio, se formaron emulsiones de perfume-en-agua con varias relaciones aceite/agua estabilizadas con distintas cantidades de nanopartículas, incluso con concentraciones de solo 1%. Se controló el tamaño de gota de las emulsiones mediante cambio en la humectabilidad, la concentración de las nanopartículas o la relación aceite/agua. Dichas emulsiones presentaron una buena estabilidad frente a la coalescencia. El cremado se pudo reducir aumentando la relación nanopartículas/aceite.

- **Formación de microcápsulas**

Con el objetivo de reducir la permeabilidad de compuestos volátiles de las emulsiones de Pickering previamente formadas, se estudió la formación de microcápsulas por reacción entre las nanopartículas de poliéster i un agente de reticulación (isocianato) en la interfase de las emulsiones según la siguiente reacción (Figure 6.15) (Thompson, 2010):

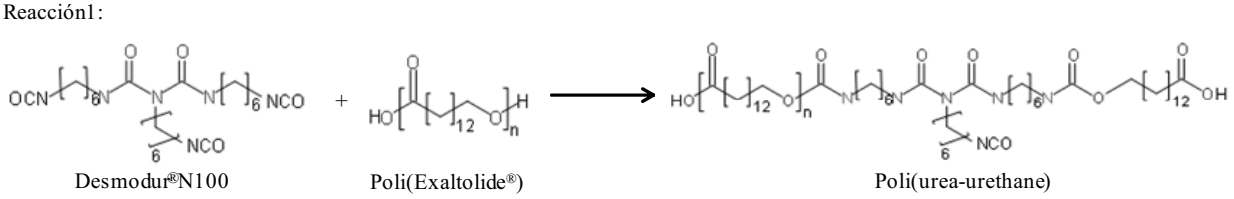

Figure 6.15 : Reacción sugerida entre el Desmodur N100 y las nanopartículas de poli(Exaltolide®).

En primer lugar, se estudió la influencia del tiempo mediante microscopia óptica, espectroscopia de infra-rojo y termogravimetria. Por microscopia óptica, se observó un cambio de forma de las gotas de emulsiones (de esféricas a no-esféricas) a partir de 4 horas de reacción. Se confirmó la presencia de nanopartículas de poli(Exaltolide®) y del isocianato en las microcápsulas formadas pero no se pudo confirmar la formación de un polímero poli(urea-uretano) por espectroscopia infra-rojo. Por ello, se estudiaron las microcápsulas por termogravimetria y se confirmó la formación del poli(urea-uretano) en aproximadamente 4 horas a 40ºC por la presencia de un pico a 300ºC en el perfil de termogravimetria. Se fijaron las condiciones de reacción a 40ºC durante 4h y se estudió la influencia de la relación entre los grupos hidroxilos del poli(Exaltolide®) y los grupos NCO del isocianato en la formación de microcápsulas mediante espectroscopia infra-rojo y termogravimetria (Figura 6.16).

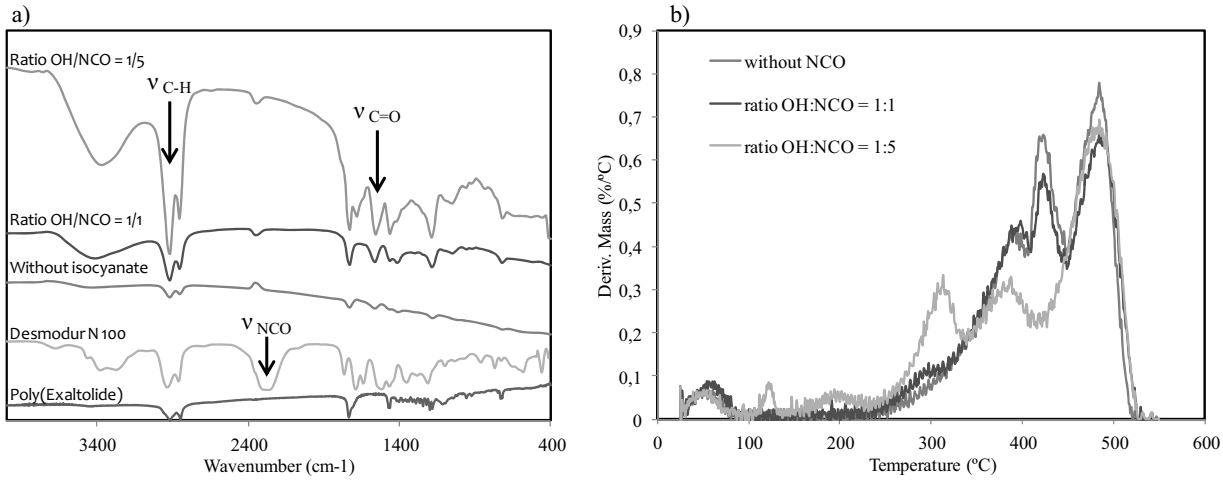

Figura 6.16 : a) espectro FTIR y b) perfile de termogravimetria de las microcápsulas formadas a partir de emulsiones de MP-en-agua con una relación aceite/agua de 10/90 estabilizadas por las nanopartículas de poli(Exaltolide®) para varias relaciones OH/NCO.

Se observaron la presencia de las bandas del poli(Exaltolide®) y de bandas de poliurea en el espectro de las microcápsulas pero no se observó la banda característica del grupo NCO del isocianato. Estos resultados sugieren la formación de microcápsulas por reacción entre un isocianato y las nanopartículas de poliéster en la interfase de una emulsión de Pickering. Se confirmó la presencia de un polímero poliurea-uretano por termogravimetria. Los resultados mostraron que las microcápsulas aumentaban en rigidez al aumentar la concentración de isocianato (Trovati, 2010). El estudio se hizo igualmente para las emulsiones estabilizadas por las nanopartículas de poli(OH-Exaltolide®) y puso de manifiesto la necesidad de una concentración menor de isocianato para formar las microcápsulas. Por microscopia electrónica de barrido, se confirmó la formación de microcápsulas con ambos tipos de nanopartículas (Figura 6.17).

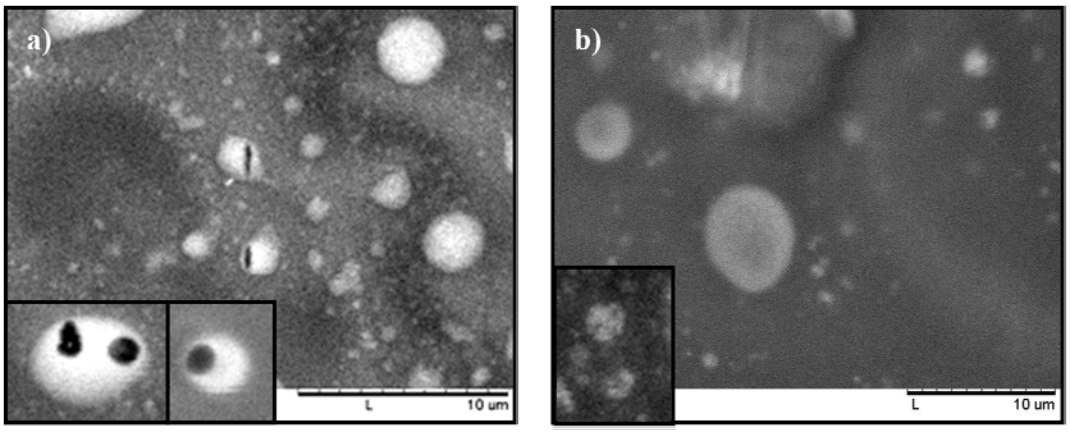

Figura 6.17 : Imagen de SEM de las microcápsulas formadas a partir de emulsiones de MP-en-agua con una relación aceite/agua de 10/90 estabilizadas por las nanopartículas de a) poli(Exaltolide®) y b) poli(OH-Exaltolide®).

Por microscopia, se confirmó la formación de microcápsulas con estructura núcleo-coraza. Finalmente, se estudió la liberación del perfume encapsulado en las microcápsulas de poli(Exaltolide®) y poli(OH-Exaltolide®) sintetizadas a distintas concentraciones de isocianato en una formulación de gel de ducha. Sin isocianato, se observó una liberación rápida del perfume, lo que indicó la elevada permeabilidad de la interfase aceite/agua cubierta únicamente por nanopartículas de poliéster. Al aumentar la concentración de isocianato, se observó una liberación del perfume más lenta debido al aumento de rigidez de las microcápsulas. Además, tal como se illustró en la Figura 6.18, se logró un control de la liberación al cambiar el tipo de nanopartículas de poli(Exaltolide®) a poli(OH-Exaltolide®) .

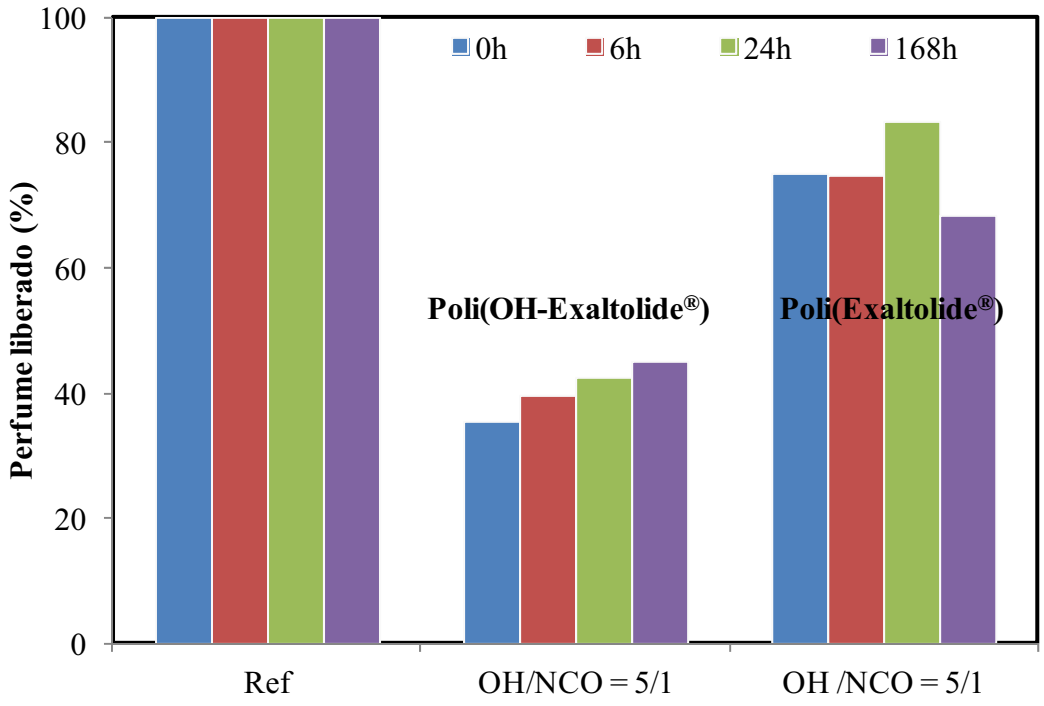

Figura 6.18 : Comparación del perfile de liberación del perfume de las microcápsulas obtenidas con nanopartículas de poli(OH-Exaltolide®) y Poli(Exaltolide®) entrecruzadas en la interfase de emulsiones de Pickering usando una proporción OH/NCO de 5/1.

El perfil de liberación del perfume obtenido, en Figura 6.18, sugiere la formación de microcápsulas menos permeable cuando se usan nanopartículas de poli(OH-Exaltolide®). Debido a su alto contenido en grupos OH (comparado con las nanopartículas de poli(Exaltolide®)), el grado de entrecruzamiento con isocianato en la interfase es mayor y así disminuye la permeabilidad de las microcápsulas permitiendo un cierto control de la liberación del perfume.

4. CONCLUSIONES GENERALES

Los resultados de esta tesis demuestran la posibilidad de formar nanopartículas de poliésteres por polimerización en condiciones suaves (enzima y baja temperatura) usando nano-emulsiones obtenidas por métodos de baja energía. Las propiedades de las nanopartículas obtenidas tales como el tamaño o la cristalinidad fueron optimizadas mediante la variación de la composición de las nano-emulsiones plantilla y/o de los parámetros de reacción. Se confirmó la posibilidad de funcionalizar las nanopartículas mediante la adición de un grupo hidroxilo en su estructura o mediante la copolimerización de monómeros cíclicos controlando así el grado de funcionalización. Las nanopartículas de poliésteres se pudieron usar para la estabilización de emulsiones de Pickering de un perfume-en-agua. Estas emulsiones fueron utilizadas como sistemas de liberación controlada de una fragancia modelo, pero no se pudo controlar eficientemente su liberación. Con el objetivo de evitar la rápida evaporación del perfume, las nanopartículas fueron covalentemente reticuladas en la interfase aceite/agua de las emulsiones de Pickering conduciendo a la formación de microcápsulas con estructura núcleo-coraza, permitiendo un mayor control de la liberación de perfume.

REFERENCES

7. REFERENCES

A

Albertsson, A.C., Varma, I.K., Recent developments in ring opening polymerization of lactones for biomedical applications, *Biomacromolecules,* **2003***, 4*, 1466-1486.

Allemann, E., Gurny, R., Doelker, E., Preparation of aqueous polymeric nanodispersions by a reversible salting-out process: Influence of process parameters on particle size, *International Journal of Pharmaceutics*, **1992**, *87*, 247-253.

Anton, N., Benoit, J-P., Saulnier, P., Design and production of nanoparticles formulated from nano-emulsion templates-a review, *Journal of Controlled Release,* **2008***, 128*, 185-199.

Anton, N., Vandamme, T., Nano-emulsions and micro-emulsions: clarifications of the critical differences, *Pharmaceutical Research, Springer Netherlands,* **2011***, 28*, 978-985.

Antonietti, M., Landfester, K., Polyreactions in miniemulsions, *Progress in Polymer Science,* **2002***, 27*, 689-757.

Aranberri, I., Binks, B., Clint, J., Fletcher, P., Synthesis of macroporous silica from solid-stabilized emulsion templates, *Journal of Porous Materials,* **2009***, 16*, 429-437.

Arditty, S., Whitby, C. P., Binks, B.P., Schmitt, V., Leal-Calderon, F., Some general features of limited coalescence in solid-stabilized emulsions, *The European Physical Journal E: Soft Matter and Biological Physics,* **2003***, 11*, 273-328.

Aschenbrenner, E., Weiss, C., Landfester, K., Enzymatic esterification in aqueous miniemulsions, *chemistry*, *A European Journal*, **2009**, *15*, 2434-2444.

Ashby, N.P., Binks, B.P., Pickering emulsions stabilised by Laponite clay particles *Physical Chemistry Chemical Physics,* **2000***, 2*, 5640-5646.

Astete, C.E., Kumar, C. S., Sabliov, C. M., Size control of poly(d,l-lactide-co-glycolide) and poly(d,l-lactide-co-glycolide)-magnetite nanoparticles synthesized by emulsion evaporation technique, *Colloids and Surfaces, A: Physicochemical and Engineering Aspects*, **2007**, *299,* 209 – 216.

Asua, J.M., Miniemulsion polymerization, *Progress in Polymer Science,* **2002***, 27*, 1283–1346.

Aveyard, R., Binks, B.P., Clint, J. H., Emulsions stabilised solely by colloidal particles, *Advances in Colloid and Interface Science,* **2003***, 100-102*, 503 – 546.

B

Bancroft, W.D., The theory of emulsification V, *The Journal of Physical Chemistry,* **1912***, 17*, 501-519.

Barichello, J.M., Morishita, M., Takayama, K., Nagai, T., Encapsulation of hydrophilic and lipophilic drugs in plga nanoparticles by the nanoprecipitation method, *Drug Development and Industrial Pharmacy*, **1999**, *25*, 471-476.

Barrère, M., Landfester, K., Polyester synthesis in aqueous miniemulsion, *Polymer*, **2003**, *44*, 2833–2841.

Benita, S., Levy, M.Y., Submicron emulsions as colloidal drug carriers for intravenous administration: Comprehensive physicochemical characterization, *Journal of Pharmaceutical Sciences*, **1993**, *82*, 1069-1079

Berthier, D.L., Schmidt, I., Fieber, W., Schatz, C., Furrer, A., Wong, K., Lecommandoux, S., Controlled Release of Volatile Fragrance Molecules from PEO-b-PPO-b-PEO Block Copolymer Micelles in Ethanol−Water Mixtures, *Langmuir*, **2010**, *26*, 7953-7961.

Bianchi, D., Cesti, P., Battistel, E., Anhydrides as acylating agents in lipase-catalyzed stereoselective esterification of racemic alcohols, *Journal of Organic Chemistry*, **1988**, *53*, 5531-5534.

Binks, B.P., Lumsdon, S., Stability of oil-in-water emulsions stabilised by silica particles, *Physical Chemistry Chemical Physics*, **1999**, 1, 3007-3016.

Binks, B.P., Lumsdon, S.O., Influence of particle wettability on the type and stability of surfactant-free emulsions, *Langmuir,* **2000a***, 16*, 8622-8631.

Binks, B.P., Lumsdon, S.O., Transitional phase inversion of solid-stabilized emulsions using particle mixtures, *Langmuir,* **2000b***, 16*, 3748-3756.

Binks, B. P., Lumsdon, S. O., Effects of oil type and aqueous phase composition on oil–water mixtures containing particles of intermediate hydrophobicity, *Physical Chemistry Chemical Physics,* **2000c***, 2*, 2959-2967.

Binks, B.P., Lumsdon, S.O., Catastrophic phase inversion of water-in-oil emulsions stabilized by hydrophobic silica, *Langmuir,* **2000d***, 16*, 2539-2547.

Binks, B.P., Lumsdon, S.O., Pickering emulsions stabilized by monodisperse latex particles: effects of particle size, *Langmuir,* **2001***, 17*, 4540-4547.

Binks, B.P., Particles as surfactants--similarities and differences, *Current Opinion in Colloid, Interface Science,* **2002a***, 7*, 21-41.

Binks, B.P., Clint, J.H., Solid wettability from surface energy components: relevance to Pickering emulsions, *Langmuir,* **2002b***, 18*, 1270-1273.

Binks, B.P., Kirkland, M., Interfacial structure of solid-stabilised emulsions studied by scanning electron microscopy, *Physical Chemistry Chemical Physics,* **2002c***, 4*, 3727-3733.

Binks, B.P., Whitby, C.P., Temperature-dependent stability of water-in-undecanol emulsions, *Colloids and Surfaces A: Physicochemical and Engineering Aspects,* **2003***, 224*, 241-249.

Binks, B.P., Whitby, C.P., Silica particle-stabilized emulsions of silicone oil and water: aspects of emulsification, *Langmuir*, **2004**, *20*, 1130-1137.

Binks, B.P., Whitby, C., Nanoparticle silica-stabilised oil-in-water emulsions: Improving emulsion stability, *Colloids and Surfaces A: Physicochemical and Engineering Aspects,* **2005***, 253*, 105-115.

Binks, B.P., Horozov, T.S., Colloidal particles at liquid interfaces, *Cambridge university press*, **2006**, ISBN: 978-0-511-33513-6.

Binks, B.P., Desforges, A., Duff, D.G., Synergistic stabilization of emulsions by a mixture of surface-active nanoparticles and surfactant, *Langmuir,* **2007a***, 23*, 1098-1106.

Binks, B.P., Rodrigues, J.A., Enhanced stabilization of emulsions due to surfactant-induced nanoparticle flocculation, *Langmuir,* **2007b***, 23*, 7436-7439.

Binks, B.P., Rodrigues, J.A., Frith, W.J., Synergistic interaction in emulsions stabilized by a mixture of silica nanoparticles and cationic surfactant, *Langmuir,* **2007c***, 23*, 3626-3636.

Binks, B.P., Rocher, A., Effects of temperature on water-in-oil emulsions stabilised solely by wax microparticles, *Journal of Colloid and Interface Science,* **2009***, 335*, 94 – 104.

Binks, B.P., Fletcher, P., Holt, B., Beaussoubre, P., Wong, K., Phase inversion of particle-stabilised perfume oil-water emulsions: Experiment and theory, *Physical Chemistry Chemical Physics,* **2010a**, *12*, 11954-11966.

Binks, B.P, Fletcher, P., Holt, B., Beaussoubre, P., Wong, K., Selective retardation of perfume oil evaporation from oil-in-water emulsions stabilized by either surfactant or nanoparticles, *Langmuir*, **2010b**, *26*, 18024-18030.

Binks, B.P, Fletcher, P., Johnson, A., Elliott, R., Membrane permeation of testosterone from either solutions, particle dispersions, or particle-stabilized emulsions, *Langmuir*, **2012**, *28*, 2510-2522.

Bisht, K.S., Henderson, L., Gross, R.A., Kaplan, D.S.G., Enzyme-catalyzed ring-opening polymerization of ω-pentadecalactone, *Macromolecules,* **1997***, 30*, 2705-2711.

Bunjes, H., Koch, M.H.J., Westesen, K., Effect of particle size on colloidal solid triglycerides, *Langmuir*, **2000**, *16*, 5234-5241.

C

Candau, F., Leong, Y.S., Pouyet, G., Candau, S., Inverse microemulsion polymerization of acrylamide: Characterization of the water-in-oil microemulsions and the final microlatexes, *Journal of Colloid and Interface Science*, **1984**, *101*, 167-183.

Calderó, G., García-Celma, M., Solans, C., Plaza, M., Pons, R., Influence of composition variables on the molecular diffusion from highly concentrated water-in-oil emulsions (gel-emulsions), *Langmuir,* **1997***, 13*, 385-390.

Calderó, G., García-Celma, M. J., Solans, C., Formation of polymeric nano-emulsions by a low-energy method and their use for nanoparticle preparation, *Journal of Colloid and Interface Science,* **2011***, 353*, 406–411.

Cai, J., Liu, C., Cai, M., Zhu, J., Zuo, F., Hsiao, B., Gross, R., Effects of molecular weight on poly(ω-pentadecalactone) mechanical and thermal properties, *Polymer,* **2010***, 51*, 1088-1099.

Cauvin, S., Sadoun, A., Santos, R., Belleney, J., Ganachaud, F., Hemery, P., Cationic polymerization of p-methoxystyrene in miniemulsion, *Macromolecules*, **2002**, *35*, 7919-7927

Cayre, O.J., Noble, P.F., Paunov, V.N., Fabrication of novel colloidosome microcapsules with gelled aqueous cores, *Journal of Materials Chemistry*, **2004**, *14*, 3351-3355.

Ceccorulli, G., Scandola, M., Kumar, A., Kalra, B., Gross, R., Cocrystallization of random copolymers of ω-pentadecalactone and ε-caprolactone synthesized by lipase catalysis, *Biomacromolecules,* **2005***, 6*, 902-907.

Cho, E.C., Cho, K., Ahn, J.K., Kim, J., Chang, I-S., Effect of particle size, composition, and thermal treatment on the crystalline structure of polycaprolactone nanoparticles, *Biomacromolecules,* **2006**, *7*, 1679-1685.

Crespy, D., Landfester, K., Miniemulsion polymerization as a versatile tool for the synthesis of functionalized polymers, *Beilstein Journal of Organic Chemistry,* **2010***, 6*, 1132-1148.

Croll, L.M., Stöver, H.D.H., Formation of tectocapsules by assembly and cross-linking of poly(divinylbenzene-alt-maleic anhydride) spheres at the oil−water interface, *Langmuir*, **2003**, *19*, 5918-5922.

D- E

Davis, S., Round, H., Purewal, T., Ostwald ripening and the stability of emulsion systems: an explanation for the effect of an added third component, *Journal of Colloid and Interface Science,* **1981***, 80*, 508-511.

Delmas, T., Piraux, H., Couffin, A.-C., Texier, I., Vinet, F., Poulin, P., Cates, M. E., Bibette, J., How to prepare and stabilize very small nanoemulsions, *Langmuir,* **2011***, 27*, 1683-1692.

Deminière, B., Colin, A., Calderon, F.L., Bibette, J., Vieillissement par coalescence et durée de vie d'une émulsion concentrée, *Comptes Rendus de l'Académie des Sciences - Series IIC - Chemistry,* **1998***, 1*, 163-165.

Derjaguin, B., Landau, L., Theory of the stability of strongly charged lyophobic sols and of the adhesion of strongly charged particles in solutions of electrolytes, *Acta Physico Chemica URSS,* **1941**, 14, 633.

Dickinson, E., Food emulsions and foams: Stabilization by particles, *Current Opinion in Colloid, Interface Science,* **2010***, 15*, 40-49.

Dinsmore, A., Hsu, M., Nikolaides, M., Marquez, M., Bausch, A., Weitz, D., Colloidosomes: Selectively permeable capsules composed of colloidal particles, *Science,* **2002***, 298*, 1006-1009.

Duda, A., Kowalski, A., Penczek, S., Uyama, H., Kobayashi, S., Kinetics of the ring-opening polymerization of 6-, 7-, 9-, 12-, 13-, 16-, and 17-membered lactones. Comparison of chemical and enzymatic polymerizations, *Macromolecules,* **2002***, 35*, 4266-4270.

F

Fessi, H., Piusieux, F., Devissaguet, J., Ammoury, N., Benita, S., Nanocapsule formation by interfacial polymer deposition following solvent displacement *International Journal of Pharmaceutics*, **1989**, *55*, R1-R4.

Finkle, P., Draper, H.D., Hildebrand, J.H., The theory of emulsification, *Journal of American chemical society*, **1923**, 45, 2780-2788.

Focarete, M., Scandola, M., Kumar, A., Gross, R. Physical characterization of poly(ω-pentadecalactone) synthesized by lipase-catalyzed ring-opening polymerization, *Journal of Polymer Science, Part B: Polymer Physics,* **2001***, 39*, 1721-1729.

Focarete, M.L., Gazzano, M., Scandola, M., Kumar, A., Gross, R.A. Copolymers of ω-pentadecalactone and trimethylene carbonate from lipase catalysis: influence of microstructure on solid-state properties, *Macromolecules*, **2002**, *35*, 8066-8071.

Forgiarini, A., Esquena, J., Gonzalez, C., Solans, C., Formation of nano-emulsions by low-energy emulsification methods at constant temperature, *Langmuir,* **2001***, 17*, 2076-2083.

Frelichowska, J., Bolzinger, M-A., Pelletier, J., Valour, J-P., Chevalier, Y., Topical delivery of lipophilic drugs from o/w Pickering emulsions, *International Journal of Pharmaceutics,* **2009***, 371*, 56-63.

Frelichowska, J., Bolzinger, M-A., Chevalier, Y., Effects of solid particle content on properties of o/w Pickering emulsions, *Journal of Colloid and Interface Science,* **2010***, 351*, 348-356.

G

Gazzano, M., Malta, V., Focarete, M. L., Scandola, M., Gross, R. A., Crystal structure of poly(ω-pentadecalactone, *Journal of Polymer Science Part B: Polymer Physics,* **2003***, 41*, 1009-1013.

Gers-Barlag, H., Miller, A., Emulsifier-free finely disperse systems of the oil-in-water and water-in-oil type, **2004,** US 6,803,049 B2.

Griffin, W.C., Classification of surface-active agents by HLB, *Journal of the society of cosmetic chemists,* **1949**, 311-326.

Gross, R., Kumar, A., Kalra, B., Polymer synthesis by in vitro enzyme catalysis, *Chemical Review,* **2001***, 101*,2097-2124.

Guterres, S.S., Alves, M.P., Pohlmann, A.R., Polymeric nanoparticles, nanospheres and nanocapsules, for cutaneous applications, *Drug Target Insights, Libertas Academica,* **2007***, 2*, 147-157.

H

Harris, J., Roos, C., Djalali, R., Rheingans, O., Maskos, M., Schmidt, M., Application of the negative staining technique to both aqueous and organic solvent solutions of polymer particles, *Micron,* **1999***, 30*, 289 -298.

Hassander, H., Johansson, B., Törnell, B., The mechanism of emulsion stabilization by small silica (Ludox) particles, *Colloids and Surfaces,* **1989***, 40*, 93-105.

He, Y., Yu, X., Preparation of silica nanoparticle-armored polyaniline microspheres in a Pickering emulsion, *Materials Letters*, **2007**, *61*, 2071-2074.

Higuchi, W.I., Misra, J., Physical degradation of emulsions via the molecular diffusion route and the possible prevention thereof, *Journal of Pharmaceutical Sciences*, **1962**, *51*, 459-466.

Holmberg, K., Jönsson, B., Krönberg, B., Lindman, B., Surfactants and polymers in aqueous solution, *Wiley edition,* **2002***,* ISBN: 047149883J.

Hopp, R., Finkelmeier, H., Koch, O., Körber, A., Derivate cyclisher Lactone, Verfahren zu ihrer Herstellung und Verfahren zur Herstellung von 15-pentadecanolid und seinen Homologen, EP 0 512 348 A1, **1992**.

Horozov, T.S., Binks, B.P., Particle-stabilized emulsions: a bilayer or a bridging monolayer, *Angewandte Chemie International Edition,* **2006***, 45*, 773-776.

I

Israelachvili, J.N., Mitchell, D.J., Ninham, B.W., Theory of self-assembly of hydrocarbon amphiphiles into micelles and bilayers, *Journal of The Chemical Society, Faraday Transactions 2,* **1976***, 72*.

Israelachvili, J., The science and applications of emulsions- an overview, *Colloids and Surfaces A: Physicochemical and Engineering Aspects,* **1994***, 91*, 1-8.

Izquierdo, P., Solans, C., Formation and stability of nano-emulsions, L*angmuir,* **2002***, 18*.

Izquierdo, P., Feng, J., Esquena, J., Tadros, T.F., Dederen, J.C., Garcia, M.J., Azemar, N., Solans, C., The influence of surfactant mixing ratio on nano-emulsion formation by the PIT method, *Journal of Colloid and Interface Science,* **2005***, 285*, 388-394.

J

Jedliski, Z., Juzwa, M.A, Kowalczuk, M., Montaudo, M., Anionic polymerization of pentadecanolide. A new route to a potentially biodegradable aliphatic polyester, *Macromolecular Chemistry and Physics.,* **1996***, 197(9)*, 2923-2929.

Jiang, Q., Yang, C.C., Li, J.C., Size-dependent melting temperature of polymers, *Macromolecular Theory and Simulations,* **2003***, 12*, 57-60.

Jiang, Z., Azim, H., Gross, R., Focarete, M., Scandola, M., Lipase-catalyzed copolymerization of ω-pentadecalactone with p-dioxanone and characterization of copolymer thermal and crystalline properties, *Biomacromolecules,* **2007***, 8*, 2262-2269.

Jiang, Z., Lipase-catalyzed synthesis of aliphatic polyesters via copolymerization of lactone, dialkyl diester, and diol, *Biomacromolecules,* **2008***, 9*, 3246-3251.

Jousma, H., Joosten, J.G.H., Junginger, H.E., Mesophases in mixtures of water and polyoxyethylene surfactant: Variations of repeat spacing with temperature and composition, *Colloid, Polymer Science,* **1988***, 266*, 640-651.

Juárez, J.A., Whitby, C.P., Oil-in-water Pickering emulsion destabilisation at low particle concentrations, *Journal of Colloid and Interface Science*, **2012**, *368*, 319 - 325

K

Kabal'nov, A., Pertzov, A., Shchukin, E., Ostwald ripening in two-component disperse phase systems: Application to emulsion stability, *Colloids and Surfaces,* **1987***, 24*, 19- 32.

Kadokawa, J.I., Kobayashi, S., Polymer synthesis by enzymatic catalysis *Current Opinion in Chemical Biology,* **2010***, 14*, 145-153.

Kikuchi, H., Uyama H., Kobayashi, S., Lipase-catalyzed ring-opening polymerization of substituted lactones, *Polymer Journal,* **2002***, 34*, 835-84.

Kim, J.W., Fernández-Nieves, A., Dan, N., Utada, A.S., Marquez, M., Weitz, D.A., Colloidal assembly route for responsive colloidosomes with tunable permeability *Nano Letters,* **2007***, 7*, 2876-2880.

Klang, V., Matsko, N. B., Valenta, C., Hofer, F., Electron microscopy of nanoemulsions: An essential tool for characterization and stability assessment, *Micron,* **2012***, 43*, 85-103.

Knani, D., Gutman, A. L. & Kohn, D. H. Enzymatic polyesterification in organic media. Enzyme-catalyzed synthesis of linear polyesters. I. Condensation polymerization of linear hydroxyesters. II. Ring-opening polymerization of ε-caprolactone, *Journal of Polymer Science, Part A: Polymer Chemistry*, **1993**, *31*, 1221-1232.

Kobayashi, S., Uyama, H., Namekawa, S., Hayakawa, H., Enzymatic ring-opening polymerization and copolymerization of 8-octanolide by lipase catalyst, *Macromolecules,* **1998a***, 31*, 5655-5659.

Kobayashi, S., Takeya, K., Suda, S., Uyama, H., Lipase-catalyzed ring-opening polymerization of medium-size lactones to polyesters, *Macromolecular Chemistry and Physics,* **1998b***, 199*, 1729-1736.

Kobayashi, S., Enzymatic ring-opening polymerization of lactones by lipase catalyst: Mechanistic aspects, *Macromolecular Symposia,* **2006***, 240*, 178-185.

Kobayashi, S., Recent developments in lipase-catalyzed synthesis of polyesters, *Macromolecular Rapid Communication,* **2009***, 30(4-5)*, 237-266.

Kobayashi, S., Lipase-catalyzed polyester synthesis-A green polymer chemistry *Proceedings of the Japan Academy Series B: Physical and Biological Sciences,* **2010***, 86*, 338-365.

Kumar, A., Kalra, B., Dekhterman, A., Gross, R., Efficient ring-opening polymerization and copolymerization of ε-caprolactone and ω-pentadecalactone catalyzed by Candida antartica lipase B, *Macromolecules,* **2000***, 33*, 6303-6309.

Kunieda, H., Friberg, S. E., Critical phenomena in a surfactant/water/oil system. Basic study on the correlation between solubilization, microemulsion, and ultralow interfacial tensions, *Bulletin of the Chemical Society of Japan,* **1981***, 54*, 1010-1014.

L

Laïb, S., Routh, A.F., Fabrication of colloidosomes at low temperature for the encapsulation of thermally sensitive compounds, *Journal of Colloid and Interface Science,* **2008***, 317*, 121-129.

Landfester, K., Bechthold, N., Tiarks, F., Antonietti, M., Formulation and stability mechanisms of polymerizable miniemulsions, *Macromolecules,* **1999***, 32*, 5222-5228.

Landfester, K., Tiarks, F., Hentze, H.-P., Antonietti, M., Polyaddition in miniemulsions: A new route to polymer dispersions, *Macromolecular Chemistry and Physics,* **2000a***, 201*, 1-5.

Landfester, K., Willert, M., Antonietti, M., Preparation of polymer particles in nonaqueous direct and inverse miniemulsions, *Macromolecules,* **2000b***, 33*, 2370-2376.

Landfester, K., The generation of nanoparticles in miniemulsions, *Advanced Materials,* **2001***, 13*, 765-768.

Landfester, K., Synthesis of colloidal particles in miniemulsions, *Annual Review of Materials Research,* **2006***, 36*, 231-279.

Landfester, K., Miniemulsion polymerization and the structure of polymer and hybrid nanoparticles, *Angewandte Chemie International Edition,* **2009***, 48*, 4488-4507.

Laredj-Bourezg, F., Chevalier, Y., Boyron, O., Bolzinger, M.-A., Emulsions stabilized with organic solid particles, *Colloids and Surfaces A: Physicochemical and Engineering Aspects,* **2012**, *413*, 252 – 259.

Leal-Calderon, F., Schmitt, V., Solid-stabilized emulsions, *Current Opinion in Colloid, Interface Science,* **2008***, 13*, 217 – 227.

Lebedev, B., Yevstropov, A., Thermodynamic properties of polylactones, *Die Makromolekulare Chemie,* **1984***, 185*, 1235-1253.

Lee, S.J., Jeong, J.R., Shin, S.C., Kim, J.C., Chang, Y.H., Chang, Y.M., Kim, J.D.D., Nanoparticles of magnetic ferric oxides encapsulated with poly(D,L latide-co-glycolide) and their applications to magnetic resonance imaging contrast agent, *Journal of Magnetism and Magnetic Materials*, **2004**, *272-276*, 2432-2433.

Lifshitz, I., Slyozov, V., The kinetics of precipitation from supersaturated solid solutions, *Journal of Physics and Chemistry of Solids,* **1961***, 19*, 35-50.

Lovell, P.A., El-Aasser, M.S, Emulsion polymerization and emulsion polymers, J. Wiley, **1997**, 801 pages, ISBN 047196746797804719674607.

M

Maitre, C., Ganachaud, F., Ferreira, O., Lutz, J.F., Paintoux, Y., Hémery, P., Anionic polymerization of phenyl glycidyl ether in nano-emulsion *Macromolecules,* **2000***, 33*, 7730-7736.

Målberg, S., Finne-Wistrand, A., Albertsson, A-C., The environmental influence in enzymatic polymerization of aliphatic polyesters in bulk and aqueous mini-emulsion, *Polymer*, **2010**, *51*, 5318-5322.

Mason, T.G., Wilking, J.N., Meleson, K., Chang, C.B., Graves, S.M., Nanoemulsions: formation, structure, and physical properties, *Journal of Physics: Condensed Matter*, **2006**, *18*, R635.

Matsumura, S., Beppu, H., Toshima, K., Enzyme-Catalyzed Ring-Opening Polymerization of Four-Membered Lactones: Preparation of Poly(propiolactone) and Poly(malic acid), *ACS Symposium Series,* **1998***, 684*, 74-89.

Matsumura, S., Enzymatic synthesis of polyesters via ring-opening polymerization *Advances in Polymer Science,* **2006***, 194*, 95-132.

May, S. New applications for biocatalysts, *Current Opinion in Biotechnology*, **1997**, *8*, 181-186.

McClements, D., Edible nanoemulsions: Fabrication, properties, and functional performance, *Soft Matter,* **2011***, 7*, 2297-2316.

McClements, D. J., Nanoemulsions versus microemulsions: terminology, differences, and similarities, *Soft Matter,* **2012***, 8*, 1719-1729.

Mee, L.v.d., Helmich, F., de Bruijn, R., Vekemans, J.A.J.M., Palmans, A.R.A., Meijer, E. W., Investigation of Lipase-Catalyzed Ring-Opening Polymerizations of Lactones with Various Ring Sizes: Kinetic Evaluation, *Macromolecules,* **2006***, 39*, 5021-5027.

Mei, Y., Kumar, A., Gross, R., Kinetics and mechanism of Candida antarctica lipase B catalyzed solution polymerization of ε-Caprolactone, *Macromolecules,* **2003***, 36*, 5530-5536.

Meulen, I.v.d., de Geus, M., Antheunis, H., Deumens, R., Joosten, E. A.J., Koning, C. E., Heise, A., Polymers from functional macrolactones as potential biomaterials: enzymatic ring opening polymerization, biodegradation, and biocompatibility, *Biomacromolecules,* **2008***, 9*, 3404-3410.

Meulen, I.v.d., Li, Y., Deumens, R., Joosten, E. A. J., Koning, C. E., Heise, A., Copolymers from unsaturated macrolactones: toward the design of cross-linked biodegradable polyesters, *Biomacromolecules,* **2011***, 12*, 837-843.

Morales, D., Gutierrez, J. M., Garcia-Celma, M. J., Solans, C., A., Study of the relation between bicontinuous microemulsions and oil/water nano-emulsion formation, *Langmuir,* **2003***, 19*, 7196-7200.

Morales, D., Solans, C., Gutierrez, J.M., Garcia-Celma, M.J., Olsson, U., Oil/Water droplet formation by temperature change in the Water/C16E6/Mineral oil system *Langmuir,* **2006***, 22*, 3014-3020.

Mundargi, R., Babu, V., Rangaswamy, V., Patel, P., Aminabhavi, T., Nano/micro technologies for delivering macromolecular therapeutics using poly(d,l-lactide-co-glycolide) and its derivatives, *Journal of Controlled Release*, **2008**, *125*, 193-20.

Musyanovych, A., Schmitz-Wienke, J., Mailänder, V., Walther, P., Landfester, K., Preparation of biodegradable polymer nanoparticles by nano-emulsion technique and their cell interactions, *Macromolecular Bioscience,* **2008***, 8*, 127-139.

N

Nakajima, H, Microemulsions in cosmetics, C. Solans, H. Kunieda (Eds.), Industrial Applications of Microemulsions, *Marcel Dekker New York*, **1997**, *66*, 175–197.

Namekawa, S., Uyama, H., Kobayashi, S., Lipase-catalyzed ring-opening polymerization of 16-hexadecanolide, *Proceedings of the Japan Academy Series B: Physical and Biological Sciences,* **1998a***, 74*, 65-68.

Namekawa, S., Uyama, H., Kobayashi, S., Lipase-catalyszed ring-opening polymerization of lactones in water, *Polymer journal,* **1998b***, 30 (3)*, 269-271.

Namekawa, S., Suda, S., Uyama, H., Kobayashi, S., Lipase-catalyzed ring-opening polymerization of lactones to polyesters and its mechanistic aspects, *International Journal of Biological Macromolecules,* **1999***, 25*, 145-151.

Namekawa, S., Uyama, H., Kobayashi, S., Enzymatic synthesis of polyesters from lactones, dicarboxylic acid divinyl esters, and glycols through combination of ring-opening polymerization and polycondensation, *Biomacromolecules,* **2000***, 1*, 335-338.

Nicolaos, G., Crauste-Manciet, S., Farinotti, R., Brossard, D., Improvement of cefpodoxime proxetil oral absorption in rats by an oil-in-water submicron emulsion, *International Journal of Pharmaceutics*, **2003**, *263*, 165-171.

O- P- Q

Okassa, L.N., Marchais, H., Douziech-Eyrolles, L., Hervé, K., Cohen-Jonathan, S., Munnier, E., Soucé, M., Linassier, C., Dubois, P., Chourpa, I., Optimization of iron oxide nanoparticles encapsulation within poly(d,l-lactide-co-glycolide) sub-micron particles, *European Journal of Pharmaceutics and Biopharmaceutics*, **2007**, *67*, 31-38.

Paunov, V.N., Binks, B.P., Ashby, N.P., Adsorption of charged colloid particles to charged liquid surfaces, *Langmuir*, **2002**, *18*, 6946-6955.

Pickering, S. U., CXCVI.-Emulsions, J. Chem. Soc., **1907**, *91*, 2001-2021.

Pinto Reis, C., Neufeld, R., Ribeiro, A., Veiga, F., Nanoencapsulation I. Methods for preparation of drug-loaded polymeric nanoparticles, *Nanomedicine: Nanotechnology, Biology, and Medicine*, **2006a**, *2*, 8-21.

Pinto Reis, C., Neufeld, R., Ribeiro, A., Veiga, F., Nanoencapsulation II. Biomedical applications and current status of peptide and protein nanoparticulate delivery systems, *Nanomedicine: Nanotechnology, Biology, and Medicine*, **2006b**, *2*, 53-65.

Prestidge, C.A., Barnes, T., Simovic, S., Polymer and particle adsorption at the PDMS droplet-water interface, *Advances in Colloid and Interfaces Science*, **2004**, *108-109*, 105-118.

Prestidge, C.A., Simovic, S., Nanoparticle encapsulation of emulsion droplets, *International Journal of Pharmaceutics,* **2006***, 324*, 92-100.

Quintanar-Guerrero, D., Allémann, E., Doelker, E., Fessi, H., A mechanistic study of the formation of polymer nanoparticles by the emulsification-diffusion technique, *Colloid, Polymer Science,* **1997***, 275*, 640-647.

R

Ramsden, W., Separation of solids in the surface-layers of solutions and 'suspensions' (observations on surface-membranes, bubbles, emulsions, and mechanical coagulation). *Preliminary Account Proceedings of the Royal Society of London*, **1903**, *72*, 156-164.

Reis, P., Holmberg, K., Watzke, H., Leser, M., Miller, R., Lipases at interfaces: A review, *Advances in Colloid and Interface Science*, **2009**, *147-148*, 237-250.

Roger, K., Cabane, B., Olsson, U., Formation of 10-100 nm size-controlled emulsions through a sub-PIT cycle, *Langmuir,* **2010***, 26*, 3860-3867.

Roger, K., Cabane, B., Olsson, U., Emulsification through surfactant hydration: The PIC Process Revisited, *Langmuir,* **2011***, 27*, 604-611.

Rosen, M., The relationship of structure to properties in surfactants. IV. Effectiveness in surface or interfacial tension reduction, *Journal of Colloid And Interface Science*, **1976**, *56*, 320-327.

Rossier-Miranda, F., Schroën, C., Boom, R., Colloidosomes: Versatile microcapsules in perspective, *Colloids and Surfaces A: Physicochemical and Engineering Aspects,* **2009***, 343*, 43-49.

Ruppert, M., Landfester, K., Ziener, U., Anionic polymerization of cyclic ester and amide in nano-emulsion: Synthesis and characterization of poly(ε-caprolactone) and poly(ε-caprolactone-co-ε-caprolactam) nanoparticles, *Journal of Polymer Science Part A: Polymer Chemistry*, **2010**, *48*, 4929-4937.

S

Sadurní, N., Solans, C., Azemar, N., García-Celma, M. J., Studies on the formation of O/W nano-emulsions, by low-energy emulsification methods, suitable for pharmaceutical applications, *European Journal of Pharmaceutical Sciences,* **2005***, 26*, 438-445.

Sagitani, H., Making homogeneous and fine droplet O/W emulsions using nonionic surfactants, *Journal of the American Oil Chemists' Society,* **1981***, 58*, 738-743.

Salari, J.W.O., van Heck, J., Klumperman, B., Steric Stabilization of Pickering Emulsions for the Efficient Synthesis of Polymeric Microcapsules, *Langmuir,* **2010***, 26*, 14929-14936.

Schork, F.J., Luo, Y., Smulders, W., Russum, J.P., Butté, A., Fontenot, K. Okubo, M., Nano-emulsion Polymerization, *Polymer Particles,* **2005***, 175*, 129-255.

Schulman, J.H., Leja, J., Control of contact angles at the oil-water-solid interfaces. Emulsions stabilized by solid particles (BaSO4), *Transaction of the Faraday Society*, **1954**, 50, 598-605.

Shinoda, K., Saito, H., The effect of temperature on the phase equilibria and the types of dispersions of the ternary system composed of water, cyclohexane, and nonionic surfactant, *Journal of Colloid and Interface Science,* **1968***, 26*, 70-74.

Shinoda, K., Saito, H., The stability of o/w type emulsions as functions of temperature and the HLB of emulsifiers: The emulsification by PIT-method, *Journal of Colloid and Interface Science,* **1969***, 30*, 258-263.

Siebert, J. M., Baumann, D., Zeller, A., Mailänder, V., Landfester, K., Synthesis of Polyester Nanoparticles in Nano-emulsion Obtained by Radical Ring-Opening of BMDO and Their Potential as Biodegradable Drug Carriers, *Macromolecular Bioscience,* **2012***, 12*, 165-175.

Simovic, S., Prestidge, C.A., Hydrophilic silica nanoparticles at the PDMS droplet-water interface, *Langmuir*, **2003**, *19*, 3785-3792.

Simovic, S., Prestidge, C.A., Nanoparticles of varying hydrophobicity at the emulsion droplet-water interface: adsorption and coalescence stability, *Langmuir*, **2004**, *20*, 8357-8365.

Simovic, S., Prestidge, C.A., Nanoparticle layers controlling drug release from emulsions, *European Journal of Pharmaceutics and Biopharmaceutics*, **2007**, *67*, 39-47.

Solans, C., Izquierdo, P., Nolla, J., Azemar, N., Garcia-Celma, M., Nano-emulsions, *Current Opinion in Colloid, Interface Science,* **2005***, 10*, 102-110.

Solans, C., Solé, I., Nano-emulsions: Formation by low-energy methods, *Current Opinion in Colloid and Interface Science,* **2012***, 17*, 246-254.

Solè, I., Maestro, A., González, C., Solans, C., Gutiérrez, J.M., Optimization of nano-emulsion preparation by low-energy methods in an ionic surfactant system, *Langmuir*, **2006**, *22*, 8326–8332.

Solè, I., Maestro, A., González, C., Solans, C., Gutiérrez, J.M., Influence of the phase behavior on the properties of ionic nanoemulsions prepared by the phase inversion composition method, *Journal of Colloids and Interface Science*, **2008**, *327*, 433–439.

Solè, I., Solans, C., Maestro, A., González, C., Gutiérrez, J., Study of nano-emulsion formation by dilution of microemulsions, *Journal of Colloid and Interface Science,* **2012***, 376*, 133-139.

Sonneville-Aubrun, O., Simonnet, J-T., L'Alloret, F., Nanoemulsions: a new vehicle for skincare products, *Advances in Colloid and Interface Science,* **2004***, 108–109*, 145-149.

Sonneville-Aubrun, O., Babayan, D., Bordeaux, D., Lindner, P., Rata, G., Cabane, B., Phase transition pathways for the production of 100 nm oil-in-water emulsions, *Physical Chemistry Chemical Physics,* **2009***, 11*, 101-110.

Soppimath, K.S., Aminabhavi, T.M., Kulkarni, A.R., Rudzinski, W.E., Biodegradable polymeric nanoparticles as drug delivery devices, *Journal of Controlled Release,* **2001***, 70*, 1-20.

Soula, R., Novat, C., Tomov, A., Spitz, R., Claverie, J., Drujon, X., Malinge, J., Saudemont, T., Catalytic polymerization of ethylene in emulsion, *Macromolecules*, **2001**, *34*, 2022-2026.

Sperling, L.H., Introduction to physical polymer science, *John Wiley&sons*, **2005**, ISBN, 047175711X, 97804717515.

Spernath, L., Magdassi, S., A new method for preparation of poly-lauryl acrylate nanoparticles from nanoemulsions obtained by the phase inversion temperature process *Polymers for Advanced Technologies,* **2007***, 18*, 705-711.

Staff, R.H., Lieberwirth, I., Landfester, K., Crespy, D., Preparation and characterization of anisotropic submicron particles from semicrystalline polymers, *Macromolecular Chemistry and Physics,* **2012***, 213*, 351-358.

Stoffer, J., Bone, T., Polymerization in water-in-oil microemulsion systems – 1, Journal of polymer science. Part A-1, *Polymer chemistry*, **1980**, *18*, 2641-2648.

T

Taden, A., Antonietti, M., Landfester, K., Enzymatic Polymerization towards Biodegradable Polyester Nanoparticles, *Macromolecular Rapid Communications,* **2003***, 14*, 512-516.

Tadros, Th.F., Vincent, B., Encyclopedia of emulsion technology (edited by Becher, P.), *Marcel Decker*, **1983**, *1*, 1-56.

Tadros, Th.F., Izquierdo, P., Esquena, J., Solans, C., Formation and stability of nano-emulsions, *Advances in Colloid and Interface Science,* **2004***, 108-109*, 303-318.

Taisne, L., Walstra, P., Cabane, B., Transfer of oil between emulsion droplets, *Journal of Colloid and Interface Science,* **1996***, 184*, 378-390.

Tambe, D.E., Sharma, M.M., The effect of colloidal particles on fluid-fluid interfacial properties and emulsion stability, *Advances in Colloid and Interface Science*, **1994**, *52*, 1-63.

Tamilvanan, S., Schmidt, S., Müller, R., Benita, S. In vitro adsorption of plasma proteins onto the surface (charges) modified-submicron emulsions for intravenous administration, *European Journal of Pharmaceutics and Biopharmaceutics*, **2005**, *59*, 1-7.

Tarimala, S., Dai, L.L., Structure of microparticles in solid-stabilized emulsions *Langmuir*, **2004**, 20, 3492-3494.

Taylor, P., Ottewill, R., Ottewill, R., Rennie, A., Ostwald ripening in O/W nano-emulsions formed by the dilution of O/W microemulsions, *Trends in Colloid and Interface Science VIII,* **1994***, 97*, 199-203.

Taylor, P., Ostwald ripening in emulsions, *Advances in Colloid and Interface Science,* **1998***, 75*, 107-163.

Teixeira, Z., Dreiss, C.A., Lawrence, M., Heenan, R.K., Machado, D., Justo, G.Z., Guterres, S.S., Durán, N., Retinyl palmitate polymeric nanocapsules as carriers of bioactives, *Journal of Colloid and Interface Science,* **2012***, 382*, 36-47.

Thieme, J., Abend, S., Lagaly, G., Aggregation in Pickering emulsions, *Colloid polymer Sci*, **1999**, 277, 257-260.

Thompson, K. L., Armes, S. P., Howse, J. R., Ebbens, S., Ahmad, I., Zaidi, J. H., York, D. W., Burdis, J. A., Covalently Cross-Linked Colloidosomes, *Macromolecules,* **2010***, 43*, 10466-10474.

Tiarks, F., Landfester, K., Antonietti, M., One-step preparation of polyurethane dispersions by nano-emulsion polyaddition, *Journal of Polymer Science Part A: Polymer Chemistry,* **2001***, 39*, 2520-2524.

Trimaille, T., Pichot, C., Elaïssari, A., Fessi, H., Briançon, S., Delair, T., Poly(D,L-lactic acid) nanoparticle preparation and colloidal characterization, *Colloid, Polymer Science,* **2003***, 281*, 1184-1190.

Trovati, G., Sanches, E. A., Neto, S. C., Mascarenhas, Y. P., Chierice, G. O., Characterization of polyurethane resins by FTIR, TGA, and XRD, *Journal of Applied Polymer Science*, **2010**, *115*, 263-268.

Tsaur,S.L., Fitch, R.M., Preparation and properties of polystyrene model colloids: I. Preparation of surface-active monomer and model colloids derived therefrom, *Journal of Colloid and Interface Science*, **1987**, *115* (2), 450–462.

U

Ugelstad, J., El-Aasser, M.S., Vanderhoff, J.W., Emulsion polymerization: Initiation of polymerization in monomer droplets, *Journal of Polymer Science: Polymer Letters,* **1973***, 11*, 503-513.

Uyama, H., Takeya, K., Hoshi, N., Kobayashi, S., Lipase-catalyzed ring-opening polymerization of 12-dodecanolide, *Macromolecules,* **1995a***, 28*, 7046-7050.

Uyama, H., Takeya, K., Kobayashi, S., Enzymatic ring-opening polymerization of lactones to polyesters by lipase catalyst: unusually high reactivity of macrolides, *Bulletin of the Chemical Society of Japan*, **1995b**, *68*, 56-61.

Uyama, H., Kikuchi, H., Takeya, K., Kobayashi, S., Lipase-catalyzed ring-opening polymerization and copolymerization of 15-pentadecanolide, *Advanced Materials,* **1996***, 8*, 357-360.

Uyama, H., Kobayashi, S., Enzymatic synthesis of polyesters via polycondensation *Advances in Polymer Science*, **2006**, *194*, 133-158

V

Vashisth, C., Whitby, C.P., Fornasiero, D., Ralston, J., Interfacial displacement of nanoparticles by surfactant molecules in emulsions, *Journal of Colloid and Interface Science,* **2010***, 349*, 537-543.

Vauthier, C., Dubernet, C., Fattal, E., Pinto-Alphandary, H., Couvreur, P., Poly(alkylcyanoacrylates) as biodegradable materials for biomedical applications, *Advanced Drug Delivery Reviews,* **2003***, 55*, 519-548.

Vauthier, C., Bouchemal, K., Methods for the preparation and manufacture of polymeric nanoparticles, *Pharmaceutical Research,* **2009***, 26*, 1025-1058.

Velev, O.D., Furusawa, K., Nagayama, K., Assembly of latex particles by using emulsion droplets as templates. 1. Microstructured hollow spheres, *Langmuir,* **1996***, 12*, 2374-2384.

Verwey, E.J.W., Overbeek, J.Th.G., Theory of the stability of lyophobic colloids, *Amsterdam: Elsevier*,**1948**.

Vignati, E., Piazza, R., Lockhart, T. P., Pickering emulsions: Interfacial tension, colloidal layer morphology, and trapped-particle motion, *Langmuir*, **2003**, 19, 6650-6656.

Vrignaud, S., Benoit, J-P., Saulnier, P., Strategies for the nanoencapsulation of hydrophilic molecules in polymer-based nanoparticles, *Biomaterials,* **2011***, 32*, 8593 – 8604.

W

Wagner, C., Theorie der Alterung von Niederschlägen durch Umlesen (Ostwald-Reifung), *Zeitschrift für Elektrochemie, Berichte der Bunsengesellschaft für physikalische Chemie,* **1961***, 65*, 581-591.

Walstra, P., Principles of emulsion formation, *Chemical Engineering Science,***1993***, 48*, 333-349.

Wang, L., Li, X., Zhang, G., Dong, J., Eastoe, J., Oil-in-water nanoemulsions for pesticide formulations, *Journal of Colloid and Interface Science*, **2007**, *314*, 230-235.

Wang, L., Mutch, K. J., Eastoe, J., Heenan, R. K., Dong, J., Nanoemulsions Prepared by a Two-Step Low-Energy Process, *Langmuir*, **2008**, *24*, 6092-6099.

Wang, L., Tabor, R., Eastoe, J., Li, X., Heenan, R.K., Dong, J., Formation and stability of nanoemulsions with mixed ionic-nonionic surfactants, *Physical Chemistry Chemical Physics*, **2009**, *11*, 9772-9778.

Warisnoicharoen, W., Lansley, A. B., Lawrence, M. J., Light-scattering investigations on dilute nonionic oil-in-water microemulsions, *AAPS Pharmsci,* **2000***, 2 (2)*, Article 12.

Whitby, C.P., Fischer, F.E., Fornasiero, D., Ralston, J., Shear-induced coalescence of oil-in-water Pickering emulsions, *Journal of Colloid and Interface Science*, **2011**, *361*, 170–177.

X-Y

Xiao, Q., Tan, X., Ji, L., Xue, J., Preparation and characterization of polyaniline/nano-Fe3O4 composites via a novel Pickering emulsion route, *Synthetic Metals*, **2007**, *157*, 784-791.

Yow, H.N., Routh, A.F., Release profiles of encapsulated actives from colloidosomes sintered for various durations, *Langmuir,* **2009***, 25*, 159-166.

Yuan, C., Xu, Y., Jiang, N., Chen, G., Xu, B., He, N., Dai, L., Colloidosomes constructed by the seamless connection of nanoparticles: a mobile and recyclable strategy to intelligent capsules, *Soft Matter,* **2011***, 7*, 3366-3372.

Yan, N., Masliyah, J.H, Solids-stabilized oil-in-water emulsions: Scavenging of emulsion droplets by fresh oil addition, *Colloids and Surfaces A*, **1993**, *75*: 123-132.

Z

Zhiyuan Z., Pieter J., Dijkstra, J.F., Controlled ring-opening polymerization of *omega*-pentadecalactone with yttrium isopropoxide as an initiator, *Macromolecular Chemistry and Physics,* **2000***, 201*, 1329-1333.

Ziani, K., Fang, Y., McClements, D., Fabrication and stability of colloidal delivery systems for flavor oils: Effect of composition and storage conditions, *Food Research International,* **2012***, 46*, 209-216.

GLOSSARY

8. GLOSSARY

8.1. ABBREVIATIONS

API	Active Pharmaceutical Ingredient
BS	BackScattering
BSE	BackScattered Electron
BLS	BackLight Scattering
BMDO	5,6-Benzo-2-methylene-1,3-dioxepane
CA	*Candida Antartica* lipase
CCC	Critical Coagulation Concentration
CC	*Candida Cylindracea* Lipase
CL	CaproLactone
CMC	Critical Micellar Concentration
DDL	DoDecanoLide
DLS	Dynamic Light Scattering
DLVO	Derjaguin- Landau- Verwey- Overbeek theory
DMA	Dynamic Mechanical Analysis
DSC	Differential Scanning Calorimetry
DTG	Derivative ThermoGravimetric
EM	Enzyme-activated Monomer
EBSD	Electron Back Scattered Diffraction
eROP	Enzymatic Ring Opening Polymerization
Exp.	Experiment
FTIR	Fourier Transform Infra Red
GC	Gas Chromatography
GPC	Gel Permeation Chromatography
HDL	HexaDecanoLide
HLB	Hydrophilic-Lipophilic Balance
HPLC	High Performance Liquid Chromatography
Int	Integration
IR	Infra Red
LBS	Light BackScattering
LSW	Lifshitz Slezov Wagner
MWCO	Molecular weight Cut-Off
NP	Nanoparticles
NMR	Nuclear Magentic Resonance
O	Oil
PC	*Pseudomonas Cepacia* lipase

PCL PolyCaproLactone
PCS Photon Correlation Spectrometer
PDI PolyDispersity Index
PDL PentaDecanoLide
PF *Pseudomonas fluorescens* lipase
PLA polyLactic Acid
PLGA Poly(Lactic-co-Glycolic) Acid
PIC Phase Inversion Composition
PIT Phase Inversion Temperature
PPDL PolyPentaDecanoLide
PPL *Porcine pancreas* lipase
PS *Pseudomonas* lipase
PSD Particle Size Distribution
PTA PhosphoTungstic Acid
ROP Ring Opening Polymerization
RJ *Rhizopus Japonicus* Lipase
S Surfactant
SAXS Small Angle X-Ray Scattering
SEM Scanning Electron Microscopy
T Transmission
TEM Transmission Electron Microscopy
TGA ThermoGravimetric Analysis
THF TetraHydroFurane
TMC TriMethylene Carbonate
UDL UnDecanoLide
UV Ultra-violet
VL ValeroLactone
W Water
WAXS Wide Angle X-ray Scattering

8.2. ROMAN LETTERS

A	Hamaker constant/ interfacial area
A_T	Total area
a	Nanoparticles radius
a_s	Superficial area per molecule
C	Concentration
C_α	Solubility of the dispersed phase in the continuous phase
c	Washburn constant
D	Diffusion coefficient
d	Diameter
d_n	Number average diameter
d_w	Weight average diameter
d_v	Volume average diameter
d_{nem}	Nano-emulsion droplet diameter
$d_{nanoparticle}$	Nanoparticle diameter
E_A	Potential due to the attractive forces
E_R	Potential due to the repulsive forces
E_T	Total potential
f	Asymmetric factor
G	Gibbs free energy
g	Gravitational acceleration
H	Enthalpy /Molar mass of the hydrophilic group of the surfactant
k_B	Boltzmann constant
L	Molar mass of the lipophilic group of the surfactant
m	Masse
M_n	Number average molecular weight
M_w	Weight average molecular weight
N_{HLB}	Number of hydrophilic-lipophilic balance
N	Total number of particles
N_A	Avogadro number
N_d	Number of droplets
N_p	Number of particles in a droplet
n_i	Number of drop with a size d_i
Q_S	Scattering efficiency factor
R	Universal gas constant
R_h	Hydrodynamic radius
r	Droplet radius
r_0	Droplet radius at t=0
S	Surfactant concentration
S_I	Surfactant concentration at the interface
S_M	Surfactant concentration in the continuous phase
T	Temperature
T_m	Melting temperature
T_c	Crystallization Temperature
t	Time
V	Volume of a drop
V_m	Volume molar of the dispersed phase
V_T	Total volume
x	Distance

8.3. GREEK LETTERS

γ	Interfacial tension
δ	Chemical shift
ε	Dielectric constant of water / solvent permeability
ε_0	Dielectric constant of vacuum
η	Viscosity
θ	Contact angle
κ	Inverse of the Debye length
λ	Wavelength
μ	Electrophoretic mobility
ν	Wave number
ξ	Zeta potential
ρ	Density
ρ_c	Density of the continuous phase
ρ_d	Density of the dispersed phase
ϕ_d	Volume fraction of dispersed phase
ϕ_p	Volume fraction of particles
φ_a	Surface coverage
χ	Crystallinity degree
ω	Rate
ω_{CR}	Creaming rate
ω_{CO}	Coalescence rate
ω_{OR}	Ostwald ripening rate

APPENDICES

9. APPENDICES

Appendix 1: Phase behavior of the water/Brij®96V/Exaltolide®: hexadecane.

Method: The phase behavior of a water/surfactant/oil system was determined by means of ternary equilibrium phase diagram at constant temperature (25ºC). Samples were prepared by mixing the oil, surfactant and water at 25ºC. Samples were homogenized on a vortex and left to equilibrate at 25ºC in a thermostated bath. Samples containing 10, 20, 30, 40, 50, 60, 70, 80 and 90 % of water were prepared for various O/S ratios. The phase equilibrium is reached when one or more phases were observed separated by a transparent interface. The presence of liquid crystals was first identified looking at the sample between crossed polarizers and a light source. Samples were then observed by optical microscopy to confirm the presence of liquid crystals using crossed polarizers. Sample preparation consists of applying a small quantity of sample on a slide and covered by a cover slip. It has to be taken into account that the liquid crystalline phases can break easily therefore, the slip has to be applied without pressure. In this thesis, the following symbols were used to designate the phase or region of the phase diagrams.

Acronym	Phase name	Appearance
L_1	Isotropic liquid phase (direct micelles)	Liquid / Transparent / no birefringent
L_2	Isotropic liquid phase (inverse micelles)	Liquid / Transparent / no birefringent
L_α	Lamellar phase	Viscous / slightly turbid / birefringent
H	Hexagonal phase	Highly viscous/ transparent/ birefringent
II	Two liquid phases	Each phase is liquid, transparent / no birefringent and a clear interface is observed between the two phases
M	Multiphase region containing or not liquid crystalline phases.	Turbid / birefringence

The equilibrium phase diagram of the water/Brij®96V/Exaltolide®:hexadecane system was determined at 25°C and the results are presented in the following figure.

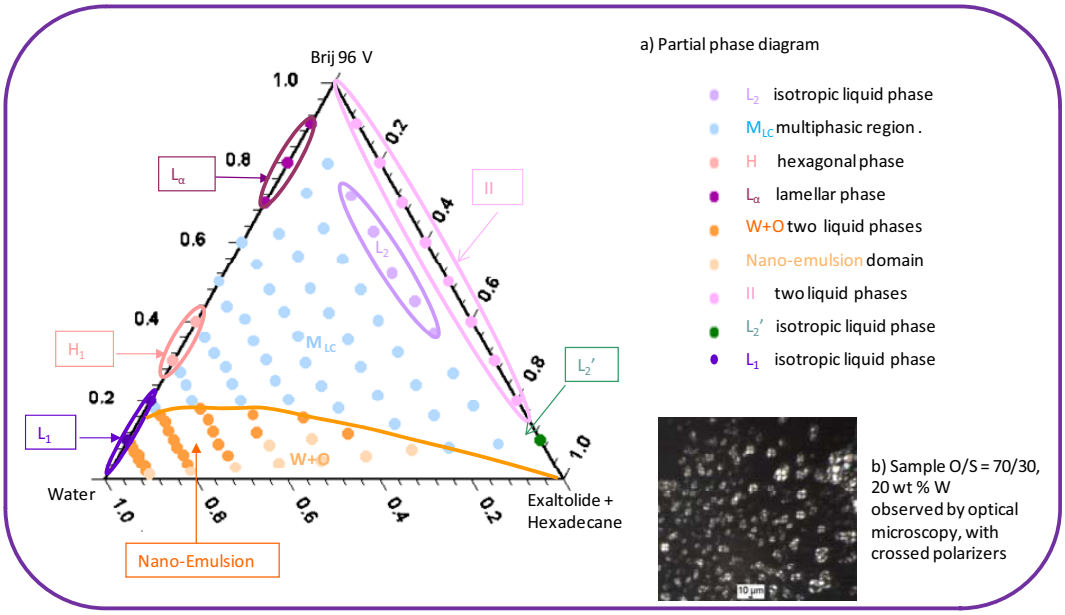

Phase diagram of the system Water /Brij®96V/ Exaltolide®:Hexadecane.

On the binary phase diagram water/Brij®96V at 25ºC, at low surfactant concentration, a liquid transparent region of isotropic liquid have been found and have been attributed to a solution of direct micelles. As the concentration of surfactant increases, two liquid crystalline phases characterized by optical microscopy are detected: Between 25 and 50 wt% of surfactant, hexagonal liquid crystal (H) has been identified. At higher surfactant concentration, mixture of liquid crystalline phases was observed where a pure lamellar phase (L_α) was characterized for surfactant concentration in the range from 70 to 90 wt%. These results agree with those described in the article of Jousma *et al.* in 1988. The pseudo binary of Brij 96V/ Exaltolide®: Hexadecane system shows an isotropic transparent liquid phase (L_2) at low surfactant concentration corresponding to inverse micelles. In the pseudo ternary Water/ Brij96V/ Exaltolide®: Hexadecane system, only one single phase is formed in a narrow region parallel to the O/S axis at low water concentrations. Considering the low amount of water in the system, the presence of inverse micelles swollen by water is expected but the system was not further characterized. The main part of the pseudo ternary phase diagram is multiphase and is formed by two multiphase regions: M_{LC} is a multiphase region that might contain liquid crystalline phases and W+O is a region where oil and water phase are separated in two liquid phases at equilibrium. Because of the high viscosity of some samples of the M_{LC} region, the types of phases at equilibrium were not characterized. As an example, a micrograph of a sample containing 20 wt% of water and O/S = 70/30 observed by optical microscopy under crossed polarized light. In the W+O region, nano-emulsions were formed, as described below, from 50 wt% of water and for O/S between 20/80 to 80/20.

Appendix 2: NMR spectra of the raw materials

NMR spectra of Brij®96V and Exaltolide®

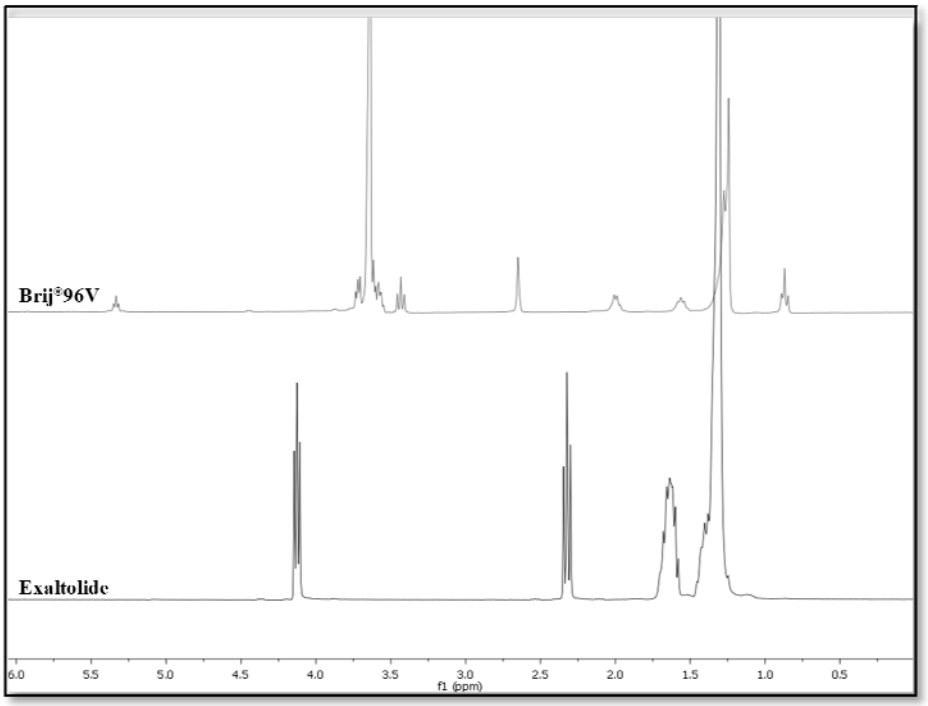

NMR spectra of Cremophor®EL and OH-Exaltolide®

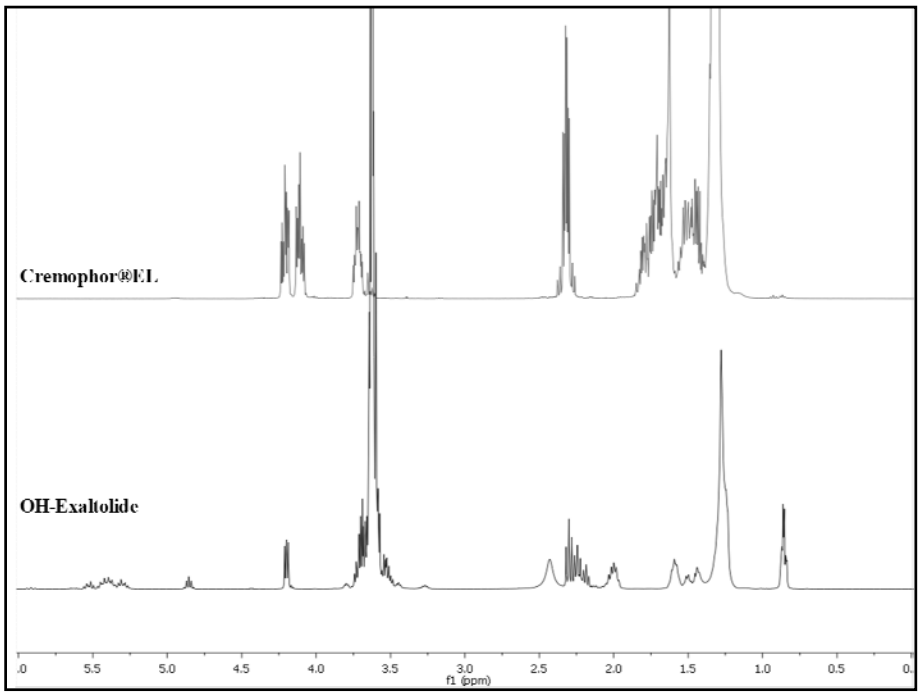

Appendix 3: NMR spectra over time of Experiments 1 to 6.

Summary of the polymerization experiments performed in nano-emulsions.

Exp.	Water content (%)	O/S ratio	Enzyme concentration (%)	Temperature (ºC)
1	90	50/50	0.1	25
2	90	50/50	0.1	45
3	90	50/50	0.035	45
4	90	50/50	0.01	45
5	90	40/60	0.1	45
6	90	60/40	0.1	45

Exp. 1

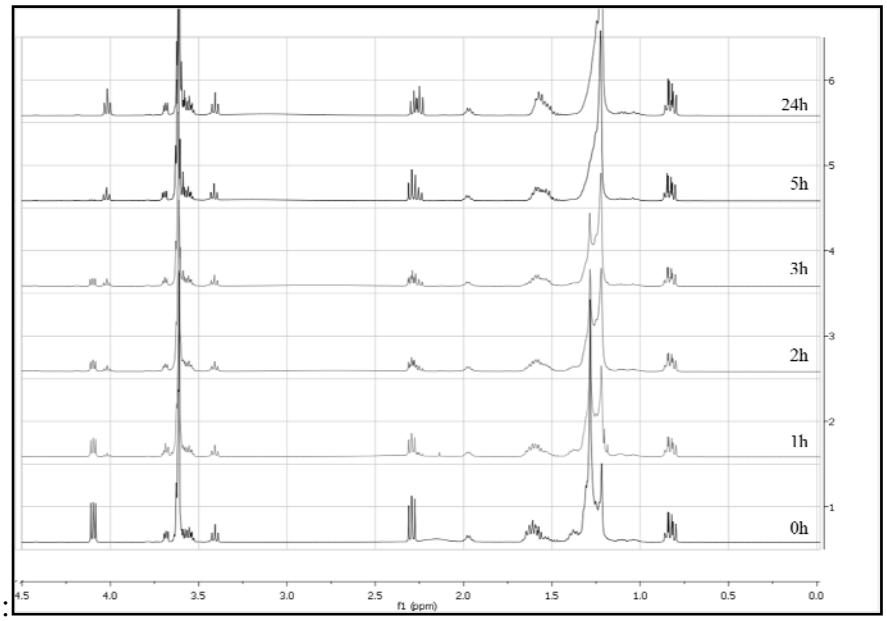

:

Exp. 2:

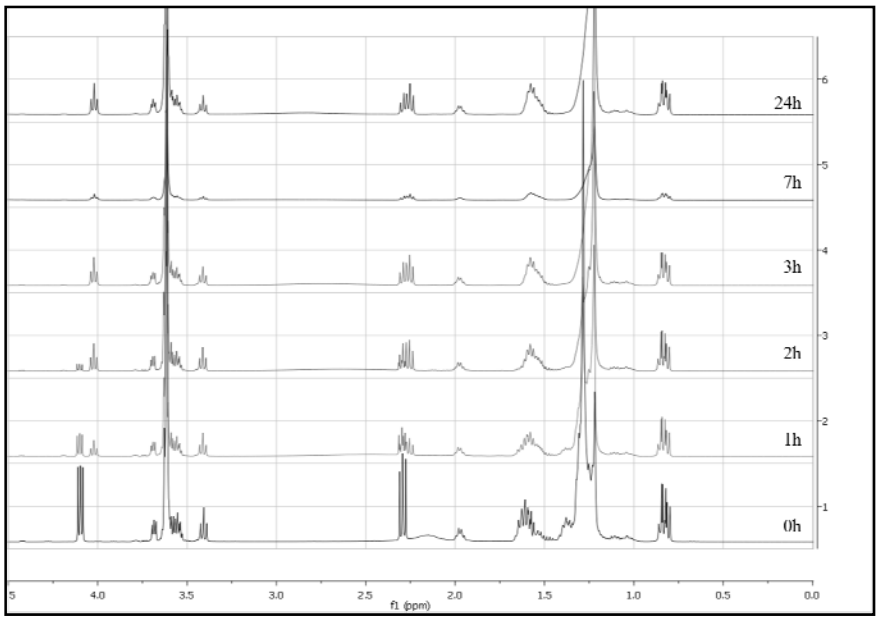

Exp. 3:

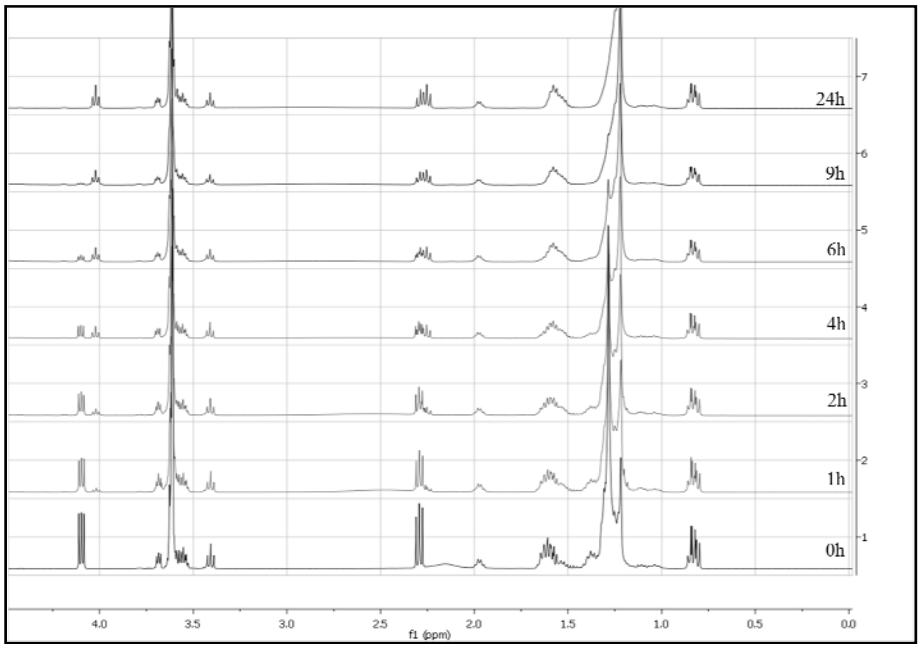
24h
9h
6h
4h
2h
1h
0h
4.0
3.5
3.0
2.5
2.0
1.5
1.0
0.5
0.0
f1 (ppm)

Exp. 4:

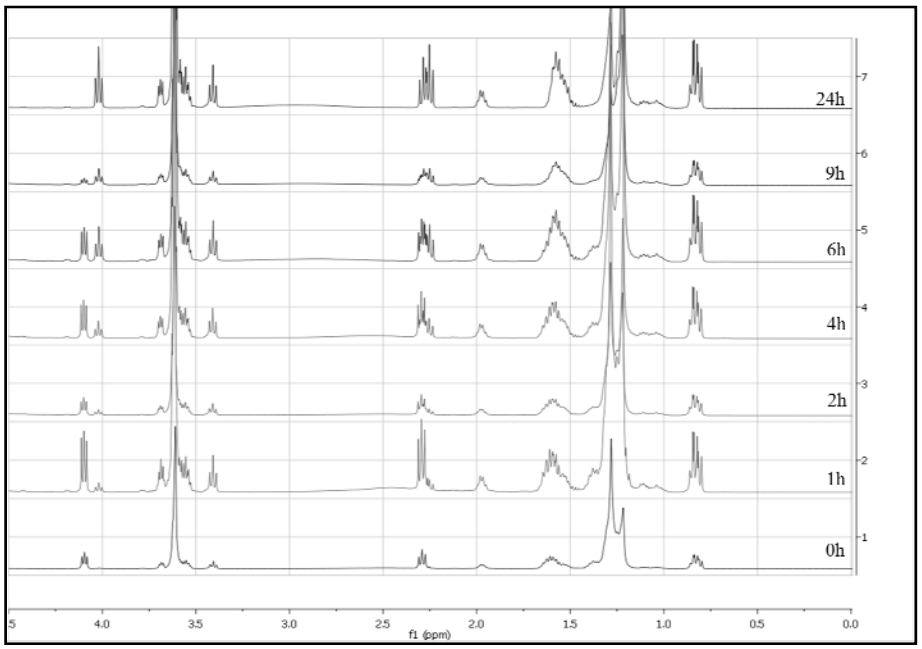
24h
9h
6h
4h
2h
1h
0h
4.0
3.5
3.0
2.5
2.0
1.5
1.0
0.5
0.0
f1 (ppm)

Exp. 5:

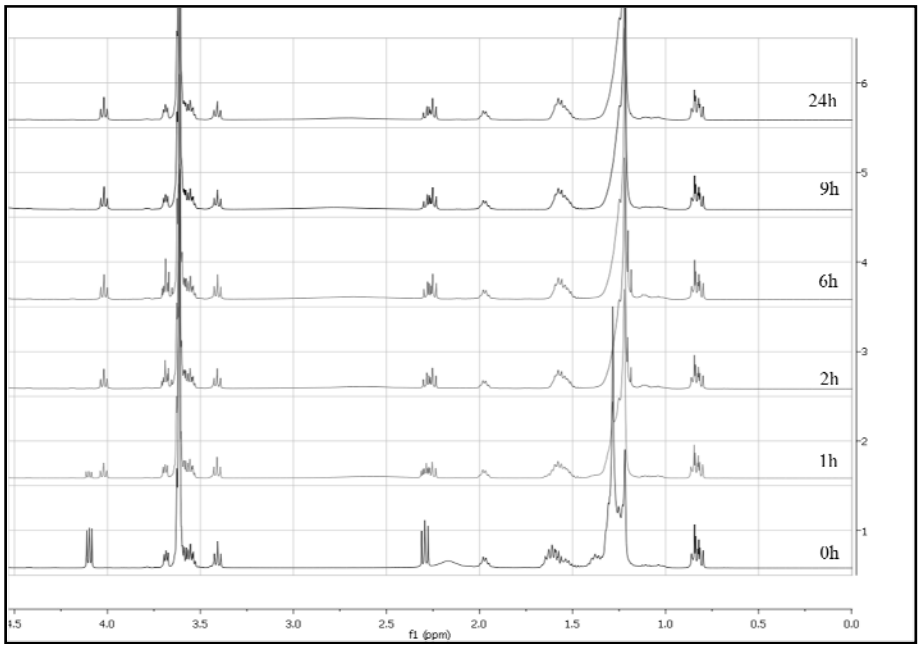

Exp. 6:

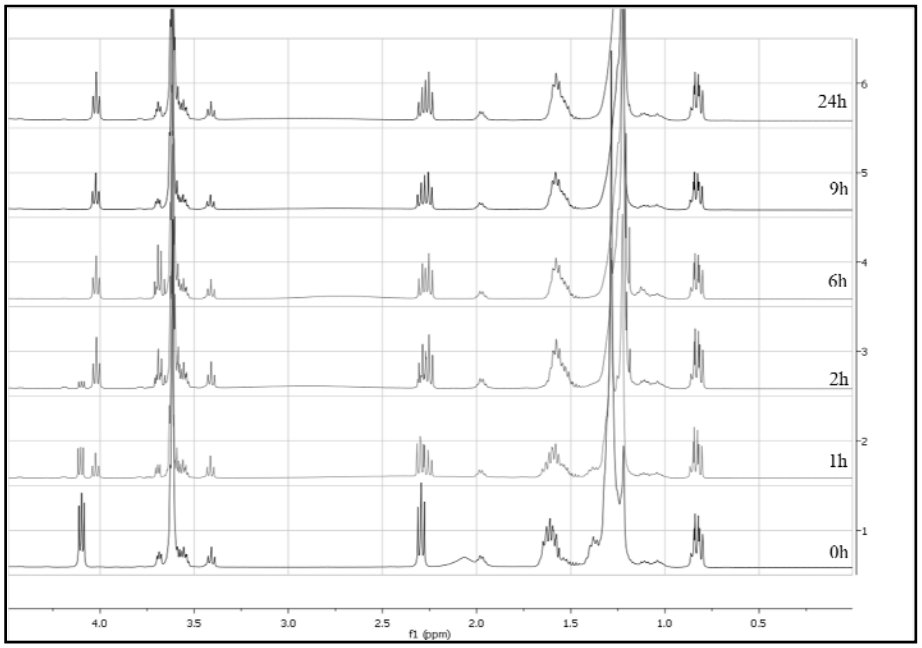

Appendix 4: DSC profile of final poly(Exaltolide®) of experiment 1 to 6.

Exp. 1:

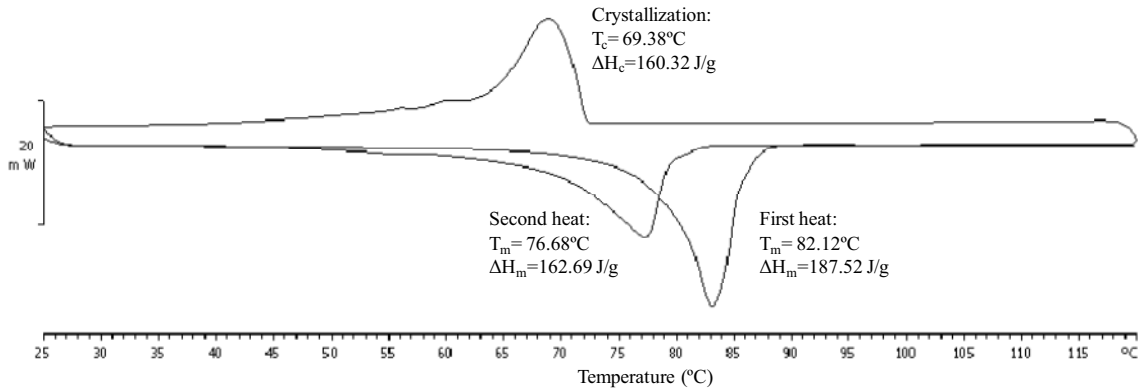

Exp. 2:

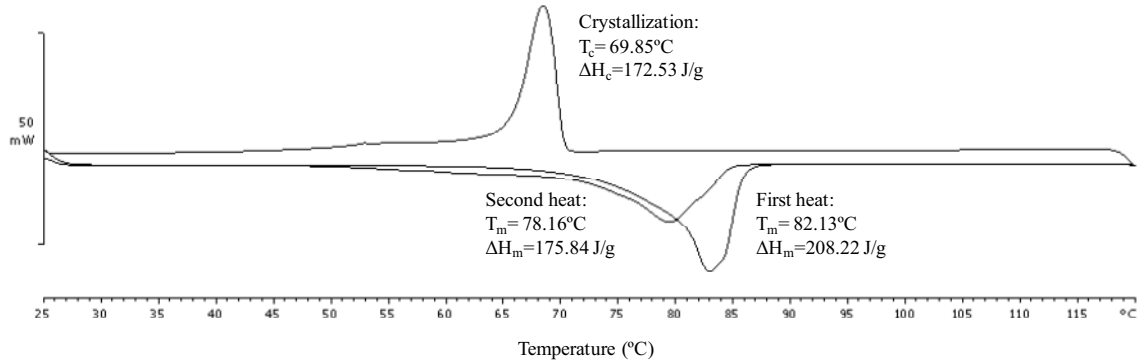

Exp. 3:

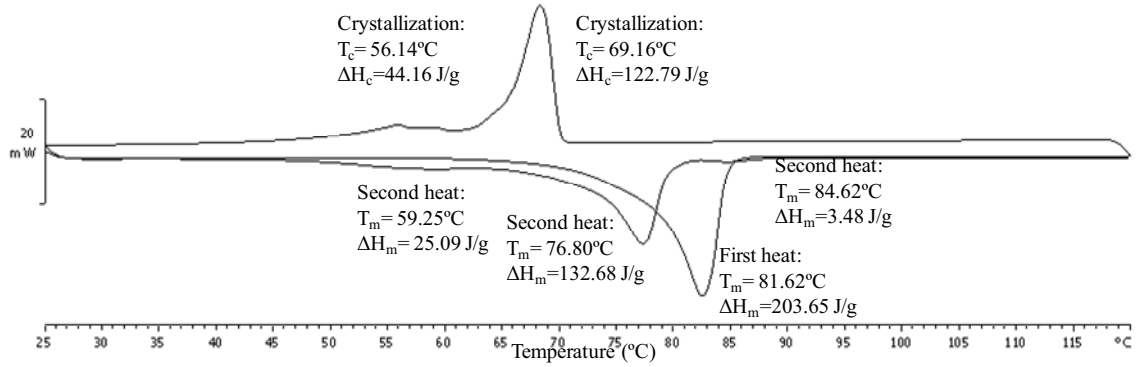

Exp. 4:

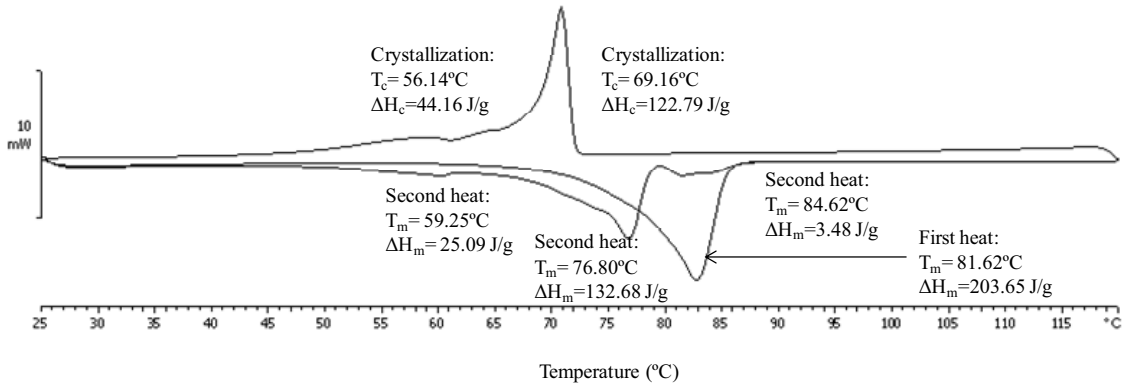

Exp. 5:

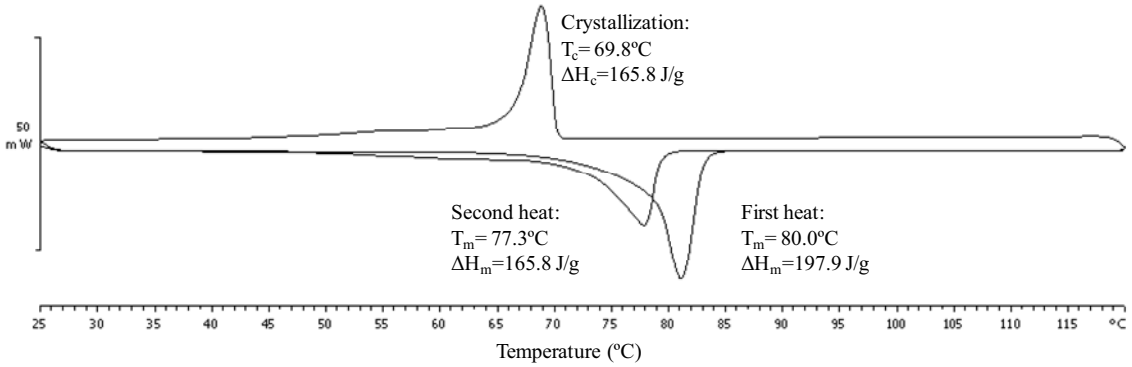

Exp.6:

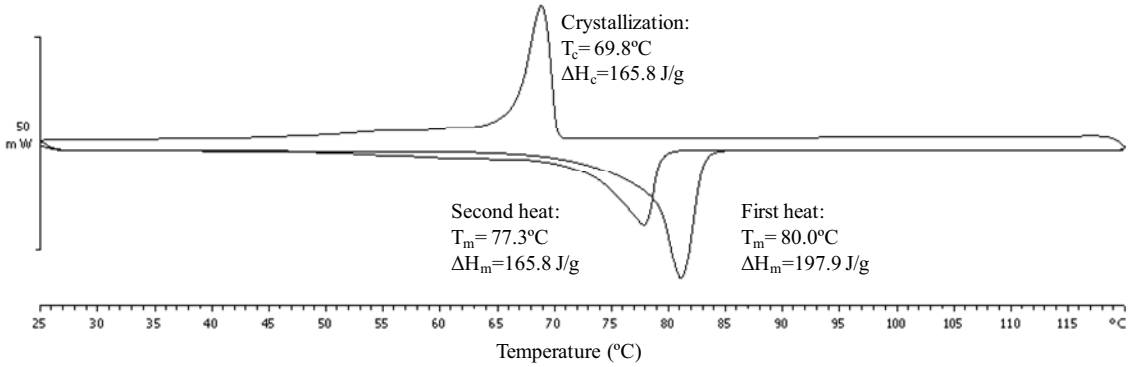

Appendix 5: Influence of the ionic strength and pH on the aqueous dispersion of poly(OH-Exaltolide®).

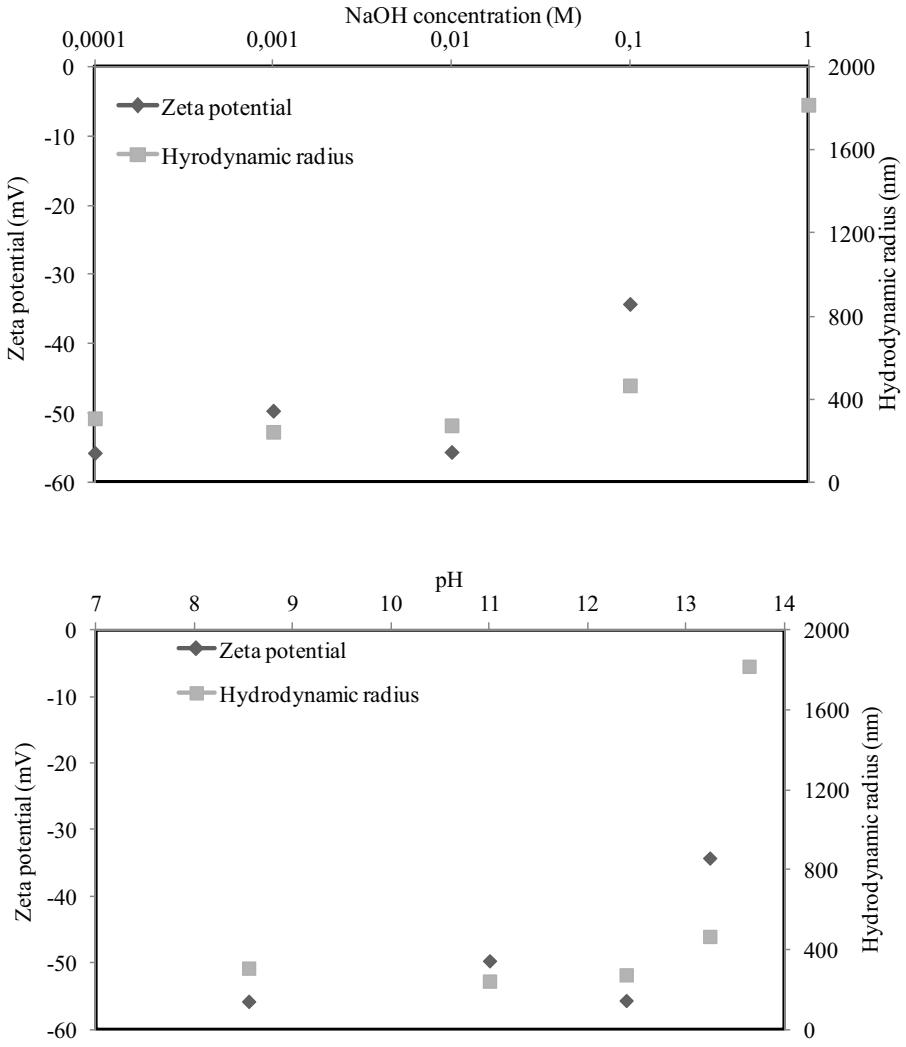

Appendix 6: DTG profile of Desmodur®N100 between 25 and 550ºC.